Treatments to expand regulatory T cells and/or deplete autoantibody production in primary membranous nephropathy

Dr Edmund Chung

Faculty of Medicine and Health

The University of Sydney

Australia

A thesis submitted to fulfil requirements for the degree of

Doctor of Philosophy

This research reported in this thesis was supported by the award of a National Health and Medical Research Council Postgraduate Research Scholarship to the PhD Candidate

2024

Statement of originality

This is to certify that to the best of my knowledge, the content of this thesis is my own work. This thesis has not been submitted for any degree or other purposes.

I certify that the intellectual content of this thesis is the product of my own work and that all the assistance received in preparing this thesis and sources have been acknowledged.

Edmund Chung

14th June 2024

Abstract

Primary membranous nephropathy is the most common cause of nephrotic syndrome in Caucasian adults and left untreated, a third of patients progress to kidney failure. In the past two decades, tremendous progress has been made in the understanding of the immunopathogenesis of membranous nephropathy, particularly the discovery of phospholipase A2 receptor as the main podocyte antigen targeted by autoantibodies in 70% of patients. However, this improved understanding has not translated into improved treatments. Currently, primary membranous nephropathy is treated with non-specific immunosuppression including cyclophosphamide and corticosteroids, calcineurin inhibitors or rituximab, which are incompletely effective and often toxic, carrying an increased risk of infection, infertility, and cancer. Since the key immune mechanism of membranous nephropathy involves a loss of immune tolerance to podocyte antigens resulting in autoantibody production and subsequent *in situ* immune complex deposition, expanding regulatory T cells to restore immune tolerance and depleting autoantibody production are attractive therapeutic strategies. In this thesis, chapter 2 reviews the existing literature to detail our current understanding of the immunopathogenesis of membranous nephropathy from both animal models and clinical studies, and how this may inform improved treatment strategies.

People with membranous nephropathy who do not respond to treatment have a poor prognosis with over half progressing to kidney failure within 10 years. While kidney transplantation is the preferred treatment for people with kidney failure, up to half will experience disease recurrence despite immunosuppression to prevent allograft rejection and half experience allograft loss five years after diagnosis since the optimal treatment of recurrent membranous nephropathy remains uncertain. Previous studies suggest predictive factors for recurrent membranous nephropathy may include human leukocyte antigen (HLA)-D risk alleles, but

other factors have not been explored with certainty. In chapter 3, we developed models to predict recurrent membranous nephropathy after kidney transplantation, which may inform clinical management such as informed consent pre-transplantation, closer monitoring post-transplantation and if more effective and safer treatments are developed in the future, identify high-risk patients who may benefit from early or pre-emptive treatment. We utilised the Australian and New Zealand Dialysis and Transplant registry and built three prediction models for recurrent membranous nephropathy (Group Least Absolute Shrinkage and Selection Operator (LASSO), penalised Cox regression and random forest), which were tuned using 10-fold cross-validation in a derivation cohort with complete HLA data while those with incomplete HLA data formed the validation cohort. Model performance was evaluated using area under the receiver operating characteristic curve (AUC-ROC). In total, 199 kidney transplant recipients with membranous nephropathy were included and 25 (13%) had recurrent disease. The Group LASSO and penalized Cox regression models (AUC-ROC 0.85, 95% confidence interval 0.76-0.94 and 0.91, 0.85-0.96 respectively) outperformed the random forest model (AUC-ROC 0.62, 0.57-0.69) in the derivation cohort, with moderate agreement in selected variables between the models (55-70%). In their validation cohorts, the penalised Cox regression model (AUC-ROC 0.73, 0.59-0.86) performed better than the Group LASSO model (AUC-ROC 0.60, 0.49-0.70). Variables of importance chosen by all models included recipient HLA-A2, donor HLA-DR12, donor-recipient HLA-B65 and HLA-DR12 match, highlighting the importance of donor-recipient HLA characteristics to recurrent membranous nephropathy though validation in larger datasets is required.

Heymann nephritis, a rat model of membranous nephropathy, recapitulates the underlying disease phenotype of membranous nephropathy of autoantibody production against a kidney antigen and is therefore a suitable model for pre-clinical testing of novel therapeutic strategies. We evaluated T cell stimulatory blockade with or without proteasome inhibition (chapter 4),

and peptide vaccination to induce $CD8^+$ regulatory T cells (chapter 5) in Heymann nephritis, which we hypothesised would deplete autoantibody production and expand regulatory T cells respectively. The anti-CD20 monoclonal antibody rituximab has been increasingly used to deplete autoantibody-producing B cells for the treatment of membranous nephropathy but has been ineffective in up to 40% of patients. T cell help is crucial for B cells to produce high affinity antibodies and differentiate into long-lived antibody-producing plasma cells, neither of which are targeted by rituximab. Therefore, we reasoned T cell costimulatory blockade (cytotoxic-T-lymphocyte-associated antigen 4 (CTLA4)-Ig) with or without a short course of proteasome inhibition (bortezomib) to deplete plasma cells may represent a complementary form of treatment in membranous nephropathy. In chapter 4, we immunised Lewis rats with Fx1A and complete Freund's adjuvant (CFA) to induce Heymann nephritis and treated them with CTLA4-Ig alone or CTLA4-Ig plus a short-course of bortezomib. CTLA4-Ig-treated and CTLA4-Ig plus bortezomib-treated rats had significant and similar reductions in serum creatinine and proteinuria, with less glomerulosclerosis, tubular injury, and interstitial infiltrate compared to untreated Heymann nephritis rats. Glomerular IgG deposition was reduced in CTLA4-Ig plus bortezomib-treated and CTLA4-Ig-treated rats compared to untreated Heymann nephritis rats but there were no significant differences in serum anti-Fx1A levels, suggesting the benefit of CTLA4-Ig with or without bortezomib was not mediated by reducing autoantibody production. Rather, CTLA4-Ig-treated rats and CTLA4-Ig plus bortezomib-treated rats exhibited significantly reduced messenger ribonucleic acid (mRNA) expression of T helper (Th) 17 cell cytokines (interleukin (IL) 6, IL7, IL21) in the kidney but also reduced mRNA expression of markers of regulatory T cells (Forkhead box P3, Transforming growth factor-β) in the kidney but not the spleen. There were no between-group differences in kidney or splenic mRNA expression of Th1 markers (interferon-γ, T-box transcription factor), splenic mRNA expression of plasma cell markers (B lymphocyte-induced maturation protein 1, X-box

binding protein 1, Interferon regulatory factor 4) or T follicular helper cell markers (B-cell lymphoma 6, IL21). CTLA4-Ig-treated rats and CTLA4-Ig plus bortezomib-treated rats also exhibited reduced infiltration of $CD4^+$ and $STAT3^+$ cells into the kidney. These data suggested CTLA4-Ig alone ameliorated experimental membranous nephropathy, potentially through suppression of Th17 cells in the kidney and may represent an effective adjunct treatment in membranous nephropathy.

Immune tolerance is mediated by regulatory T cells, of which $CD4^+$ regulatory T cells are the best-characterised population. However, $CD4^+$ regulatory T cells numbers are unchanged in Heymann nephritis whereas previous studies have shown $CD8^+$ regulatory T cells to be protective in Heymann nephritis. Furthermore, $CD8^+$ regulatory T cells are equally cross-protective across multiple mouse models of autoimmunity and specific peptides that expanded $CD8^+$ regulatory T cells in murine experimental multiple sclerosis have been recently reported. Therefore, in chapter 5 we hypothesised these peptides would also expand $CD8^+$ regulatory T cells and protect against Heymann nephritis. Lewis rats with Heymann nephritis received peptide vaccination 1 week before (prevention vaccination) or 1 week after disease induction (treatment vaccination). Prevention vaccination, but not treatment vaccination, significantly reduced anti-Fx1A autoantibody levels and serum creatinine. Both prevention and treatment vaccination reduced histological kidney injury. mRNA expression of Helios, the major transcription factor of $CD8^+$ regulatory T cells, was upregulated in both the spleen and kidney with prevention vaccination and in the kidney with treatment vaccination. To understand whether the effect of peptide vaccination was mediated by $CD8^+$ regulatory T cells, we adoptively transferred $CD8^+$ T cells 1 week after peptide vaccination into Heymann nephritis rats, which significantly reduced serum creatinine, proteinuria, histological kidney injury, anti-Fx1A autoantibody levels, germinal centre formation, and mRNA expression of markers of T follicular helper cells (B-cell lymphoma 6, IL21), Th1 cells (interferon-γ, T-box transcription

factor) and Th17 cells (IL6, IL17). This demonstrated peptide vaccination induces $CD8^+$ regulatory T cells that ameliorate induction of experimental membranous nephropathy which may represent a further peripheral control against autoimmunity.

B-cell activating factor (BAFF) is a cytokine which is critical for B cell survival and maturation, and is involved in the development of autoreactive B cells that cause membranous nephropathy. Serum BAFF concentrations also correlate with disease activity in membranous nephropathy. Therefore, in chapter 6 we generated chimeric antigen receptor (CAR) T cells that genetically express BAFF to redirect T-cell killing towards autoreactive B cells that require a high level of BAFF for survival. Since BAFF has multiple isoforms including a monomer and trimer, we have generated three BAFF CAR constructs consisting of the extracellular domain of human BAFF: 1) full-length BAFF monomer, 2) truncated BAFF monomer and 3) truncated BAFF trimer. We generated CAR T cells using lentiviral gene delivery and using a PiggyBac transposon, a non-viral gene delivery method. Cytotoxicity against Raji B cells (a lymphoma B cell line) and human embryonic kidney (HEK)-293T cells as a negative control were evaluated using the Calcein assay. Intracellular cytokine release, memory phenotype and exhaustion phenotype were assessed on flow cytometry. All three forms of BAFF CAR T cells demonstrated increased cytotoxicity against Raji B-cells compared to unmodified T-cells without significant cytotoxicity against HEK293T cells. Co-culture of BAFF CAR T cells with Raji B-cells resulted in induction of the degranulation marker CD107a and proinflammatory cytokines (tumour necrosis factor-α, interferon-γ and IL2), compared to unmodified T-cells co-cultured with Raji-B cells. Overall, BAFF CAR T cells did not show an increased expression of markers of T-cell exhaustion (programmed death 1, T cell immunoglobulin and mucin domain-containing protein 3, lymphocyte activation gene 3). These results demonstrate BAFF T cells eliminate B cells *in vitro* and may represent a novel treatment for B cell-mediated autoimmunity, which underpins membranous nephropathy. The findings from this thesis

supports novel treatment strategies for depleting autoantibodies and expanding regulatory T cells in membranous nephropathy as well as utilising prediction models to identify patients at high risk of recurrent disease after kidney transplantation, which can guide clinical decision-making regarding pre-transplantation risk and post-transplantation monitoring. This thesis should also stimulate future research and clinical trials of novel treatments in membranous nephropathy, which has the potential to reveal more effective and safer treatment options for this complex disease.

Authorship attribution statement

I undertook this thesis as a full-time student at the Centre for Kidney Research, The Children's Hospital at Westmead, under the supervision of Professor Stephen Alexander, Dr Yuan Min Wang, Dr Karen Keung and Dr Min Hu.

The thesis is presented as a combination of traditional chapters (Chapter 1, 6 and 7) and publications (Chapter 2 and 3). The manuscripts for Chapters 4 and 5 are under submission.

I, Edmund Chung, am responsible for developing the research methodology in liaison with my supervisors, conducting the research experiments, analysing and interpreting the data, and drafting and revising both manuscripts and the thesis.

For chapters 1 and 7, I was responsible for the concepts, review of literature, synthesis of findings, drafting and revision of the chapters. For chapters 2 to 6, I was responsible for concept development, developing the research proposals, selection of research methods, data analysis, interpretation of results, drafting and revision of manuscripts for publication. Data from chapter 2 was obtained from the Australian and New Zealand Dialysis and Transplant registry, which had recruited and published results prior to the commencement of my PhD candidature. Studies were approved by the Animal Ethics Committee at Western Sydney Local Health District and the Human Research Ethics Committee at the Sydney Children's Hospital Network.

Supervisor statement

As supervisor for the candidature upon which this thesis is based, I can confirm that the authorship attribution statements above are correct.

Prof Stephen Inglis Alexander

17th October 2024

List of included publications arising from this thesis

Location in thesis	Status	Details
Chapter 2	Published	**Chung EYM**, Wang YM, Keung K, Hu M, McCarthy H, Wong G, Kairaitis L, Bose B, Harris DCH and Alexander SI. Membranous nephropathy: Clearer pathology and mechanisms identify potential strategies for treatment. *Front Immunol*. 2022;13:1036249. doi: 10.3389/fimmu.2022.1036249
Chapter 3	Published	**Chung EYM**, Blazek K, Teixeira-Pinto A, Sharma A, Kim S, Lin Y, Keung K, Bose B, Kairaitis L, McCarthy H, Ronco P, Alexander SI, and Wong G. Predictive models for recurrent membranous nephropathy after kidney transplantation. *Transplant Direct*. 2022; 8(9): e1357. doi: 10.1097/TXD.0000000000001357
Chapter 4	Manuscript under submission	**Chung EYM**, Wang YM, Shaw K, Ronning E, Wang Y, Zhang GY, Hu M, Keung K, McCarthy H, Harris DCH and Alexander SI. T cell costimulatory blockade ameliorates experimental membranous nephropathy potentially through T-helper 17 cell suppression in the kidney. [Manuscript under submission]
Chapter 5	Manuscript under submission	**Chung EYM**, Wang YM, Shaw K, Ronning E, Wang Y, Zhang GY, Hu M, Keung K, McCarthy H, Harris DCH and Alexander SI. $CD8^+$ regulatory T cells induced by peptide vaccination ameliorates

experimental model of membranous nephropathy**.**

[Manuscript under submission]

Conferences and presentations during PhD candidature

2021 **Chung EYM**, Blazek K, Teixeira-Pinto A, Sharma A, Kim S, Lin Y, Keung K, Bose B, Kairaitis L, McCarthy H, Ronco P, Alexander SI, and Wong G. Association between recipient-donor HLA genotypes and recurrent membranous nephropathy after kidney transplantation. *American Society of Nephrology Kidney Week*, USA. Online.

2022 **Chung EYM**, Blazek K, Teixeira-Pinto A, Sharma A, Kim S, Lin Y, Keung K, Bose B, Kairaitis L, McCarthy H, Ronco P, Alexander SI, and Wong G. Predictive factors for recurrent membranous nephropathy after kidney transplantation. *Transplantation Society of Australia and New Zealand Annual Scientific Meeting*, Adelaide, SA, Australia

2022 **Chung EYM**, Wang YM, Shaw K, Ronning E, Zhang GY, Hu M, Keung K, McCarthy H, Harris DCH and Alexander SI. T cell costimulatory blockade with CTLA4-Ig ameliorates Heymann nephritis via Th17 suppression in the kidney independent of autoantibody production. *Australia and New Zealand Society of Nephrology Annual Scientific Meeting*, Sydney, NSW, Australia.

2023 **Chung EYM**, Wang YM, Shaw K, Ronning E, Wang Y, Zhang GY, Hu M, Keung K, McCarthy H, Harris DCH and Alexander SI. $CD8^+$ regulatory T cells induced by peptide vaccination ameliorates experimental model of membranous nephropathy (Finalist for Young Investigator Award). *Australia and New Zealand Society of Nephrology Annual Scientific Meeting*, Christchurch, New Zealand.

2024 **Chung EYM**, Gowrishankar K, Gore S, Tan A, Du S, Shaw K, Halpin J, Wang YM, Keung K, McCarthy HJ, Micklethwaite K, Harris DC and Alexander SI. BAFF-expressing chimeric antigen receptor T-cells specifically eliminate B-cells *in vitro*. *Australia and New Zealand Society of Nephrology Annual Scientific Meeting*, Adelaide, Australia.

Acknowledgements

I gratefully acknowledge the guidance and support of my supervisors. I thank Prof Stephen Alexander for his supervision, mentorship, warmth, support, and generosity with his time. I thank Dr Yuan Min Wang for sharing her expertise in core laboratory protocols, patience in teaching me, and support. I thank Dr Karen Keung for her advice, support, mentorship, and guidance in both my research and clinical career. I thank Dr Min Hu for her advice, support, and sharing her expertise in core laboratory protocols.

My colleagues at The Centre for Kidney Research and Children's Cancer Research Unit at The Children's Hospital at Westmead, and at the Westmead Institute for Medical Research have provided invaluable help and support. I am especially grateful to Prof Germaine Wong, Dr Katrina Blazek, Dr Ankit Sharma and Prof Armando Teixeira-Pinto for sharing their statistical expertise, to Dr Ya Wang and Dr Li Ma for sharing their histological expertise, to Dr Edwin Lau for his flow cytometry expertise, and to Dr Kavitha Gowrishankar, A/Prof Kenneth Micklethwaite, Dr Karli Shaw, Ms Sayali Gore, Ms Samantha Du, Dr Amanda Tan and Dr Joshua Halpin for sharing their expertise in cell culture and chimeric antigen receptor T cell protocols. I thank all the co-authors who contributed to works comprising this thesis.

I thank the National Health and Medical Research Council who supported my PhD candidature through their Postgraduate Research Scholarship.

I wish to thank my family (Angelica, Celeste, Luke, Ivy, Tim, and Clara) for their endless love and support. I thank God for this opportunity to pursue a PhD in an area I am passionate in, surrounding me with a team of caring, patient, and knowledgeable researchers, and for the skills and relationships I have developed, which I hope to apply to improve the lives of people with kidney disease.

Table of Contents

Abbreviations

ABBA: Anti brush border antibody

AHN: Active Heymann nephritis

ANCA: Anti-neutrophil cytoplasmic antibody

ANOVA: Analysis of variance

ANZDATA: Australia and New Zealand Dialysis and Transplant

APC: Antigen-presenting cells

APRIL: A proliferation-inducing ligand

AR: Aldose reductase

AUC-ROC: Area under the receiver operating characteristic curve

BAFF: B-cell activating factor

BAFF-R: B-cell activating factor receptor

Bcl6: B-cell lymphoma 6

BCMA: B cell maturation antigen

BCR: B cell receptor

BIM: BCL2-interacting mediator of cell death

Blimp1: B lymphocyte-induced maturation protein 1

Bregs: Regulatory B cells

BSA: Bovine serum albumin

C3aR: Complement 3a receptor

CAAR: Chimeric autoantigen receptor

CAR: Chimeric antigen receptor

CCL20: C-C chemokine ligand 20

CCR6: C-C chemokine receptor 6

cDNA: Complementary DNA

CDR-H3: Third complementarity-determining region of the heavy chain

CFA: Complete Freund's adjuvant

CFH: Complement factor H

CI: confidence interval

CNTN1: Contactin 1

COVID-19: Coronavirus Disease 2019

CpG: Cytosine phosphate guanine

CR1: Complement receptor 1

CTLA4: cytotoxic-T-lymphocyte-associated antigen 4

CTLD: C-type lectin-like domains

CXCL12: CXC motif chemokine ligand 12

DMEM: Dulbecco's Modified Eagle Medium

DNA: Deoxyribonucleic acid

DNMT: DNA methyltransferase

dNTP: Deoxynucleotide triphosphate

DOC: Deoxycholic acid

EAE: Experimental autoimmune encephalomyelitis

ECACC: European Collection of Cell Cultures

E.coli: Escherichia coli

EDTA: Ethylenediaminetetraacetic acid

EF1α: Elongation factor 1-alpha

EGFP: Enhanced green fluorescent protein

ELISA: Enzyme-linked immunosorbent assay

EphA2: EPH receptor A2

E:T: Effector:target

EXT1/EXT2: exostosin 1/exostosin 2

FACS: Fluorescence-activated cell sorting

FAT1: Protocadherin FAT1

FBS: Fetal bovine serum

FDA: Food and Drug Administering

FMNL1: Formin-like 1

Foxp3: Forkhead box P3

GAPDH: Glyceraldehyde 3-phosphate dehydrogenase

GBM: Glomerular basement membrane

GFP: Green fluorescent protein

GWAS: Genome-wide association studies

HEK: Human embryonic kidney

HIV: Human immunodeficiency virus

HLA: Human leukocyte antigen

HN: Heymann nephritis

HTRA1: High temperature requirement A serine peptidase 1

IFA: Incomplete Freud's Adjuvant

IFN: Interferon

IgG: Immunoglobulin G

IL: Interleukin

IQR: interquartile range

IRF4: Interferon regulatory factor 4

JAK: Janus Kinase

KDIGO: Kidney Disease: Improving Global Outcomes

LAG3: Lymphocyte activation gene 3

LASSO: Least Absolute Shrinkage and Selection Operator

LB: Luria-Bertani

LRP2: Low-density lipoprotein receptor-related protein 2

MASP: MBL-associated serine protease

MBL: Mannan-binding lectin

MCP-1: Monocyte chemoattractant protein-1

MGB: Minor groove binder

MLV: Murine leukaemia virus

MN: Membranous nephropathy

MOI: Multiplicity of infection

mRNA: messenger RNA

mTOR: Mammalian target of rapamycin

NCAM1: Neural cell adhesion molecule 1

NELL1: Neural epidermal growth factor-like 1 protein

NEP/CD10: Neutral endopeptidase

NFKB: Nuclear factor-kappa-B

NFQ: Non-fluorescent quencher

NTNG1: Netrin G1

PAS: Periodic Acid-Schiff

PBMC: Peripheral blood mononuclear cells

PBS: Phosphate-buffered saline

PBX2: Pre-B-cell leukemia transcription factor 2

PCDH7: Protocadherin 7

PCR: Polymerase chain reaction

PD1: Programmed death 1

PHN: Passive Heymann nephritis

PLA2R: M-type phospholipase A2 receptor 1

PMN: Primary membranous nephropathy

PNA: Peanut agglutinin

PNPP: P-nitrophenyl phosphate

PTPRB: Protein Tyrosine Phosphatase Receptor Type B

RAG: Recombination activating gene

RANTES: Regulated upon activation normal T-cell expressed and secreted

RAP: Receptor associated protein

Rh-α3NC1: Recombinant human non-collagenous domain 1 of α3(IV) collagen

RNA: Ribonucleic acid

ROR: RAR-related orphan nuclear receptor

SD: Standard deviation

Sema3B: Semaphorin 3B

SLE: Systematic lupus erythematosus

SNP: Single nucleotide polymorphism

SOC: Super optimal medium with catabolic repressor

SOD2: Superoxide dismutase 2

STAT3: Signal transducer and activator of transcription 3

TACI: Transmembrane activator and cyclophilin ligand interactor

TAE: Tris-acetate-ethylenediaminetetraacetic acid

TAP: Transporter associated with antigen processing

Tbet: T-box transcription factor

Tcm: Central memory T cell

TCR: T cell receptor

Tem: Effector memory T cell

Terma: Terminally differentiated effector memory re-expressing CD45RA T cell

TET: Tet methylcytosine dioxygenase

Tfh: T follicular helper

Tfr: T follicular regulatory

TGF-β: Transforming growth factor-β

TGFBR3: Transforming growth factor-β receptor 3

Th: T helper

THSD7A: Thrombospondin type-1 domain-containing protein 7A

Tim3: T cell immunoglobulin and mucin domain-containing protein 3

TNF: Tumour necrosis factor

Tregs: Regulatory T cells

TRIPOD: Transparent Reporting of a multivariable prediction model for Individual Prognosis or Diagnosis

Tscm: Stem-like central memory T cell

ULK1: Unc-51 like autophagy activating kinase 1

UV: Ultraviolet

VCN: Vector copy number

VDJ: Variable, Diversity, Joining gene segments

XBP1: X-box binding protein 1

1. Introduction

1.1 Rationale of the thesis

Primary membranous nephropathy is an autoimmune kidney disease characterised by autoantibody formation against podocyte antigens, which cause glomerular injury, nephrotic syndrome, progressive kidney impairment and kidney failure. It is the most common cause of primary nephrotic syndrome in Caucasian adults with an annual incidence of around 10 per million and predominantly affects men aged 50-60 years.[1] Despite spontaneous remission occurring in 20-30%, left untreated around 30-40% of patients progress to kidney failure and of those unresponsive to treatment, 50% progress to kidney failure within 10 years.[1-3] Those who are unresponsive to treatment tend to have significant proteinuria and persistent nephrotic syndrome, which carries an increased risk of cardiovascular disease, up to 50% incidence of thromboembolism, and up to 42% incidence of death.[2] Despite existing treatments, primary membranous nephropathy remains the second and third leading cause of kidney failure due to glomerulonephritis in the USA and Europe respectively.[4] This reflects the incurable relapsing nature of primary membranous nephropathy, which is associated with a 25-50% relapse rate after treatments induce disease remission.[5-8] Furthermore, after kidney transplantation, the preferred treatment for kidney failure, membranous nephropathy recurs in 35-50% of patients and is associated with a 50% risk of allograft loss after 5 years, which highlights the need for better treatments for primary membranous nephropathy.[9-11]

Current treatments for primary membranous nephropathy broadly suppress the immune system and are incompletely effective and associated with significant adverse effects. The Kidney Disease: Improving Global Outcomes (KDIGO) Clinical Practice Guideline for the Management of Glomerular Diseases recommends three potential treatments for primary

membranous nephropathy: 1. Cyclophosphamide and corticosteroids; 2. Calcineurin inhibitors; or 3. Rituximab.[12] Combination cyclophosphamide and corticosteroids is the only treatment regimen proven to reduce the risk the long-term risk of kidney failure but is associated with increased risk of infertility, infection, and cancer.[7, 13] Calcineurin inhibitors such as cyclosporin induce partial disease remission but are associated with disease relapse in 40% when weaned and prolonged use results in hypertension, hypercholesterolaemia, diabetes mellitus and decline in kidney function.[5] More recently, rituximab, a monoclonal antibody against CD20 on B cells, has been used however it failed to induce complete or partial disease remission in 40% of patients.[6] While rituximab is generally well-tolerated in the short-term, it impairs vaccine responses, which is relevant in light of the recent Coronavirus Disease 2019 (COVID-19) global pandemic where vaccination prevented severe disease and death.[14] In the long-term, rituximab is associated with hypogammaglobulinaemia and subsequent infection risk.[15]

Over the past two decades, tremendous progress has been made in our understanding of the immunopathogenesis of primary membranous nephropathy, which has provided insights into potential novel therapeutic targets. Phospholipase A2 receptor (PLA2R) was discovered in 2009 as the main podocyte antigen targeted by autoantibodies in 70% of patients with primary membranous nephropathy.[16] Since then, over 20 antigens have been associated with PLA2R-negative membranous nephropathy, though apart from thrombospondin type-1 domain-containing protein 7A (THSD7A), the pathogenicity of other implicated antigens remains to be determined.[17-19] However, despite the discovery of PLA2R as the main disease autoantigen revolutionising the management of PLA2R-associated membranous nephropathy, from providing a non-invasive method of diagnosis in certain patients and foregoing the need for a kidney biopsy, to allowing the detection of immunological remission that precedes clinical remission by 18 months (facilitating earlier and safe tapering of treatment), it has not translated into improved therapeutic strategies.[1, 20] Genome-wide association studies (GWAS) of primary

membranous nephropathy have identified key immunological drivers of disease such as genetic variants in the PLA2R gene and in human leukocyte antigens (HLA) class II on antigen-presenting cells, suggesting a role for $CD4^+$ T cells in disease pathogenesis.[21, 22] This also suggests alterations in the PLA2R protein structure or PLA2R gene expression leads to a loss of immune tolerance in individuals carrying risk HLA alleles and subsequent autoimmunity and autoantibody production. Therefore, depleting autoantibody-producing cells or promoting immune tolerance through expanding regulatory T cells are attractive therapeutic targets.

While our understanding of the immunology underpinning primary membranous nephropathy has greatly improved, recurrent membranous nephropathy after kidney transplantation remains poorly understood. Accordingly, the KDIGO Clinical Practice Guideline for the Management of Glomerular Diseases do not make any strong recommendations for when and how to treat recurrent membranous nephropathy.[12] Like primary membranous nephropathy, there is an association between recurrent membranous nephropathy and class II HLA risk variants, though only when present in the kidney donor rather than kidney transplant recipient.[23] Another study had conflicting findings, demonstrating an association between recurrent membranous nephropathy and class I HLA-A3 in the kidney transplant recipient, though both studies were limited by small sample sizes.[24] With the rise of machine learning to generate novel insights from large datasets,[25] we hypothesised that machine learning algorithms have the potential to build prediction models in the Australia and New Zealand Dialysis and Transplant (ANZDATA) registry to identify predictive factors of and patients at high risk for recurrent membranous nephropathy (Aim 1).

The focus on rituximab in recent clinical trials of primary membranous nephropathy reflects the increased recognition of autoantibody production as central to the immunopathogenesis of disease. However, B cell depletion with rituximab remains incompletely ineffective, potentially due to T cells and plasma cells, neither of which are depleted by rituximab. T cells,

in particular T follicular helper (Tfh) cells, are crucial to the development and maturation of B cells into memory B cells and plasma cells. In germinal centres, Tfh cells provide help for B cells to undergo somatic hypermutation and immunoglobulin class switching, which is essential for the development of high affinity immunoglobulin G (IgG) which characterise primary membranous nephropathy.[26, 27] Furthermore, T cells also facilitate B cell differentiation into plasma cells, which produce high affinity IgG independent of T cell help.[28] While plasma cell depletion can be readily achieved using a proteasome inhibitor such as bortezomib, prolonged use is associated with significant toxicity such as infection risk and neurotoxicity. In kidney transplantation, T cell costimulatory blockade with belatacept has been shown to reduce antibodies directed at the transplant (donor-specific antibodies) and preserve kidney function compared to calcineurin inhibitors.[29] Therefore, we hypothesised that a short-course of bortezomib to initially deplete plasma cells followed by T cell costimulatory blockade with cytotoxic-T-lymphocyte-associated antigen 4 (CTLA4)-Ig to prevent B cell maturation may effectively deplete autoantibody production in Heymann nephritis, a rat model of membranous nephropathy (Aim 2).

Immune tolerance is mediated by regulatory T cells, of which the two main subsets are $CD4^+$ regulatory T cells and $CD8^+$ regulatory T cells. While the mechanisms by which $CD4^+$ regulatory T cells protect against autoimmunity in both animals and humans are better understood, their role in Heymann nephritis remains relatively unclear. Rather, $CD8^+$ regulatory T cells have been demonstrated to protect against Heymann nephritis by eliminating autoreactive $CD4^+$ T cells and reducing autoantibody production.[30, 31] While the precise mechanisms by which $CD8^+$ regulatory T cells protect against autoimmunity are yet to be delineated, they appear to be equally cross-protective when transferred between two mouse models of autoimmunity (type 1 diabetes and multiple sclerosis), suggesting this mechanism is independent of the specific disease antigen.[32] In comparison, antigen specific $CD4^+$ regulatory

T cells exhibit stronger protection against autoimmunity than polyclonal $CD4^+$ regulatory T cells.[33, 34] Recently, specific peptides that expanded $CD8^+$ regulatory T cells and protected mice against experimental multiple sclerosis were reported.[35] Therefore, we hypothesised that immunisation of these same peptides might also expand $CD8^+$ regulatory T cells and protect rats against Heymann nephritis (Aim 3).

While regulatory T cells maintain peripheral immune tolerance against autoreactive T cells, central immune tolerance in primary lymphoid organs (thymus or bone marrow) is maintained in part by negative selection in which autoreactive T and B cells undergo cell death. B-cell activating factor (BAFF) is a cytokine produced by myeloid cells, which is critical for B cell survival and maturation, and has been implicated in the development of autoreactive B cells since excess BAFF overcomes death signals triggered by self-antigens binding to the B-cell receptor during the process of negative selection.[36] The positive correlation between serum BAFF levels and disease activity in primary membranous nephropathy also highlights their likely importance in the development of autoreactive B cells.[37] Chimeric antigen receptor (CAR) T cells are genetically altered T cells that redirect T cell killing towards a target of interest, and most CAR T cell products are directed against CD19 on B cells. While CD19-targeting CAR T cells have been predominantly used for the treatment of B cell leukaemia and lymphomas, more recently they have shown remarkable potency in preliminary data from a case series in refractory autoimmune disease.[38] We hypothesised that CAR T cells expressing BAFF could eliminate B cells that require high levels of BAFF for their survival, which may preferentially eliminate autoreactive B cells and thus deplete autoantibody levels (Aim 4).

1.2 Aims

The primary aim of this thesis is to develop and implement novel treatment strategies to deplete autoantibodies and/or expand regulatory T cells and/or deplete B cells and plasma cells in membranous nephropathy.

The specific objectives of this thesis were to:

(i) Develop prediction models for recurrent membranous nephropathy after kidney transplantation.

(ii) Deplete autoantibody production in Heymann nephritis, a rat model of membranous nephropathy, using CTLA4-Ig with or without bortezomib.

(iii) Expand $CD8^+$ regulatory T cells in Heymann nephritis using peptide vaccination.

(iv) Develop CAR T cells expressing BAFF to specifically eliminate B cells *in vitro*.

1.3 Outline of chapters

This thesis consists of two published papers in peer-reviewed journals (Chapters 2 and 3), two manuscripts under submission (Chapters 4 and 5), a thesis chapter (Chapter 6) and discussion chapter (Chapter 7). Figure 1 illustrates how aims 1 to 4 fit in the development of novel treatments to deplete autoantibodies and/or expand regulatory T cells in primary membranous nephropathy and develop prediction models for recurrent membranous nephropathy after kidney transplantation to facilitate treatment implementation.

Chapter 2 provides a review of our current understanding of the immunopathogenesis of primary membranous nephropathy and how that informs novel therapeutic strategies explored in later chapters. Chapter 3 aims to develop prediction models for recurrent membranous nephropathy after kidney transplantation to identify patients at high risk for recurrent disease to assist treatment implementation and identify predictive factors for recurrent membranous nephropathy, the pathogenesis of which remains poorly understood. Chapter 4 and 5 utilise a

rat model of membranous nephropathy, Heymann nephritis, to test whether CTLA4-Ig with or without bortezomib depletes autoantibodies and whether peptide vaccination expands $CD8^+$ regulatory T cells respectively. Chapter 6 aims to develop CAR T cells expressing BAFF that specifically target B cells *in vitro*, which represents a novel treatment to deplete autoantibody-producing cells in primary membranous nephropathy. Chapter 7 summarises the principal findings of the thesis, the strengths and limitations of each chapter, the implications of the findings for management of primary membranous nephropathy and future research, and the contribution of this thesis to the existing literature on primary membranous nephropathy.

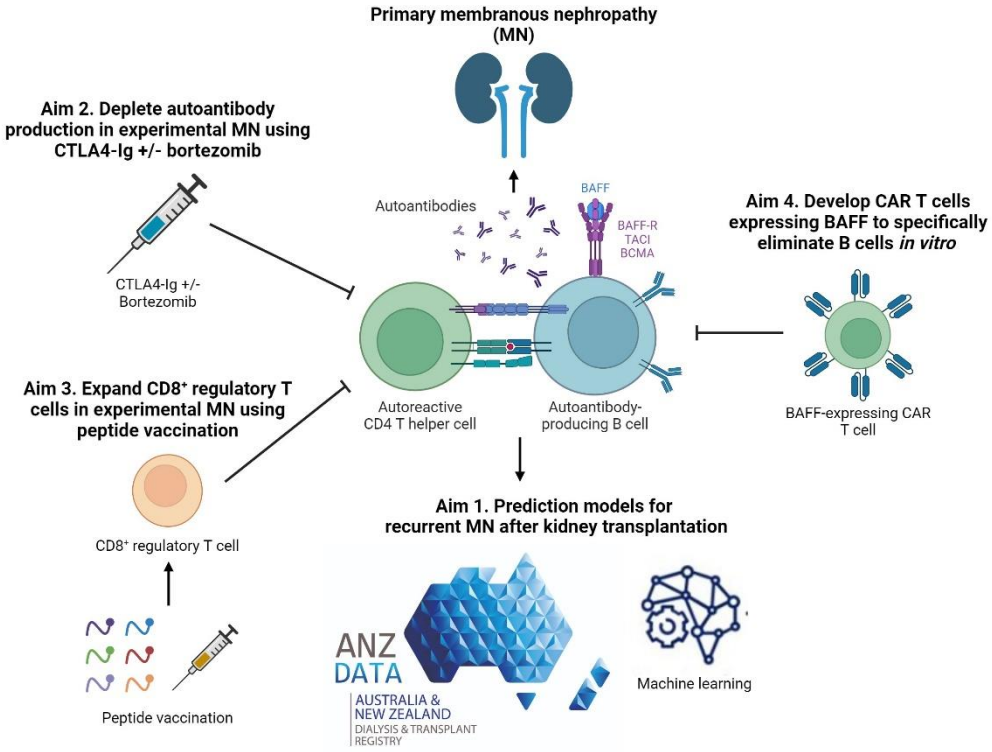

Figure 1. Outline of aims within the development and implementation of novel treatment strategies for primary membranous nephropathy.

1.4 References

1. Ronco P, Beck L, Debiec H, et al. Membranous nephropathy. Nat Rev Dis Primers. 2021;7(1):69.

2. Fervenza FC, Sethi S, Specks U. Idiopathic membranous nephropathy: diagnosis and treatment. Clin J Am Soc Nephrol. 2008;3(3):905-19.

3. Troyanov S, Wall CA, Miller JA, et al. Idiopathic membranous nephropathy: definition and relevance of a partial remission. Kidney Int. 2004;66(3):1199-205.

4. Maisonneuve P, Agodoa L, Gellert R, et al. Distribution of primary renal diseases leading to end-stage renal failure in the United States, Europe, and Australia/New Zealand: results from an international comparative study. Am J Kidney Dis. 2000;35(1):157-65.

5. Cattran DC, Appel GB, Hebert LA, et al. Cyclosporine in patients with steroid-resistant membranous nephropathy: a randomized trial. Kidney Int. 2001;59(4):1484-90.

6. Fervenza FC, Appel GB, Barbour SJ, et al. Rituximab or Cyclosporine in the Treatment of Membranous Nephropathy. N Engl J Med. 2019;381(1):36-46.

7. Jha V, Ganguli A, Saha TK, et al. A randomized, controlled trial of steroids and cyclophosphamide in adults with nephrotic syndrome caused by idiopathic membranous nephropathy. J Am Soc Nephrol. 2007;18(6):1899-904.

8. Ponticelli C, Altieri P, Scolari F, et al. A randomized study comparing methylprednisolone plus chlorambucil versus methylprednisolone plus cyclophosphamide in idiopathic membranous nephropathy. J Am Soc Nephrol. 1998;9(3):444-50.

9. Dabade TS, Grande JP, Norby SM, et al. Recurrent idiopathic membranous nephropathy after kidney transplantation: a surveillance biopsy study. Am J Transplant. 2008;8(6):1318-22.

10. Grupper A, Cornell LD, Fervenza FC, et al. Recurrent Membranous Nephropathy After Kidney Transplantation: Treatment and Long-Term Implications. Transplantation. 2016;100(12):2710-6.

11. Moroni G, Gallelli B, Quaglini S, et al. Long-term outcome of renal transplantation in patients with idiopathic membranous glomerulonephritis (MN). Nephrol Dial Transplant. 2010;25(10):3408-15.

12. Rovin BH, Adler SG, Barratt J, et al. Executive summary of the KDIGO 2021 Guideline for the Management of Glomerular Diseases. Kidney Int. 2021;100(4):753-79.

13. Ponticelli C, Zucchelli P, Passerini P, et al. A 10-year follow-up of a randomized study with methylprednisolone and chlorambucil in membranous nephropathy. Kidney Int. 1995;48(5):1600-4.

14. Watson OJ, Barnsley G, Toor J, et al. Global impact of the first year of COVID-19 vaccination: a mathematical modelling study. Lancet Infect Dis. 2022;22(9):1293-302.

15. Tieu J, Smith RM, Gopaluni S, et al. Rituximab Associated Hypogammaglobulinemia in Autoimmune Disease. Front Immunol. 2021;12:671503.

16. Beck LH, Jr., Bonegio RG, Lambeau G, et al. M-type phospholipase A2 receptor as target antigen in idiopathic membranous nephropathy. N Engl J Med. 2009;361(1):11-21.

17. Avasare R, Andeen N, Beck L. Novel Antigens and Clinical Updates in Membranous Nephropathy. Annu Rev Med. 2024;75:219-332.

18. Tomas NM, Hoxha E, Reinicke AT, et al. Autoantibodies against thrombospondin type 1 domain-containing 7A induce membranous nephropathy. J Clin Invest. 2016;126(7):2519-32.

19. Tomas NM, Meyer-Schwesinger C, von Spiegel H, et al. A Heterologous Model of Thrombospondin Type 1 Domain-Containing 7A-Associated Membranous Nephropathy. J Am Soc Nephrol. 2017;28(11):3262-77.

20. Lerner GB, Virmani S, Henderson JM, et al. A conceptual framework linking immunology, pathology, and clinical features in primary membranous nephropathy. Kidney Int. 2021;100(2):289-300.

21. Stanescu HC, Arcos-Burgos M, Medlar A, et al. Risk HLA-DQA1 and PLA(2)R1 alleles in idiopathic membranous nephropathy. N Engl J Med. 2011;364(7):616-26.

22. Xie J, Liu L, Mladkova N, et al. The genetic architecture of membranous nephropathy and its potential to improve non-invasive diagnosis. Nat Commun. 2020;11(1):1600.

23. Berchtold L, Letouzé E, Alexander MP, et al. Corrigendum to Berchtold L, Letouzé E, Alexander MP, et al. HLA-D and PLA2R1 risk alleles associate with recurrent primary membranous nephropathy in kidney transplant recipients. Kidney Int. 2021;99:671-685. Kidney Int. 2021;100(1):243.

24. Batal I, Vasilescu ER, Dadhania DM, et al. Association of HLA Typing and Alloimmunity With Posttransplantation Membranous Nephropathy: A Multicenter Case Series. Am J Kidney Dis. 2020;76(3):374-83.

25. Connor KL, O'Sullivan ED, Marson LP, et al. The Future Role of Machine Learning in Clinical Transplantation. Transplantation. 2021;105(4):723-35.

26. Fresquet M, Jowitt TA, Gummadova J, et al. Identification of a major epitope recognized by PLA2R autoantibodies in primary membranous nephropathy. J Am Soc Nephrol. 2015;26(2):302-13.

27. van de Logt AE, Fresquet M, Wetzels JF, et al. The anti-PLA2R antibody in membranous nephropathy: what we know and what remains a decade after its discovery. Kidney Int. 2019;96(6):1292-302.

28. Crotty S. A brief history of T cell help to B cells. Nat Rev Immunol. 2015;15(3):185-9.

29. Vincenti F, Rostaing L, Grinyo J, et al. Belatacept and Long-Term Outcomes in Kidney Transplantation. N Engl J Med. 2016;374(4):333-43.

30. de Heer E, Daha MR, Burgers J, et al. Reestablishment of self tolerance by suppressor T-cells after active Heymann's nephritis. Cell Immunol. 1986;98(1):28-33.

31. Wang YM, Zhang GY, Hu M, et al. CD8+ regulatory T cells induced by T cell vaccination protect against autoimmune nephritis. J Am Soc Nephrol. 2012;23(6):1058-67.

32. Wu Y, Zheng Z, Jiang Y, et al. The specificity of T cell regulation that enables self-nonself discrimination in the periphery. Proc Natl Acad Sci U S A. 2009;106(2):534-9.

33. Tang Q, Henriksen KJ, Bi M, et al. In vitro-expanded antigen-specific regulatory T cells suppress autoimmune diabetes. J Exp Med. 2004;199(11):1455-65.

34. Tarbell KV, Yamazaki S, Olson K, et al. CD25+ CD4+ T cells, expanded with dendritic cells presenting a single autoantigenic peptide, suppress autoimmune diabetes. J Exp Med. 2004;199(11):1467-77.

35. Saligrama N, Zhao F, Sikora MJ, et al. Opposing T cell responses in experimental autoimmune encephalomyelitis. Nature. 2019;572(7770):481-7.

36. Mackay F, Browning JL. BAFF: a fundamental survival factor for B cells. Nat Rev Immunol. 2002;2(7):465-75.

37. Netti GS, Infante B, Spadaccino F, et al. Serum Levels of BAFF and APRIL Predict Clinical Response in Anti-PLA2R-Positive Primary Membranous Nephropathy. J Immunol Res. 2019;2019:8483650.

38. Müller F, Taubmann J, Bucci L, et al. CD19 CAR T-Cell Therapy in Autoimmune Disease - A Case Series with Follow-up. N Engl J Med. 2024;390(8):687-700.

2.Background

2.1 Overview

Primary membranous nephropathy (PMN) is one of the common causes of adult-onset nephrotic syndrome and is characterized by autoantibodies against podocyte antigens causing *in situ* immune complex deposition. Much of our understanding of the disease mechanisms underpinning this kidney-limited autoimmune disease originally came from studies of Heymann nephritis, a rat model of PMN, where autoantibodies against megalin produced a similar disease phenotype though megalin is not implicated in human disease. In PMN, the major target antigen was identified to be M-type phospholipase A2 receptor 1 (PLA2R) in 2009. Further utilization of mass spectrometry on immunoprecipitated glomerular extracts and laser microdissected glomeruli has allowed the rapid discovery of other antigens (thrombospondin type-1 domain-containing protein 7A, neural epidermal growth factor-like 1 protein, semaphorin 3B, protocadherin 7, high temperature requirement A serine peptidase 1, netrin G1) targeted by autoantibodies in PMN. Despite these major advances in our understanding of the pathophysiology of PMN, treatments remain non-specific, often ineffective, or toxic. In this review, we summarize our current understanding of the immune mechanisms driving PMN from animal models and clinical studies, and the implications on the development of future targeted therapeutic strategies.

2.2 Introduction

Primary membranous nephropathy (PMN) is one of the commonest causes of adult-onset nephrotic syndrome with an incidence of 12 cases per million per year.[1] It is a kidney-limited autoimmune disease characterized by *in situ* formation of subepithelial glomerular immune deposits containing immunoglobulin G (IgG) autoantibodies and complement.[2] While spontaneous disease remission occurs in around 32% of patients, approximately a third ultimately progress to kidney failure needing dialysis or kidney transplantation.[1] The podocyte antigens responsible for eliciting an autoimmune response in PMN remained elusive until 2009 when M-type phospholipase A2 receptor 1 (PLA2R) was discovered, followed by thrombospondin type-1 domain-containing protein 7A (THSD7A) in 2014.[3, 4] These discoveries improved the diagnosis of PMN with anti-PLA2R autoantibody testing having a specificity of 99%, which together with the kidney biopsy light microscopy findings of subepithelial "spikes" of the glomerular basement membrane (GBM) on silver methenamine stain, immunofluorescence finding of granular deposits of IgG along the glomerular capillary wall, and electron microscopy finding of exclusive subepithelial localization of electron-dense deposits, differentiate PMN from other forms of nephrotic syndrome.[1, 5] However, despite this improved understanding, treatments for PMN remain non-specific. Cytotoxic therapy (chlorambucil or cyclophosphamide) plus glucocorticoids lower the 10-year incidence of kidney failure to approximately 10% (compared to 40% in those receiving supportive treatment) but is associated with significant toxicity such as infertility, infection and malignancy.[6-10] Calcineurin inhibitors have proven short-term efficacy though are limited by high relapse rate of 40% and long-term nephrotoxicity.[11] The anti-CD20 monoclonal antibody rituximab targeting B cells is the most targeted treatment to date but may not eliminate autoreactive B cells due to changes in the CD20 antigen, does not eliminate high-affinity antibody-producing plasma cells that do not express CD20, and fails to induce complete or

partial remission in up to 40% of patients.[12, 13] In comparing these existing treatments, a recent trial found cyclophosphamide plus glucocorticoids to be superior to calcineurin inhibitors plus single-dose rituximab (total 1g) though there was a higher anti-PLA2R autoantibody titre at baseline in the calcineurin inhibitor/rituximab group, which together with the low dose of rituximab used, may have contributed to worse outcomes.[14] In contrast, rituximab (total 3g) was superior to calcineurin inhibitors,[12] but rituximab (total 2g) was comparable to cyclophosphamide plus glucocorticoids.[15] Lastly, recurrent membranous nephropathy (MN) after kidney transplantation also occurs in 35-50% of patients and accounts for 50% allograft loss 5 years after diagnosis, highlighting the unmet need for targeted treatments in PMN.[16-19]

Antigen-independent treatments targeting autoantibody production is attractive and feasible given the multitude of disease antigens implicated in PMN particularly with improved antibodies targeting plasma cells. Targeted treatments against antigen-specific B cells or antigen-specific T cells helpers directed against antigens linked to PMN, using chimeric antigen receptor (CAR) T cells, chimeric autoantigen receptor expressing (CAAR) T cells, or CAR regulatory T cells (Tregs) to eliminate or suppress antigen-specific effectors are also conceivable. However, these experimental treatments remain untested in human autoimmune disease and rigorous testing in animal models of PMN is required.[20] In this review, we compare the immune mechanisms driving PMN and associated animal models, and implications for evaluating novel targeted therapeutics.

2.3 Pathological Features in Animal Models of Membranous Nephropathy

2.3.1 Heymann nephritis

Heymann et al described active Heymann nephritis (AHN) in 1959, where immunization of the proximal tubular antigen Fx1A with complete Freund's adjuvant in Lewis rats caused development of anti-Fx1A antibodies and *in situ* glomerular subepithelial immune complex formation after 4 weeks, and proteinuria after 8-10 weeks.[21] Passive Heymann nephritis (PHN) is a more limited model induced by administration of sheep anti-rat Fx1A antibodies with cell- and blood-free perfusion to prevent immune complex formation in the circulation.[22, 23] While PHN was widely used to study the effector mechanisms caused by glomerular IgG deposition, it does not recapitulate autologous formation of podocyte autoantibodies seen in AHN and which leads to PMN.

2.3.2 Passive administration of anti-PLA2R or anti-THSD7A antibodies in mice

The identification of antigens implicated in PMN has led to the development of mouse models where passive administration of anti-PLA2R and anti-THSD7A antibodies into transgenic mice with murine full-length PLA2R on podocytes and wild-type mice respectively were able to induce similar disease to PMN with subepithelial glomerular IgG deposition, C3 deposition and proteinuria.[24-27]

2.3.3 Transgenic mice expressing human PLA2R specifically on podocytes

Recently, Tomas et al have described transgenic knock-in mice expressing human PLA2R specifically on podocytes. These mice spontaneously developed anti-human PLA2R autoantibodies after 3 weeks, nephrotic syndrome with glomerular deposition of murine IgG1 (equivalent of human IgG4) and complement activation after 4 weeks, and glomerular subepithelial electron-dense deposits after 6 weeks.[28] Overall, this model faithfully recapitulates human PMN.

2.3.4 Passive administration of anti-aminopeptidase A, anti-dipeptidyl peptidase IV, or anti-podocyte antibodies in rats or mice

Passive administration of antibodies against mouse aminopeptidase A,[29, 30] dipeptidyl peptidase IV,[31] and anti-mouse podocyte antibodies were also able to induce glomerular IgG deposition with proteinuria but without complement activation, unlike human PMN.[32, 33] Furthermore, these antigens are not implicated in human PMN.

2.3.5 Exogenous antigen deposition onto the glomerular basement membrane in rabbits or mice

Intravenous injections of cationic bovine serum albumin (BSA) and immunization of recombinant human non-collagenous domain 1 of α3(IV) collagen (rh-α3NC1) both produced significant albuminuria and subepithelial deposits of IgG and C3.[34, 35] However, glomerular deposition of exogenous antigen (BSA and rh-α3NC1) in these models significantly differs from the pathogenesis of human PMN.[35]

2.4 Pathological Features in Human Membranous Nephropathy

Human PMN is characterized by heterogeneous presentation and clinical course with around a third of patients undergoing spontaneous remission, a third experiencing persistent proteinuria, and a third progressing to kidney failure.[36] While light microscopy findings on kidney biopsy also exhibit some variability, ranging from a normal appearance early in disease to thickened GBM as disease progresses, granular deposition of IgG and C3 in glomeruli on immunofluorescence and electron-dense subepithelial deposits on electron microscopy are seen at any stage of disease.[1, 36]

2.5 Antigens and Autoantibodies in Animal Models of Membranous Nephropathy

2.5.1 Heymann nephritis

The pathogenic antigen in Fx1A was identified as a 330-kDa glycoprotein called megalin, which is a low-density lipoprotein receptor involved in protein endocytosis and transcytosis (Table 1).[37-40] Another autoantibody in AHN was subsequently identified targeting the 44-kDa receptor associated protein (RAP), which acts as an endoplasmic reticulum chaperone for megalin.[39]

AHN is characterized by anti-Fx1A autoantibodies without circulating IgG subclass predominance but induce proteinuria via complement-fixing rat IgG2b (equivalent to human IgG1) (Figure 1A.1).[41-43] The main pathogenic epitope on megalin at its N-terminal domain is glycosylation- and conformation-dependent though epitope spreading occurs, similar to PMN, whereby the immune response to a disease antigen may extend to non-cross-reactive peptide sequences on the same antigen (intramolecular spreading) or adjacent antigens (intermolecular spreading) over time.[44, 45] Accordingly, anti-RAP autoantibodies likely represent intermolecular epitope spreading due to the association of RAP with megalin (Figure 1A.2).

2.5.2 Passive administration of anti-PLA2R or anti-THSD7A antibodies in mice

For the passive administration of anti-PLA2R antibodies, transgenic mice expressing murine PLA2R were required due to a lack of PLA2R expression normally on murine podocytes.[24] Murine PLA2R has 72% sequence homology with human PLA2R and adoptive transfer of human anti-PLA2R autoantibodies could not bind murine PLA2R. Instead disease induction

required transfer of rabbit anti-PLA2R antibodies.[24] Therefore, the pathogenicity of human anti-PLA2R antibodies remains to be definitively proven *in vivo*.

In contrast, murine podocytes normally express THSD7A. Interestingly, human sera containing anti-THSD7A antibodies but not purified human anti-THSD7A antibodies activated the lectin complement pathway on murine podocytes and caused oxidative stress, disruption of nephrin, and rearrangement of the podocyte actin cytoskeleton.[25-27] In comparison, rabbit anti-THSD7A antibodies (with or without sera) induced significant proteinuria in the absence of complement activation.[25, 27] These discrepant results could be related to lower amounts of injected purified human antibody, alteration of autoantibodies when purified using acid-elution or the presence of other proteins within human sera required for complement activation. Furthermore, it is unclear whether generation of rabbit anti-PLA2R and anti-THSD7A antibodies are predominantly of IgG4 subclass (like their human counterparts) and therefore whether disease pathophysiology caused by passive administration of these antibodies is homologous to human PMN.[24, 27]

2.5.3 Transgenic mice expressing human PLA2R specifically on podocytes

Full length human PLA2R was expressed on podocytes of these mice and anti-human PLA2R antibodies recognized the cysteine-rich domain as well as C-type lectin domains (CTLD) 1, 7 and 8, which are the same epitopes recognized by anti-PLA2R antibodies in patients with PMN.[28, 46-48] Therefore, this represents the ideal model for confirming the pathogenicity of human anti-PLA2R autoantibodies.

2.6 Antigens and Autoantibodies in Human Membranous Nephropathy

While there are many similarities between Heymann nephritis and PMN, they are not homologous primarily due to differences in the disease antigen. Megalin (called low-density lipoprotein receptor-related protein 2 (LRP2) in humans) is 77% homologous between rodents and humans, though human tissue expression is predominantly on proximal tubular brush border and glomerular staining is weak.[40, 49] Accordingly, anti-LRP2 antibodies in humans cause ABBA (anti brush border antibody) disease, characterized by tubular immune deposits with segmental glomerular subepithelial deposits, subnephrotic proteinuria, and kidney failure.[50]

Unlike Heymann nephritis, IgG4 is the predominant IgG subclass in most patients with PMN though IgG1 is predominantly found in neural epidermal growth factor-like 1 protein (NELL1)- and semaphorin 3B (Sema3B)-associated PMN without significant activation of the classical complement pathway based on rare C1q deposition.[51, 52]

2.6.1 PLA2R

PLA2R is the primary disease antigen in 70% of PMN and while the pathogenicity of anti-PLA2R autoantibodies is highly likely due to the strong correlation of antibody titres with disease activity, *in vitro* evidence of podocyte injury caused by anti-PLA2R sera and lectin pathway activation by anti-PLA2R IgG4, definitive *in vivo* evidence of pathogenicity is yet to be confirmed (Figure 1B.1).[3, 53-56] The major epitope targeted by anti-PLA2R antibodies is located at the 31-mers peptide sequence of the cysteine-rich domain of PLA2R (specifically the N-terminal linear stretch VIQSES and C-terminal stretch SVLTLENC regions) with additional antibody epitopes identified at CTLD1, CTLD7 and CTLD8.[46, 48, 57] Epitope spreading from the cysteine-rich domain to the CTLD1 and/or 7 domains occurs in 25-66% of patients over the course of 3 months to 2 years.[58, 59] However, data are inconsistent regarding whether epitope spreading is associated with treatment resistance.[48, 58, 59]

Genome-wide association studies have greatly enhanced our understanding of how self-antigens such as PLA2R trigger an autoimmune response. The risk of PMN was substantially increased in individuals with both single nucleotide polymorphisms (SNP) in class II human leukocyte antigen (HLA-DQA1*0501 in Europeans, -DRB1*1501 in East Asians, and -DRB1*0301 in both ethnicities) on antigen-presenting cells (APC) and SNPs in the PLA2R locus (rs4664308 in Europeans and rs17831251 in both Europeans and East Asians).[60, 61] These non-coding region SNPs were either associated with other SNPs within the PLA2R coding region or an enhancer element resulting in an altered amino acid sequence or increased tissue expression respectively.[61] This may enhance antigen presentation by APCs expressing risk HLA variants to their cognate $CD4^+$ T cell, thereby initiating the process of autoimmunity. *In silico* analysis predicted HLA-DRB1*1501 and HLA-DRB1*0301 preferentially bound to PLA2R peptides in the CTLD1, CTLD7 and between CTLD4 and CTLD5 regions compared to the 31-mers peptide, though experimental validation is required.[62]

In recurrent PLA2R-associated MN after kidney transplantation, detectable anti-PLA2R autoantibody titres pre-transplantation and steroid-free immunosuppression are known risk factors.[16, 63-65] Positive glomerular staining for PLA2R in these cases also suggest the same antigen is implicated in recurrent MN.[64] However, the HLA risk alleles (HLA-DQA1*0501, -DRB1*1501, and -DRB1*0301) associated with PMN were not associated with recurrent MN but rather two non-coding HLA-D SNPs (rs9271550 and rs9271705) and three PLA2R SNPs (rs3828323, rs17830558, and rs3749117)) when present on the donor but not the recipient.[66] Another study found an association between recurrent MN and recipient HLA-A3.[67] Discrepancies between studies may be due to the relatively small sample sizes and different diagnostic criteria for recurrent MN. Overall, the pathogenesis of recurrent MN remains poorly understood and further studies are required.

2.6.2 THSD7A

THSD7A was the second podocyte antigen discovered in PMN, implicated in 10% of PLA2R-negative PMN (Figure 1B.2).[4] THSD7A and PLA2R are structurally similar as are their associated autoantibodies, which are predominantly of IgG4 subclass, activate complement with glomerular C5b-9 staining, bind initially to the immunodominant epitope on the N-terminal domain of their target antigen exclusively in non-reducing conditions, and are associated with epitope-spreading.[4, 25, 47, 68] Contrary to the prevailing paradigm of a single podocyte antigen being targeted in PMN, dual anti-PLA2R and anti-THSD7A antibodies and staining on biopsy has been reported in 1% of cases.[69]

2.6.3 Other antigens implicated in primary membranous nephropathy

Laser microdissection and mass spectrometry on kidney biopsies of PLA2R-negative PMN has led to the discovery of many more disease antigens such as NELL1, Sema3B, protocadherin 7 (PCDH7), high temperature requirement A serine peptidase 1 (HTRA1), and netrin G1 (NTNG1) (Figure 1B.3). These antigens account for less than 10% of PMN and their associated autoantibodies vary in their predominant IgG subclass, ability to activate complement, and the association of their pathogenic epitope with disulfide bonds based on whether autoantibodies were detected under reducing or non-reducing conditions (Table 1).[51, 52, 70-77] Anti-Sema3B autoantibodies correlated with disease activity in a case report of severe pediatric PMN, suggestive of pathogenicity.[78] However, the pathogenicity of other autoantibodies remains to be determined and the mechanism by which these self-antigens trigger an autoimmune response remain unclear. Furthermore, it remains unclear how some of these antigens such as NELL1 and PCDH7 display weak or no staining in normal glomeruli but are implicated in PMN, whereby the subepithelial localization of deposits on electron microscopy in NELL1- and PCDH7-associated MN strongly suggest shedding from podocytes rather than mesangial or endothelial cells. NELL1 and PCDH7 are known to be secretory proteins and highly glycosylated proteins respectively,[79] which may impact their expression under healthy

conditions. However, further research on the expression and localization of these novel antigens in normal podocytes are required. Overall, it is apparent that PMN is not a single disease entity but rather a group of diseases characterized by autoantibodies against different antigens causing kidney-limited autoimmune disease.

2.6.4 Antigens implicated in secondary and neonatal membranous nephropathy

MN podocyte antigens exostosin 1/eoxstosin 2 (EXT1/EXT2), neural cell adhesion molecule 1 (NCAM1), and transforming growth factor-β receptor 3 (TGFBR3) are associated with other autoimmune diseases, especially systematic lupus erythematosus (SLE).[71, 73, 75] In particular, EXT1/EXT2-associated membranous lupus nephritis confers a better prognosis than EXT1/EXT2-negative membranous lupus nephritis.[80] This may be due to EXT1/EXT2-related glycosylation of heparan sulfate, which protects the GBM against immune injury. Contactin 1 (CNTN1) is associated with chronic inflammatory demyelinating polyneuropathy-related MN and protocadherin FAT1 (FAT1) is associated with allogeneic hematopoietic stem cell transplant-related MN.[76, 77]

In contrast, while MN secondary to infections such as hepatitis B have been well described and hypothesized to be due to molecular mimicry, the associated podocyte antigen remains unclear.[81] Evidence of molecular mimicry due to malignancy is more convincing for THSD7A- and NELL1-associated MN. THSD7A was found in tumour and follicular dendritic cells of tumour-infiltrated lymph nodes in separate cases of gallbladder adeno-neuroendocrine carcinoma and endometrial carcinoma[82, 83] Up to 33% of NELL1-associated MN were secondary to malignancy with NELL1 tumour expression demonstrated in 2 cases (invasive ductal carcinoma of the breast and follicular lymphoma).[84] Lastly, neutral endopeptidase (NEP/CD10) is a podocyte antigen implicated in neonatal MN, which is caused by placental

transfer of anti-NEP antibodies to the fetus from NEP-deficient mothers (truncating mutations in the *MME* gene) who undergo alloimmunization during the pregnancy or from previous miscarriages.[85, 86]

2.6.5 Other antigens reported in primary membranous nephropathy

IgG4 against aldose reductase (AR) and superoxide dismutase 2 (SOD2) have also been described in multiple PMN cohorts.[87, 88] However, these antigens are not expressed on the surface of normal podocytes, antibody titres do not correlate with disease activity, and both AR and SOD2 are involved in oxidative stress, a known downstream effect of podocyte injury.[87, 88] Accordingly, *in vitro* and *in vivo* evidence demonstrated podocyte membrane expression of SOD2 increasing with intracellular oxidation and after passive transfer of anti-THSD7A IgG respectively.[27, 87] These data suggest antibodies targeted AR and SOD2 are a secondary phenomenon to autoantibody-mediated podocyte injury exposing neoantigens rather than autoantibodies driving PMN pathogenesis. More recently, autoantibodies against Formin-like 1 (FMNL1) were detected in patients with PMN as well as other forms of glomerular disease (IgA nephropathy and focal segmental glomerulosclerosis), which recognize FMNL1 expression on macrophages.[89] Whether FMNL1 positive macrophages contribute to the pathogenesis of PMN (ie. M1 macrophages) or highlight a reparative role of macrophages (ie. M2 macrophages) in PMN requires further study.

2.7 T and B cell Immunity in Animal Models of Membranous Nephropathy

2.7.1 Heymann nephritis

There is a clear T cell role in Heymann nephritis with $CD4^+$ T cell depletion abolishing IgG and C3 deposition as well as proteinuria, demonstrating the essential role of $CD4^+$ T cell-B cell interaction in autoantibody formation.[90] In contrast, $CD8^+$ T cell depletion reduced proteinuria with intact glomerular IgG and C3 deposition in AHN,[43, 91] and reduced proteinuria in the autologous phase (week 2-4) in PHN but not during the heterologous phase (week 1) where infused anti-Fx1A antibodies cause complement-mediated podocyte injury.[92] Therefore, the small $CD8^+$ T cell infiltrate seen in Heymann nephritis likely occurs downstream of podocyte antibody deposition and proteinuria.

Development of anti-Fx1A autoantibodies in AHN suggest loss of immune tolerance, likely due to escape from thymic deletion by megalin-specific effector T cells and/or impaired induction of megalin-specific $Foxp3^+$ $CD4^+$ Tregs, though overall levels of $Foxp3^+$ $CD4^+$ Tregs are unchanged in AHN.[93] In contrast, evidence of regulation that dampen autoimmunity in AHN were found to be mediated by thymus-derived $CD8^+$ T cells, which reduced autoantibody production and proteinuria upon adoptive transfer.[94, 95] In particular, $CD8^+$ Tregs reduced anti-Fx1A antibody production in AHN by targeting $CD4^+$ T follicular helper (Tfh) cells expressing the non-classical MHC class I molecule Qa-1 (Figure 1A.5). In PMN, $CD8^+$ Tregs have yet to be described while $CD4^+$ Tregs were reduced in patients with active disease prior to receiving immunosuppression.[96]

2.7.2 Transgenic mice expressing human PLA2R specifically on podocytes

Tomas et al demonstrated that human PLA2R was not expressed in the thymus of their transgenic mice, explaining the spontaneous formation of anti-human PLA2R antibodies is likely due to a lack of central tolerance.[28] In contrast, another study described transgenic knock-in mice with ubiquitous expression of human PLA2R that did not develop a PMN phenotype, likely due to establishment of immune tolerance to human PLA2R, though expression of

human PLA2R in the thymus of these mice was not reported.[97] Lastly, in the study by Tomas et al, a PMN phenotype did not develop in recombination activating gene (RAG) 2 knock-out mice expressing human PLA2R specifically on podocytes, indicating the requirement of mature T and B cells for the formation of anti-human PLA2R autoantibodies.[28]

2.8 T and B cell and Innate Immunity in Human Membranous Nephropathy

Study of T cell subsets in PMN have revealed an increased $CD4^+$:$CD8^+$ T cell ratio.[98, 99] Further analysis of $CD4^+$ T cells in PMN showed increased Th2 cells without change in Th1 cells, increased Tfh cells, and lower $CD4^+$ Tregs, which were associated with increased IgG4 production, increased plasma cells and a loss of immune tolerance respectively (Figure 1B.4).[96, 98, 100-103] Our understanding of PMN disease antigens and class II HLA linkage suggest that HLA-driven effector T cells and/or the loss of Tregs likely play a role in loss of immune tolerance, similar to Goodpasture disease, another autoimmune kidney disease caused by autoantibodies directed against a glomerular antigen.[104] Indeed, reduced $CD4^+$ Treg number and/or function have been described in various autoimmune diseases, demonstrating its critical role in maintaining immune tolerance.[105-108] Accordingly, enhanced ability of Tregs to suppress the anti-PLA2R response in PMN has also been hypothesized to be the mechanism underlying the spontaneous remission observed in a third of patients, however data supporting this theory are lacking.[109]

More recently, increased Th17 cells have been demonstrated to correlate with disease activity, relapse and thrombotic complications in PMN,[110, 111] and IL-17 signalling was differentially expressed in single-cell RNA sequencing of kidney biopsy specimens in patients with PLA2R-

associated PMN.[112] Whether Th17 activation is triggered by glomerular antibody deposition, proteinuria or tissue injury requires further study. Single-cell RNA sequencing of kidney biopsy specimens in PMN also identified tumour necrosis factor (TNF) signalling and NOD-like receptor signalling in glomerular endothelial cells, pericytes and tubular cells compared to healthy controls, suggesting a role of innate immunity.[112] In comparison, bulk RNA sequencing and microarray expression profiles of the glomerular compartment of kidney biopsies revealed a PMN-specific signature significantly enriched in NF-kB1 targets compared to other glomerulopathies, which is consistent with a GWAS finding of a variant at the NF-kB1 locus conferring an increased risk of PMN.[61, 113] Regarding the significance of TNF signalling in PMN, circulating TNF receptors correlated with proteinuria and tubular TNF receptor expression but not anti-PLA2R autoantibody titres, which may reflect a downstream effect of heavy proteinuria on stimulating tubular cell chemokine production and infiltration of TNF-α-producing macrophages and lymphocytes.[114, 115] Indeed, TNF inhibition reduced kidney inflammatory infiltrates but not proteinuria or immune complex deposition in BSA-induced murine MN, highlighting the need to validate the findings of transcriptomic profiling with *in vivo* studies to improve our understanding of disease pathophysiology.[116]

Analysis of B cell populations in PMN have demonstrated an increase in naive B cells and reduced memory B cells, which could be secondary to Tfh-mediated differentiation of B cells into autoantibody-producing plasma cells or B cell infiltration into the kidney.[99, 117] B cell depletion with rituximab was associated with increased $CD4^+$ Tregs, potentially due to B cell expression of interferon-γ, which suppressed $CD4^+$ Tregs in animal studies (Figure 1B.4).[99, 118, 119] Regulatory B cells (Bregs) have been implicated in the suppression of B-cell-mediated autoimmunity through IL-10 production. Breg levels in PMN have varied between studies due to differences in surface markers assessed,[96, 120, 121] though overall higher Bregs correlated with better treatment responses.[96, 120]

Despite the rapid discovery of antigens targeted by autoantibodies in PMN, identification of antigen-specific T and B cells has yet to be described. T cell receptor (TCR) gene sequencing in patients with PMN revealed lower diversity of the VDJ cassette combination compared to healthy controls, which may represent expansion of antigen-specific T cells.[122] The same group analysed the B cell receptor (BCR) sequences in patients with PMN and found increased somatic hypermutation and length distribution of the third complementarity-determining region of the heavy chain (CDR-H3) of all immunoglobulin isotypes compared to healthy controls, indicative of overall increased B cell activation in PMN.[123] Future studies linking TCR and BCR sequences with pathogenic epitopes of PLA2R (or other antigens implicated in MN) may assist in identifying autoreactive T and B cells.

2.9 The Complement System in Animal Models of Membranous Nephropathy

2.9.1 Heymann nephritis

While megalin alone could recapitulate AHN, immunization with Fx1A caused more severe proteinuria suggesting additional antigens targeted by anti-Fx1A autoantibodies contributed to podocyte injury.[124] Such antigens include solid-phase complement regulatory proteins such as Crry (murine equivalent of complement receptor 1 (CR1)) and CD59 (Figure 1A.3, Figure 2). Indeed, Crry-deficient Fx1A could not induce AHN without administration of anti-Crry antibodies.[125] Lower glomerular CR1 and CD59 are reported in PMN though without evidence of associated autoantibodies and may simply represent podocyte loss.[126, 127] Overall, these data suggest complement activation plays an important role in mediating podocyte injury after antibody deposition in Heymann nephritis.

The crucial role of complement-mediated glomerular injury in Heymann nephritis was demonstrated by the prevention of proteinuria in PHN with complement depletion using cobra venom factor.[128] In AHN, proteinuria was dependent on glomerular deposition of rat complement-fixing IgG2b suggesting classical pathway activation,[41, 42] and increased podocyte expression of complement factor H (CFH) in PHN also suggests alternative pathway activation.[129] More recently, classical and alternative pathway but not lectin pathway activation was confirmed in PHN with associated increases in plasma C3a and glomerular expression of C3a receptor (C3aR). Accordingly, C3aR antagonism ameliorated disease by inhibiting the downregulation of synaptopodin (actin-associated protein in podocytes) and Bcl2 (apoptosis inhibition gene), and the upregulation of β-catenin on podocytes, which was recapitulated in human podocyte cell lines exposed to PMN sera.[130] Interestingly, C3aR antagonism did not alter inflammatory cell infiltration (including $CD4^+$ T cells, $CD8^+$ T cells, and macrophages) in the kidney of PHN rats despite C3a, an anaphylatoxin, being a potent chemoattractant.[130]

Glomerular deposition of terminal complement component C5b-9 has been demonstrated in both Heymann nephritis and PMN.[56] PVG/c rats with or without C6 deficiency induced with PHN or AHN demonstrated no differences in proteinuria, though C6 depletion using goat anti-rat C6 IgG in Sprague-Dawley rats with PHN significantly reduced proteinuria.[92, 131, 132] Nevertheless, C5b-9 has been shown to cause sublethal podocyte injury, leading to activation of cytosolic phospholipase A2, oxidative stress, lipid peroxidation, DNA damage, and disruption of the podocyte slit diaphragm (Figure 1A.4).[133]

2.10 The Complement System and Other Mechanisms of Glomerular Injury in Human Membranous Nephropathy

2.10.1 Complement System

Despite glomerular IgG and complement deposition being well-described in PMN, this finding long appeared to be inconsistent with the predominance of non-complement fixing IgG4. While there is a predominance of complement-fixing IgG1 deposition in early stages of PMN,[134, 135] the lack of glomerular C1q but almost universal C4d deposition suggested activation of the lectin pathway rather than the classical pathway (Table 2).[136] Indeed, glomerular deposition of mannan-binding lectin (MBL) co-localized with anti-PLA2R IgG4 and correlated with disease activity.[137, 138] Recently, Haddad et al provided important insights into the mechanism of lectin pathway activation in PMN by showing glycosylation patterns on anti-PLA2R IgG4 allow binding of MBL (Figure 1B.5). Such glycosylation patterns were not demonstrated in IgG4 of PLA2R-negative PMN, secondary MN or other glomerular diseases, demonstrating distinct autoimmune responses against different antigens implicated in PMN. Furthermore, anti-PLA2R IgG4 but not IgG4-depleted sera from patients with PLA2R-associated PMN was essential for the proteolysis of two podocyte proteins synaptopodin and NEPH1 via C3aR and C5aR activation on podocytes (Figure 1B.6), which could be prevented by inhibiting MBL-associated serine protease (MASP) or using C6-depleted sera.[56] Increased serum C3a and glomerular expression of C3aR have also been demonstrated in PMN patients, which correlated with disease activity and was associated with increased podocyte expression of PLA2R and reduced expression of synaptopodin.[130]

Despite growing evidence of lectin pathway activation in PMN, PLA2R-associated PMN has also been described in patients with MBL deficiency in whom disease activity was mediated by alternative pathway activation.[139] However, the mechanism of alternative pathway activation in PMN without initial activation of the lectin pathway remains unclear though one could postulate the role of traditional activators of the alternative pathway such as infection, which increase C3a levels and subsequent overexpression of PLA2R on podocytes that predisposes to autoimmunity. Anti-CFH autoantibodies are an unlikely mechanism of

alternative pathway activation, detected in only 3% of patients with PMN.[140] CFH also binds to human glomeruli via interaction with heparan sulfate, which is downregulated in PMN, AHN and PHN though whether this results in alternative pathway activation remains unproven.[141-144]

2.10.2 Other mechanisms of glomerular injury in primary membranous nephropathy

Impaired podocyte autophagy, fumarate accumulation in podocytes causing oxidative stress, and disruption of podocyte adhesion to collagen IV in the GBM have also been implicated in glomerular injury in PMN. Impairment of podocyte autophagy in PMN causes internalization of nephrin and α-actinin-4 (podocyte actin cytoskeleton protein), which in PLA2R-associated PMN may be mediated by activation of the mTOR/ULK1^{ser757} signalling pathway (Figure 1B.7).[145-148] Fumarate hydratase, which co-localizes with podocalyxin on podocytes, is reduced in PLA2R-associated PMN in an oxidative stress- and C5b-9-dependent manner (Figure 1B.8).[149] Inhibition of fumarate hydratase using small interfering RNA results in fumarate accumulation within podocytes causing oxidative stress and reduction in zonula occludens-1 (podocyte slit diaphragm protein) and Wilm's tumor 1 (podocyte transcription factor).[149, 150] Lastly, *in vitro* evidence suggests human sera containing anti-PLA2R antibodies impair podocyte adhesion to collagen IV on the GBM though the exact mechanism remains unclear.[151]

2.11 Novel Therapeutics: Potential Targets and Challenges

2.11.1 Targeting autoantibody production by B cells and plasma cells

PMN appears to be different disease entities rather than a uniform disease but with a unified immunological phenotype of autoantibody formation against an antigen mostly expressed on

podocytes. Therefore, targeting antibody generation through B-cells, plasma cells and Tfh cells is an attractive strategy (Figure 3). While rituximab, a chimeric anti-CD20 monoclonal antibody, is effective at depleting B cells, treatment response in PMN is variable (60-85% complete or partial remission at 24 months).[12, 15] This may be related to autoantibody production by CD20-negative plasma cells, changes in the CD20 antigen that may be restricted to autoreactive B cells, or the development of neutralizing antibodies against rituximab. Ofatumumab and obinutuzumab are humanized anti-CD20 monoclonal antibodies, which have successfully treated patients with PMN who developed serum sickness to rituximab or anti-rituximab antibodies,[152, 153] and demonstrated superior B-cell depletion compared to rituximab respectively.[154] The efficacy of obinutuzumab and belimumab (humanized monoclonal antibody against B-cell activating factor (BAFF)) in lupus nephritis, another disease mediated in part by autoreactive B cells, and CD19 CAR T cells in treatment-refractory SLE are also promising alternative B cell-depleting therapies, which require further evaluation in PMN.[155-158]

Treatment resistance to B-cell depletion may also be attributable to persistent memory plasma cells, which produce autoantibodies independent of T and B cell interactions. The proteasome inhibitor bortezomib effectively depletes plasma cells and has been effective in both treatment-resistant and treatment-naïve PMN.[159, 160] Plasma cells express CD38 and CD138, which could be targeted by anti-CD38 monoclonal antibodies such as daratumumab. However, safety concerns of neurotoxicity with bortezomib and infection with both bortezomib and daratumumab may limit their use. An alternative approach could be a short course of plasma cell-depleting therapy followed by B cell depletion or T cell co-stimulatory blockade to inhibit the Tfh-mediated B cell differentiation into plasma cells. In an uncontrolled cohort study and a case series of kidney transplant recipients with antibody-mediated rejection, short-duration bortezomib (on average 4 doses of 1.3 mg/m^2) followed by adjunctive therapy (including

rituximab, plasmapheresis, or intravenous immunoglobulin) or T cell co-stimulatory blockade with belatacept respectively were effective.[161, 162] However, controlled clinical trials are needed to confirm the efficacy of these treatment regimens.

2.11.2 Targeting antigen-specific B and T cells

The discovery of the disease antigens driving PMN also raises the possibility of antigen-specific therapeutics such as CAR or CAAR T cell therapies against PLA2R-specific B cells. In pemphigus vulgaris, an antibody-mediated autoimmune blistering skin disease, CAAR T cells expressing the disease autoantigen desmoglein 3 was able to eliminate desmoglein 3-specific B cells in a mouse model even in the presence of circulating autoantibodies and without off-target toxicity.[163] A similar approach is conceivable in PMN where B cell-mediated autoimmunity is driven by a single autoantigen in most cases.

2.11.3 Establishing immune tolerance

Inducing immune tolerance without abrogating anti-infection and anti-tumour immunity is the ultimate therapeutic strategy. CAR $CD4^+$ Tregs targeting organ-specific antigens suppressed autoimmunity in animal models of type 1 diabetes, multiple sclerosis and autoimmune colitis.[164-166] In particular, CAR Tregs in the autoimmune colitis model were able to suppress disease activity despite being specific for an antigen distinct from the disease antigen.[166] This demonstrates the phenomenon of infectious tolerance whereby $CD4^+$ Tregs can confer suppressive activity to conventional T cells via membrane-bound transforming growth factor-β (TGF-β).[167, 168] PLA2R may represent an ideal tissue marker to direct CAR Tregs to the glomerulus in PMN. An alternative strategy may be selective expansion of Tregs using low-dose IL-2, which was effective in animal models of rheumatoid arthritis and autoimmune colitis.[169] However, a mechanism of IL-2 delivery to the kidney remains unclear.

Two distinct regulatory T cell subsets also exist to maintain immune tolerance at the germinal centre: $CD8^+$ Tregs and T follicular regulatory (Tfr) cells. In a mouse model of multiple sclerosis, yeast libraries have been used to identify peptides that engage the $CD8^+$ Treg TCR and vaccination of these peptides suppressed disease activity.[170] Neuritin, a protein produced by Tfr cells to prevent differentiation of B cells into plasma cells has also been shown to suppress autoantibody production in Tfr-deficient mice.[171] However, the importance of $CD8^+$ Tregs and Tfr cells in PMN remains to be established and development of these promising though experimental therapies will require rigorous pre-clinical evaluation.

2.11.4 Are current animal models suitable for preclinical testing of novel therapeutics?

Heymann nephritis has significantly contributed to our understanding of the disease mechanisms causing PMN but distinct differences in the underlying disease antigen, predominant autoantibody IgG subclass, and mechanism of complement activation and glomerular injury remain. Despite this, AHN remains a relevant and feasible model that recapitulates the unifying disease phenotype of PMN and therefore is suitable for testing novel therapeutics targeting autoantibody production. Activation of the alternative complement pathway is also a hallmark of both AHN/PHN and PMN with C3aR antagonism ameliorating disease in PHN,[130] and an ongoing trial will evaluate the factor B inhibitor iptacopan (LNP023) compared to rituximab in PMN (NCT04154787).

Models of PMN induced by passive administration of anti-PLA2R and anti-THSD7A autoantibodies may better resemble the mechanism of glomerular injury in human PMN. However, PLA2R and THSD7A in these models were not humanized, reflecting the inability of transferred human anti-PLA2R autoantibodies or purified human anti-THSD7A to recapitulate disease. Furthermore, rabbit anti-THSD7A antibodies lack the ability to activate

complement, a hallmark of THSD7A-associated PMN. These animal models also require the passive administration of antibodies and therefore do not reproduce the immunological mechanism of autoantibody production in PMN.

Most recently, transgenic knock-in mice expressing human PLA2R specifically on podocytes faithfully recapitulates human PMN phenotype, representing an important and exciting development that opens opportunities to further understand the disease mechanisms driving PMN and test novel antigen-specific therapeutics such as CAR or CAAR T cells. It remains unclear whether a similar approach can be replicated to model MN associated with non-PLA2R antigens, though developing transgenic mice with podocyte-specific expression of the numerous non-PLA2R MN disease antigens present a significant challenge as well as feasibility issues. An alternative approach would be to immunize susceptible murine strains with a specific PMN-associated antigen and adjuvant. However, while expression of Sema3B and serine protease HTRA1 have been demonstrated in murine podocytes, PCDH7 is not detectable in rat kidneys and it is unclear whether murine podocytes express NELL1 or NTNG1.[172-175]

2.12 Conclusion

Our understanding of PMN is rapidly evolving with the promise of targeted therapeutics now emerging. Integrating technologies such as mapping T and B cell receptor sequences to their cognate antigen, HLA-peptide tetramer analysis, and single-cell RNA sequencing of lymphocytes will likely offer greater insights into the immune mechanisms causing PMN leading to the development of more effective and targeted treatments in this challenging disease.

2.13 References

1. Couser WG. Primary Membranous Nephropathy. Clin J Am Soc Nephrol. 2017;12(6):983.

2. Ronco P, Debiec H. Molecular Pathogenesis of Membranous Nephropathy. Annu Rev Pathol. 2020;15(1):287-313.

3. Beck Jr LH, Bonegio RG, Lambeau G, Beck DM, Powell DW, Cummins TD, et al. M-type phospholipase A2 receptor as target antigen in idiopathic membranous nephropathy. N Engl J Med. 2009;361(1):11-21.

4. Tomas NM, Beck LH, Meyer-Schwesinger C, Seitz-Polski B, Ma H, Zahner G, et al. Thrombospondin Type-1 Domain-Containing 7A in Idiopathic Membranous Nephropathy. N Engl J Med. 2014;371(24):2277-87.

5. Du Y, Li J, He F, Lv Y, Liu W, Wu P, et al. The diagnosis accuracy of PLA2R-AB in the diagnosis of idiopathic membranous nephropathy: a meta-analysis. PLoS One. 2014;9(8):e104936.

6. Ponticelli C, Zucchelli P, Imbasciati E, Cagnoli L, Pozzi C, Passerini P, et al. Controlled trial of methylprednisolone and chlorambucil in idiopathic membranous nephropathy. N Engl J Med. 1984;310(15):946-50.

7. Ponticelli C, Zucchelli P, Passerini P, Cagnoli L, Cesana B, Pozzi C, et al. A randomized trial of methylprednisolone and chlorambucil in idiopathic membranous nephropathy. N Engl J Med. 1989;320(1):8-13.

8. Ponticelli C, Zucchelli P, Passerini P, Cesana B. Methylprednisolone plus chlorambucil as compared with methylprednisolone alone for the treatment of idiopathic membranous nephropathy. The Italian Idiopathic Membranous Nephropathy Treatment Study Group. N Engl J Med. 1992;327(9):599-603.

9. Ponticelli C, Altieri P, Scolari F, Passerini P, Roccatello D, Cesana B, et al. A randomized study comparing methylprednisolone plus chlorambucil versus methylprednisolone plus cyclophosphamide in idiopathic membranous nephropathy. J Am Soc Nephrol. 1998;9(3):444-50.

10. Jha V, Ganguli A, Saha TK, Kohli HS, Sud K, Gupta KL, et al. A randomized, controlled trial of steroids and cyclophosphamide in adults with nephrotic syndrome caused by idiopathic membranous nephropathy. J Am Soc Nephrol. 2007;18(6):1899-904.

11. Cattran DC, Appel GB, Hebert LA, Hunsicker LG, Pohl MA, Hoy WE, et al. Cyclosporine in patients with steroid-resistant membranous nephropathy: a randomized trial. Kidney Int. 2001;59(4):1484-90.

12. Fervenza FC, Appel GB, Barbour SJ, Rovin BH, Lafayette RA, Aslam N, et al. Rituximab or Cyclosporine in the Treatment of Membranous Nephropathy. N Engl J Med. 2019;381(1):36-46.

13. Ruggenenti P, Fervenza FC, Remuzzi G. Treatment of membranous nephropathy: time for a paradigm shift. Nat Rev Nephrol. 2017;13(9):563-79.

14. Fernández-Juárez G, Rojas-Rivera J, Logt AV, Justino J, Sevillano A, Caravaca-Fontán F, et al. The STARMEN trial indicates that alternating treatment with corticosteroids and cyclophosphamide is superior to sequential treatment with tacrolimus and rituximab in primary membranous nephropathy. Kidney Int. 2021;99(4):986-98.

15. Scolari F, Delbarba E, Santoro D, Gesualdo L, Pani A, Dallera N, et al. Rituximab or Cyclophosphamide in the Treatment of Membranous Nephropathy: The RI-CYCLO Randomized Trial. J Am Soc Nephrol. 2021;32(4):972-82.

16. Grupper A, Cornell LD, Fervenza FC, Beck LH, Jr., Lorenz E, Cosio FG. Recurrent Membranous Nephropathy After Kidney Transplantation: Treatment and Long-Term Implications. Transplantation. 2016;100(12).

17. Stahl R, Hoxha E, Fechner K. PLA2R autoantibodies and recurrent membranous nephropathy after transplantation. N Engl J Med. 2010;363(5):496-8.

18. Dabade TS, Grande JP, Norby SM, Fervenza FC, Cosio FG. Recurrent idiopathic membranous nephropathy after kidney transplantation: a surveillance biopsy study. Am J Transplant. 2008;8(6):1318-22.

19. Moroni G, Gallelli B, Quaglini S, Leoni A, Banfi G, Passerini P, et al. Long-term outcome of renal transplantation in patients with idiopathic membranous glomerulonephritis (MN). Nephrol Dial Transplant. 2010;25(10):3408-15.

20. Sadeqi Nezhad M, Seifalian A, Bagheri N, Yaghoubi S, Karimi MH, Adbollahpour-Alitappeh M. Chimeric Antigen Receptor Based Therapy as a Potential Approach in Autoimmune Diseases: How Close Are We to the Treatment? Front Immunol. 2020;11:603237.

21. Heymann W, Hackel DB, Harwood S, Wilson SG, Hunter JL. Production of nephrotic syndrome in rats by Freund's adjuvants and rat kidney suspensions. Proc Soc Exp Biol Med. 1959;100(4):660-4.

22. Couser W, Steinmuller D, Stilmant M, Salant D, Lowenstein L. Experimental glomerulonephritis in the isolated perfused rat kidney. J Clin Invest. 1978;62(6):1275-87.

23. Adler S, Baker PJ, Pritzl P, Couser WG. Detection of terminal complement components in experimental immune glomerular injury. Kidney Int. 1984;26(6):830-7.

24. Meyer-Schwesinger C, Tomas NM, Dehde S, Seifert L, Hermans-Borgmeyer I, Wiech T, et al. A novel mouse model of phospholipase A2 receptor 1-associated membranous nephropathy mimics podocyte injury in patients. Kidney Int. 2020;97(5):913-9.

25. Tomas NM, Hoxha E, Reinicke AT, Fester L, Helmchen U, Gerth J, et al. Autoantibodies against thrombospondin type 1 domain–containing 7A induce membranous nephropathy. J Clin Invest. 2016;126(7):2519-32.

26. Wang Z, Wen L, Dou Y, Zhao Z. Human anti-thrombospondin type 1 domain-containing 7A antibodies induce membranous nephropathy through activation of lectin complement pathway. Biosci Rep. 2018;38(3).

27. Tomas NM, Meyer-Schwesinger C, von Spiegel H, Kotb AM, Zahner G, Hoxha E, et al. A Heterologous Model of Thrombospondin Type 1 Domain-Containing 7A-Associated Membranous Nephropathy. J Am Soc Nephrol. 2017;28(11):3262.

28. Tomas NM, Dehde S, Meyer-Schwesinger C, Huang M, Hermans-Borgmeyer I, Maybaum J, et al. Podocyte expression of human phospholipase A2 receptor 1 causes immune-mediated membranous nephropathy in mice. Kidney Int. 2022.

29. Assmann K, Van Son J, Dijkman H, Koene R. A nephritogenic rat monoclonal antibody to mouse aminopeptidase A. Induction of massive albuminuria after a single intravenous injection. J Exp Med. 1992;175(3):623-35.

30. Dijkman HB, Gerlofs-Nijland ME, van der Laak JA, Wetzels JF, Groenen PJ, Assmann KJ. Podocyte changes after induction of acute albuminuria in mice by anti-aminopeptidase A mAb. Nephron Exp Nephrol. 2003;94(3):e85-e93.

31. Natori Y, Hayakawa I, Shibata S. Identification of gp108, a pathogenic antigen of passive Heymann nephritis, as dipeptidyl peptidase IV. Clin Exp Immunol. 1987;70(2):434.

32. Meyer-Schwesinger C, Dehde S, Klug P, Becker JU, Mathey S, Arefi K, et al. Nephrotic syndrome and subepithelial deposits in a mouse model of immune-mediated anti-podocyte glomerulonephritis. J Immunol. 2011;187(6):3218-29.

33. Meyer T, Schwesinger C, Wahlefeld J, Dehde S, Kerjaschki D, Becker J, et al. A new mouse model of immune-mediated podocyte injury. Kidney Int. 2007;72(7):841-52.

34. Border WA, Harry JW, Kamil ES, Cohen AH. Induction of membranous nephropathy in rabbits by administration of an exogenous cationic antigen: Demonstration of a pathogenic role for electrical charge. J Clin Invest. 1982;69(2):451-61.

35. Zhang J-J, Malekpour M, Luo W, Ge L, Olaru F, Wang X-P, et al. Murine membranous nephropathy: Immunization with α3 (IV) collagen fragment induces subepithelial immune complexes and FcγR-independent nephrotic syndrome. J Immunol. 2012;188(7):3268-77.

36. Lerner GB, Virmani S, Henderson JM, Francis JM, Beck LH, Jr. A conceptual framework linking immunology, pathology, and clinical features in primary membranous nephropathy. Kidney Int. 2021;100(2):289-300.

37. Edgington TS, Glassock RJ, Dixon FJ. Autologous immune complex nephritix induced with renal tubular antigen: I. Identification and isolation of the pathogenic antigen. J Exp Med. 1968;127(3):555-72.

38. Kerjaschki D, Farquhar MG. The pathogenic antigen of Heymann nephritis is a membrane glycoprotein of the renal proximal tubule brush border. Proc Natl Acad Sci U S A. 1982;79(18):5557-61.

39. Farquhar MG, Saito A, Kerjaschki D, Orlando RA. The Heymann nephritis antigenic complex: megalin (gp330) and RAP. J Am Soc Nephrol. 1995;6(1):35.

40. Kukida M, Sawada H, Daugherty A, Lu HS. Megalin: a bridge connecting kidney, the renin-angiotensin system, and atherosclerosis. Pharmacol Res. 2020;151:104537.

41. Brüggemann M, Teale C, Clark M, Bindon C, Waldmann H. A matched set of rat/mouse chimeric antibodies. Identification and biological properties of rat H chain constant regions mu, gamma 1, gamma 2a, gamma 2b, gamma 2c, epsilon, and alpha. J Immunol. 1989;142(9):3145-50.

42. Noble B, Van Liew JB, Andres GA, Brentjens JR. Factors influencing susceptibility of LEW rats to Heymann nephritis. Clin Immunol Immunopathol. 1984;30(2):241-54.

43. Penny MJ, Boyd RA, Hall BM. Permanent CD8+ T Cell Depletion Prevents Proteinuria in Active Heymann Nephritis. J Exp Med. 1998;188(10):1775-84.

44. Shah P, Tramontano A, Makker SP. Intramolecular epitope spreading in Heymann nephritis. J Am Soc Nephrol. 2007;18(12):3060-6.

45. Tramontano A, Makker SP. Conformation and Glycosylation of a Megalin Fragment Correlate with Nephritogenicity in Heymann Nephritis. J Immunol. 2004;172(4):2367.

46. Fresquet M, Jowitt TA, Gummadova J, Collins R, O'Cualain R, McKenzie EA, et al. Identification of a Major Epitope Recognized by PLA2R Autoantibodies in Primary Membranous Nephropathy. J Am Soc Nephrol. 2015;26(2):302.

47. Fresquet M, Rhoden SJ, Jowitt TA, McKenzie EA, Roberts I, Lennon R, et al. Autoantigens PLA2R and THSD7A in membranous nephropathy share a common epitope motif in the N-terminal domain. J Autoimmun. 2020;106:102308.

48. Reinhard L, Zahner G, Menzel S, Koch-Nolte F, Stahl RAK, Hoxha E. Clinical Relevance of Domain-Specific Phospholipase A(2) Receptor 1 Antibody Levels in Patients with Membranous Nephropathy. J Am Soc Nephrol. 2020;31(1):197-207.

49. Perez-Gomez MV, Sanchez-Niño MD, Ortiz A. Megalin/lipoprotein receptor-related protein 2 autoimmunity and kidney disease. Clin Kidney J. 2020;13(3):281-6.

50. Larsen CP, Trivin-Avillach C, Coles P, Collins AB, Merchant M, Ma H, et al. LDL receptor-related protein 2 (Megalin) as a target antigen in human kidney anti-brush border antibody disease. J Am Soc Nephrol. 2018;29(2):644-53.

51. Sethi S, Debiec H, Madden B, Charlesworth MC, Morelle J, Gross L, et al. Neural epidermal growth factor-like 1 protein (NELL-1) associated membranous nephropathy. Kidney Int. 2020;97(1):163-74.

52. Sethi S, Debiec H, Madden B, Vivarelli M, Charlesworth MC, Ravindran A, et al. Semaphorin 3B-associated membranous nephropathy is a distinct type of disease predominantly present in pediatric patients. Kidney Int. 2020;98(5):1253-64.

53. Hofstra JM, Beck LH, Beck DM, Wetzels JF, Salant DJ. Anti-phospholipase A2 receptor antibodies correlate with clinical status in idiopathic membranous nephropathy. Clin J Am Soc Nephrol. 2011;6(6):1286-91.

54. Rao SJ, Shen Q, Wang HM, Tang S, Wang XY. The association of anti-PLA2R with clinical manifestations and outcomes in idiopathic membranous nephropathy: a meta-analysis. Int Urol Nephrol. 2020;52(11):2123-33.

55. Ruggenenti P, Debiec H, Ruggiero B, Chianca A, Pellé T, Gaspari F, et al. Anti-Phospholipase A2 Receptor Antibody Titer Predicts Post-Rituximab Outcome of Membranous Nephropathy. J Am Soc Nephrol. 2015;26(10):2545.

56. Haddad G, Lorenzen JM, Ma H, de Haan N, Seeger H, Zaghrini C, et al. Altered glycosylation of IgG4 promotes lectin complement pathway activation in anti-PLA2R1–associated membranous nephropathy. J Clin Invest. 2021;131(5).

57. Fresquet M, Lockhart-Cairns MP, Rhoden SJ, Jowitt TA, Briggs DC, Baldock C, et al. Structure of PLA2R reveals presentation of the dominant membranous nephropathy epitope and an immunogenic patch. Proc Natl Acad Sci U S A. 2022;119(29):e2202209119.

58. Seitz-Polski B, Debiec H, Rousseau A, Dahan K, Zaghrini C, Payré C, et al. Phospholipase A2 Receptor 1 Epitope Spreading at Baseline Predicts Reduced Likelihood of Remission of Membranous Nephropathy. J Am Soc Nephrol. 2018;29(2):401.

59. Seitz-Polski B, Dolla G, Payré C, Girard CA, Polidori J, Zorzi K, et al. Epitope Spreading of Autoantibody Response to PLA2R Associates with Poor Prognosis in Membranous Nephropathy. J Am Soc Nephrol. 2016;27(5):1517.

60. Stanescu HC, Arcos-Burgos M, Medlar A, Bockenhauer D, Kottgen A, Dragomirescu L, et al. Risk HLA-DQA1 and PLA(2)R1 alleles in idiopathic membranous nephropathy. N Engl J Med. 2011;364(7):616-26.

61. Xie J, Liu L, Mladkova N, Li Y, Ren H, Wang W, et al. The genetic architecture of membranous nephropathy and its potential to improve non-invasive diagnosis. Nat Commun. 2020;11(1):1600.

62. Cui Z, Xie LJ, Chen FJ, Pei ZY, Zhang LJ, Qu Z, et al. MHC Class II Risk Alleles and Amino Acid Residues in Idiopathic Membranous Nephropathy. J Am Soc Nephrol. 2017;28(5):1651-64.

63. Debiec H, Martin L, Jouanneau C, Dautin G, Mesnard L, Rondeau E, et al. Autoantibodies specific for the phospholipase A2 receptor in recurrent and de novo membranous nephropathy. Am J Transplant. 2011;11(10):2144-52.

64. Kattah A, Ayalon R, Beck LH, Jr., Sethi S, Sandor DG, Cosio FG, et al. Anti-phospholipase A_2 receptor antibodies in recurrent membranous nephropathy. Am J Transplant. 2015;15(5):1349-59.

65. Quintana LF, Blasco M, Seras M, Pérez NS, López-Hoyos M, Villarroel P, et al. Antiphospholipase A2 Receptor Antibody Levels Predict the Risk of Posttransplantation Recurrence of Membranous Nephropathy. Transplantation. 2015;99(8):1709-14.

66. Berchtold L, Letouzé E, Alexander MP, Canaud G, Logt AV, Hamilton P, et al. HLA-D and PLA2R1 risk alleles associate with recurrent primary membranous nephropathy in kidney transplant recipients. Kidney Int. 2021;99(3):671-85.

67. Batal I, Vasilescu ER, Dadhania DM, Adel AA, Husain SA, Avasare R, et al. Association of HLA Typing and Alloimmunity With Posttransplantation Membranous Nephropathy: A Multicenter Case Series. Am J Kidney Dis. 2020;76(3):374-83.

68. Seifert L, Hoxha E, Eichhoff AM, Zahner G, Dehde S, Reinhard L, et al. The Most N-Terminal Region of THSD7A Is the Predominant Target for Autoimmunity in THSD7A-Associated Membranous Nephropathy. J Am Soc Nephrol. 2018;29(5):1536.

69. Larsen CP, Cossey LN, Beck LH. THSD7A staining of membranous glomerulopathy in clinical practice reveals cases with dual autoantibody positivity. Mod Pathol. 2016;29(4):421-6.

70. Al-Rabadi LF, Caza T, Trivin-Avillach C, Rodan AR, Andeen N, Hayashi N, et al. Serine Protease HTRA1 as a Novel Target Antigen in Primary Membranous Nephropathy. J Am Soc Nephrol. 2021.

71. Caza TN, Hassen SI, Kuperman M, Sharma SG, Dvanajscak Z, Arthur J, et al. Neural cell adhesion molecule 1 is a novel autoantigen in membranous lupus nephritis. Kidney Int. 2020.

72. Sethi S, Madden B, Debiec H, Morelle J, Charlesworth MC, Gross L, et al. Protocadherin 7-Associated Membranous Nephropathy. J Am Soc Nephrol. 2021;32(5):1249-61.

73. Sethi S, Madden BJ, Debiec H, Charlesworth MC, Gross L, Ravindran A, et al. Exostosin 1/Exostosin 2–Associated Membranous Nephropathy. J Am Soc Nephrol. 2019;30(6):1123.

74. Reinhard L, Machalitza M, Wiech T, Groene HJ, Lassé M, Rinschen M, et al. Netrin G1 is a Novel Target Antigen in Primary Membranous Nephropathy. J Am Soc Nephrol. 2022.

75. Caza TN, Hassen SI, Kenan DJ, Storey A, Arthur JM, Herzog C, et al. Transforming Growth Factor Beta Receptor 3 (TGFBR3)-Associated Membranous Nephropathy. Kidney360. 2021;2(8):1275-86.

76. Le Quintrec M, Teisseyre M, Bec N, Delmont E, Szwarc I, Perrochia H, et al. Contactin-1 is a novel target antigen in membranous nephropathy associated with chronic inflammatory demyelinating polyneuropathy. Kidney Int. 2021;100(6):1240-9.

77. Sethi S, Madden B, Casal Moura M, Nasr SH, Klomjit N, Gross L, et al. Hematopoietic Stem Cell Transplant-Membranous Nephropathy Is Associated with Protocadherin FAT1. J Am Soc Nephrol. 2022;33(5):1033-44.

78. Fila M, Debiec H, Perrochia H, Djouadi N, Verpont MC, Buob D, et al. Recurrence of Anti-Semaphorin 3B-Mediated Membranous Nephropathy after Kidney Transplantation. J Am Soc Nephrol. 2022;33(3):503-9.

79. Sethi S. New 'Antigens' in Membranous Nephropathy. J Am Soc Nephrol. 2021;32(2):268-78.

80. Ravindran A, Casal Moura M, Fervenza FC, Nasr SH, Alexander MP, Fidler ME, et al. In Patients with Membranous Lupus Nephritis, Exostosin-Positivity and Exostosin-Negativity Represent Two Different Phenotypes. J Am Soc Nephrol. 2021;32(3):695-706.

81. Xie Q, Li Y, Xue J, Xiong Z, Wang L, Sun Z, et al. Renal Phospholipase A2 Receptor in Hepatitis B Virus-Associated Membranous Nephropathy. Am J Nephrol. 2015;41(4-5):345-53.

82. Hoxha E, Wiech T, Stahl PR, Zahner G, Tomas NM, Meyer-Schwesinger C, et al. A Mechanism for Cancer-Associated Membranous Nephropathy. N Engl J Med. 2016;374(20):1995-6.

83. Hoxha E, Beck LH, Jr., Wiech T, Tomas NM, Probst C, Mindorf S, et al. An Indirect Immunofluorescence Method Facilitates Detection of Thrombospondin Type 1 Domain-Containing 7A-Specific Antibodies in Membranous Nephropathy. J Am Soc Nephrol. 2017;28(2):520-31.

84. Caza TN, Hassen SI, Dvanajscak Z, Kuperman M, Edmondson R, Herzog C, et al. NELL1 is a target antigen in malignancy-associated membranous nephropathy. Kidney Int. 2021;99(4):967-76.

85. Debiec H, Guigonis V, Mougenot B, Decobert F, Haymann JP, Bensman A, et al. Antenatal membranous glomerulonephritis due to anti-neutral endopeptidase antibodies. N Engl J Med. 2002;346(26):2053-60.

86. Debiec H, Nauta J, Coulet F, van der Burg M, Guigonis V, Schurmans T, et al. Role of truncating mutations in MME gene in fetomaternal alloimmunisation and antenatal glomerulopathies. Lancet. 2004;364(9441):1252-9.

87. Prunotto M, Carnevali ML, Candiano G, Murtas C, Bruschi M, Corradini E, et al. Autoimmunity in membranous nephropathy targets aldose reductase and SOD2. J Am Soc Nephrol. 2010;21(3):507-19.

88. Murtas C, Bruschi M, Candiano G, Moroni G, Magistroni R, Magnano A, et al. Coexistence of different circulating anti-podocyte antibodies in membranous nephropathy. Clin J Am Soc Nephrol. 2012;7(9):1394-400.

89. Bruschi M, Cavalli A, Moll S, Candiano G, Scapozza L, Patel JJ, et al. Discovery of anti-Formin-like 1 protein (FMNL1) antibodies in membranous nephropathy and other glomerular diseases. Sci Rep. 2022;12(1):13659.

90. Quiza CG, Leenaerts PL, Hall BM. The role of T cells in the mediation of glomerular injury in Heymann's nephritis in the rat. Int Immunol. 1992;4(4):423-32.

91. Penny MJ, Boyd RA, Hall BM. Role of T cells in the mediation of Heymann nephritis. ii. Identification of Th1 and cytotoxic cells in glomeruli. Kidney Int. 1997;51(4):1059-68.

92. Spicer ST, Tran GT, Killingsworth MC, Carter N, Power DA, Paizis K, et al. Induction of passive Heymann nephritis in complement component 6-deficient PVG rats. J Immunol. 2007;179(1):172-8.

93. Wang YM, Zhang GY, Hu M, Polhill T, Sawyer A, Zhou JJ, et al. CD8+ Regulatory T Cells Induced by T Cell Vaccination Protect Against Autoimmune Nephritis. J Am Soc Nephrol. 2012;23(6):1058.

94. de Heer E, Daha MR, Burgers J, van Es LA. Reestablishment of self tolerance by suppressor T-cells after active Heymann's nephritis. Cell Immunol. 1986;98(1):28-33.

95. de Heer E, Daha MR, van Es LA. The autoimmune response in active Heymann's nephritis in Lewis rats is regulated by T-lymphocyte subsets. Cell Immunol. 1985;92(2):254-64.

96. Cantarelli C, Jarque M, Angeletti A, Manrique J, Hartzell S, O'Donnell T, et al. A Comprehensive Phenotypic and Functional Immune Analysis Unravels Circulating Anti-Phospholipase A2 Receptor Antibody Secreting Cells in Membranous Nephropathy Patients. Kidney Int Rep. 2020;5(10):1764-76.

97. Jaber S, Goehrig D, Bertolino P, Massemin A, Bihl F, Chabry J, et al. Generation of a conditional transgenic mouse model expressing human Phospholipase A2 Receptor 1. Sci Rep. 2020;10(1):8190.

98. Kuroki AKI, Iyoda M, Shibata T, Sugisaki T. Th2 cytokines increase and stimulate B cells to produce IgG4 in idiopathic membranous nephropathy. Kidney Int. 2005;68(1):302-10.

99. Rosenzwajg M, Languille E, Debiec H, Hygino J, Dahan K, Simon T, et al. B- and T-cell subpopulations in patients with severe idiopathic membranous nephropathy may predict an early response to rituximab. Kidney Int. 2017;92(1):227-37.

100. Masutani K, Taniguchi M, Nakashima H, Yotsueda H, Kudoh Y, Tsuruya K, et al. Up-regulated interleukin-4 production by peripheral T-helper cells in idiopathic membranous nephropathy. Nephrol Dial Transplant. 2004;19(3):580-6.

101. Shi X, Qu Z, Zhang L, Zhang N, Liu Y, Li M, et al. Increased ratio of ICOS+/PD-1+ follicular helper T cells positively correlates with the development of human idiopathic membranous nephropathy. Clin Exp Pharmacol Physiol. 2016;43(4):410-6.

102. Zhang Z, Shi Y, Yang K, Crew R, Wang H, Jiang Y. Higher frequencies of circulating ICOS+, IL-21+ T follicular helper cells and plasma cells in patients with new-onset membranous nephropathy. Autoimmunity. 2017;50(8):458-67.

103. Hirayama K, Ebihara I, Yamamoto S, Kai H, Muro K, Yamagata K, et al. Predominance of type-2 immune response in idiopathic membranous nephropathy. Cytoplasmic cytokine analysis. Nephron. 2002;91(2):255-61.

104. Ooi JD, Petersen J, Tan YH, Huynh M, Willett ZJ, Ramarathinam SH, et al. Dominant protection from HLA-linked autoimmunity by antigen-specific regulatory T cells. Nature. 2017;545(7653):243-7.

105. Viglietta V, Baecher-Allan C, Weiner HL, Hafler DA. Loss of functional suppression by CD4+CD25+ regulatory T cells in patients with multiple sclerosis. J Exp Med. 2004;199(7):971-9.

106. Ehrenstein MR, Evans JG, Singh A, Moore S, Warnes G, Isenberg DA, et al. Compromised function of regulatory T cells in rheumatoid arthritis and reversal by anti-TNFalpha therapy. J Exp Med. 2004;200(3):277-85.

107. Crispin JC, Martínez A, Alcocer-Varela J. Quantification of regulatory T cells in patients with systemic lupus erythematosus. J Autoimmun. 2003;21(3):273-6.

108. Kukreja A, Cost G, Marker J, Zhang C, Sun Z, Lin-Su K, et al. Multiple immuno-regulatory defects in type-1 diabetes. J Clin Invest. 2002;109(1):131-40.

109. Cattran DC, Brenchley PE. Membranous nephropathy: integrating basic science into improved clinical management. Kidney Int. 2017;91(3):566-74.

110. Cremoni M, Brglez V, Perez S, Decoupigny F, Zorzi K, Andreani M, et al. Th17-Immune Response in Patients With Membranous Nephropathy Is Associated With Thrombosis and Relapses. Front Immunol. 2020;11:574997.

111. Dan T, JiGuang G, Z J. Variation of Peripheral Th17/Treg Imbalance in Patients with Idiopathic Membranous Nephropathy After Cyclosporin a Treatment: A Prognostic Marker of Idiopathic Membranous Nephropathy. Biomed J Sci & Tech Res. 2018;7(5).

112. Xu J, Shen C, Lin W, Meng T, Ooi JD, Eggenhuizen PJ, et al. Single-Cell Profiling Reveals Transcriptional Signatures and Cell-Cell Crosstalk in Anti-PLA2R Positive Idiopathic Membranous Nephropathy Patients. Front Immunol. 2021;12:683330.

113. Sealfon R, Mariani L, Avila-Casado C, Nair V, Menon R, Funk J, et al. Molecular Characterization of Membranous Nephropathy. J Am Soc Nephrol. 2022;33(6):1208-21.

114. Lee SM, Yang S, Cha RH, Kim M, An JN, Paik JH, et al. Circulating TNF receptors are significant prognostic biomarkers for idiopathic membranous nephropathy. PLoS One. 2014;9(8):e104354.

115. Remuzzi G, Bertani T. Pathophysiology of progressive nephropathies. N Engl J Med. 1998;339(20):1448-56.

116. Huang YS, Fu SH, Lu KC, Chen JS, Hsieh HY, Sytwu HK, et al. Inhibition of tumor necrosis factor signaling attenuates renal immune cell infiltration in experimental membranous nephropathy. Oncotarget. 2017;8(67):111631-41.

117. Wang B, Zuo K, Wu Y, Huang Q, Qin WS, Zeng CH, et al. Correlation between B lymphocyte abnormality and disease activity in patients with idiopathic membranous nephropathy. J Int Med Res. 2011;39(1):86-95.

118. Olalekan SA, Cao Y, Hamel KM, Finnegan A. B cells expressing IFN-γ suppress Treg-cell differentiation and promote autoimmune experimental arthritis. Eur J Immunol. 2015;45(4):988-98.

119. Roccatello D, Sciascia S, Di Simone D, Solfietti L, Naretto C, Fenoglio R, et al. New insights into immune mechanisms underlying response to Rituximab in patients with

membranous nephropathy: A prospective study and a review of the literature. Autoimmun Rev. 2016;15(6):529-38.

120. Ramachandran R, Kaundal U, Girimaji N, Rakha A, Rathi M, Gupta KL, et al. Regulatory B Cells Are Reduced and Correlate With Disease Activity in Primary Membranous Nephropathy. Kidney Int Rep. 2020.

121. Dong Z, Liu Z, Dai H, Liu W, Feng Z, Zhao Q, et al. The Potential Role of Regulatory B Cells in Idiopathic Membranous Nephropathy. J Immunol Res. 2020;2020:7638365.

122. Zhang Y, Jin Y, Guan Z, Li H, Su Z, Xie C, et al. The Landscape and Prognosis Potential of the T-Cell Repertoire in Membranous Nephropathy. Front Immunol. 2020;11:387.

123. Su Z, Jin Y, Zhang Y, Guan Z, Li H, Chen X, et al. The Diagnostic and Prognostic Potential of the B-Cell Repertoire in Membranous Nephropathy. Front Immunol. 2021;12:635326.

124. Kamata K, Baird L, Erikson M, Collins A, McCluskey R. Characterization of antigens and antibody specificities involved in Heymann nephritis. J Immunol. 1985;135(4):2400-8.

125. Schiller B, He C, Salant DJ, Lim A, Alexander JJ, Quigg RJ. Inhibition of complement regulation is key to the pathogenesis of active Heymann nephritis. J Exp Med. 1998;188(7):1353-8.

126. Moll S, Miot S, Sadallah S, Gudat F, Mihatsch MJ, Schifferli JA. No complement receptor 1 stumps on podocytes in human glomerulopathies. Kidney Int. 2001;59(1):160-8.

127. Ravindran A, Madden B, Charlesworth MC, Sharma R, Sethi A, Debiec H, et al. Proteomic Analysis of Complement Proteins in Membranous Nephropathy. Kidney Int Rep. 2020;5(5):618-26.

128. Salant DJ, Belok S, Madaio MP, Couser WG. A new role for complement in experimental membranous nephropathy in rats. J Clin Invest. 1980;66(6):1339-50.

129. Ren G, Doshi M, Hack BK, Alexander JJ, Quigg RJ. Rat glomerular epithelial cells produce and bear factor H on their surface that is up-regulated under complement attack. Kidney Int. 2003;64(3):914-22.

130. Gao S, Cui Z, Zhao MH. Complement C3a and C3a Receptor Activation Mediates Podocyte Injuries in the Mechanism of Primary Membranous Nephropathy. J Am Soc Nephrol. 2022.

131. Leenaerts PL, Hall BM, Van Damme BJ, Daha MR, Vanrenterghem YF. Active Heymann nephritis in complement component C6 deficient rats. Kidney Int. 1995;47(6):1604-14.

132. Baker PJ, Ochi RF, Schulze M, Johnson RJ, Campbell C, Couser WG. Depletion of C6 prevents development of proteinuria in experimental membranous nephropathy in rats. Am J Pathol. 1989;135(1):185-94.

133. Cybulsky AV, Quigg RJ, Salant DJ. Experimental membranous nephropathy redux. Am J Physiol Renal Physiol. 2005;289(4):F660-71.

134. Huang CC, Lehman A, Albawardi A, Satoskar A, Brodsky S, Nadasdy G, et al. IgG subclass staining in renal biopsies with membranous glomerulonephritis indicates subclass switch during disease progression. Mod Pathol. 2013;26(6):799-805.

135. Hoxha E, Kneißler U, Stege G, Zahner G, Thiele I, Panzer U, et al. Enhanced expression of the M-type phospholipase A2 receptor in glomeruli correlates with serum receptor antibodies in primary membranous nephropathy. Kidney Int. 2012;82(7):797-804.

136. Ma H, Sandor DG, Beck LH, Jr. The role of complement in membranous nephropathy. Semin Nephrol. 2013;33(6):531-42.

137. Zhang Y, Liu Y, Liang L, Liu L, Tang X, Tang L, et al. Effect of Glomerular Mannose-Binding Lectin Deposition on the Prognosis of Idiopathic Membranous Nephropathy. Kidney Blood Press Res. 2020;45(5):713-26.

138. Hayashi N, Okada K, Matsui Y, Fujimoto K, Adachi H, Yamaya H, et al. Glomerular mannose-binding lectin deposition in intrinsic antigen-related membranous nephropathy. Nephrol Dial Transplant. 2017;33(5):832-40.

139. Bally S, Debiec H, Ponard D, Dijoud F, Rendu J, Fauré J, et al. Phospholipase A2 Receptor–Related Membranous Nephropathy and Mannan-Binding Lectin Deficiency. J Am Soc Nephrol. 2016;27(12):3539.

140. Sethi A, Miao J, Willrich MAV, Frinack JL, Cattran DC, Fervenza FC, et al. Limited Significance of Antifactor H Antibodies in Patients with Membranous Nephropathy. Clin J Am Soc Nephrol. 2021.

141. Luo W, Olaru F, Miner JH, Beck LH, van der Vlag J, Thurman JM, et al. Alternative Pathway Is Essential for Glomerular Complement Activation and Proteinuria in a Mouse Model of Membranous Nephropathy. Front Immunol. 2018;9(1433).

142. Raats C, Luca M, Bakker M, Van der Wal A, Heeringa P, Van Goor H, et al. Reduction in glomerular heparan sulfate correlates with complement deposition and albuminuria in active Heymann nephritis. J Am Soc Nephrol. 1999;10(8):1689-99.

143. Van Den Born J, van den Heuvel LP, Bakker MA, Veerkamp JH, Assmann KJ, Weening JJ, et al. Distribution of GBM heparan sulfate proteoglycan core protein and side chains in human glomerular diseases. Kidney Int. 1993;43(2):454-63.

144. Clark SJ, Ridge LA, Herbert AP, Hakobyan S, Mulloy B, Lennon R, et al. Tissue-specific host recognition by complement factor H is mediated by differential activities of its glycosaminoglycan-binding regions. J Immunol. 2013;190(5):2049-57.

145. Kabuta T, Furuta A, Aoki S, Furuta K, Wada K. Aberrant interaction between Parkinson disease-associated mutant UCH-L1 and the lysosomal receptor for chaperone-mediated autophagy. J Biol Chem. 2008;283(35):23731-8.

146. Hartleben B, Gödel M, Meyer-Schwesinger C, Liu S, Ulrich T, Köbler S, et al. Autophagy influences glomerular disease susceptibility and maintains podocyte homeostasis in aging mice. J Clin Invest. 2010;120(4):1084-96.

147. Meyer-Schwesinger C, Meyer T, Münster S, Klug P, Saleem M, Helmchen U, et al. A new role for the neuronal ubiquitin C-terminal hydrolase-L1 (UCH-L1) in podocyte process formation and podocyte injury in human glomerulopathies. J Pathol. 2009;217(3):452-64.

148. Yang L, Wu Y, Lin S, Dai B, Chen H, Tao X, et al. sPLA2-IB and PLA2R mediate insufficient autophagy and contribute to podocyte injury in idiopathic membranous nephropathy by activation of the p38MAPK/mTOR/ULK1(ser757) signaling pathway. FASEB J. 2021;35(2):e21170.

149. Jo HA, Hyeon JS, Yang SH, Jung Y, Ha H, Jeong CW, et al. Fumarate modulates phospholipase A2 receptor autoimmunity-induced podocyte injury in membranous nephropathy. Kidney Int. 2021;99(2):443-55.

150. You YH, Quach T, Saito R, Pham J, Sharma K. Metabolomics Reveals a Key Role for Fumarate in Mediating the Effects of NADPH Oxidase 4 in Diabetic Kidney Disease. J Am Soc Nephrol. 2016;27(2):466-81.

151. Škoberne A, Behnert A, Teng B, Fritzler MJ, Schiffer L, Pajek J, et al. Serum with phospholipase A2 receptor autoantibodies interferes with podocyte adhesion to collagen. Eur J Clin Invest. 2014;44(8):753-65.

152. Podestà MA, Ruggiero B, Remuzzi G, Ruggenenti P. Ofatumumab for multirelapsing membranous nephropathy complicated by rituximab-induced serum-sickness. BMJ Case Rep. 2020;13(1).

153. Boyer-Suavet S, Andreani M, Lateb M, Savenkoff B, Brglez V, Benzaken S, et al. Neutralizing Anti-Rituximab Antibodies and Relapse in Membranous Nephropathy Treated With Rituximab. Front Immunol. 2019;10:3069.

154. Tobinai K, Klein C, Oya N, Fingerle-Rowson G. A Review of Obinutuzumab (GA101), a Novel Type II Anti-CD20 Monoclonal Antibody, for the Treatment of Patients with B-Cell Malignancies. Adv Ther. 2017;34(2):324-56.

155. Amoura Z, Remy P, Quintana Porras L, Chiche L, Chauveau D, Roccatello D, et al. Alternative Renal Response Definitions in a Randomized, Controlled Trial of Obinutuzumab for Proliferative Lupus Nephritis [abstract]. Arthritis Rheumatol. 2020;72(suppl 10).

156. Furie R, Rovin BH, Houssiau F, Malvar A, Teng YKO, Contreras G, et al. Two-Year, Randomized, Controlled Trial of Belimumab in Lupus Nephritis. N Engl J Med. 2020;383(12):1117-28.

157. Mougiakakos D, Krönke G, Völkl S, Kretschmann S, Aigner M, Kharboutli S, et al. CD19-Targeted CAR T Cells in Refractory Systemic Lupus Erythematosus. N Engl J Med. 2021;385(6):567-9.

158. Mackensen A, Müller F, Mougiakakos D, Böltz S, Wilhelm A, Aigner M, et al. Anti-CD19 CAR T cell therapy for refractory systemic lupus erythematosus. Nat Med. 2022.

159. Geara AS, Bhoj V, Hogan JJ. Bortezomib Treatment for Refractory PLA2R-Positive Membranous Nephropathy. Glomerular Dis. 2021;1(1):40-3.

160. Hartono C, Chung M, Kuo SF, Seshan SV, Muthukumar T. Bortezomib therapy for nephrotic syndrome due to idiopathic membranous nephropathy. J Nephrol. 2014;27(1):103-6.

161. Kizilbash S, Claes D, Ashoor I, Chen A, Jandeska S, Matar RB, et al. Bortezomib in the treatment of antibody-mediated rejection in pediatric kidney transplant recipients: A multicenter Midwest Pediatric Nephrology Consortium study. Pediatr Transplant. 2017;21(3).

162. Jain D, Rajab A, Young JS, Yin D, Nadasdy T, Chong AS, et al. Reversing donor-specific antibody responses and antibody-mediated rejection with bortezomib and belatacept in mice and kidney transplant recipients. Am J Transplant. 2020;20(10):2675-85.

163. Ellebrecht CT, Bhoj VG, Nace A, Choi EJ, Mao X, Cho MJ, et al. Reengineering chimeric antigen receptor T cells for targeted therapy of autoimmune disease. Science. 2016;353(6295):179-84.

164. Tenspolde M, Zimmermann K, Weber LC, Hapke M, Lieber M, Dywicki J, et al. Regulatory T cells engineered with a novel insulin-specific chimeric antigen receptor as a candidate immunotherapy for type 1 diabetes. J Autoimmun. 2019;103:102289.

165. Fransson M, Piras E, Burman J, Nilsson B, Essand M, Lu B, et al. CAR/FoxP3-engineered T regulatory cells target the CNS and suppress EAE upon intranasal delivery. J Neuroinflammation. 2012;9:112.

166. Elinav E, Waks T, Eshhar Z. Redirection of regulatory T cells with predetermined specificity for the treatment of experimental colitis in mice. Gastroenterology. 2008;134(7):2014-24.

167. Jonuleit H, Schmitt E, Kakirman H, Stassen M, Knop J, Enk AH. Infectious tolerance: human CD25(+) regulatory T cells convey suppressor activity to conventional CD4(+) T helper cells. J Exp Med. 2002;196(2):255-60.

168. Andersson J, Tran DQ, Pesu M, Davidson TS, Ramsey H, O'Shea JJ, et al. CD4+ FoxP3+ regulatory T cells confer infectious tolerance in a TGF-beta-dependent manner. J Exp Med. 2008;205(9):1975-81.

169. Ottolenghi A, Bolel P, Sarkar R, Greenshpan Y, Iraqi M, Ghosh S, et al. Life-extended glycosylated IL-2 promotes Treg induction and suppression of autoimmunity. Sci Rep. 2021;11(1):7676.

170. Saligrama N, Zhao F, Sikora MJ, Serratelli WS, Fernandes RA, Louis DM, et al. Opposing T cell responses in experimental autoimmune encephalomyelitis. Nature. 2019;572(7770):481-7.

171. Gonzalez-Figueroa P, Roco JA, Papa I, Núñez Villacís L, Stanley M, Linterman MA, et al. Follicular regulatory T cells produce neuritin to regulate B cells. Cell. 2021;184(7):1775-89.e19.

172. Guan F, Villegas G, Teichman J, Mundel P, Tufro A. Autocrine class 3 semaphorin system regulates slit diaphragm proteins and podocyte survival. Kidney Int. 2006;69(9):1564-9.

173. Rinschen MM, Gödel M, Grahammer F, Zschiedrich S, Helmstädter M, Kretz O, et al. A Multi-layered Quantitative In Vivo Expression Atlas of the Podocyte Unravels Kidney Disease Candidate Genes. Cell Rep. 2018;23(8):2495-508.

174. Sano K, Tanihara H, Heimark RL, Obata S, Davidson M, St John T, et al. Protocadherins: a large family of cadherin-related molecules in central nervous system. EMBO J. 1993;12(6):2249-56.

175. Meerabux JM, Ohba H, Fukasawa M, Suto Y, Aoki-Suzuki M, Nakashiba T, et al. Human netrin-G1 isoforms show evidence of differential expression. Genomics. 2005;86(1):112-6.

176. Chatelet F, Brianti E, Ronco P, Roland J, Verroust P. Ultrastructural localization by monoclonal antibodies of brush border antigens expressed by glomeruli. I. Renal distribution. Am J Pathol. 1986;122(3):500.

177. Chatelet F, Brianti E, Ronco P, Roland J, Verroust P. Ultrastructural localization by monoclonal antibodies of brush border antigens expressed by glomeruli. II. Extrarenal distribution. Am J Pathol. 1986;122(3):512.

178. Zheng G, Bachinsky DR, Stamenkovic I, Strickland DK, Brown D, Andres G, et al. Organ distribution in rats of two members of the low-density lipoprotein receptor gene family, gp330 and LRP/alpha 2MR, and the receptor-associated protein (RAP). J Histochem Cytochem. 1994;42(4):531-42.

179. Erhuma M, Köbel M, Mustafa T, Wulfänger J, Dralle H, Hoang-Vu C, et al. Expression of neutral endopeptidase (NEP/CD10) on pancreatic tumor cell lines, pancreatitis and pancreatic tumor tissues. Int J Cancer. 2007;120(11):2393-400.

2.14 Tables and Figures

Table 1. Disease antigens implicated in Heymann nephritis and membranous nephropathy

Antigen	Normal tissue expression (References)	Function of antigen	Prevalence of antigen in disease	IgG subclass deposited in glomeruli	Serum antibody	Patho-genicity of antibody	Complement activation	Mean age (yrs)	Sex (M: F)	Other disease associations
Heymann nephritis										
Megalin (in Fx1A)	Podocyte, proximal tubular brush border, type II pneumocytes,	Low-density lipoprotein receptor, calcium handling, mediates transcytosis of certain proteins (eg. albumin, retinol binding protein) and	100%	Rat IgG2b[a] >> Rat IgG1[b]	Yes	Yes	C3, C5b-9	NA	NA	Human ABBA disease

	epididymis [176, 177]	degradation of other proteins in lysosomes								
RAP	All cells, primarily in kidney and brain[178]	Endoplasmic reticulum chaperone for lipid receptors such as megalin	Unclear	Unclear	Yes	Yes	Unclear	NA	NA	None
Primary membranous nephropathy										
PLA2R	Podocyte[3]	Unclear in kidney. Regulates cellular senescence, migration, hormone and cytokine release	70%	IgG4	Yes (non-reducing)	Highly likely	C3, C5b-9, MBL	48	2:1	None

THSD7A	Podocyte[4]	Stabilizes and enhances podocyte adhesion	2.5%	IgG4	Yes (non-reducing)	Yes	C5b-9, MBL,[c] C3b[c]	50	1:3	Malignancy (33%)
NELL1	Osteoblast, brain, kidney tubule[51]	Unclear in kidney	2%[d]	IgG1	Yes (non-reducing)	Unclear	C3, rarely C1q	63	1:1	Malignancy (33%)
Sema3B	Most organs (especially CNS), kidney tubule, endothelial cells,	Unclear in kidney. CNS development	Unclear[e]	IgG1 >> IgG4	Yes (reducing)	Unclear	C3, rarely C1q	15	3:2	None

	podocyte[52, 172]								
PCDH7	Brain, kidney tubule[72]	Unclear in kidney. Cell signalling	2%	IgG4 >> IgG1, IgG2, IgG3	Yes (non-reducing)	Unclear	Trace C3	61	3:1	Autoimmune disease (21%), malignancy (14%)
Serine protease HTRA1	Non-specific, podocyte [70]	Unclear in kidney. Cell growth, apoptosis, and inflammation	1-2%	IgG4	Yes (non-reducing or reducing)	Unclear	C3, rarely C1q	67	1:1	None

NTNG1	Brain, podocyte[74]	Unclear in kidney. Axonal adhesion molecule	0.4%	IgG4	Yes (non-reducing)	Unclear	Unclear	58	Male in all 3 cases	None
Secondary membranous nephropathy										
EXT1/EXT2	Non-specific, podocyte in kidney[73]	Synthesise heparan-sulfate backbone of glycosaminoglycan residues on proteins	28% MLN	IgG1	No	Unclear	C3, C1q	36	1:4	Autoimmune disease (71%), malignancy (8%)
NCAM1	CNS, thyroid, adrenal, heart, stomach,	Unclear in kidney. Synaptic plasticity, neuronal migration, axonal branching,	7% MLN	IgG1 > IgG3 > IgG2, IgG4	Yes (non-reducing)	Unclear	C3, C1q	34	1:2	Autoimmune disease, especially SLE (90%)

	immune cells, kidney interstitial cells, podocyte[71]	fasciculation and synaptogenesis in CNS								
TGFBR3	Podocyte, mesangial cell, endothelial cell[75]	Accessory receptor for TGF-β signalling, protecting against autoimmunity	6% MLN	IgG1, IgG2 or IgG3	No	Unclear	C3, C1q	40	1:16	Autoimmune disease, especially SLE (82%)
CNTN1	CNS, PNS, kidney glomeruli[76]	Unclear in kidney. Neuronal cell adhesion molecule that regulates myelination and	Unclear	IgG4	Yes	Unclear[f]	C3	70	Male in all 5 cases	CIDP (100%)

		nodal/paranodal organization in CNS									
FAT1	Podocyte, kidney proximal tubular epithelial cells, CNS, skin, esophagus, lung[77]	Unclear in kidney. Mediates calcium-dependent cell-cell recognition and adhesion	Unclear	IgG4	Yes (non-reducing or reducing)	Unclear	Mild (0-1+)	C3	60	9:5	Allogeneic HSCT (100%)
Neonatal membranous nephropathy											
NEP	Podocyte, lung, intestine,	Regulate levels of various peptides (eg.	Unclear	IgG1	Yes	Yes	C3, C1q		From birth	1:1	None

	adrenal, prostate, breast, uterus, CNS[85, 179]	atrial peptide) natriuretic

RAP: receptor associated protein; NA: not applicable; ABBA: kidney anti brush border antibodies and kidney failure; PLA2R: M-type phospholipase A2 receptor 1; MBL: mannan-binding lectin; THSD7A: thrombospondin type-1 domain-containing protein 7A; NELL1: Neural epidermal growth factor-like 1 protein; Sema3B: Semaphorin 3B; CNS: central nervous system; PCDH7: Protocadherin 7; SLE: systemic lupus erythematosus; HTRA1: high temperature requirement A serine peptidase 1; NTNG1: netrin G1; EXT1/EXT2: exostosin 1/exostosin 2; MLN: membranous lupus nephritis; NCAM1: neural cell adhesion molecule 1; SLE: systemic lupus erythematosus; TGFBR3: type III transforming growth factor β receptor; CNTN1: contactin 1; PNS: peripheral nervous system; CIDP: chronic inflammatory demyelinating polyneuropathy; FAT1: protocadherin FAT1; HSCT: hematopoietic stem cell transplant; NEP: neutral endopeptidase

[a]Rat IgG2b equivalent to human IgG1

[b]Rat IgG1 equivalent to human IgG4

[c]Only in experimental data of murine glomeruli exposed to human sera containing anti-THSD7A antibodies

[d]Prevalence derived from “Wang et al. Neural Epidermal Growth Factor–Like 1 Protein–Positive Membranous Nephropathy in Chinese Patients. *Clin J Am Soc Nephrol*. 2021 May 8;16(5):727-35” since discovery cohort only reported prevalence of NELL1-associated PMN of 16% in PLA2R-negative PMN

[e]Discovery cohort only reported prevalence of Sema3B-associated PMN of 9% in PLA2R-, THSD7A-, EXT1/EXT2-, and NELL-1-negative PMN

[f]Anti-CNTN1 proven to be pathogenic in CIDP but not MN

Table 2. Complement system involvement in Heymann nephritis and membranous nephropathy

Component of the complement pathway	Change in membranous nephropathy	Comments
Classical pathway		
C1q	HN: ↑	Glomerular deposition of IgG2b in HN binds C1q.
	PMN: ↔	IgG4 (predominant IgG subclass in PLA2R-, THSD7A-, PCDH7-, HTRA1- and NTNG1-associated PMN) does not bind C1q. Predominant IgG1 (NELL-1- and Sema3B-associated PMN) not associated with C1q deposition.
	SMN: ↑/↔	IgG1 (predominant IgG subclass in EXT1/EXT2- and NCAM-1-associated MN) binds C1q. IgG4 (predominant IgG subclass in CNTN1- and FAT1-associated MN) does not bind C1q.
Lectin pathway		
MBL	HN: ↔	Glomerular MBL staining negative in HN.
	PMN: ↑	Glycosylated anti-PLA2R IgG4 allows MBL binding. MBL deposition also demonstrated in THSD7A-associated PMN.
	SMN: ?	

Alternative pathway		
Factor B / Properdin	HN: ↑ PMN: ↑ SMN: ?	Increased glomerular deposition of factor B in HN. Factor B and properdin deposition in PMN patients with MBL deficiency. Mechanism of activation unclear.
Common pathway		
C3	HN: ↑ PMN: ↑ SMN: ↑	C3 deposition is a hallmark of HN and MN (primary and secondary). Increased serum C3a and glomerular expression of C3aR demonstrated in both HN and PMN.
C5b-9	HN: ↑ PMN: ↑ SMN: ?	Glomerular deposition of C5b-9 in HN. C5b-9 deposition demonstrated in PLA2R- and THSD7A-associated PMN.
Complement regulatory proteins		
Fluid-phase	HN: ↑ PMN: ↑ SMN: ?	Increased factor H reflecting alternative pathway activation. Increased factor H reflecting alternative pathway activation. Increased vitronectin and clusterin reflecting C5b-9 activation.
Solid-phase	HN: ↓ PMN: ↓ SMN: ?	Anti-Fx1A antibodies bind Crry and CD59. Decreased CR1 and CD59, potentially reflecting podocyte loss.

HN: Heymann nephritis; PMN: primary membranous nephropathy; SMN: secondary membranous nephropathy; NA: not applicable; PLA2R: M-type phospholipase A2 receptor 1; THSD7A: thrombospondin type-1 domain-containing protein 7A; NELL-1: Neural epidermal growth factor-like 1 protein; Sema3B: Semaphorin 3B; CNS: central nervous system; PCDH7: Protocadherin 7; NTNG1: netrin G1; SLE: systemic lupus erythematosus; HTRA1: high temperature requirement A serine peptidase 1; EXT1/EXT2: exostosin 1/exostosin 2; NCAM-1: neural cell adhesion molecule 1; CNTN1: contactin 1; FAT1: protocadherin FAT1; MBL: mannan-binding lectin; C3aR: complement 3a receptor; CR1: complement receptor 1.

Figure 1.

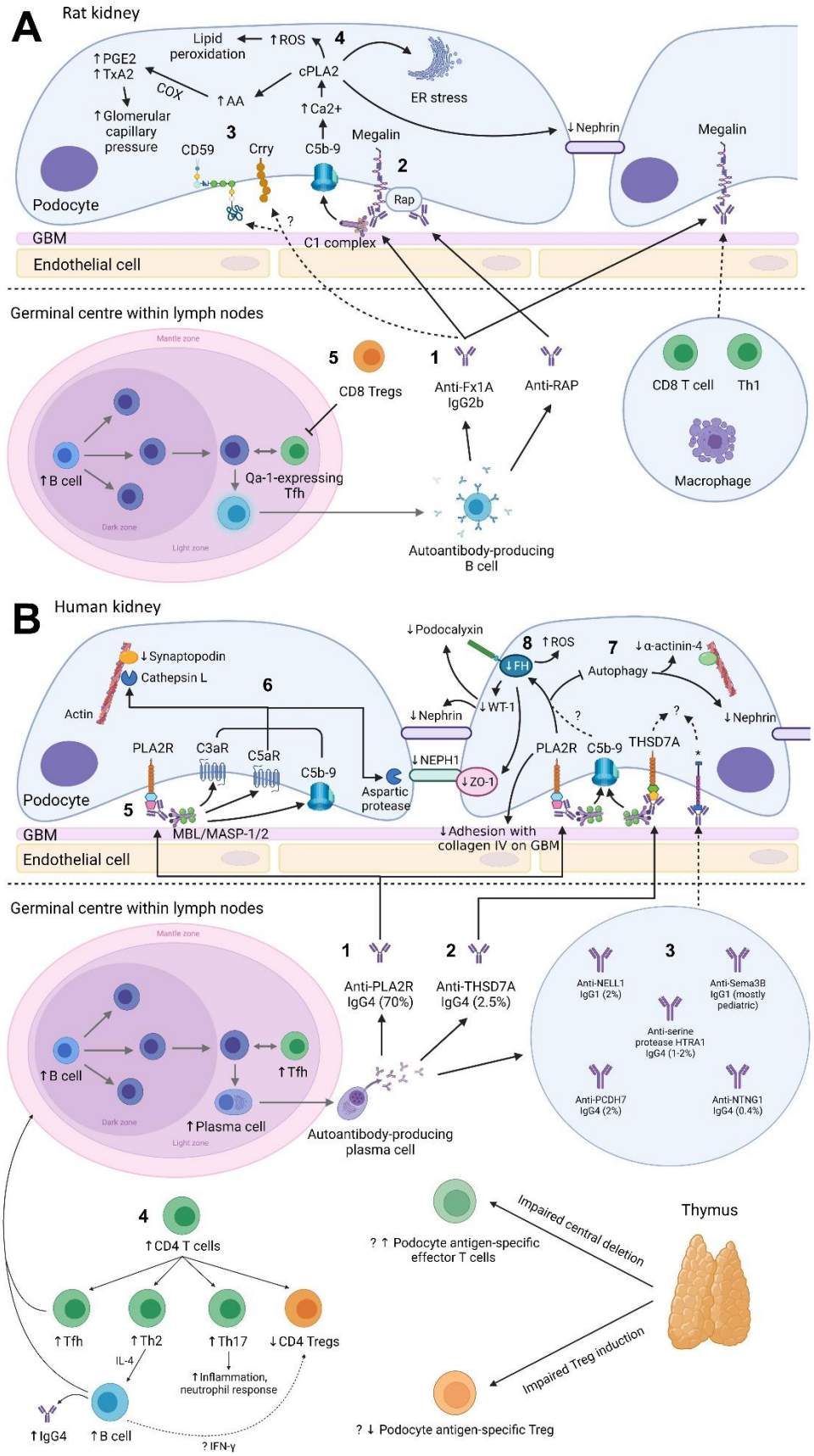
A
Rat kidney
Lipid peroxidation
↑ROS
4
↑PGE2
↑TxA2
COX
↑AA
cPLA2
ER stress
↑Glomerular capillary pressure
3
CD59
Crry
C5b-9
↑Ca2+
Megalin
↓Nephrin
Megalin
2
Rap
Podocyte
?
C1 complex
GBM
Endothelial cell
Germinal centre within lymph nodes
Mantle zone
5
CD8 Tregs
1
Anti-Fx1A IgG2b
Anti-RAP
CD8 T cell
Th1
↑B cell
Qa-1-expressing Tfh
Dark zone
Light zone
Macrophage
Autoantibody-producing B cell
B
Human kidney
↓Podocalyxin
8
↑ROS
↓FH
7
↓α-actinin-4
Autophagy
↓Synaptopodin
Cathepsin L
6
Actin
↓Nephrin
↓WT-1
?
?
↓Nephrin
PLA2R
C3aR
C5aR
C5b-9
↓NEPH1
↓ZO-1
PLA2R
C5b-9
THSD7A
Podocyte
5
Aspartic protease
GBM
MBL/MASP-1/2
↓Adhesion with collagen IV on GBM
Endothelial cell
Germinal centre within lymph nodes
Mantle zone
1
Anti-PLA2R IgG4 (70%)
2
Anti-THSD7A IgG4 (2.5%)
3
Anti-NELL1 IgG1 (2%)
Anti-Sema3B IgG1 (mostly pediatric)
Anti-serine protease HTRA1 IgG4 (1-2%)
Anti-PCDH7 IgG4 (2%)
Anti-NTNG1 IgG4 (0.4%)
↑B cell
↑Tfh
Dark zone
↑Plasma cell
Light zone
Autoantibody-producing plasma cell
4
↑CD4 T cells
? ↑ Podocyte antigen-specific effector T cells
Impaired central deletion
Thymus
↑Tfh
↑Th2
↑Th17
↓CD4 Tregs
IL-4
↑Inflammation, neutrophil response
Impaired Treg induction
↑IgG4
↑B cell
? IFN-γ
? ↓ Podocyte antigen-specific Treg

Figure 2.

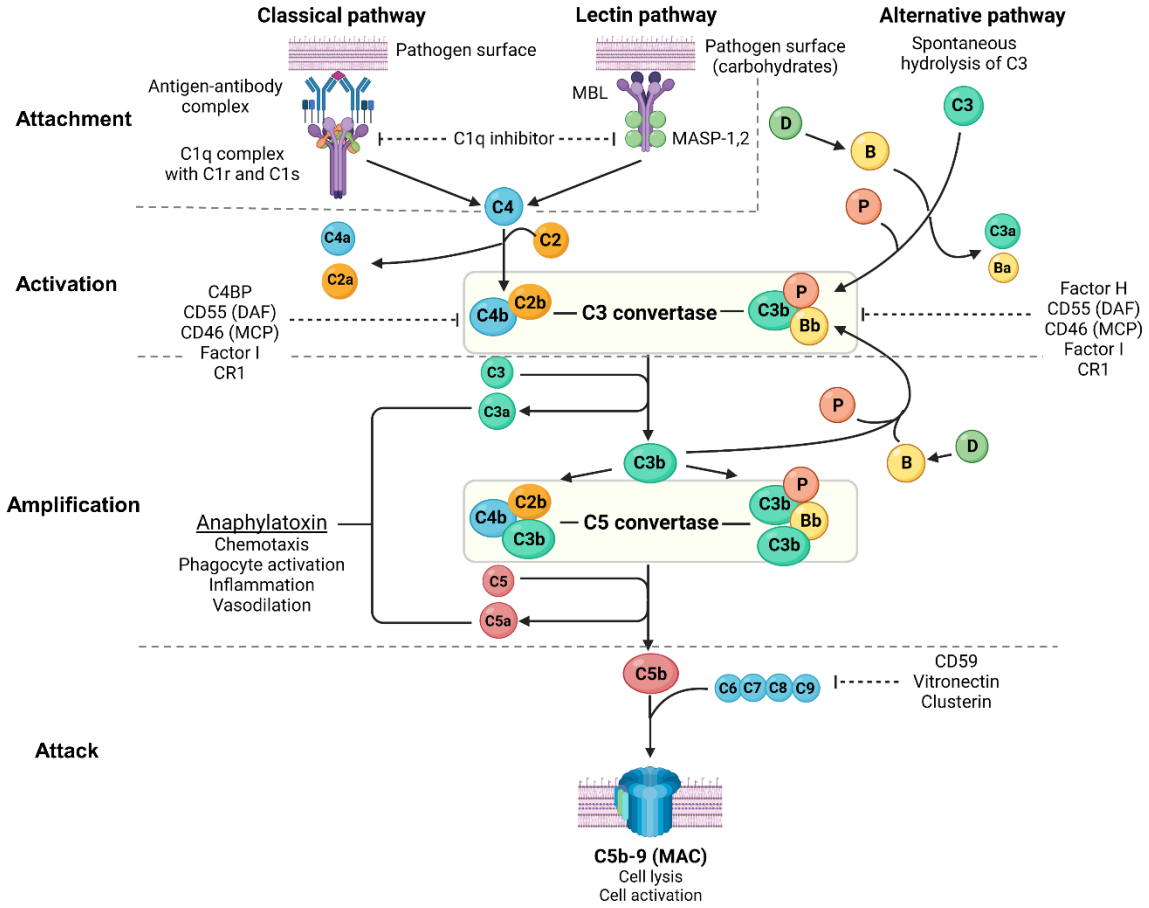

Figure 3.

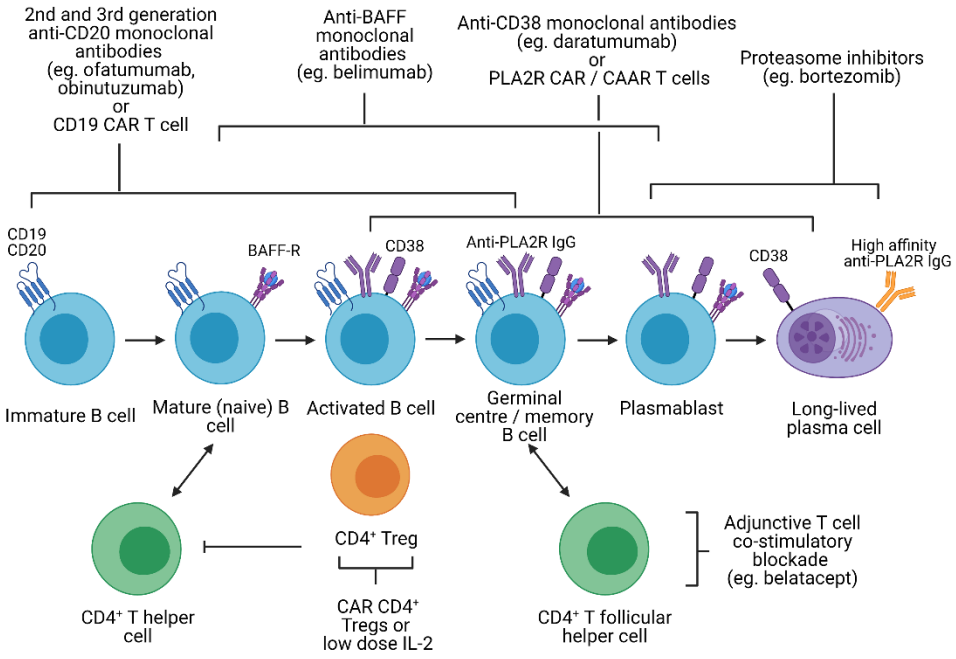

Figure legends

Figure 1. Mechanism of podocyte injury in Heymann nephritis (A) and primary membranous nephropathy (B)

Created with BioRender.com

GBM: glomerular basement membrane; ROS: reactive oxygen species; cPLA2: cytosolic phospholipase A2; PGE2: prostaglandin E2; TxA2: thromboxane A2; COX: cyclo-oxygenase; AA: arachidonic acid; ER: endoplasmic reticulum; RAP: receptor associated protein; Treg: regulatory T cell; Th1: $CD4^+$ T helper-1 cell; Tfh: $CD4^+$ T follicular helper cell; FH: fumarate hydratase; WT-1: Wilms tumor-1; PLA2R: M-type phospholipase A2 receptor 1; C3aR: C3a receptor; C5aR: C5a receptor; MBL: mannan-binding lectin; MASP: mannan-binding lectin serine protease; ZO-1: zonula occludens-1; THSD7A: thrombospondin type-1 domain-containing protein 7A; NELL1: neural epidermal growth factor-like 1 protein; Sema3B: semaphorin 3B; PCDH7: protocadherin 7; HTRA1: high temperature requirement A serine peptidase 1; NTNG1: netrin G1; Th2: $CD4^+$ T helper-2 cell; Th17: $CD4^+$ T helper-17 cell; IFN-γ: interferon-γ; *: cognate antigen for anti-NELL1, anti-Sema3B, anti-PCDH7, anti-serine protease HTRA1, and anti-NTNG1 autoantibodies respectively.

A: 1. In Heymann nephritis, anti-Fx1A antibodies bind primarily to megalin on podocytes and activate the classical complement pathway (via the IgG2b subclass). 2. Anti-RAP antibodies are also detected and may represent epitope spreading due to the association between megalin and RAP, which assists the transport of megalin from ER to cell surface. 3. Complement activation may be potentially exacerbated by binding of anti-Fx1A antibodies to complement regulatory proteins Crry and CD59. 4. Sublethal C5b-9 injury causes intracellular calcium influx, activating cPLA2, which hydrolyzes membrane phospholipids of the podocyte, ER and nuclear envelope. This causes ER stress, generation of ROS, disruption of the slit diaphragm

protein nephrin, and release of AA with subsequent COX-mediated generation of prostanoids (PGE2, TxA2) that increase glomerular filtration pressure, exacerbating proteinuria. Glomerular IgG and complement deposition attract glomerular infiltrates of $CD8^+$ T cells, Th1 cells, and macrophages, potentially via the IgG Fc receptor and anaphylatoxins C3a/C5a. 5. Autoantibody production in Heymann nephritis is at least in part dependent on Qa-1-expressing Tfh cells, which are inhibited by $CD8^+$ Tregs.

B: 1. In primary membranous nephropathy (PMN), autoantibodies are predominantly directed against PLA2R, and 2. less commonly against THSD7A, 3. NELL1, PCDH7, serine protease HTRA1 and NTNG1, except in pediatric PMN where Sema3B is the most common podocyte antigen targeted by autoantibodies. 4. Increased B cells and Tfh cells are observed, which interact in the germinal centre of lymph nodes to induce differentiation of B cells into high-affinity antibody-producing plasma cells. Autoantibodies in PMN are primarily of the IgG4 subclass, potentially due to Th2-mediated IL-4 production. Loss of tolerance to podocyte antigens such as PLA2R may be due to loss of thymus-derived podocyte antigen-specific Tregs. 5. Glycosylated anti-PLA2R IgG4 bind the MBL/MASP-1/2 complex to activate the lectin complement pathway. 6. This causes activation of C3aR and C5aR as well as deposition of C5b-9, which activates cathepsin L- and an aspartic protease-mediated proteolysis of the actin cytoskeleton protein synaptopodin and slit diaphragm protein NEPH1 respectively. Anti-PLA2R antibody-containing serum is also associated with reduced FH, impaired autophagy and reduced adhesion to the GBM, though it is unclear whether these effects are mediated via complement activation. 7. Impairment in autophagy results in internalization of nephrin and the actin cytoskeleton protein α-actinin-4. 8. Reduced FH leads to intracellular fumarate accumulation, which is associated with increased generation of ROS, reduced slit diaphragm protein ZO-1 and reduced transcription of WT-1, which normally activates the expression of

podocyte proteins nephrin and podocalyxin. The mechanisms of podocyte injury of other autoantibodies associated with PMN remain incompletely understood.

Figure 2. Overview of the complement system

Created with BioRender.com

MBL: mannan-binding lectin; MASP: mannan-binding lectin serine protease; C4BP: C4b-binding protein; DAF: decay-accelerating factor; MCP: membrane cofactor protein; CR1: complement receptor 1; MAC: membrane attack complex; C3aR: C3a receptor; C5aR: C5a receptor; PMN: primary membranous nephropathy; PLA2R: M-type phospholipase A2 receptor 1; THSD7A: thrombospondin type-1 domain-containing protein 7A.

The complement system consists of 3 pathways: classical pathway, lectin pathway and alternative pathway, which can be conceptually understood using 4A's: **attachment**, **activation**, **amplification**, and **attack** (steps of complement activation in bold text below). In the classical pathway, complement C1q **attaches** to the Fc receptor of antigen-bound antibodies (IgG1, IgG3 and IgM in humans, and IgG2a and IgG2b in rodents). The lectin pathway is similar to the classical pathway where lectins (such as ficolins, MBLs or collectins) **attach** to carbohydrates on pathogens, activating MASP-1 and MASP-2 (analogous to C1r and C1s of the classical pathway), which cleave C4 and C2 to form C3 convertase (C4b2b). In the alternative pathway, small amounts of C3 are spontaneously **activated** ("C3 tickover") due to a labile thioester bond, forming a C3b fragment that binds to factor B (B), which in turn is cleaved by factor D (D) to form the alternative pathway C3 convertase (C3bBb) that is stabilised by properdin (P), forming C3bBbP. Regardless of the pathway of activation, C3 convertase cleaves C3 into C3a and C3b, which **amplifies** alternative pathway activation whereby further factor B binds to C3b forming more C3 convertase. Apart from amplifying C3 convertase formation, C3b also acts as an opsonin and binds to C3 convertase to form C5

convertase (C4b2b3b and C3bBbC3bP), which cleaves C5 into C5a and C5b. C3a and C5a act as potent anaphylatoxins via their respective receptors (C3aR and C5aR). Complement **attack** is initiated by C5b sequentially binding C6, C7, C8, and C9 to form the MAC (C5b-9), which causes transmembrane pores that cause osmotic cell lysis or sublethal cell injury, activating internal cellular processes.

The complement system is tightly regulated by proteins present in plasma (fluid-phase) and on cell surfaces including the podocyte (solid-phase). Fluid-phase regulators include C1q inhibitor (binds C1r/C1s and MASP-1/MASP-2 to prevent classical and lectin pathway activation), C4BP (binds C4b to prevent formation of the classical/lectin pathway C3 convertase), factor H (binds C3b to prevent formation of the alternative pathway C3 convertase), factor I (cofactor for factor H and MCP, which both inhibit C3 convertase formation), vitronectin (binds the C5b-7 complex to prevent MAC formation) and clusterin (binds C7, C8, C9 to prevent MAC formation). Solid-phase regulators include DAF (dissociates C2b from C4b and Bb from C3b to inactivate C3 convertase), MCP (binds C3b and C4b to prevent C3 convertase formation), CR1 (binds C3b and C4b to prevent C3 convertase formation) and CD59 (binds C8 and C9 to prevent MAC formation).

Figure 3. Potential immunological targets for novel therapeutics in primary membranous nephropathy

Created with BioRender.com

BAFF-R: B-cell activating factor receptor; CAR: chimeric antigen receptor; CAAR: chimeric autoantibody receptor; PLA2R: M-type phospholipase A2 receptor 1; Treg: regulatory T cell.

In primary membranous nephropathy, autoreactive B cells produce autoantibodies targeting podocyte antigens (represented by PLA2R in this figure but also include thrombospondin type-1 domain-containing protein 7A, neural epidermal growth factor-like 1 protein, semaphorin

3B, protocadherin 7, high temperature requirement A serine peptidase 1, and netrin G1). These autoreactive B cells originate from the bone marrow, mature from immature B cells to mature B cells, become activated upon interaction with $CD4^+$ T helper cells (via cytokines and CD40 ligation) and undergo isotype switching. Activated B cells subsequently migrate to the germinal centre of secondary lymphoid organs where they interact with $CD4^+$ T follicular helper cells, resulting in B cell proliferation and somatic hypermutation, ultimately differentiating into plasmablast and long-lived plasma cells which secrete high-affinity autoantibodies. Immature, mature, activated and germinal centre B cells express CD19 and CD20, which can be targeted by 2^{nd} and 3^{rd} generation anti-CD20 monoclonal antibodies (eg. ofatumumab and obinutuzumab), which may be superior to rituximab, or CD19 CAR T cells. However, in cases of primary membranous nephropathy resistant to 1^{st} generation anti-CD20 monoclonal antibodies (eg. rituximab) that respond to 2^{nd} or 3^{rd} generation anti-CD20 monoclonal antibodies, this may be due to changes in the CD20 antigen that may be restricted to autoreactive B cells. CD19 and CD20 are also not expressed on plasmablasts or long-lived plasma cells which continue to secrete autoantibodies despite B cell depletion. Monoclonal antibodies targeting BAFF (eg. belimumab), preventing binding to the BAFF receptor, target both B cells and plasmablasts but not long-lived plasma cells. Proteasome inhibitors have been shown to be effective in depleting plasmablasts and plasma cells. Anti-CD38 monoclonal antibodies (eg. daratumumab) may also be effective against plasma cells, plasmablasts and B cells. However, proteasome inhibitors and anti-CD38 monoclonal antibodies are associated significant toxicity and short-duration therapy to deplete plasma cells followed by adjunctive therapy (eg. B cell depletion or T cell co-stimulatory blockade to prevent B cell activation) may be better tolerated. With the discovery of disease antigens underpinning primary membranous nephropathy, CAR T cells or CAAR T cells targeting autoantibodies (eg. anti-PLA2R) on autoreactive B cells, plasmablasts and plasma cells are conceivable. Lastly,

harnessing the capacity of $CD4^+$ regulatory T cells to induce immune tolerance at sites of inflammation independent of antigen specificity (infectious tolerance) is attractive. Such strategies may involve CAR regulatory T cells directed to the kidney (eg. targeting PLA2R on the podocyte) or low-dose IL-2, which preferentially expands regulatory T cells not effector T cells.

3.Predictive models for recurrent membranous nephropathy after kidney transplantation

3.1 Overview

Background: Recurrent membranous nephropathy (MN) post-transplantation affects 35-50% of kidney transplant recipients (KTR) and accounts for 50% allograft loss 5 years after diagnosis. Predictive factors for recurrent MN may include human leukocyte antigen (HLA)-D risk alleles, but other factors have not been explored with certainty.

Methods: The Australian and New Zealand Dialysis and Transplant (ANZDATA) registry was used to develop three prediction models for recurrent MN (Group Least Absolute Shrinkage and Selection Operator (LASSO), penalized Cox regression and random forest), which were tuned using 10-fold cross-validation in a derivation cohort with complete HLA data. KTRs with MN but incomplete HLA data formed the validation cohort. Model performance was evaluated using area under the receiver operating characteristic curve (AUC-ROC).

Results: 199 KTRs with MN were included and 25 (13%) had recurrent MN (median follow-up 5.9 years). The AUC-ROC for Group LASSO, penalized Cox regression and random forest models were 0.85 (95% confidence interval 0.76-0.94), 0.91 (0.85-0.96) and 0.62 (0.57-0.69) respectively in the derivation cohort, with moderate agreement in selected variables between the models (55-70%). In their validation cohorts, the AUC-ROC for Group LASSO and penalized Cox regression were 0.60 (0.49-0.70) and 0.73 (0.59-0.86) respectively. Variables of importance chosen by all models included recipient HLA-A2, donor HLA-DR12, donor-recipient HLA-B65 and HLA-DR12 match.

Conclusions: A penalized Cox regression performed reasonably for predicting recurrent MN and was superior to Group LASSO and random forest models. These models highlighted the importance of donor-recipient HLA characteristics to recurrent MN, though validation in larger datasets is required.

3.2 Introduction

Primary membranous nephropathy (MN) is one of the commonest causes of primary nephrotic syndrome in adults and is associated with progression to kidney failure in approximately one-third of patients.[1] While kidney transplantation is the preferred treatment modality in kidney failure, recurrent MN occurs in 35-50% of kidney allografts and is associated with subsequent graft loss in half of these patients.[2-4] Autoantibodies against the podocyte antigen phospholipase-A2 receptor (PLA2R) underpins 70% of primary MN and in two small case series, detectable anti-PLA2R antibodies at time of kidney transplantation was associated with recurrent MN with a positive predictive value of 57-83% and negative predictive value of 42-60%.[5, 6]

Genome-wide association studies (GWAS) have also revealed the importance of the immune system in the pathogenesis of MN, identifying risk alleles associated with primary MN in the general population: human leukocyte antigen (HLA)-DQA1*0501 (DQ2 by serology) in Europeans, DRB1*1501 (DR15 by serology) in East Asians, and HLA-DRB1*0301 (DR17 by serology) in both ethnicities.[7, 8] In kidney transplant recipients with MN, a multicenter case series of 93 recipients (55 with recurrent MN) found an association with recipient HLA-A3 but not HLA-DR or HLA-DQ serotypes.[9] Targeted PLA2R1 and HLA-D loci sequencing in 145 kidney transplant recipients with primary MN (54 with recurrent MN) found an association with two non-coding HLA-D single nucleotide polymorphisms (SNP) (rs9271550 and rs9271705) when present on the donor but not the recipient.[10] Prediction models for recurrent MN were improved using a genetic risk score built using these risk SNPs at the HLA-D locus and PLA2R1 locus in addition to clinical variables (area under the curve (AUC) 0.81 compared to AUC 0.71 with clinical variables alone).[10] These studies, however, are largely focused on Caucasian populations and next-generation sequencing of HLA-D and PLA2R1 loci are not routinely available to assist in the prediction of recurrent MN after kidney transplantation. In this study, we aimed to develop prediction models for recurrent MN in a national

cohort of kidney transplant recipients using routinely collected clinical data including donor-recipient HLA serotypes and HLA mismatch characteristics.

3.3 Material and Methods

3.3.1 Study population

This study was reported in adherence to the Transparent Reporting of a multivariable prediction model for Individual Prognosis Or Diagnosis (TRIPOD) statement.[11] Ethics approval was obtained from the Sydney Children's Hospitals Network Human Research Ethics Committee (HREC/ETH00021). We performed a cohort study in kidney transplant recipients with MN as the primary kidney disease from the Australian and New Zealand Dialysis and Transplant (ANZDATA) registry between 1963 and 2020. Indications for kidney allograft biopsy were determined by each individual transplant unit and were not standardized across the cohort. Recurrent MN was defined as biopsy-proven MN post-transplantation and non-recurrent MN was defined as the absence of biopsy-proven MN post-transplantation since data on proteinuria and anti-PLA2R antibody titers were not available in ANZDATA. Due to the association between HLA and MN, donor and recipient pairs without complete HLA serotyping for HLA-A/B/DR/DQ were excluded from the derivation cohort used for building the prediction models. While imputation based on HLA serological typing is potentially feasible using the Allele Frequencies Net Database (AFND),[12] Haplostats,[13, 14] and the international ImMunoGeneTics project (IMGT)/HLA Database,[15] these are unlikely to be as accurate as using computational analysis with modern next-generation sequencing techniques.[16-19] For recipients who had recurrent MN in more than one kidney transplant, only the first episode of recurrence was included.

3.3.2 Data collection

Biopsy-proven recurrent MN was the outcome of interest. Covariates of interest included recipient characteristics (age, ethnicity, weight, dialysis vintage, blood group, and comorbidities), donor characteristics (age and blood group), and transplant characteristics (HLA-A/B/DR/DQ serotypes from donor and recipient pairs, HLA-matched serotypes from donor and recipient pairs, total HLA mismatch, donor type, regraft status, maximum pre-transplant panel reactive antibody, biopsy-proven rejection, induction immunosuppression regime, maintenance immunosuppression regime upon transplantation, and transplant era based on decade of transplantation). We also assessed HLA-matched serotypes from donor and recipient pairs in the same model due to an association between zero HLA-mismatch and recurrent glomerulonephritis after kidney transplantation.[20, 21]

3.3.3 Statistical analysis

In the derivation cohort, Group Least Absolute Shrinkage and Selection Operator (LASSO) regression, a form of penalized logistic regression, was performed for variable selection using the R package 'grpreg'. In a simple regression, the model may put considerable weighting on certain variables that are deemed to be important, resulting in overfitting. In contrast, LASSO regression performs L1 regularization where a penalization parameter (λ) is multiplied to the sum of the absolute values of the regression coefficients, imposing a penalty on the size of regression coefficients and shrinking some coefficients to zero during model building. As a result, regularization incorporates both model fitting and variable selection simultaneously, which is useful in high dimensional datasets.[22, 23] Multinomial variables (ethnicity, recipient and donor blood group, and smoking status) and ordinal variables (total HLA mismatch and HLA-A/B/DR/DQ loci mismatch) were grouped together. Group LASSO was chosen over ridge regression since LASSO performs variable selection and yields a sparse model by shrinking coefficient estimates of some variables to zero. In comparison, ridge regression performs L2 regularization, which also shrinks some coefficient estimates but not to zero and therefore does not eliminate variables. Group LASSO was chosen over stepwise logistic

regression, which would be prone to false positive variable selection due to multiple testing in a high dimensional dataset. Furthermore, LASSO handles sparse events well and therefore is suitable for building prediction models for rare events such as recurrent MN.[24, 25] The λ that minimized the binomial deviance was chosen by 10-fold cross-validation, which involved dividing our dataset into 10 subsets (9 for training and one for validation). The error rates are then averaged across 10 trials to obtain the total efficiency of the modelling. Multiple imputation for missing data was performed using the R package 'mice' prior to variable selection. We generated 100 imputed datasets in which cross-validated Group LASSO was performed. Model performance was assessed using the mean area under the receiver operating characteristic curve (AUC-ROC) and model accuracy (defined as the number of correct classifications divided by the total number of classifications) in the datasets created by 10-fold cross-validation with their corresponding 95% confidence interval (CI), which was calculated by the R package 'pROC'. Variable importance was determined by calculating its frequency of being selected in the 10-fold cross-validation.

3.3.4 Sensitivity analysis

In the subgroup of kidney transplant recipients in the derivation cohort with recorded time-to-recurrent MN, we performed group penalized Cox regression using the 'cv.grpsurv' function in the R package 'grpreg'. Time-to-graft loss was chosen as the time variable for kidney transplant recipients without recurrent MN. The λ which minimized the partial likelihood deviance was chosen by 10-fold cross-validation. Random forest was also performed in the derivation cohort to determine the sensitivity of algorithm variable selection using penalized regression. Random forest was chosen over single decision tree regression since it builds multiple decision trees (reducing high variance associated with single trees) on bootstrapped training samples using a random selection of variables at each split to decorrelate the trees (reducing correlation associated with multiple decision trees utilizing all variables) and therefore reduces overfitting. We performed 10-fold cross-validation

repeated five times to select the number of random variables used at each split and number of trees used in the forest which maximized the AUC-ROC. Variable importance plots based on the mean decrease of accuracy over all out-of-bag cross validated predictions were evaluated in the 100 imputed datasets using the tuned random forest model. Variables are ranked in descending order of importance in the variable importance plot, and variables above the inflection point when the curve of the variable importance plot flattens were selected as previously described.[26] Variables selected in at least 50 of the 100 variable importance plots were compared with variables selected using Group LASSO. Random forest, parameter tuning, and variable importance plots were performed using the R package 'caret'. Model performance of penalized Cox regression and random forest were assessed using the cross-validated AUC-ROC and model accuracy calculated by the R package 'pROC'.

3.3.5 Validation cohort

To further evaluate the model performance of the Group LASSO, penalized Cox regression and random forest models, we created separate validation cohorts from kidney transplant recipients initially excluded due to incomplete HLA serotyping though retaining predictors driving each model. Model performance was assessed using AUC-ROC and model accuracy with their corresponding 95% CI calculated by the R package 'pROC'. Multiple imputation on non-HLA variables was performed in the validation cohort separate from the derivation cohort.

3.4 Results

3.4.1 Population characteristics

Of the 32,858 kidney transplant recipients in the ANZDATA registry, 554 recipients had MN as their primary kidney disease of whom 199 donor-recipient pairs (36%) had complete HLA serotyping for donor and recipient HLA-A/B/DR/DQ and were included in the study (Figure 1). Nine variables (4%)

had missing values (range 2-25%) (Figure 2). The median age of kidney transplant recipients was 48 years (interquartile range [IQR] 21) and the majority were male (73%) of Caucasian ethnicity (82%) (Table 1). The median donor age was 42 years (IQR 24). The median follow-up time was 8.04 years (IQR 14.90). The majority of kidney transplants occurred during the periods of 1990-1999 (42%) and 2010-2019 (41%). Living donation occurred in 27% and blood group incompatible transplants occurred in 3% of recipients. The proportion of recipients with a total HLA mismatch of 0 was 6%, 1 or 2 was 32%, 3 or 4 was 39%, and 5 or 6 was 23%. Biopsy-proven acute cellular rejection occurred in 19%, biopsy-proven acute antibody-mediated rejection occurred in 3%, and the median maximum pre-transplant panel-reactive antibody was 0% (IQR 20). The most common induction immunosuppression was interleukin-2 (IL2) receptor blocker (37%), and the most common maintenance immunosuppressive agents were tacrolimus (50%) or cyclosporin (56%), mycophenolate (67%) and corticosteroids (99%).

A total of 25 kidney transplant recipients experienced recurrent MN (13%), predominantly during the period of 1990-1999 (68%). The time to biopsy-proven disease recurrence was reported in 17 of 25 kidney transplant recipients experiencing recurrent MN (median 4.72 [IQR 4.13] years). Two recipients had recurrent MN in more than one kidney transplant and only the first episode of recurrence was included in the study. HLA serotypes in donor-recipient pairs are shown in Table 2.

3.4.2 Group LASSO

Model performance using Group LASSO for predicting recurrent MN in the derivation cohort was good (AUC-ROC 0.85, 95% CI 0.76-0.94 and model accuracy 88%, 84-93%) (Figure 3). Ten-fold cross-validation in the derivation cohort yielded an average error rate of 12.6%. Of the 222 variables (Table 3), Group LASSO selected 10 variables in at least 50 of the 100 imputed datasets as driving model predictions (Figure 4). Of these 10 selected variables, 6 were selected in at least 90 of the 100 imputed datasets. Variables driving model prediction were prior history of hepatitis C, IL2 receptor

blocker induction, mycophenolate maintenance, azathioprine maintenance, other maintenance immunosuppression (medications included in this variable are detailed in Table 1), recipient HLA-A2, recipient HLA-B65, donor HLA-DR12, donor-recipient HLA-B65 match, and donor-recipient HLA-DR12 match. Six variables were chosen in all cross-validated folds and of equal importance: mycophenolate maintenance, other maintenance immunosuppression, recipient HLA-A2, recipient HLA-B65, donor-recipient HLA-B65 match, and donor-recipient HLA-DR12 match (Table 4).

3.4.3 Sensitivity analysis

In the subgroup of kidney transplant recipients experiencing recurrent MN with recorded time-to-recurrence (17 of 25 recipients), penalized Cox regression performed well in predicting recurrent MN in the derivation cohort (AUC-ROC 0.91, 0.85-0.96 and model accuracy 69%, 63-76%) (Figure 3). Nine variables, all chosen in at least 90 of the 100 imputed datasets, were selected as driving model predictions, including recipient HLA-A2, recipient HLA-B65, recipient HLA-DR17, donor HLA-DR12, donor HLA-DQ4, donor-recipient HLA-B51 match, donor-recipient HLA-B65 match, donor-recipient HLA-DR12 match, and donor-recipient HLA-DR17 match (Figure 4). Of these 9 variables, 5 (55%) were also chosen by Group LASSO. Eight variables were chosen in all cross-validated folds and of equal importance: recipient HLA-A2, recipient HLA-B65, recipient HLA-DR17, donor HLA-DR12, donor HLA-DQ4, donor-recipient HLA-B65 match, donor-recipient HLA-DR12 match, and donor-recipient HLA-DR17 match (Table 4).

Random forest performed poorer for predicting recurrent MN in the derivation cohort than Group LASSO (AUC-ROC 0.62, 0.57-0.69 and model accuracy 51%, 44-58%) (Figure 3). Random forest selected 7 variables in at least 50 of the 100 imputed datasets as driving model predictions (Figure 4), all of which were also selected by Group LASSO. The top 3 variables driving model predictions were donor-recipient HLA-DR12 match, recipient HLA-A2, and mycophenolate maintenance (Table 4).

3.4.4 Model validation

The validation cohort for the Group LASSO model was created from kidney transplant recipients with MN and complete HLA serotyping for recipient HLA-A/B/DR and donor HLA-B/DR (required for model predictors) but missing data for donor HLA-A/DQ and recipient HLA-DQ (therefore excluded from the derivation cohort). This comprised 275 kidney transplant recipients, 34 (12%) of whom had recurrent MN (Table 5). Group LASSO model performance in the validation cohort was poor (AUC-ROC 0.60, 0.49-0.70 and model accuracy 61%, 55-67%) (Figure 5). In comparison, the penalized Cox regression model performance in its validation cohort was reasonable (AUC-ROC 0.73, 0.59-0.86 and model accuracy 59%, 49-68%) (Figure 5). Kidney transplant recipients in this validation cohort had complete HLA serotyping for recipient HLA-A/B/DR and donor HLA-B/DR/DQ but missing data for donor HLA-A and recipient HLA-DQ (99 kidney transplant recipients, 7 (7%) with recurrent MN (Table 6)). In the random forest model, variables from all recipient and donor HLA serotype groups contributed to model predictions and a validation cohort could not be generated.

3.5 Discussion

In this study of almost 200 kidney transplant recipients with MN, we developed cross-validated prediction models for recurrent MN using Group LASSO, penalized Cox regression and random forest, which incorporated routinely collected clinical data from a nation-wide transplant cohort (ANZDATA) including donor-recipient HLA serotypes and HLA mismatch characteristics. We found Group LASSO and penalized Cox regression performed well at predicting recurrent MN in the derivation cohort and had superior performance to random forest. However, Group LASSO and penalized Cox regression model performance in their respective validation cohort was poor and reasonable respectively, though differences in the validation cohorts for each model preclude direct comparison of model performance. There was reasonable agreement in variables driving predictions

across the Group LASSO and random forest models, which were recipient HLA-A2, donor HLA-DR12, donor-recipient HLA-B65 match and donor-recipient HLA-DR12 match, mycophenolate maintenance, azathioprine maintenance, and IL2 receptor blocker induction. Caution is needed in interpreting the importance of immunosuppression variables chosen as it may reflect differences in the transplant era between kidney transplant recipients with recurrent MN and those without recurrent MN in the ANZDATA registry. We investigated whether the association between zero HLA mismatch and recurrent glomerulonephritis was driven by specific HLA and found donor-recipient HLA-B65 match and donor-recipient HLA-DR12 match contributed to prediction models for recurrent MN.[21] While this suggests mechanisms independent of allograft rejection contribute to recurrent MN, the potential mechanism by which HLA matching contributes to recurrent glomerulonephritis remains poorly understood and its role should be interpreted with caution since this association has been mostly reported in retrospective studies. Variables were chosen by supervised feature selection using penalized regression and ensemble tree machine learning techniques, which addressed the issues of overfitting and multiple testing associated with stepwise feature selection in our high dimensional dataset.[27, 28]

While multiple studies have identified risk factors for recurrent MN after kidney transplantation such as detectable pre-transplant anti-PLA2R autoantibody, steroid-free immunosuppression, recipient HLA-A3 and donor risk HLA-D and PLA2R1 alleles,[3, 6, 9, 10, 29] prediction models to identify patients at high risk of recurrent MN (or other forms of glomerulonephritis) using routine pre-transplant clinical data have not been comprehensively evaluated. These predictive approaches may inform clinicians on patients requiring closer monitoring of proteinuria, anti-PLA2R antibody titer and/or protocol allograft biopsies to detect recurrent MN post-transplantation. Early diagnosis of recurrent MN may facilitate timely treatment with rituximab.[30] However, external and prospective validation of our prediction models are required.

Agreement between the Group LASSO, penalized Cox regression and random forest models in our study regarding the importance of donor-recipient HLA in predicting recurrent MN offer potential

insights into the pathogenesis of recurrent MN, which remains incompletely understood. Class I HLA such as HLA-A2 may play a role in directly activating cytotoxic CD8 T cells, which mediate glomerular injury downstream of antibody-deposition in Heymann nephritis, a rat model of MN.[31] However, the role of CD8 T cells in MN is less clear with conflicting reports on the proportion of CD8 T cells in MN compared to healthy.[32, 33]

The mechanism underpinning class II HLA-mediated autoimmune effector mechanisms or immune tolerance are better understood.[34] In recurrent MN, class II HLA-DR12 may activate autoreactive CD4 T cells. However, HLA-DR12 is different from MN risk alleles in the general population, which is unlikely explained by differences in podocyte antigens driving recurrent MN due to positive glomerular staining for PLA2R in recipients with recurrent PLA2R-associated MN.[6]

Alternatively, HLA-A2 and HLA-DR12 may contribute indirectly to recurrent MN via molecular mimicry whereby donor HLA-recipient HLA complexes are also recognized by PLA2R-specific recipient T cells.[35] Finally, HLA-A2 and HLA-DR12 may not be mechanistically involved in recurrent MN but represent haplotypes associated with recurrent MN via linkage disequilibrium..[36] HLA-DR12 is in linkage disequilibrium with HLA-DQA1*0501, which is not consistent with a study by Berchtold et al that identified two donor non-coding HLA-D SNPs associated with recurrent MN, none of which were in linkage disequilibrium with MN risk alleles such as HLA-DQA1*0501.[10] While Berchtold et al performed molecular HLA typing and validated their results in a replication cohort, their analysis did not include class I HLA loci. Our results also disagree with a multi-center case series by Batal et al, which analyzed HLA-A/B/DR/DQ serotypes and identified an association between recurrent MN and older recipient age, living related donors, steroid-free immunosuppression, and recipient HLA-A3.[9] These discrepancies may be due to different diagnostic criteria for recurrent MN.

Our study has several strengths and limitations. We developed prediction models for recurrent MN in a large national transplant registry, which minimizes the potential risk of selection bias associated

with case-series studies. These models utilized routinely collected pre-transplant clinical data including donor-recipient HLA serotypes and HLA mismatch characteristics, which improves the potential translation of these models. We addressed the issue of missing data using multiple imputation, and the issue of high dimensional data using Group LASSO penalized regression. We demonstrated the robustness of our results with another machine learning method (random forest) and used penalized Cox regression to analyze the subgroup of our cohort with time-to-recurrent MN data. Despite the relatively small derivation cohort used to build the prediction models, we utilized patients initially excluded for incomplete HLA data to form validation cohorts for our models, representing an efficient use of our limited dataset.

However, there were many limitations in this study. Firstly, our study sample size was small despite analyzing a national cohort of kidney transplant recipients, and the certainty of our results were low with wide confidence intervals. Therefore, the findings of our study are solely exploratory. Furthermore, our study population was limited to Australia and New Zealand, and predominantly of Caucasian ethnicity, limiting the generalizability of our results. Second, molecular HLA typing was not available for any kidney transplant recipients with MN in the ANZDATA registry. It is likely that recurrent MN is driven by specific HLA allelic variants and the lack of granular HLA data for all recipients and donors in transplant registries may potentially bias our findings since even single amino-acid substitutions in the HLA-DR alpha-chain can modify the peptide-binding groove and affect T cell responses.[37] Furthermore, HLA-DQ serotyping was unavailable in 267 (48%) of the 554 kidney transplant recipients with MN and HLA-DP serotyping was mostly unavailable. This may have limited our models' predictive performance since class II HLA are frequently associated with autoimmunity.[38, 39] We also did not perform HLA imputation due to the inaccuracy of HLA serotype imputation compared to HLA allelic imputation. Third, detection and misclassification bias is likely present with a lower rate of recurrent MN in ANZDATA (13%) compared to existing literature (35-50%).[2-4] This may represent incomplete reporting and/or differences in clinical practice between treatment sites and time periods such as protocol biopsies post-transplantation, which have been

associated with higher rates and earlier detection of disease recurrence (median time to recurrence 4-15 months in studies implementing protocol biopsies compared to 56 months in ANZDATA).[2, 5, 6] This suggests that the clinical practice of protocol biopsies were limited in our cohort and that biopsy-proven diagnosis of recurrent MN occurred late after detection of relatively high levels of proteinuria, though proteinuria at time of diagnosis was not available in our cohort. As a result, it is likely that mild forms of recurrent MN were not diagnosed, representing misclassification bias. Fourth, our findings were not confirmed in an external validation cohort. Despite evaluating a large transplant registry, cases of recurrent MN were small and HLA serotyping incomplete, which prevented us from dividing into separate derivation and validation cohorts. We addressed this issue by using 10-fold cross validation to balance efficient data usage and avoid individual splits in our dataset that may be poor choices. Furthermore, we developed separate validation cohorts for the Group LASSO and penalized Cox regression models using kidney transplant recipients initially excluded for incomplete HLA data but retained predictors driving each model. However, validation cohorts differed between models, preventing direct comparison of model performance. Fifth, anti-PLA2R antibody titer at transplantation, pre-transplant proteinuria, and pre-transplant serum albumin, known predictors of recurrent MN post-transplantation, were not available in the ANZDATA registry.[3] However, anti-PLA2R antibody data would be unavailable for most recipients since PLA2R was discovered 46 years after the inception of the ANZDATA registry. Furthermore, discovery of other podocyte antigens targeted by autoantibodies in MN over the past decade suggest MN is comprised of different disease entities with distinct drivers of disease recurrence.[40, 41] Lastly, our relatively small sample size with high proportion of missingness may affect the statistical validity of using multiple imputation to handle missing data.

In conclusion, we developed Group LASSO, penalized Cox regression and random forest prediction models for recurrent MN in kidney transplant recipients, which remains incompletely understood, challenging to predict and an important cause of allograft loss in recipients with MN. Donor-recipient HLA characteristics were major drivers of model predictions. Our findings are exploratory and

require further external and prospective validation in larger datasets. Future studies evaluating prediction models for recurrent MN utilizing molecular HLA typing, stratified by underlying disease antigen and associated autoantibody status before transplantation may be possible using data linkage between transplant registries and existing biorepositories, which may assist clinical decision-making and management of kidney transplant recipients with MN.

3.6 References

1. Lerner GB, Virmani S, Henderson JM, et al. A conceptual framework linking immunology, pathology, and clinical features in primary membranous nephropathy. Kidney Int. 2021;100(2):289-300.

2. Dabade TS, Grande JP, Norby SM, et al. Recurrent idiopathic membranous nephropathy after kidney transplantation: a surveillance biopsy study. Am J Transplant. 2008;8(6):1318-22.

3. Grupper A, Cornell LD, Fervenza FC, et al. Recurrent Membranous Nephropathy After Kidney Transplantation: Treatment and Long-Term Implications. Transplantation. 2016;100(12):2710-6.

4. Moroni G, Gallelli B, Quaglini S, et al. Long-term outcome of renal transplantation in patients with idiopathic membranous glomerulonephritis (MN). Nephrol Dial Transplant. 2010;25(10):3408-15.

5. Debiec H, Martin L, Jouanneau C, et al. Autoantibodies specific for the phospholipase A2 receptor in recurrent and De Novo membranous nephropathy. Am J Transplant. 2011;11(10):2144-52.

6. Kattah A, Ayalon R, Beck LH, Jr., et al. Anti-phospholipase A_2 receptor antibodies in recurrent membranous nephropathy. Am J Transplant. 2015;15(5):1349-59.

7. Stanescu HC, Arcos-Burgos M, Medlar A, et al. Risk HLA-DQA1 and PLA(2)R1 alleles in idiopathic membranous nephropathy. N Engl J Med. 2011;364(7):616-26.

8. Xie J, Liu L, Mladkova N, et al. The genetic architecture of membranous nephropathy and its potential to improve non-invasive diagnosis. Nat Commun. 2020;11(1):1600.

9. Batal I, Vasilescu ER, Dadhania DM, et al. Association of HLA Typing and Alloimmunity With Posttransplantation Membranous Nephropathy: A Multicenter Case Series. Am J Kidney Dis. 2020;76(3):374-83.

10. Berchtold L, Letouzé E, Alexander MP, et al. HLA-D and PLA2R1 risk alleles associate with recurrent primary membranous nephropathy in kidney transplant recipients. Kidney Int. 2021;99(3):671-85.

11. Collins GS, Reitsma JB, Altman DG, et al. Transparent Reporting of a multivariable prediction model for Individual Prognosis or Diagnosis (TRIPOD): the TRIPOD statement. Ann Intern Med. 2015;162(1):55-63.

12. Gonzalez-Galarza FF, McCabe A, Santos E, et al. Allele frequency net database (AFND) 2020 update: gold-standard data classification, open access genotype data and new query tools. Nucleic Acids Res. 2020;48(D1):D783-d8.

13. Gragert L, Madbouly A, Freeman J, et al. Six-locus high resolution HLA haplotype frequencies derived from mixed-resolution DNA typing for the entire US donor registry. Hum Immunol. 2013;74(10):1313-20.

14. Paunić V, Gragert L, Madbouly A, et al. Measuring ambiguity in HLA typing methods. PLoS One. 2012;7(8):e43585.

15. Robinson J, Halliwell JA, Hayhurst JD, et al. The IPD and IMGT/HLA database: allele variant databases. Nucleic Acids Res. 2015;43(Database issue):D423-31.

16. Cook S, Choi W, Lim H, et al. Accurate imputation of human leukocyte antigens with CookHLA. Nat Commun. 2021;12(1):1264.

17. Jia X, Han B, Onengut-Gumuscu S, et al. Imputing amino acid polymorphisms in human leukocyte antigens. PLoS One. 2013;8(6):e64683.

18. Zheng X, Shen J, Cox C, et al. HIBAG--HLA genotype imputation with attribute bagging. Pharmacogenomics J. 2014;14(2):192-200.

19. Naito T, Suzuki K, Hirata J, et al. A deep learning method for HLA imputation and trans-ethnic MHC fine-mapping of type 1 diabetes. Nat Commun. 2021;12(1):1639.

20. Allen PJ, Chadban SJ, Craig JC, et al. Recurrent glomerulonephritis after kidney transplantation: risk factors and allograft outcomes. Kidney Int. 2017;92(2):461-9.

21. Jeon HJ, Kim YS, Lee SM, et al. The effect of recurrent glomerulonephritis and acute rejection episodes in zero human leukocyte antigen-mismatched kidney transplantation. Transplant Proc. 2012;44(3):600-6.

22. Au EH, Francis A, Bernier-Jean A, et al. Prediction modeling-part 1: regression modeling. Kidney Int. 2020;97(5):877-84.

23. Coorey CP, Sharma A, Muller S, et al. Prediction modeling-part 2: using machine learning strategies to improve transplantation outcomes. Kidney Int. 2021;99(4):817-23.

24. Huang J, Ma S, Zhang CH. Adaptive Lasso for sparse high-dimensional regression models. Stat Sin. 2008;1:1603-18.

25. Simon N, Friedman J, Hastie T, et al. A sparse-group lasso. J Comput Graph Stat. 2013;22(2):231-45.

26. Genuer R, Poggi JM, Tuleau-Malot C. Variable selection using random forests. Pattern Recognit Lett. 2010;31(14):2225-36.

27. Emmert-Streib F, Dehmer M. High-Dimensional LASSO-Based Computational Regression Models: Regularization, Shrinkage, and Selection. Mach Learn Knowl Extr. 2019;1(1):359-83.

28. Borboudakis G, Tsamardinos I. Forward-Backward Selection with Early Dropping. J Mach Learn Res. 2019;20(1):276-314.

29. Quintana LF, Blasco M, Seras M, et al. Antiphospholipase A2 Receptor Antibody Levels Predict the Risk of Posttransplantation Recurrence of Membranous Nephropathy. Transplantation. 2015;99(8):1709-14.

30. Sprangers B, Lefkowitz GI, Cohen SD, et al. Beneficial effect of rituximab in the treatment of recurrent idiopathic membranous nephropathy after kidney transplantation. Clin J Am Soc Nephrol. 2010;5(5):790-7.

31. Penny MJ, Boyd RA, Hall BM. Permanent CD8(+) T cell depletion prevents proteinuria in active Heymann nephritis. J Exp Med. 1998;188(10):1775-84.

32. Cagnoli L, Tabacchi P, Pasquali S, et al. T cell subset alterations in idiopathic glomerulonephritis. Clin Exp Immunol. 1982;50(1):70-6.

33. Rosenzwajg M, Languille E, Debiec H, et al. B- and T-cell subpopulations in patients with severe idiopathic membranous nephropathy may predict an early response to rituximab. Kidney Int. 2017;92(1):227-37.

34. Ooi JD, Petersen J, Tan YH, et al. Dominant protection from HLA-linked autoimmunity by antigen-specific regulatory T cells. Nature. 2017;545(7653):243-7.

35. Robson KJ, Kitching AR. Recurrent membranous nephropathy after transplantation: donor antigen and HLA converge in defining risk. Kidney Int. 2021;99(3):545-8.

36. Morris DL, Taylor KE, Fernando MM, et al. Unraveling multiple MHC gene associations with systemic lupus erythematosus: model choice indicates a role for HLA alleles and non-HLA genes in Europeans. Am J Hum Genet. 2012;91(5):778-93.

37. Zeliszewski D, Golvano JJ, Gaudebout P, et al. Implication of HLA-DR residues at positions 67, 71, and 86 in interaction between HLA-DR11 and peptide HA306-320. J Immunol. 1993;151(11):6237-47.

38. Gough SC, Simmonds MJ. The HLA Region and Autoimmune Disease: Associations and Mechanisms of Action. Current genomics. 2007;8(7):453-65.

39. Gebe JA, Swanson E, Kwok WW. HLA class II peptide-binding and autoimmunity. Tissue Antigens. 2002;59(2):78-87.

40. Tomas NM, Beck LH, Jr., Meyer-Schwesinger C, et al. Thrombospondin type-1 domain-containing 7A in idiopathic membranous nephropathy. N Engl J Med. 2014;371(24):2277-87.

41. Sethi S. New 'Antigens' in Membranous Nephropathy. J Am Soc Nephrol. 2021;32(2):268-78.

3.7 Tables and Figures

Table 1. Characteristics of kidney transplant recipients with recurrent membranous nephropathy and non-recurrent membranous nephropathy in the derivation cohort

Variables	**Recurrent membranous nephropathy (n=25)**	**Non-recurrent membranous nephropathy (n=174)**
Age (years; median (IQR))		
-Recipient	42 (32-54)	49 (38-58)
-Donor	37 (23-48)	44 (31-54)
Recipient sex; male (%)	18 (72)	127 (73)
Recipient weight (kg; median (IQR))	75 (66-81)	76 (65-89)
Recipient ethnicity (%)		
-Caucasian	20 (80)	143 (82)
-Asian	3 (12)	11 (8)
-Central or South American	0 (0)	2 (1)
-South Pacific Island	0 (0)	3 (2)
-Middle Eastern	0 (0)	4 (2)
-African	0 (0)	1 (0.6)
-Australian Aboriginal	1 (4)	3 (2)
Dialysis vintage (months; median (IQR))	22 (5-43)	23 (10-65)
Transplant era (%)		
-1980-1989	3 (12)	5 (3)
-1990-1999	17 (68)	67 (38)
-2000-2009	2 (8)	24 (14)

-2010-2019	3 (12)	78 (45)
Recipient blood group (%)		
-A	10 (40)	71 (41)
-AB	1 (4)	6 (3)
-B	5 (20)	23 (13)
-O	9 (36)	74 (43)
Donor blood group (%)		
-A	8 (32)	66 (38)
-AB	1 (4)	1 (0.6)
-B	3 (12)	20 (11)
-O	13 (52)	87 (50)
ABO blood group incompatible (%)	0 (0)	5 (3)
HLA A loci mismatch (%)		
-0	3 (12)	40 (23)
-1	16 (64)	87 (50)
-2	6 (24)	47 (27)
HLA B loci mismatch (%)		
-0	5 (20)	30 (17)
-1	18 (72)	86 (49)
-2	2 (8)	58 (33)
HLA DR loci mismatch (%)		
-0	10 (40)	57 (33)
-1	11 (44)	75 (43)
-2	4 (16)	42 (24)
HLA DQ loci mismatch (%)		
-0	14 (56)	78 (45)

-1	10 (40)	75 (43)
-2	1 (4)	21 (12)
Total HLA mismatch (%)		
-0	2 (8)	10 (6)
-1 to 2	7 (28)	56 (32)
-3 to 4	12 (48)	66 (38)
-5 to 6	4 (16)	42 (24)
Living donor (%)	9 (36)	44 (25)
Regraft (%)	3 (12)	32 (18)
Biopsy-proven rejection (%)		
-Acute cellular rejection	2 (8)	30 (17)
-Acute humoral rejection	0 (0)	6 (3)
Maximum panel reactive antibodies (%; median (IQR))	3 (0-16)	0 (0-20)
Recipient comorbidities (%)		
-Type 1 diabetes	0 (0)	1 (0.6)
-Type 2 diabetes	0 (0)	15 (9)
-Coronary artery disease	1 (4)	18 (10)
-Cerebrovascular disease	1 (4)	2 (1)
-Peripheral vascular disease	0 (0)	6 (3)
-Chronic lung disease	0 (0)	7 (4)
-Hepatitis C virus	0 (0)	1 (0.6)
-Cancer	2 (8)	26 (15)
Smoking status (%)		
-Never	13 (52)	81 (47)
-Former	5 (20)	57 (33)

-Current	1 (4)	14 (8)
Induction immunosuppression (%)		
-IL2 receptor blocker	2 (8)	72 (41)
-T cell depletion	3 (12)	17 (6)
-B cell depletion	0 (0)	1 (0.5)
-IVIG induction	0 (0)	5 (2)
-Any induction	5 (20)	90 (52)
Maintenance immunosuppression (%)		
-Tacrolimus	5 (20)	95 (55)
-Cyclosporin	20 (80)	91 (52)
-Mycophenolate	7 (28)	126 (72)
-Azathioprine	19 (76)	63 (36)
-mTOR inhibitor	1 (4)	23 (13)
-Corticosteroids	25 (100)	172 (99)
-Other maintenance therapy*	2 (8)	2 (1)

IQR = interquartile range, HLA = human leukocyte antigen, IL2 = interleukin-2, IVIG = intravenous immunoglobulin, mTOR = mammalian target of rapamycin.

*Other maintenance immunosuppression includes chlorambucil, cyclophosphamide, leflunomide, sotrastaurin, and janus kinase 3 inhibitor

Table 2. Donor-recipient HLA serotypes and matched HLA serotypes in kidney transplant recipients with recurrent membranous nephropathy and non-recurrent membranous nephropathy in the derivation cohort

Variables	Recurrent membranous nephropathy (n=25)	Non-recurrent membranous nephropathy (n=174)
Recipient HLA (%)		
A loci		
-A1	11 (44)	78 (43)
-A2	15 (60)	53 (30)
-A3	3 (12)	35 (20)
-A11	2 (8)	26 (15)
-A23	1 (4)	4 (2)
-A24	4 (16)	31 (18)
-A25	0 (0)	8 (5)
-A26	0 (0)	9 (5)
-A28	0 (0)	9 (5)
-A29	3 (12)	15 (9)
-A30	0 (0)	14 (8)
-A31	1 (4)	11 (6)
-A32	3 (12)	11 (6)
-A33	1 (4)	4 (2)
-A34	0 (0)	2 (1)
-A68	0 (0)	4 (2)
B loci		

-B7	2 (8)	27 (16)
-B8	12 (48)	75 (43)
-B13	0 (0)	11 (6)
-B14	0 (0)	3 (2)
-B18	5 (20)	31 (18)
-B27	2 (8)	12 (7)
-B35	2 (8)	25 (14)
-B37	0 (0)	4 (2)
-B38	0 (0)	4 (2)
-B39	1 (4)	3 (2)
-B41	0 (0)	2 (1)
-B44	6 (24)	33 (19)
-B45	1 (4)	1 (0.6)
-B49	0 (0)	3 (2)
-B50	0 (0)	3 (2)
-B51	4 (16)	14 (8)
-B52	0 (0)	6 (3)
-B55	1 (4)	5 (3)
-B56	0 (0)	4 (2)
-B57	1 (4)	9 (5)
-B58	1 (4)	3 (2)
-B60	2 (8)	13 (7)
-B61	1 (4)	5 (3)
-B62	2 (8)	17 (10)
-B65	3 (12)	4 (2)
DR loci		

-DR1	3 (12)	16 (9)
-DR2	2 (8)	2 (1)
-DR3	6 (24)	65 (37)
-DR4	8 (32)	39 (22)
-DR5	1 (4)	2 (1)
-DR6	1 (4)	3 (2)
-DR7	4 (16)	23 (13)
-DR8	2 (8)	9 (5)
-DR9	1 (4)	3 (2)
-DR10	0 (0)	4 (2)
-DR11	5 (20)	43 (25)
-DR12	3 (12)	7 (4)
-DR13	4 (16)	18 (10)
-DR14	1 (4)	13 (7)
-DR15	1 (4)	28 (16)
-DR16	0 (0)	3 (2)
-DR17	6 (24)	28 (16)
-DR103	0 (0)	2 (1)
DQ loci		
-DQ1	7 (28)	40 (23)
-DQ2	14 (56)	102 (59)
-DQ3	8 (32)	46 (26)
-DQ4	1 (4)	2 (1)
-DQ5	2 (8)	18 (10)
-DQ6	2 (8)	25 (14)
-DQ7	4 (16)	27 (16)

-DQ8	1 (4)	12 (7)
-DQ9	2 (8)	2 (1)
Donor HLA (%)		
A loci		
-A1	13 (52)	74 (43)
-A2	11 (44)	74 (43)
-A3	6 (24)	43 (25)
-A11	3 (12)	17 (10)
-A23	1 (4)	5 (3)
-A24	5 (20)	23 (13)
-A25	0 (0)	7 (4)
-A26	1 (4)	10 (6)
-A28	1 (4)	6 (3)
-A29	2 (8)	9 (5)
-A30	1 (4)	11 (6)
-A31	2 (8)	10 (6)
-A32	1 (4)	11 (6)
-A33	0 (0)	4 (2)
-A34	0 (0)	2 (1)
-A68	2 (8)	8 (5)
B loci		
-B5	0 (0)	3 (2)
-B7	6 (24)	31 (18)
-B8	12 (48)	63 (36)
-B13	2 (8)	10 (6)
-B14	1 (4)	7 (4)

-B18	2 (8)	15 (9)
-B27	2 (8)	10 (6)
-B35	2 (8)	26 (15)
-B37	2 (8)	3 (2)
-B38	0 (0)	7 (4)
-B39	1 (4)	7 (4)
-B41	0 (0)	5 (3)
-B44	5 (20)	40 (23)
-B47	0 (0)	2 (1)
-B49	1 (4)	5 (3)
-B51	1 (4)	16 (9)
-B52	0 (0)	3 (2)
-B55	1 (4)	3 (2)
-B56	0 (0)	3 (2)
-B57	0 (0)	12 (7)
-B58	0 (0)	2 (1)
-B60	2 (8)	14 (8)
-B61	1 (4)	4 (2)
-B62	4 (16)	20 (11)
-B64	0 (0)	2 (1)
-B65	2 (8)	4 (2)
-B70	0 (0)	3 (2)
DR loci		
-DR1	2 (8)	25 (14)
-DR2	2 (8)	6 (3)
-DR3	5 (20)	45 (26)

-DR4	6 (24)	44 (25)
-DR5	1 (4)	3 (2)
-DR6	1 (4)	3 (2)
-DR7	5 (20)	41 (24)
-DR8	2 (8)	6 (3)
-DR9	0 (0)	3 (2)
-DR10	1 (4)	3 (2)
-DR11	5 (20)	31 (18)
-DR12	3 (12)	2 (1)
-DR13	4 (16)	26 (15)
-DR14	2 (8)	12 (7)
-DR15	5 (20)	30 (17)
-DR16	1 (4)	5 (3)
-DR17	3 (12)	29 (17)
-DR52	0 (0)	2 (1)
-DR103	0 (0)	3 (2)
DQ loci		
-DQ1	8 (32)	42 (24)
-DQ2	12 (48)	98 (56)
-DQ3	9 (36)	38 (22)
-DQ4	2 (8)	4 (2)
-DQ5	3 (12)	29 (17)
-DQ6	4 (16)	32 (18)
-DQ7	4 (16)	31 (18)
-DQ8	0 (0)	15 (9)
-DQ9	0 (0)	5 (3)

Donor-recipient HLA match (%)		
A loci		
-A1	9 (36)	49 (28)
-A2	7 (28)	34 (20)
-A3	1 (4)	14 (8)
-A11	1 (4)	6 (3)
-A24	2 (8)	10 (6)
-A25	0 (0)	2 (1)
-A29	1 (4)	1 (0.6)
-A30	0 (0)	7 (4)
-A31	0 (0)	3 (2)
-A32	0 (0)	5 (3)
B loci		
-B7	1 (4)	10 (6)
-B8	11 (44)	48 (28)
-B13	0 (0)	3 (2)
-B14	0 (0)	2 (1)
-B18	2 (8)	10 (6)
-B27	0 (0)	2 (1)
-B35	1 (4)	10 (6)
-B44	2 (8)	14 (8)
-B51	1 (4)	1 (0.6)
-B55	1 (4)	1 (0.6)
-B56	0 (0)	2 (1)
-B60	1 (4)	3 (2)
-B62	2 (8)	10 (6)

-B65	2 (8)	1 (0.6)
DR loci		
-DR1	1 (4)	7 (4)
-DR3	4 (16)	35 (20)
-DR4	3 (12)	26 (15)
-DR6	1 (4)	1 (0.6)
-DR7	3 (12)	14 (8)
-DR11	2 (8)	18 (10)
-DR12	2 (8)	0 (0)
-DR13	2 (8)	11 (6)
-DR14	1 (4)	4 (2)
-DR15	1 (4)	8 (5)
-DR17	3 (12)	11 (6)
DQ loci		
-DQ1	1 (4)	21 (12)
-DQ2	11 (44)	70 (40)
-DQ3	5 (20)	23 (13)
-DQ5	1 (4)	10 (6)
-DQ6	1 (4)	12 (7)
-DQ7	3 (12)	13 (7)
-DQ8	0 (0)	7 (4)

Table 3. Summary of variables included in Group LASSO, penalized Cox regression and random forest models

Type of variable	**Number of variables (total n = 222)**
Recipient characteristics	
-Age	1
-Sex	1
-Ethnicity	1
-Weight	1
-Dialysis vintage	1
-Blood group	1
-Comorbidities	8
-Smoking status	1
Donor characteristics	
-Age	1
-Blood group	1
Transplant characteristics	
-HLA mismatch (A, B, DR, DQ, total)	5
-Donor status (living or deceased)	1
-Blood group incompatibility status	1
-Regraft status	1
-Maximum panel-reactive antibodies	1
-Biopsy-proven rejection (acute cellular, acute antibody-mediated)	2 5
-Induction immunosuppression	7

-Maintenance immunosuppression	1
-Transplant era	
HLA characteristics	
-Recipient HLA-A serotype	16
-Donor HLA-A serotype	16
-Recipient HLA-B serotype	25
-Donor HLA-B serotype	27
-Recipient HLA-DR serotype	18
-Donor HLA-DR serotype	19
-Recipient HLA-DQ serotype	9
-Donor HLA-DQ serotype	9
-Donor-recipient HLA-A match	10
-Donor-recipient HLA-B match	14
-Donor-recipient HLA-DR match	11
-Donor-recipient HLA-DQ match	7

HLA = human leukocyte antigen

Table 4. Variable importance in Group LASSO, penalized Cox regression and random forest models

Variable ranking (1 = highest importance, 10 = lowest importance)	**Group LASSO**	**Penalised Cox regression**	**Random forest**
1	Mycophenolate maintenance Other maintenance immunosuppression* Recipient HLA-A2 Recipient HLA-B65 Donor-recipient HLA-B65 match Donor-recipient HLA-DR12 match	Recipient HLA-A2 Recipient HLA-B65 Recipient HLA-DR17 Donor HLA-DR12 Donor HLA-DQ4 Donor-recipient HLA-B65 match Donor-recipient HLA-DR12 match Donor-recipient HLA-DR17 match	Donor-recipient HLA-DR12 match
2			Recipient HLA-A2
3			Mycophenolate maintenance

4		Donor HLA-DR12
5		Donor-recipient HLA-B65 match
6		Azathioprine maintenance
7	Donor HLA-DR12	IL2 receptor blocker induction
8	Azathioprine maintenance	
9	Hepatitis C	
10	IL2 receptor blocker induction	

HLA = human leukocyte antigen; IL2 = interleukin-2

*Other maintenance immunosuppression includes chlorambucil, cyclophosphamide, leflunomide, sotrastaurin, and janus kinase 3 inhibitor

Table 5. Characteristics of kidney transplant recipients with recurrent membranous nephropathy and non-recurrent membranous nephropathy in the validation cohort for the Group LASSO model

Variables	**Recurrent membranous nephropathy (n=34)**	**Non-recurrent membranous nephropathy (n=241)**
Age (years; median (IQR))		
-Recipient	49 (14)	53 (19)
-Donor	41 (15)	43 (27)
Recipient sex; male (%)	27 (79)	184 (76)
Recipient weight (kg; median (IQR))	80 (20)	76 (17)
Recipient ethnicity (%)		
-Caucasian	31 (91)	203 (84)
-Asian	1 (3)	12 (5)
-Central or South American	0 (0)	0 (0)
-South Pacific Island	0 (0)	3 (9)
-Middle Eastern	0 (0)	1 (3)
-African	0 (0)	0 (0)
-Australian Aboriginal	1 (3)	4 (12)
Dialysis vintage (months; median (IQR))	12 (27)	28 (47)
Transplant era (%)		
-1980-1989	7 (21)	42 (17)
-1990-1999	6 (18)	34 (14)
-2000-2009	16 (47)	77 (32)
-2010-2019	5 (15)	87 (36)

Recipient blood group (%)		
-A	10 (29)	104 (43)
-AB	1 (3)	7 (3)
-B	6 (18)	27 (11)
-O	17 (50)	103 (43)
Donor blood group (%)		
-A	10 (29)	97 (40)
-AB	1 (3)	6 (2)
-B	5 (15)	17 (7)
-O	18 (53)	121 (50)
ABO blood group incompatible (%)	0 (0)	6 (2)
HLA A loci mismatch (%)		
-0	5 (15)	53 (22)
-1	19 (56)	130 (54)
-2	10 (29)	58 (24)
HLA B loci mismatch (%)		
-0	10 (29)	48 (20)
-1	16 (47)	115 (48)
-2	8 (24)	78 (32)
HLA DR loci mismatch (%)		
-0	13 (38)	94 (39)
-1	16 (47)	86 (36)
-2	5 (15)	60 (25)
Total HLA mismatch (%)		
-0	4 (12)	17 (7)
-1 to 2	10 (29)	83 (34)

-3 to 4	14 (41)	87 (36)
-5 to 6	6 (18)	53 (22)
Living donor (%)	14 (41)	71 (29)
Regraft (%)	1 (3)	25 (10)
Biopsy-proven rejection (%)		
-Acute cellular rejection	11 (32)	49 (20)
-Acute humoral rejection	2 (6)	16 (7)
Maximum panel reactive antibodies (%; median (IQR))	0 (7)	0 (13)
Recipient comorbidities (%)		
-Type 1 diabetes	0 (0)	3 (1)
-Type 2 diabetes	1 (3)	16 (7)
-Coronary artery disease	3 (9)	34 (14)
-Cerebrovascular disease	0 (0)	7 (3)
-Peripheral vascular disease	0 (0)	6 (2)
-Chronic lung disease	1 (9)	19 (8)
-Hepatitis C virus	0 (0)	1 (0.4)
-Cancer	2 (6)	32 (13)
Smoking status (%)		
-Never	15 (44)	111 (46)
-Former	12 (35)	74 (31)
-Current	4 (12)	25 (10)
Induction immunosuppression (%)		
-IL2 receptor blocker	15 (44)	116 (48)
-T cell depletion	0 (0)	10 (4)
-B cell depletion	0 (0)	1 (0.4)

-IVIG induction	0 (0)	3 (1)
-Any induction	15 (44)	126 (52)
Maintenance immunosuppression (%)		
-Tacrolimus	16 (47)	126 (52)
-Cyclosporin	24 (71)	128 (53)
-Mycophenolate	27 (79)	178 (74)
-Azathioprine	11 (32)	86 (36)
-mTOR inhibitor	3 (9)	27 (11)
-Corticosteroids	32 (94)	230 (95)
-Other maintenance therapy*	2 (6)	5 (2)
Recipient HLA (%)		
A loci		
-A1	18 (53)	108 (45)
-A2	9 (26)	106 (44)
-A3	6 (18)	48 (20)
-A11	7 (21)	36 (15)
-A23	2 (6)	6 (2)
-A24	8 (24)	39 (16)
-A25	1 (3)	5 (2)
-A26	0 (0)	11 (5)
-A28	2 (6)	6 (2)
-A29	4 (12)	12 (5)
-A30	2 (6)	14 (6)
-A31	4 (12)	9 (4)
-A32	1 (3)	14 (6)
-A33	0 (0)	5 (2)

-A34	0 (0)	4 (2)
-A68	1 (3)	5 (2)
B loci		
-B7	7 (21)	37 (15)
-B8	17 (50)	115 (48)
-B13	2 (6)	12 (5)
-B14	0 (0)	3 (1)
-B18	4 (12)	23 (10)
-B27	3 (9)	18 (7)
-B35	2 (6)	23 (10)
-B37	2 (6)	3 (1)
-B38	2 (6)	5 (2)
-B39	0 (0)	13 (5)
-B41	0 (0)	1 (0.4)
-B44	7 (21)	49 (20)
-B45	1 (3)	2 (0.8)
-B49	0 (0)	6 (2)
-B50	1 (3)	3 (1)
-B51	3 (9)	13 (5)
-B52	0 (0)	4 (2)
-B55	1 (3)	13 (5)
-B56	0 (0)	3 (2)
-B57	1 (3)	10 (4)
-B58	0 (0)	5 (2)
-B60	1 (3)	22 (9)
-B61	1 (3)	3 (2)

-B62	2 (6)	20 (8)
-B65	0 (0)	9 (4)
DR loci		
-DR1	1 (3)	26 (11)
-DR2	0 (0)	9 (4)
-DR3	17 (50)	98 (41)
-DR4	9 (26)	52 (22)
-DR5	1 (3)	6 (2)
-DR6	0 (0)	6 (2)
-DR7	7 (21)	34 (14)
-DR8	0 (0)	8 (3)
-DR9	1 (3)	9 (4)
-DR10	1 (3)	1 (0.4)
-DR11	6 (18)	41 (17)
-DR12	0 (0)	8 (3)
-DR13	4 (12)	22 (9)
-DR14	2 (6)	18 (7)
-DR15	5 (15)	36 (15)
-DR16	1 (3)	9 (4)
-DR17	6 (18)	37 (15)
-DR103	0 (0)	6 (2)
DQ loci		
-DQ1	0 (0)	3 (1)
-DQ2	5 (15)	14 (6)
-DQ3	2 (6)	5 (2)
-DQ4	0 (0)	0 (0)

-DQ5	0 (0)	2 (0.8)
-DQ6	0 (0)	1 (0.4)
-DQ7	1 (3)	3 (1)
-DQ8	1 (3)	1 (0.4)
-DQ9	0 (0)	1 (0.4)
Donor HLA (%)		
A loci		
-A1	19 (56)	103 (43)
-A2	14 (41)	109 (45)
-A3	8 (24)	63 (26)
-A11	2 (6)	32 (13)
-A23	1 (3)	15 (6)
-A24	5 (15)	36 (15)
-A25	0 (0)	6 (2)
-A26	1 (3)	8 (3)
-A28	1 (3)	5 (2)
-A29	3 (9)	11 (5)
-A30	2 (6)	14 (6)
-A31	1 (3)	9 (4)
-A32	2 (6)	12 (5)
-A33	1 (3)	5 (2)
-A34	1 (3)	1 (0.4)
-A68	3 (9)	12 (5)
B loci		
-B5	0 (0)	2 (0.8)
-B7	10 (29)	68 (28)

-B8	17 (50)	95 (39)
-B13	3 (9)	7 (3)
-B14	0 (0)	9 (4)
-B18	5 (15)	26 (11)
-B27	1 (3)	13 (5)
-B35	3 (9)	25 (10)
-B37	1 (3)	4 (2)
-B38	0 (0)	6 (2)
-B39	2 (6)	11 (5)
-B41	1 (3)	4 (2)
-B44	8 (24)	49 (20)
-B47	0 (0)	2 (0.8)
-B49	2 (6)	6 (2)
-B51	1 (3)	17 (7)
-B52	0 (0)	1 (0.4)
-B55	0 (0)	8 (3)
-B56	0 (0)	5 (2)
-B57	0 (0)	14 (6)
-B58	1 (3)	3 (1)
-B60	2 (6)	21 (9)
-B61	2 (6)	4 (2)
-B62	1 (3)	27 (11)
-B64	0 (0)	1 (0.4)
-B65	0 (0)	9 (4)
-B70	0 (0)	0 (0)
DR loci		

-DR1	2 (6)	41 (17)
-DR2	3 (9)	13 (5)
-DR3	16 (47)	63 (26)
-DR4	11 (32)	75 (31)
-DR5	0 (0)	8 (3)
-DR6	0 (0)	7 (3)
-DR7	5 (15)	50 (21)
-DR8	2 (6)	11 (5)
-DR9	1 (3)	7 (3)
-DR10	0 (0)	2 (0.8)
-DR11	7 (21)	24 (10)
-DR12	0 (0)	6 (2)
-DR13	6 (18)	28 (12)
-DR14	1 (3)	12 (5)
-DR15	7 (21)	46 (19)
-DR16	0 (0)	7 (3)
-DR17	3 (9)	43 (18)
-DR52	0 (0)	0 (0)
-DR103	0 (0)	4 (2)
DQ loci		
-DQ1	3 (9)	23 (10)
-DQ2	4 (12)	49 (20)
-DQ3	1 (3)	15 (6)
-DQ4	1 (3)	8 (3)
-DQ5	0 (0)	13 (5)
-DQ6	0 (0)	14 (6)

-DQ7	2 (6)	15 (6)
-DQ8	1 (3)	12 (5)
-DQ9	0 (0)	7 (3)
Donor-recipient HLA match (%)		
A loci		
-A1	13 (38)	72 (30)
-A2	5 (15)	64 (27)
-A3	2 (6)	20 (8)
-A11	1 (3)	6 (2)
-A24	3 (9)	15 (6)
-A25	0 (0)	1 (0.4)
-A29	2 (6)	2 (0.8)
-A30	0 (0)	6 (2)
-A31	0 (0)	0 (0)
-A32	0 (0)	3 (1)
B loci		
-B7	5 (15)	27 (11)
-B8	13 (38)	75 (31)
-B13	2 (6)	3 (1)
-B14	0 (0)	1 (0.4)
-B18	2 (6)	8 (3)
-B27	0 (0)	5 (2)
-B35	1 (3)	9 (4)
-B44	5 (15)	24 (10)
-B51	1 (3)	5 (2)
-B55	0 (0)	3 (1)

-B56	0 (0)	0 (0)
-B60	1 (3)	4 (2)
-B62	0 (0)	4 (2)
-B65	0 (0)	3 (1)
DR loci		
-DR1	0 (0)	15 (6)
-DR3	12 (35)	51 (21)
-DR4	6 (18)	35 (15)
-DR6	0 (0)	2 (0.8)
-DR7	3 (9)	23 (10)
-DR11	3 (9)	13 (5)
-DR12	0 (0)	1 (0.4)
-DR13	4 (12)	11 (5)
-DR14	1 (3)	6 (2)
-DR15	4 (12)	24 (10)
-DR17	2 (6)	18 (7)
DQ loci		
-DQ1	0 (0)	0 (0)
-DQ2	0 (0)	0 (0)
-DQ3	0 (0)	0 (0)
-DQ5	0 (0)	0 (0)
-DQ6	0 (0)	0 (0)
-DQ7	0 (0)	0 (0)
-DQ8	0 (0)	0 (0)

*Other maintenance immunosuppression includes chlorambucil, cyclophosphamide, leflunomide, sotrastaurin, and janus kinase 3 inhibitor

Table 6. Characteristics of kidney transplant recipients with recurrent membranous nephropathy and non-recurrent membranous nephropathy in the validation cohort for the penalized Cox regression model

Variables	**Recurrent membranous nephropathy (n=7)**	**Non-recurrent membranous nephropathy (n=92)**
Age (years; median (IQR))		
-Recipient	57 (15)	56 (16)
-Donor	33 (25)	45 (23)
Recipient sex; male (%)	7 (100)	68 (74)
Recipient weight (kg; median (IQR))	84 (10)	77 (15)
Recipient ethnicity (%)		
-Caucasian	7 (100)	74 (80)
-Asian	0 (0)	5 (5)
-Central or South American	0 (0)	0 (0)
-South Pacific Island	0 (0)	4 (4)
-Middle Eastern	0 (0)	0 (0)
-African	0 (0)	0 (0)
-Australian Aboriginal	0 (0)	7 (8)
Dialysis vintage (months; median (IQR))	27 (26)	42 (50)
Transplant era (%)		
-1980-1989	0 (0)	4 (4)
-1990-1999	1 (14)	15 (16)
-2000-2009	3 (43)	13 (14)

-2010-2019	3 (43)	60 (65)
Recipient blood group (%)		
-A	2 (29)	34 (37)
-AB	0 (0)	2 (2)
-B	2 (29)	15 (16)
-O	3 (43)	41 (45)
Donor blood group (%)		
-A	2 (29)	35 (38)
-AB	0 (0)	2 (2)
-B	2 (29)	9 (10)
-O	3 (43)	46 (50)
ABO blood group incompatible (%)	0 (0)	3 (3)
HLA A loci mismatch (%)		
-0	1 (14)	22 (24)
-1	3 (43)	41 (45)
-2	3 (43)	29 (32)
HLA B loci mismatch (%)		
-0	2 (29)	22 (24)
-1	2 (29)	36 (39)
-2	3 (43)	34 (37)
HLA DR loci mismatch (%)		
-0	3 (43)	33 (36)
-1	4 (57)	31 (34)
-2	0 (0)	28 (30)
Total HLA mismatch (%)		
-0	1 (14)	5 (5)

-1 to 2	1 (14)	36 (39)
-3 to 4	3 (43)	23 (25)
-5 to 6	2 (29)	28 (30)
Living donor (%)	0 (0)	8 (9)
Regraft (%)	1 (14)	12 (13)
Biopsy-proven rejection (%)		
-Acute cellular rejection	2 (29)	20 (22)
-Acute humoral rejection	1 (14)	9 (10)
Maximum panel reactive antibodies (%; median (IQR))	0 (8)	0 (10)
Recipient comorbidities (%)		
-Type 1 diabetes	0 (0)	3 (3)
-Type 2 diabetes	0 (0)	7 (8)
-Coronary artery disease	1 (14)	18 (20)
-Cerebrovascular disease	0 (0)	6 (7)
-Peripheral vascular disease	0 (0)	1 (1)
-Chronic lung disease	1 (14)	9 (10)
-Hepatitis C virus	0 (0)	1 (1)
-Cancer	1 (14)	15 (16)
Smoking status (%)		
-Never	3 (43)	44 (48)
-Former	4 (57)	33 (36)
-Current	0 (0)	9 (10)
Induction immunosuppression (%)		
-IL2 receptor blocker	5 (71)	60 (65)
-T cell depletion	0 (0)	2 (2)

-B cell depletion	0 (0)	0 (0)
-IVIG induction	0 (0)	1 (1)
-Any induction	5 (71)	62 (67)
Maintenance immunosuppression (%)		
-Tacrolimus	5 (71)	61 (66)
-Cyclosporin	4 (57)	39 (42)
-Mycophenolate	6 (86)	80 (87)
-Azathioprine	1 (14)	22 (24)
-mTOR inhibitor	1 (14)	8 (9)
-Corticosteroids	7 (100)	90 (98)
-Other maintenance therapy*	1 (14)	1 (1)
Recipient HLA (%)		
A loci		
-A1	3 (43)	39 (42)
-A2	1 (14)	41 (45)
-A3	1 (14)	20 (22)
-A11	3 (43)	11 (12)
-A23	1 (14)	3 (3)
-A24	4 (57)	17 (18)
-A25	0 (0)	3 (3)
-A26	0 (0)	4 (4)
-A28	0 (0)	1 (1)
-A29	0 (0)	5 (5)
-A30	0 (0)	5 (5)
-A31	1 (14)	1 (1)
-A32	0 (0)	6 (7)

-A33	1 (14)	1 (1)
-A34	0 (0)	2 (2)
-A68	0 (0)	2 (2)
B loci		
-B7	2 (29)	11 (12)
-B8	3 (43)	42 (46)
-B13	0 (0)	5 (5)
-B14	0 (0)	0 (0)
-B18	1 (14)	10 (11)
-B27	0 (0)	10 (11)
-B35	0 (0)	5 (5)
-B37	0 (0)	0 (0)
-B38	0 (0)	1 (1)
-B39	0 (0)	5 (5)
-B41	0 (0)	1 (1)
-B44	0 (0)	20 (22)
-B45	0 (0)	1 (1)
-B49	0 (0)	3 (3)
-B50	1 (14)	0 (0)
-B51	1 (14)	7 (8)
-B52	0 (0)	0 (0)
-B55	1 (14)	7 (8)
-B56	0 (0)	1 (1)
-B57	0 (0)	5 (5)
-B58	0 (0)	1 (1)
-B60	1 (14)	6 (7)

-B61	1 (14)	1 (1)
-B62	2 (29)	8 (9)
-B65	0 (0)	5 (5)
DR loci		
-DR1	0 (0)	6 (7)
-DR2	0 (0)	2 (2)
-DR3	3 (43)	33 (36)
-DR4	2 (29)	23 (25)
-DR5	0 (0)	0 (0)
-DR6	0 (0)	2 (2)
-DR7	1 (14)	14 (15)
-DR8	0 (0)	4 (4)
-DR9	1 (14)	2 (2)
-DR10	0 (0)	1 (1)
-DR11	1 (14)	16 (17)
-DR12	0 (0)	3 (3)
-DR13	2 (29)	10 (11)
-DR14	0 (0)	6 (7)
-DR15	2 (29)	15 (16)
-DR16	0 (0)	6 (7)
-DR17	1 (14)	17 (18)
-DR103	0 (0)	5 (5)
DQ loci		
-DQ1	0 (0)	0 (0)
-DQ2	0 (0)	0 (0)
-DQ3	0 (0)	0 (0)

-DQ4	0 (0)	0 (0)
-DQ5	0 (0)	0 (0)
-DQ6	0 (0)	0 (0)
-DQ7	0 (0)	0 (0)
-DQ8	0 (0)	0 (0)
-DQ9	0 (0)	0 (0)
Donor HLA (%)		
A loci		
-A1	4 (57)	35 (38)
-A2	2 (29)	46 (50)
-A3	2 (29)	29 (32)
-A11	0 (0)	11 (12)
-A23	0 (0)	6 (7)
-A24	2 (29)	13 (13)
-A25	0 (0)	5 (5)
-A26	0 (0)	1 (1)
-A28	0 (0)	1 (1)
-A29	0 (0)	5 (5)
-A30	0 (0)	4 (4)
-A31	0 (0)	6 (7)
-A32	0 (0)	3 (3)
-A33	0 (0)	1 (1)
-A34	1 (14)	0 (0)
-A68	1 (14)	4 (4)
B loci		
-B5	0 (0)	0 (0)

-B7	2 (29)	23 (25)
-B8	4 (57)	33 (36)
-B13	0 (0)	2 (2)
-B14	0 (0)	4 (4)
-B18	1 (14)	8 (9)
-B27	0 (0)	5 (5)
-B35	0 (0)	7 (8)
-B37	0 (0)	2 (2)
-B38	0 (0)	3 (3)
-B39	1 (14)	4 (4)
-B41	1 (14)	1 (1)
-B44	0 (0)	25 (27)
-B47	0 (0)	1 (1)
-B49	1 (14)	4 (4)
-B51	0 (0)	4 (4)
-B52	0 (0)	0 (0)
-B55	0 (0)	5 (5)
-B56	0 (0)	3 (3)
-B57	0 (0)	4 (4)
-B58	0 (0)	1 (1)
-B60	1 (14)	9 (10)
-B61	0 (0)	2 (2)
-B62	0 (0)	9 (10)
-B64	0 (0)	1 (1)
-B65	0 (0)	5 (5)
-B70	0 (0)	0 (0)

DR loci		
-DR1	0 (0)	18 (20)
-DR2	1 (14)	2 (2)
-DR3	3 (43)	15 (16)
-DR4	2 (29)	34 (37)
-DR5	0 (0)	1 (1)
-DR6	0 (0)	0 (0)
-DR7	1 (14)	19 (21)
-DR8	1 (14)	4 (4)
-DR9	0 (0)	5 (5)
-DR10	0 (0)	1 (1)
-DR11	1 (14)	7 (8)
-DR12	0 (0)	4 (4)
-DR13	2 (29)	13 (14)
-DR14	0 (0)	5 (5)
-DR15	1 (14)	19 (21)
-DR16	0 (0)	2 (2)
-DR17	1 (14)	14 (15)
-DR52	0 (0)	0 (0)
-DR103	0 (0)	2 (2)
DQ loci		
-DQ1	3 (43)	23 (25)
-DQ2	4 (57)	49 (53)
-DQ3	1 (14)	15 (16)
-DQ4	1 (14)	8 (9)
-DQ5	0 (0)	13 (14)

-DQ6	0 (0)	14 (15)
-DQ7	2 (29)	15 (16)
-DQ8	1 (14)	12 (13)
-DQ9	0 (0)	7 (8)
Donor-recipient HLA match (%)		
A loci		
-A1	2 (29)	25 (27)
-A2	0 (0)	26 (28)
-A3	1 (14)	9 (10)
-A11	0 (0)	0 (0)
-A24	1 (14)	5 (5)
-A25	0 (0)	1 (1)
-A29	0 (0)	1 (1)
-A30	0 (0)	3 (3)
-A31	0 (0)	0 (0)
-A32	0 (0)	1 (1)
B loci		
-B7	1 (14)	7 (8)
-B8	3 (43)	26 (28)
-B13	0 (0)	2 (2)
-B14	0 (0)	0 (0)
-B18	0 (0)	3 (3)
-B27	0 (0)	2 (2)
-B35	0 (0)	2 (2)
-B44	0 (0)	14 (15)
-B51	0 (0)	1 (1)

-B55	0 (0)	2 (2)
-B56	0 (0)	0 (0)
-B60	1 (14)	1 (1)
-B62	0 (0)	1 (1)
-B65	0 (0)	1 (1)
DR loci		
-DR1	0 (0)	5 (5)
-DR3	2 (29)	13 (14)
-DR4	1 (14)	14 (15)
-DR7	0 (0)	10 (11)
-DR11	1 (14)	4 (4)
-DR12	0 (0)	1 (1)
-DR13	2 (29)	5 (5)
-DR14	0 (0)	1 (1)
-DR15	1 (14)	9 (10)
-DR17	0 (0)	10 (11)
DQ loci		
-DQ1	0 (0)	0 (0)
-DQ2	0 (0)	0 (0)
-DQ3	0 (0)	0 (0)
-DQ5	0 (0)	0 (0)
-DQ6	0 (0)	0 (0)
-DQ7	0 (0)	0 (0)
-DQ8	0 (0)	0 (0)

*Other maintenance immunosuppression includes sotrastaurin

Figure 1. TRIPOD flow diagram: patient identification and selection

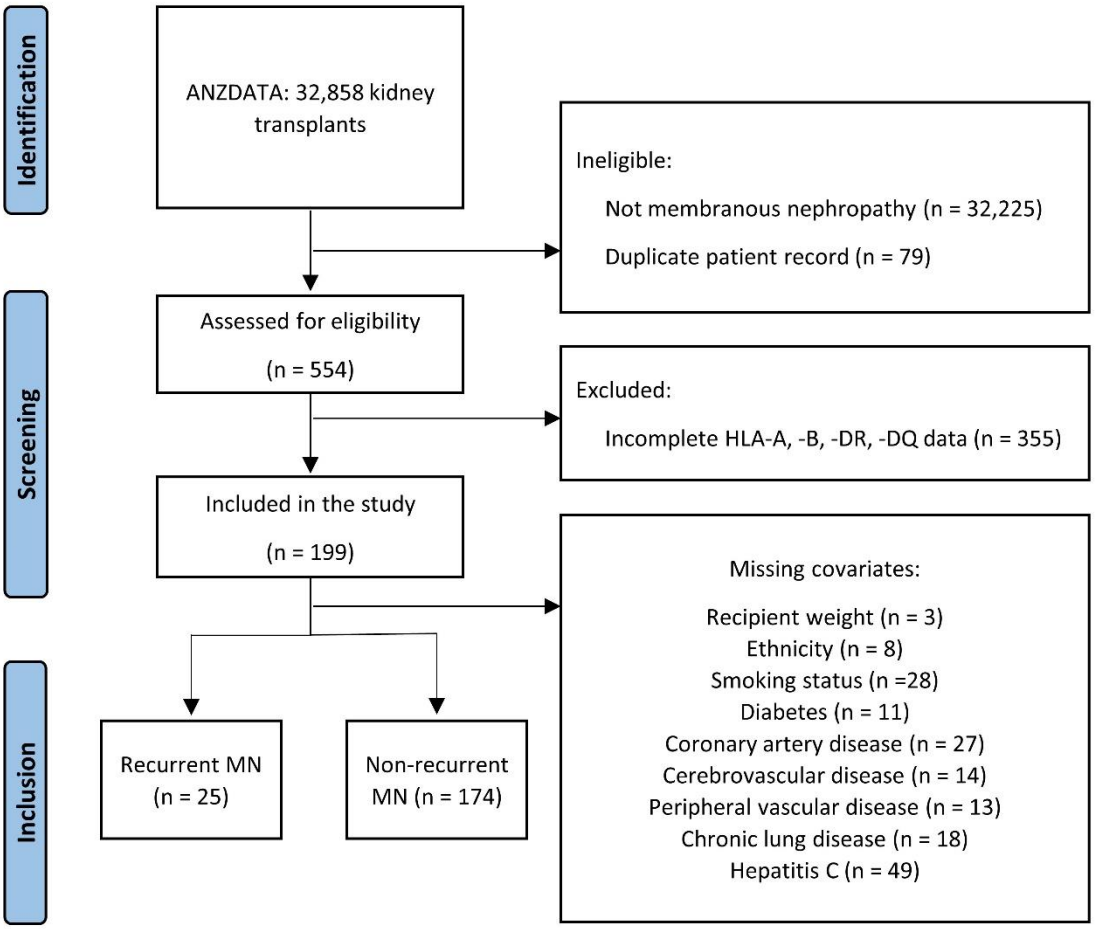

Figure 2. Variables with missing data in the derivation cohort

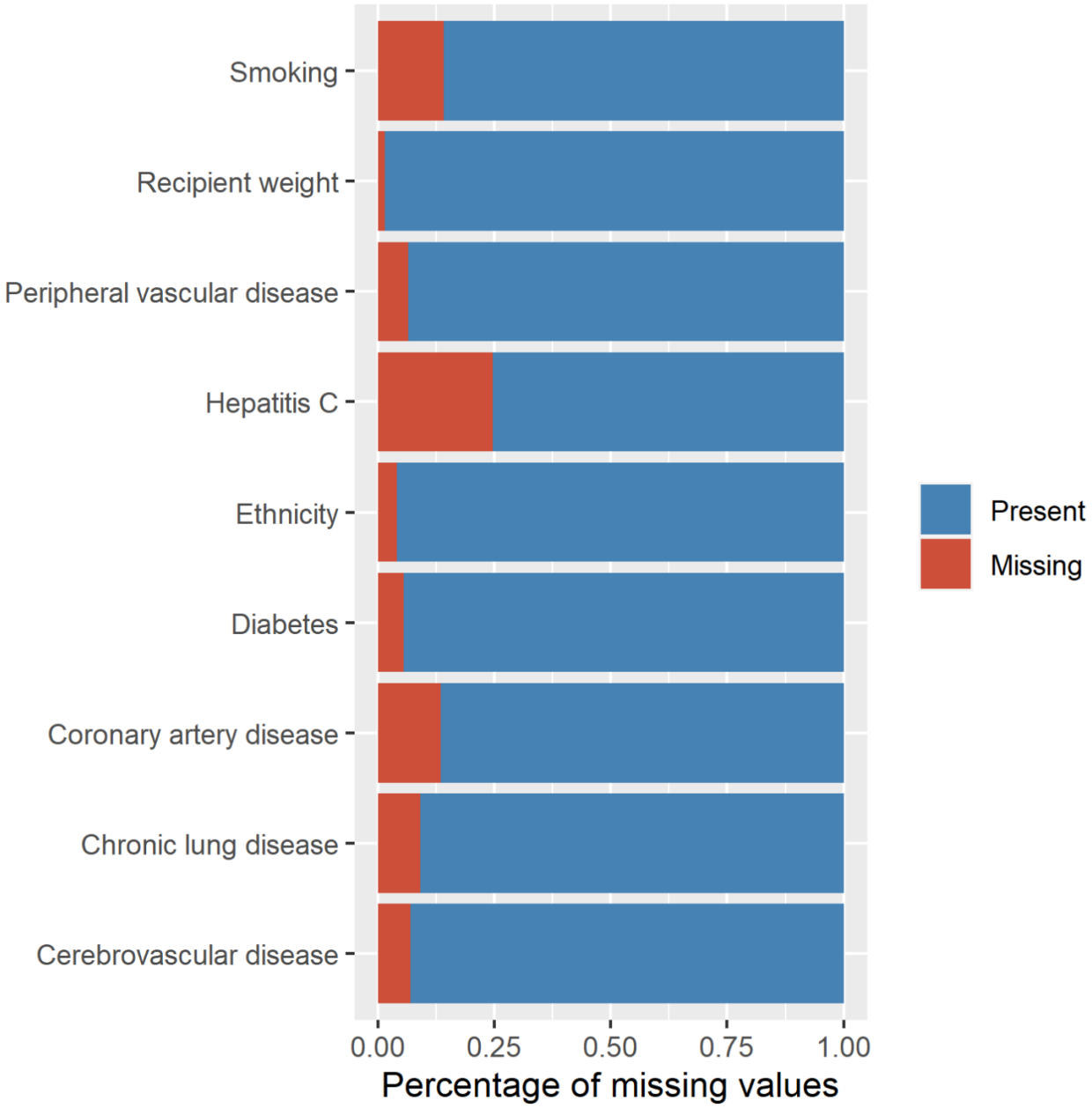

Figure 3. Receiver operating characteristic curves of the Group LASSO, penalized Cox regression and Random Forest models in the derivation cohort

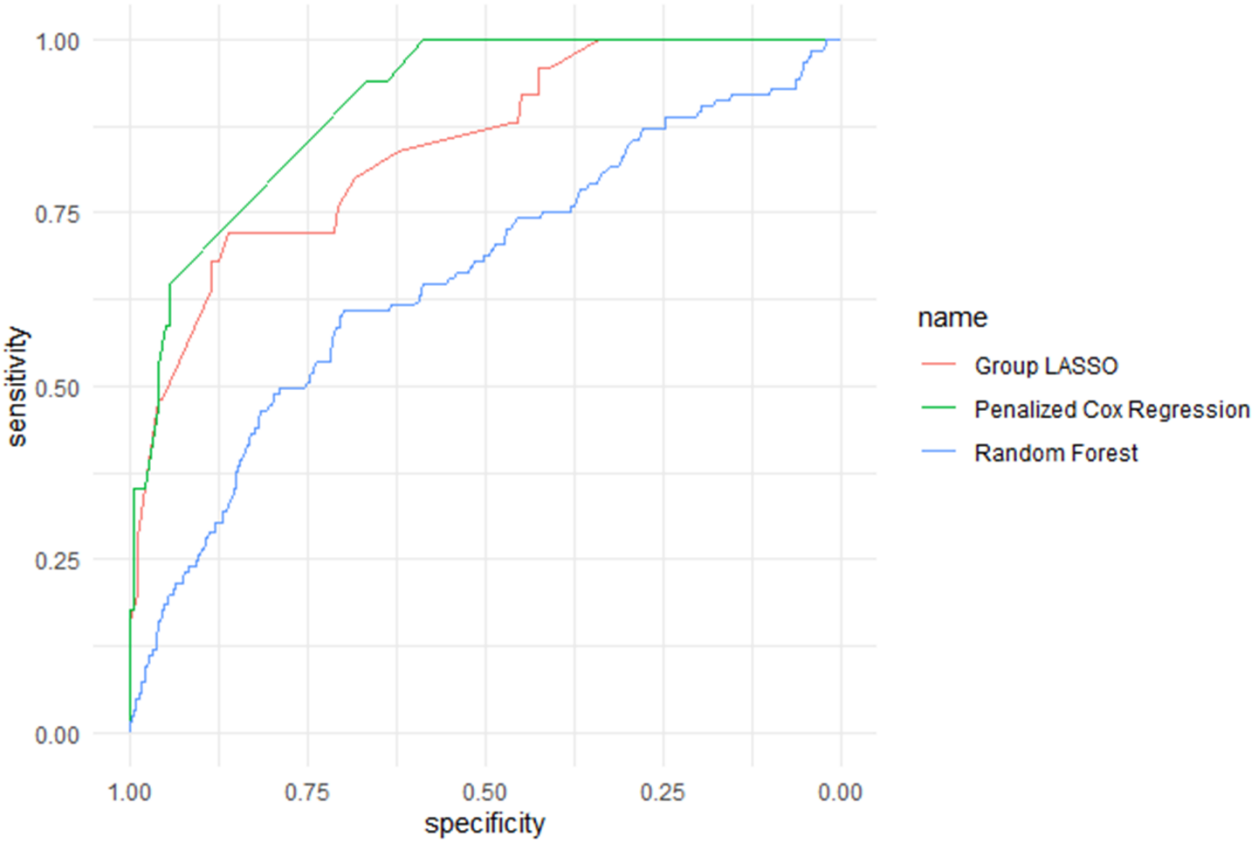

Figure 4. Variables selected by Group LASSO, penalized Cox regression and Random Forest models as predictive of recurrent membranous nephropathy in kidney transplant recipients

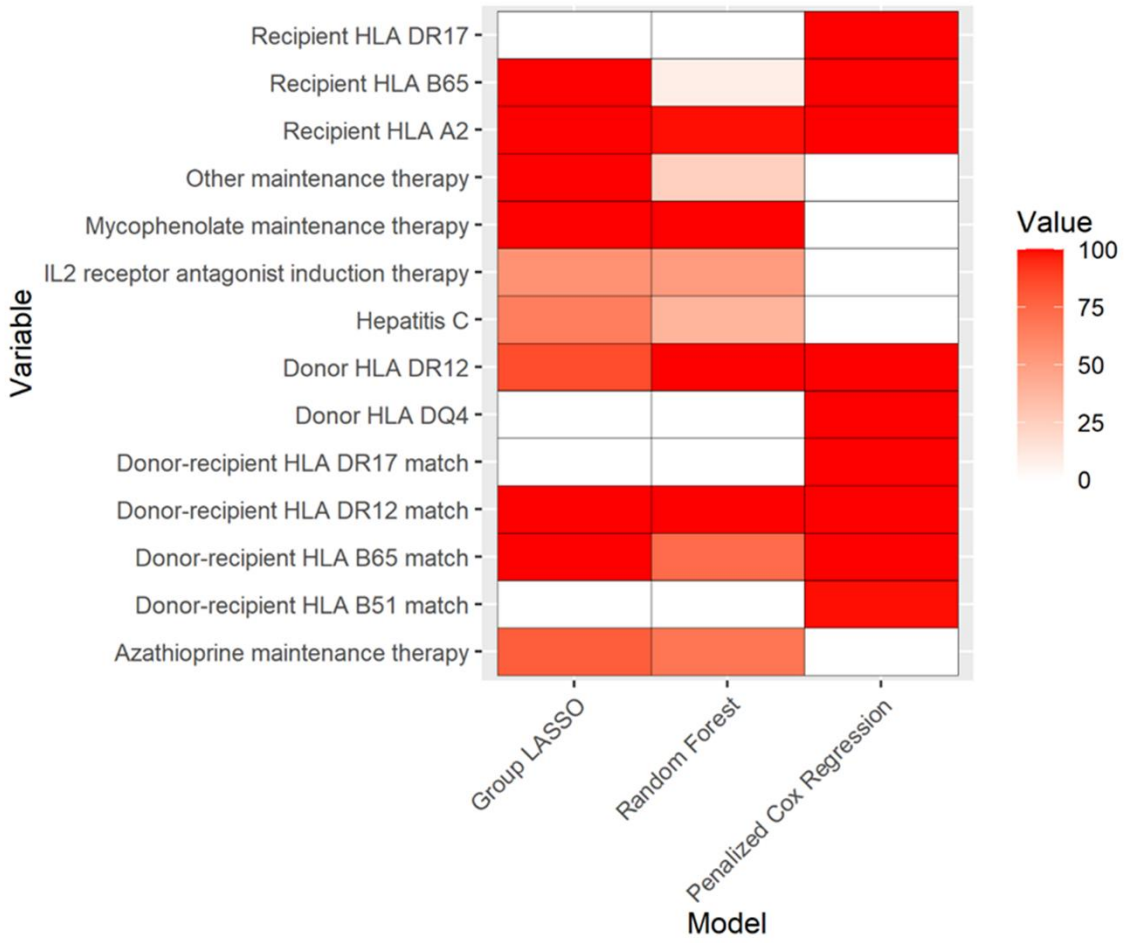

Figure 5. Receiver operating characteristic curves of the Group LASSO and penalized Cox regression models in their respective validation cohorts

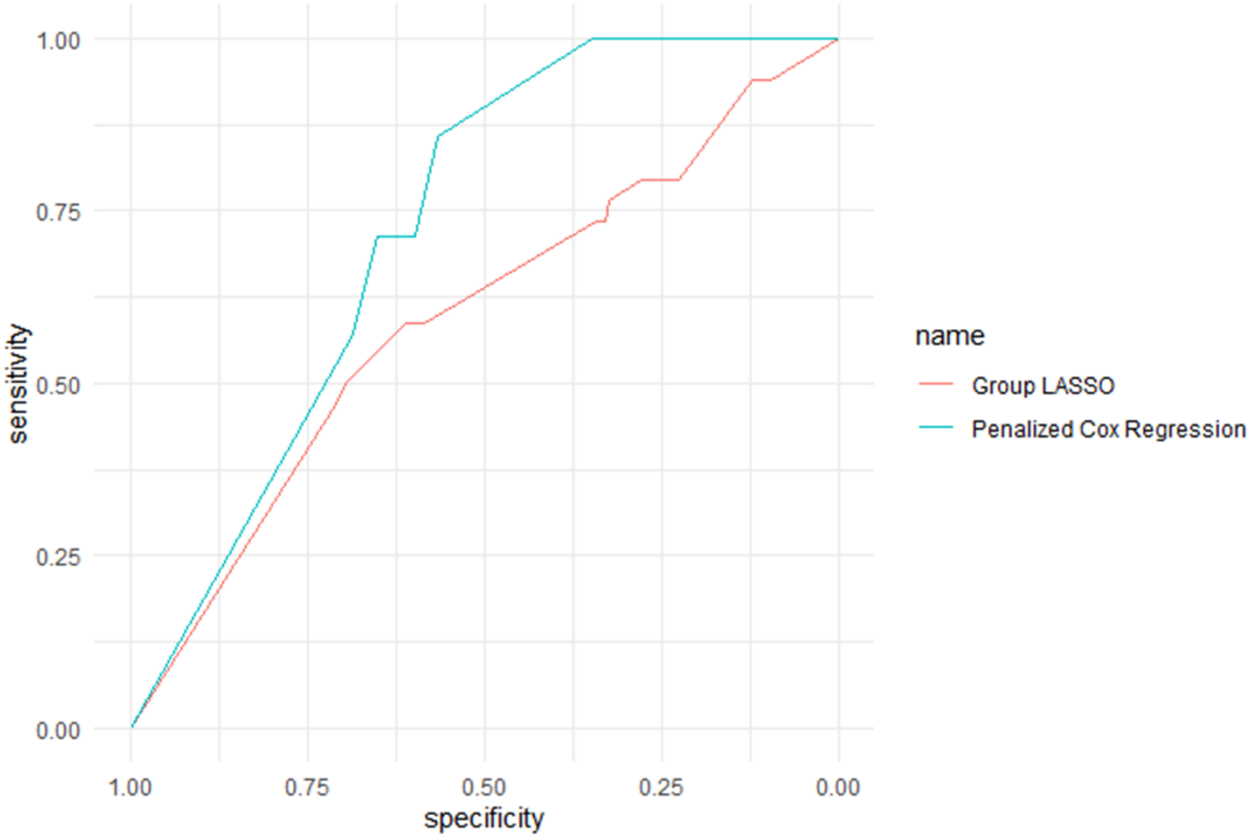

Figure legends

Figure 1. TRIPOD flow diagram: patient identification and selection

Figure 2. Variables with missing data in the derivation cohort

Figure 3. Receiver operating characteristic curves of the Group LASSO, penalized Cox regression and Random Forest models in the derivation cohort

Figure 4. Variables selected by Group LASSO, penalized Cox regression and Random Forest models as predictive of recurrent membranous nephropathy in kidney transplant recipients

Figure 5. Receiver operating characteristic curves of the Group LASSO and penalized Cox regression models in their respective validation cohorts

4.CTLA4-Ig with or without Bortezomib in Heymann Nephritis

4.1 Overview

Background and hypothesis: Recent advances in membranous nephropathy treatment have focused on B cell depletion, which is incompletely effective, potentially due to persistent autoantibody-producing plasma cells or alternative pathways of injury. T cell costimulatory blockade (cytotoxic-T-lymphocyte-associated antigen 4 (CTLA4)-Ig) to prevent T cell-dependent B cell activation and short-course proteasome inhibition (bortezomib) to deplete plasma cells may represent a complementary form of treatment.

Methods: Lewis rats were immunized with Fx1A and complete Freund's adjuvant (CFA) to induce experimental membranous nephropathy (Heymann nephritis or HN) and treated with CTLA4-Ig alone or CTLA4-Ig plus a short-course of bortezomib. Serum creatinine, proteinuria, kidney histology, serum anti-Fx1A levels, kidney and spleen messenger RNA expression, and flow cytometry on splenocytes were evaluated at 12 weeks.

Results: CTLA4-Ig-treated and CTLA4-Ig plus bortezomib-treated rats had significant and similar reductions in serum creatinine and proteinuria, with less histological kidney injury compared to untreated HN rats. Glomerular IgG deposition was reduced in CTLA4-Ig-treated and CTLA4-Ig plus bortezomib-treated rats compared to untreated HN rats but there were no significant differences in serum anti-Fx1A levels. CTLA4-Ig-treated and CTLA4-Ig plus bortezomib-treated rats exhibited significantly reduced T helper (Th)-17 cell cytokines (interleukin (IL)-6, IL-17, IL-21) and regulatory T cell (Foxp3, TGF-β) expression in the kidney but not the spleen. Immunohistochemical staining of $CD4^+$ and intracellular $STAT3^+$ cells were reduced in CTLA4-Ig plus bortezomib-treated and CTLA4-Ig-treated compared to untreated HN rats. On flow cytometry, CTLA4-Ig reduced B cells and plasma cells but not T cell subsets.

Conclusion: CTLA4-Ig ameliorated induction of experimental membranous nephropathy, potentially through suppression of Th17 cells in the kidney and may represent an effective adjunct treatment in membranous nephropathy.

4.2 Key Learning Points

What is known: Despite the importance of autoantibodies targeting podocyte antigens (primarily against the phospholipase A2 receptor) in primary membranous nephropathy, B cell depletion with rituximab remains incompletely effective in up to 40% of patients, potentially due to autoreactive T cells or autoantibody-producing plasma cells, which are not eliminated by rituximab.

This study adds: Here, we report that T cell costimulatory blockade with cytotoxic-T-lymphocyte-associated antigen 4 (CTLA4)-Ig protected against experimental membranous nephropathy, potentially by suppressing T helper-17 cells in the kidney without significantly reducing autoantibody production. The addition of bortezomib, a proteasome inhibitor that depletes plasma cells, did not provide further benefit.

Potential impact: T helper-17 cells may play an important role in kidney injury in primary membranous nephropathy, in addition to autoantibody-mediated injury, which warrants further study. Abatacept (CTLA4-Ig approved for human use), may potentially be an effective adjunct in treating primary membranous nephropathy.

Keywords: CTLA4-Ig, Heymann nephritis, Membranous nephropathy, T cell costimulatory blockade, Th17 cells

4.3 Introduction

Primary membranous nephropathy (MN) is one of the most common causes of adult-onset nephrotic syndrome, characterized by autoantibodies against podocyte antigens (phospholipase A2 receptor (PLA2R) in 70%).[1] Current treatments for primary MN remain incompletely effective and are associated with significant toxicity (eg. cyclophosphamide and glucocorticoids) or high rates of disease relapse (eg. calcineurin inhibitors). B cell depletion with rituximab also fails to induce remission in up to 40% of patients.[2]

Heymann nephritis (HN) is an experimental model of MN caused by immunization of the crude tubular protein Fx1A in Lewis rats, which mimics the immunological phenotype of MN with autoantibodies against a podocyte antigen causing *in situ* immune complex deposition.[3] There is also a cellular immune response in HN with small infiltrates of $CD8^+$ T cells and $CD4^+$ T helper (Th)-1 cells.[4] $CD4^+$ T cell subsets in human MN exhibit increased Th2 cells,[5] increased T follicular helper (Tfh) cells,[6] and reduced regulatory T cells (Tregs),[7] with an increasing recognition of Th17 cells. Single-cell RNA sequencing of kidney biopsies in human MN revealed the key role of interleukin (IL)-17 signalling and immune activation of $CD4^+$ T cells,[8, 9] and increased markers of Th17 cells correlated with disease severity.[10-12] Therefore, control of both humoral and cellular immunity is important in the treatment of MN.

Cytotoxic-T-lymphocyte-associated antigen 4 (CTLA4) is a member of the immunoglobulin (Ig) superfamily that acts as the inhibitory homolog to the T cell costimulatory protein CD28 by outcompeting it for interaction with B7-1/B7-2 (CD80/CD86) on antigen-presenting cells (APCs).[13] CTLA4-Ig has successfully treated preclinical autoimmune models of multiple sclerosis,[14] and systemic lupus erythematosus,[15] by suppressing autoreactive T cell migration and autoantibody

production due to the critical role of CD80/CD86 in Ig class switching and germinal center formation.[15, 16]

The proteasome inhibitor bortezomib depletes plasma cells by inducing endoplasmic reticulum stress and has been effective in a case report of treatment-resistant primary MN.[17] However, the risk of neurotoxicity and infection with bortezomib limits repeated or prolonged use. Bortezomib monotherapy did not reduce donor-specific antibody production in allosensitized non-human primates despite depleting plasma cells due to a compensatory increase in germinal center formation by B cells and Tfh cells, which could be abrogated by T cell costimulatory blockade.[18] A short course of bortezomib plus CTLA4-Ig was effective in treating a donor-specific antibody mouse model and kidney transplant recipients with antibody-mediated rejection.[19]

In this study, we investigated the effects of CTLA4-Ig with or without a short course of bortezomib in HN. CTLA4-Ig alone ameliorated kidney disease without a significant effect on autoantibody production, which appears to be through suppression of Th17 cells in the kidney.

4.4 Material and Methods

4.4.1 Induction of active Heymann nephritis and treatment with CTLA4-Ig with or without bortezomib

Male Lewis rats (4-6 weeks old weighing 120-200 g) were obtained from the Animal Resources Centre in Perth, Australia. Outbred male Sprague-Dawley (SD) rats were used for producing Fx1A as described below.[3] Each group of six rats were immunized subcutaneously into one hind footpad and tail base each with 100 µl Fx1A emulsified in Complete Freund's Adjuvant (CFA), containing a total of 15 mg of Fx1A, 1mg mycobacterium tuberculosis HRa37 (BD Biosciences #231141), 100 µl

of Incomplete Freund's Adjuvant (IFA) (Sigma-Aldrich #F5506), and 100 µl of phosphate-buffered saline (PBS). The control rats were immunized with an equivalent CFA emulsion prepared without Fx1A. A total of 24 rats were used and randomization was not performed. All rat procedures carried out were approved by the Western Sydney Local Health District Animal Ethics Committee (protocol 4346.12.20).

We treated HN rats with recombinant human CTLA4-Ig (300 µg intraperitoneal twice weekly for 6 weeks from Fx1A induction) (Bio X Cell #BE0099) with or without bortezomib (0.2 mg/kg intraperitoneal twice weekly for 3 weeks from Fx1A induction) (Baxter #2347B0016). We based the dose of CTLA4-Ig on a previous rat study in autoimmune anti-glomerular basement membrane glomerulonephritis.[20] We used a finite treatment course of CTLA4-Ig and a short course of bortezomib to improve the translational potential of these treatment regimes, which we hypothesized could control disease and limit toxicity. We also tested the therapeutic effect of CTLA4-Ig by treating HN rats after the onset of significant proteinuria at 8 weeks after Fx1A induction[21] (300 µg intraperitoneal twice weekly from weeks 8 to 12 after Fx1A induction).

4.4.2 Production of Fx1A

Adult male SD rats of at least 12 weeks age were used to prepare Fx1A, a crude tubular antigen, which is also expressed in the podocytes of rats. SD rats were anaesthetized using isoflurane and abdominal aorta puncture performed to perfuse PBS (Thermofisher #14190250) *in vivo* until kidneys became white. The kidney cortices were dissected and pushed through a 150-mesh steel sieve (bore size 104-106) in PBS. Filtrates were centrifuged twice with PBS (400g, 10 min, 4ºC) and supernatant collected each time. The supernatant (compromising of the tubular fraction containing the Fx1A antigen) was ultracentrifuged three times (Sorvall rotor SW-28 at 50,000g for 45 min at 4ºC), each time discarding the supernatant and resuspending the pellet in cold ultrapure Milli-Q water. The pellet

was lyophilized and then stored at -80ºC. Experiments were performed using Fx1A from the same batch.

4.4.3 Purification of Fx1A by fractional salt precipitation

Fx1A 200 mg was solubilized in 10 ml of 1% deoxycholic acid (DOC) in 0.1M sodium chloride, 0.01M ethylenediaminetetraacetic acid and 0.01M Tris buffer at a pH of 8.0 and the suspension was stirred for 2 hours at 4ºC. The sample was ultracentrifuged (Sorvall rotor SW-55 Ti at 50,000g for 45 min at 4ºC) and supernatant (containing Fx1A) collected, to which 4.75 ml of saturated ammonium sulphate was slowly added with constant stirring at 4ºC. The sample was ultracentrifuged (Sorvall rotor SW-55 Ti at 50,000g for 45 min at 4ºC) again then supernatant collected and dialyzed in 0.9% NaCl overnight at 4ºC, then stored at -80ºC.

4.4.4 Anti-Fx1A autoantibody detection by enzyme-linked immunosorbent assay (ELISA)

Anti-Fx1A autoantibody titers were determined by ELISA at 12 weeks after Fx1A or CFA immunization. Fx1A for ELISA was solubilized and purified by fractional salt precipitation.[3] Immulon 1B ELISA plates (John Morris Scientific #8045155) were coated with 100 µl of purified Fx1A (40 µg/mL, diluted in PBS) overnight at 4°C. The ELISA plate was washed with PBS + 0.05% Tween 20 twice and blocked with 300 µl of 2% bovine serum albumin (BSA, Sigma-Aldrich #A3983) for 1 hour at room temperature. The plate was washed with PBS + 0.05% Tween 20 three times and incubated with 100 µl of rat sera (diluted 1:20 in BSA 2%) for 1 hour at 37°C. The plate was subsequently washed with PBS + 0.05% Tween 20 three times and incubated with 100 µl of alkaline phosphatase-conjugated pre-absorbed goat antibody to rat IgG (Abcam #ab7098, diluted 1:1000 in BSA 2%) for 1 hour at 37°C. After washing the plate with PBS + 0.05% Tween 20 four times, 100 µl of p-nitrophenyl phosphate (PNPP) substrate (Thermofisher #37621) was added for 30 minutes. The yellow color reaction was read on a SpectraMax iD3 machine at 405 nm in triplicated samples.

Anti-Fx1A autoantibodies were quantified as a percentage of positive binding, calculated by dividing the sample optical density by the optical density of a positive control sample of known strongly positive serum containing anti-Fx1A. Background based on blank wells incubated with BSA 2% was subtracted from optical density values.

4.4.5 Flow cytometry analysis

For surface staining, splenocytes were incubated with fluorochrome-conjugated anti-rat antibodies for 25 min on ice in the dark. Intracellular labelling of was performed using fixed and permeabilized cells using PE Anti-mouse/rat forkhead box P3 (Foxp3) Staining Set (eBioscience #72-5775-40) according to manufacturer's instructions. All samples were analyzed by flow cytometry using a LSRII-10 and Fortessa Color Flow Cytometer (BD Biosciences, San Jose, USA). Data analyses were performed using the FlowJo™ software (Tree Star, Ashland, USA).

The following surface markers were measured on splenocytes via flow cytometry at week 12 (CD3-FITC, Biolegend #201403; CD4-FITC, Biolegend #203406; CD4-APC/Cy7, Biolegend #201518; CD8-PE/Cy7, Biolegend #201716; CD45RA-PE, Biolegend #202307; IgM-AF647, Biolegend #408909; ICOS-Pacific Blue, Biolegend #313522; PD1-CoraLite647, Proteintech #CL647-66220; CD45R-FITC, BD Bioscience #561876; CD138-PE, Abcam #ab209584; CD98-APC, Biolegend #206403; CD25-APC, Biolegend #202114; Live/Dead Fixable Aqua Dead Cell Stain Kit, Thermofisher #L34965). Intracellular labelling of forkhead box P3 (Foxp3) (Foxp3-PE, Biolegend #320008) was performed using fixed and permeabilized cells using PE Anti-mouse/rat Foxp3 Staining Set (eBioscience #72-5775-40) and according to manufacturer's instructions.

4.4.6 Measurement of protein and creatinine

Urine protein and creatinine levels, along with serum albumin and creatinine levels were measured at week 12. Blood samples for serum albumin and creatinine were obtained by inferior vena cava puncture at week 12. Urine protein/creatinine ratio was measured from a 16-hour urine collection using metabolic cages in which rats had access to water but not food. Serum and urine creatinine was measured using the CREA method on the Ortho Vitros Fusion 5600 (Ortho Clinical Diagnostics, Egypt), serum albumin measured using the ALB method on the Ortho Vitros Fusion 5600, and total urine protein was measured using the Biuretic method (Randox Total Protein) on the Ortho Vitros Fusion 5600.

4.4.7 Histology and morphometric evaluation

The kidneys were removed at week 12. Sagittal slices of kidney tissue were fixed in neutral buffered formalin at room temperature for 24 hours and embedded in paraffin to evaluate their pathology. 4 μm slices were stained with Periodic Acid-Schiff (PAS) reagent and assessed by light microscopy. The remaining cortex of the same kidney was snap frozen in liquid nitrogen and used for RNA analysis and immunohistochemistry. In each biopsy, a semi-quantitative score from two blinded trained observers was used to evaluate the degree of kidney injury as previously described.[22] The degree of glomerulosclerosis, tubular injury and interstitial infiltrate was evaluated on kidney sections embedded in paraffin, sections cut into 4 μm slices and stained with PAS stain. A minimum of 10 consecutive fields at 400x magnification were assessed and scored in one section per rat. Glomerulosclerosis was defined as glomeruli demonstrating any degree of sclerosis. Tubular injury was defined as tubular dilatation, epithelial cellular atrophy, and luminal cast formation. Interstitial infiltrate was defined as PAS-positive mononuclear cellular infiltration in the tubulointerstitial compartment. Each score was graded according to the extent of cortical involvement on a scale of 0 to 4: 0, normal; 1, involvement of 10-24% of the cortex; 2, involvement of 25-49% of the cortex; 3, involvement of up to 50–75% of the cortex; and 4, extensive damage involving >75% of the cortex.

The degree of kidney injury was estimated by averaging each score across the 10 consecutive fields between two blinded trained observers.

4.4.8 Immunofluorescence

Immunofluorescence staining was performed for glomerular IgG deposition using the primary antibody goat anti-rat IgG H&L Alexa Fluor®-594 (Abcam #ab150160, diluted 1:100, incubated for 1 hour at room temperature). Frozen kidney specimens were embedded in Tissue-Tek OCT (ProSciTech #IA018), 5 μm sections were cut on a Cryostat, dried overnight at room temperature, fixed in cold acetone at -20°C for 8 minutes, and dried for 30 minutes. Sections were incubated in blocking horse serum 2.5% (Vector Labs #S-2012) for 10 minutes. Images (magnification X400) were taken using a DeltaVision core microscope (Applied Precision, Washington). Total fluorescence density was quantified by the ratio of the integrated density over area of a representative glomerulus using the Fiji software.[23]

4.4.9 Immunohistochemistry

Immunohistochemical staining was performed for $CD4^+$ T cells, $CD8^+$ T cells and macrophages. Primary antibodies used in immunohistochemistry were: rabbit anti-mouse/rat CD4 (CAL4 clone) (Abcam #ab237722, diluted 1:2000, incubated at 4ºC overnight), mouse anti-rat CD8 (MRC OX8 clone) (Biorad #MCA48GA, diluted 1:75, incubated for 1 hour at room temperature), mouse anti-rat CD68 (ED1 clone) for macrophages (Biorad #MCA341GA, diluted 1:100, incubated for 1 hour at room temperature), rabbit anti-rat/mouse/human signal transduction and activators of transcription (STAT)3 (Abcam #ab31370, diluted 1:250, incubated at 4ºC overnight) and rabbit anti-rat/mouse/human Ki67 (SP6 clone) (Abcam #ab16667, diluted 1:100, incubated at 4ºC overnight). The secondary antibody was obtained from the ImmPRESS Universal PLUS Polymer Kit, Peroxidase

(horse anti-mouse/rabbit IgG) (Vector Labs #MP-7800). Peroxidase (horse anti-mouse/rabbit IgG) (Vector Labs #MP-7800) (Supplementary material). TUNEL assay (Abcam #ab206386) for evaluate lymphocyte apoptosis was performed according to manufacturer's instructions.

Kidney and spleen specimens were embedded in paraffin, 5 μm sections of kidney and spleen were cut, deparaffinized in Xylene (three times for 5 minutes), rehydrated in alcohol 100% (three times for 5 minutes) and alcohol 70% (once for 5 minutes), then washed in tap water. Antigen retrieval was performed by placing slides in citrate buffer pH 6.0 (Sigma-Aldrich #C9999) and using a Decloaking Chamber NxGen at 95°C for 20 minutes. Endogenous peroxidase activity was blocked by incubating sections for 15 minutes in 0.3% (vol/vol) H_2O_2 solution. Blocking and slide development with peroxidase substrate were performed using the ImmPRESS Universal PLUS Polymer Kit according to manufacturer's instructions except for $CD4^+$ staining in which the secondary ImmPRESS Universal Polymer was diluted 1:3. Slides were counterstained with hematoxylin (Sigma-Aldrich). To assess levels of interstitial infiltration, positively stained cells were counted from five random cortical fields (magnification X400).

4.4.10 Real-time polymerase chain reaction (PCR)

RNA was isolated from the rat spleen and kidney samples using TRIzol reagent (Thermofisher #15596018) to analyze messenger RNA (mRNA) expression. The total RNA was reverse transcribed to get cDNA as described previously.[24] To extract RNA, rat spleen and kidney samples were homogenized in an Eppendorf tube containing 1ml TRIzol reagent (Thermofisher #15596018). After 5 minutes to permit complete dissociation of the nucleoproteins complex, 0.2ml of chloroform (Sigma-Aldrich #C2432-500ml) was added, vortexed thoroughly and incubated for 3 minutes. Samples were subsequently centrifuged (12,000g for 15 min at 4ºC) and aqueous phase supernatant (containing the RNA) transferred into a new Eppendorf tube. Isopropanol 0.5ml (Sigma-Aldrich

#I9516-500ml) was added, incubated for 10 minutes then centrifuged (12,000g for 10 min at 4ºC), supernatant discarded, and pellet resuspended in 1ml of 75% ethanol. The sample was centrifuged (7500g for 5 min at 4ºC), supernatant discarded and RNA pellet air dried then resuspended in RNase-free water.

To synthesize complementary DNA (cDNA), 20 µl reaction mixture was made of 1 µg of RNA was combined with 1 µl of random primers (Thermofisher #48190011) and 1 µl of deoxynucleotide triphosphate (dNTP) mix (Thermofisher #10297018) (comprised of 10 µl each of adenine (dATP), cytosine (dCTP), guanine (dGTP), and thymine (dTTP) in 60 µl of DNase/RNase-free water (Thermofisher #10977015)) and up to 12 µl of sterile distilled water. This reaction mixture was heated at 65°C for 5 minutes then chilled on ice to which 4 µl of 5x First-Strand Buffer, 2 µl of 0.1M dithiothreitol (DTT), and 1 µl of RNaseOUT (40 units/µl) (Thermofisher #10777019) was added, then incubated at 25°C for 2 minutes. Subsequently, 1 µl (200 units) of SuperScript II Reverse Transcriptase (Thermofisher #18064-014) was added then incubated at 25°C for 10 minutes followed by 42°C for 50 minutes, then reaction inactivated by heating at 70°C for 15 minutes.

Real-time PCR was performed for 40 cycles (initial denaturation at 95°C for 5 minutes, denaturation at 95°C for 20 seconds, and primer annealing and elongation at 60°C for 50 seconds) with l µl of cDNA sample in the presence of 20 µl of PCR reaction mixture (consisting of 2 µl 10x PCR buffer, 1.6 µl dNTP mixture, 0.1 µl Taq polymerase, 0.3 µl TaqMan Gene Expression Assay, and 16 µl RNase free water) (Sigma-Aldrich #11596594001, Thermofisher #10297018). TaqMan Gene Expression Assays consisted of a pair of unlabelled PCR primers and a Taqman probe with a dye label (FAM) on the 5' end and a minor groove binder (MGB) and non-fluorescent quencher (NFQ) on the 3' end. Primers were obtained specific for rat IL-6 (Thermofisher #Rn0140330_m1), IL-17 (Thermofisher #Rn01757168_m1), RAR-related orphan nuclear receptor C (RORC) (Thermofisher

#Rn01533717_g1), forkhead box P3 (Foxp3) (Thermofisher #Rn01525092_m1), IL-10 (Thermofisher #Rn99999012_m1), transforming growth factor (TGF)-β (Thermofisher #Rn00572010_m1), B cell lymphoma 6 (Bcl6) (Thermofisher #Rn01404339_m1), IL-21 (Thermofisher #Rn01755623_m1), interferon (IFN)-γ (Thermofisher #Rn00594078_m1), T-box transcription factor 21 (Tbet) (Thermofisher #Rn01461633_m1), B-lymphocyte-induced maturation protein 1 (Blimp-1) (Thermofisher #Rn03416161_m1), Interferon Regulatory Factor 4 (IRF4) (Thermofisher #Rn01435145_m1), X-box binding protein 1 (XBP1) (Thermofisher #Rn01443523_m1) and glyceraldehyde 3-phosphate dehydrogenase (GAPDH) (Thermofisher #Rn01775763_g1), and each sample was run in triplicate, normalized to GAPDH to account for complementary DNA variability. All samples were analyzed using the Rotogene Q PCR machine.

4.4.11 Statistical analysis

Results are expressed as group mean ± standard deviation (SD). Statistical analysis for multiple comparisons was performed using the one-way analysis of variance (ANOVA) test for normally distributed data and Kruskal-Wallis one-way ANOVA test for non-parametric data. Two group differences were analyzed using the student's *t*-test for normally distributed data and the Mann-Whitney U test for non- normally distributed data. A two-tailed p value <0.05 was considered statistically significant. Statistical calculations were performed using GraphPad Prism 9.2.0.

4.5 Results

4.5.1 CTLA4-Ig alone and CTLA4-Ig plus a short course of bortezomib reduced proteinuria and serum creatinine without altering anti-Fx1A antibody levels in Heymann nephritis rats

Lewis rats with HN were treated with CTLA4-Ig with or without bortezomib (**Figure 1A**). At 12 weeks after Fx1A immunization, rats treated with CTLA4-Ig or CTLA4-Ig plus bortezomib had significantly reduced proteinuria and serum creatinine compared to untreated HN rats (**Figure 1B-C**, $p<0.05$ or $p<0.001$). There was no significant difference in serum anti-Fx1A antibody levels between HN rats treated with CTLA4-Ig or CTLA4-Ig plus bortezomib and untreated HN rats (**Figure 1D**).

4.5.2 CTLA4-Ig alone and CTLA4-Ig plus a short course of bortezomib limited kidney injury, reduced glomerular IgG deposition and reduced Th17 cell infiltration into the kidney

Kidney histology revealed significantly less glomerulosclerosis, tubular injury, and interstitial mononuclear cell infiltrates in HN rats treated with CTLA4-Ig or CTLA4-Ig plus bortezomib compared to untreated HN rats (**Figure 2A-2D,** $p<0.05$ or $p<0.01$). Glomerular IgG deposition was reduced in HN rats treated with CTLA4-Ig or CTLA4-Ig plus bortezomib compared to untreated HN rats (**Figure 2E-2F,** $p<0.05$ or $p<0.01$).

To assess the extent of the cellular infiltration, we performed immunohistochemistry on the week 12 kidney sections. CTLA4-Ig or CTLA4-Ig plus bortezomib reduced infiltrating $CD4^+$ T cells and $STAT3^+$ cells, consistent with a reduction in Th17 cell infiltration, and also reduced infiltration of $CD8^+$ T cells and macrophages compared to untreated HN rats (**Figure 3A-D,** $p<0.01$, $p<0.001$ or $p<0.0001$). There were no significant differences in infiltration between CTLA4-Ig or CTLA4-Ig plus bortezomib groups suggesting the effects were mediated by CTLA4-Ig alone. A reduction in Ki67 staining and increase in TUNEL staining was also observed in splenic lymphocytes with both CTLA4-Ig and CTLA4-Ig plus bortezomib compared to untreated HN rats, suggesting CTLA4-Ig mediated its effects in part by reducing lymphocyte proliferation and increasing lymphocyte apoptosis (**Figure 3E-F,** $p<0.0001$, $p<0.001$ and $p<0.05$).

4.5.3 CTLA4-Ig alone and CTLA4-Ig plus a short course of bortezomib suppressed Th17 cytokines and regulatory T cell markers in the kidney but not the spleen

Twelve weeks post-Fx1A immunization, mRNA expression of Th17 cytokines (IL-6, IL-17, IL-21) and Treg markers (Foxp3, and TGF-β) quantified by real-time quantitative PCR (normalized to GAPDH to account for complementary DNA variability) were significantly reduced in the kidney but not spleen in HN rats treated with CTLA4-Ig or CTLA4-Ig plus bortezomib compared to untreated HN rats (**Figure 4A and 4B**, $p<0.05$ or $p<0.01$). There were no between-group differences in mRNA expression of Tfh (Bcl6, IL-21) or plasma cell (Blimp1, IRF4, XBP1) markers in the spleen. There were also no between-group differences in mRNA expression of Th1 markers (IFN-γ, Tbet)) or RORC, encoding ROR-γ, of which an isoform ROR-γt is a Th17 cell-specific transcription factor) in the kidney and spleen.

4.5.4 CTLA4-Ig alone and CTLA4-Ig plus a short course of bortezomib reduced B cells and plasma cells but not T follicular helper cells in the spleen

Flow cytometry analyses of splenocytes showed CTLA4-Ig reduced total B cells ($CD3^-$ $CD45RA^+IgM^+$), and CTLA4-Ig or CTLA4-Ig plus bortezomib reduced plasma cells ($CD45R^-$ $CD138^+CD98^+$) compared to untreated rats (**Figure 5B and 5D**, $p<0.05$ or $p<0.01$). There were no between-group differences in $CD4^+$ T cells ($CD3^+CD4^+$), $CD8^+$ T cells ($CD3^+CD8^+$), Tfh cells ($CD4^+$ $PD1^+ICOS^+$) or Tregs ($CD4^+CD25^+Foxp3^+$) (**Figure 5**).

4.5.5 Delayed CTLA4-Ig treatment after onset of proteinuria limited kidney injury by lowering serum creatinine, reduced interstitial infiltrate in the kidney but did not affect proteinuria or autoantibody production

Lewis rats with HN were treated with CTLA4-Ig 8 weeks after Fx1A immunization, when significant proteinuria develops. At 12 weeks after Fx1A immunization, rats treated with CTLA4-Ig had significantly reduced serum creatinine compared to untreated HN rats but there were no differences in proteinuria (**Figure 6A-B**, $p<0.05$). There was no significant difference in serum anti-Fx1A antibody levels between HN rats treated with CTLA4-Ig after 8 weeks and untreated HN rats (**Figure 6C**). Kidney histology revealed significantly less interstitial mononuclear cell infiltrates in HN rats treated with CTLA4-Ig after 8 weeks compared to untreated HN rats but there were no differences in glomerulosclerosis or tubular injury (**Figure 6D-G,** $p<0.05$).

4.6 Discussion

In this study, we found CTLA4-Ig ameliorated experimental MN with a reduction in proteinuria, serum creatinine and histological kidney injury, potentially mediated through suppression of Th17 cells in the kidney. A short course of bortezomib provided no additional protection. CTLA4-Ig reduced total B cells and plasma cells but did not suppress Tfh cells and no significant differences were found in anti-Fx1A autoantibody levels. However, CTLA4-Ig also suppressed markers of Tregs in the kidney, suggesting CTLA4-Ig has both protective effects against pro-inflammatory Th17 cells but might also reduce anti-inflammatory Tregs. There were no between-group differences in RORC expression, which may reflect non-specific expression of ROR-γ on non-hematopoietic cells whereas ROR-γt, the ROR-γ isoform that is a Th17-cell-specific transcription factor, is exclusively expressed on lymphoid cells.[25] When CTLA4-Ig was given after the onset of significant proteinuria, kidney injury was attenuated by reducing interstitial inflammation without significant changes in proteinuria or anti-Fx1A autoantibody levels, suggesting CTLA4-Ig primarily ameliorates disease mechanisms downstream of proteinuria or disease mechanisms independent of autoantibody production.

Th17 cells are involved in autoimmune kidney diseases (both in animal models and humans) including ANCA vasculitis, lupus nephritis, anti-glomerular basement membrane disease, and IgA nephropathy.[26] However, this is the first description of Th17 involvement in HN. CFA is a known inducer of IL-6 production from APCs, which in the presence of TGF-β activates Th17 cells.[27] While IL-6 is a key driver of Th17 differentiation, IL-6 deficient mice could still generate a Th17 immune response through IL-21, providing an alternative pathway for Th17 differentiation.[28] IL-21 production is dependent on STAT3 but not ROR-γ,[29] and IL-21-dependent Th17 differentiation in HN may explain the lack of between-group differences in RORC expression in our study. However, in autoimmune models of multiple sclerosis also induced by CFA, IL-21 was dispensable for Th17 cells due to the large amount of IL-6 induced by CFA. Regardless of the etiology of Th17 differentiation in HN, kidney proximal tubular epithelial cells are activated by IL-17A, which causes IL-6 release and together with IL-21, amplifies Th17 cell activation.[31, 32]

CTLA4-Ig has also been shown to ameliorate adriamycin-induced nephropathy in rats by suppressing IL-17.[33] However CD28/B7 costimulation, which is inhibited by CTLA4-Ig, is not required for human Th17 differentiation but is for Treg development.[34] Furthermore, studies in both mice and humans have demonstrated Th17 cells express high levels of CTLA4 compared to Th1 cells and are resistant to costimulatory blockade by CTLA4-Ig.[35] In experimental nephrotoxic nephritis, upregulation of the chemokine receptor CCR6 ligand CCL20 results in infiltration of both CCR6-expressing Th17 cells and Tregs but not Th1 cells.[36] Indeed, CCR6 expression required CD28 costimulation,[37] which would be inhibited by CTLA4-Ig. This is consistent with our study results where CTLA4-Ig reduced mRNA expression of Th17-associated cytokines and Treg markers in the kidney but not the spleen and had no effect on Th1 cells. Our study is also consistent with previous studies in HN and experimental autoimmune glomerulonephritis treated with CD40 DNA vaccines, which upregulated CTLA4 mRNA expression in the draining lymph nodes and suppressed Th17 cells but not Th1 cells.[38, 39]

CD40 DNA vaccines also reduced CD86 on B cells with no change in numbers, whereas we found CTLA4Ig reduced B cell numbers.[38] Despite the reduction in B cells and plasma cells, our study did not demonstrate a significant effect of CTLA4-Ig on autoantibody production, which is consistent with clinical data in patients with rheumatoid arthritis where CTLA4-Ig monotherapy did not alter anti-citrullinated protein autoantibody levels.[40] We also found CTLA4-Ig reduced expression of Tregs markers (FoxP3 and TGF-β) in the kidney, which is consistent with the known deleterious effect of CTLA4-Ig on Tregs due to blockade of CD28/B7-mediated Treg homeostasis.[40] However, clinical use of CTLA4-Ig has been shown to be powerfully immunosuppressive, providing an alternative to calcineurin inhibitors post-transplant.[41]

In human MN, French and Chinese cohorts have demonstrated higher levels of Th17 cells and IL-17 compared to healthy controls, which were associated with increased disease severity.[10-12] An earlier study reported lower serum IL-17 in MN patients, which may reflect urinary protein loss of IL-17 due to higher proteinuria in this cohort.[42] Regarding potential causes of Th17 activation in MN, higher exposure to fine air particulate matter have correlated with higher serum levels of IL-17A and incidence of MN, since air pollution may act as a danger signal resulting in IL-6 production by APCs and the innate immune system, ultimately activating autoreactive T cells.[10, 43] Other potential triggers for Th17 activation include migration of Th17 cells from the gut or infections activating $CD4^+$ tissue-resident memory cells with a Th17 signature, which have been implicated in experimental crescentic glomerulonephritis though its role remains unclear in MN.[44, 45] In patients with MN, cyclosporin but not rituximab effectively suppressed Th17 cytokines, demonstrating the importance of addressing autoreactive T cells in MN, which CTLA4-Ig may also achieve.[10, 11] The increasingly recognized role of Th17 cells in MN is reflected in the ALPHAGEM trial targeting Th17 activation in MN (NCT05941845) using interferon alfa.

However, there were limitations with our study. Similar to data in human MN, we showed association between Th17 cells and kidney injury in HN but did not show causation. Furthermore, we did not assess absolute cell numbers on flow cytometry, which is relevant because costimulation inhibits lymphocyte proliferation and increases apoptosis, though this was demonstrated in our immunohistochemical staining. We also did not evaluate whether reduction in Treg markers due to CTLA4-Ig impaired Treg function. Lastly, we did not perform power calculations for our study, which may be underpowered to detect differences in serum anti-Fx1A levels.

In conclusion, our study demonstrates CTLA4-Ig ameliorates the induction of experimental MN potentially through suppression of Th17 cells in the kidney and without significant effect on autoantibody production. This reflects our understanding that MN is both a T cell and antibody mediated disease. With our increasing understanding the role of Th17 cells in MN, CTLA4-Ig may be an effective adjunctive treatment targeting T cells combined with strategies targeting autoantibody production such as anti-CD20 antibodies.

4.7 References

1. Couser WG. Primary Membranous Nephropathy. Clin J Am Soc Nephrol. 2017;12(6):983-97.

2. Fervenza FC, Appel GB, Barbour SJ, et al. Rituximab or Cyclosporine in the Treatment of Membranous Nephropathy. N Engl J Med. 2019;381(1):36-46.

3. Edgington TS, Glassock RJ, Dixon FJ. Autologous immune complex nephritis induced with renal tubular antigen. I. Identification and isolation of the pathogenetic antigen. J Exp Med. 1968;127(3):555-72.

4. Penny MJ, Boyd RA, Hall BM. Role of T cells in the mediation of Heymann nephritis. ii. Identification of Th1 and cytotoxic cells in glomeruli. Kidney Int. 1997;51(4):1059-68.

5. Kuroki A, Iyoda M, Shibata T, et al. Th2 cytokines increase and stimulate B cells to produce IgG4 in idiopathic membranous nephropathy. Kidney Int. 2005;68(1):302-10.

6. Zhang Z, Shi Y, Yang K, et al. Higher frequencies of circulating ICOS(+), IL-21(+) T follicular helper cells and plasma cells in patients with new-onset membranous nephropathy. Autoimmunity. 2017;50(8):458-67.

7. Cantarelli C, Jarque M, Angeletti A, et al. A Comprehensive Phenotypic and Functional Immune Analysis Unravels Circulating Anti-Phospholipase A2 Receptor Antibody Secreting Cells in Membranous Nephropathy Patients. Kidney Int Rep. 2020;5(10):1764-76.

8. Xu J, Shen C, Lin W, et al. Single-Cell Profiling Reveals Transcriptional Signatures and Cell-Cell Crosstalk in Anti-PLA2R Positive Idiopathic Membranous Nephropathy Patients. Front Immunol. 2021;12:683330.

9. Shi M, Wang Y, Zhang H, et al. Single-cell RNA sequencing shows the immune cell landscape in the kidneys of patients with idiopathic membranous nephropathy. Front Immunol. 2023;14:1203062.

10. Cremoni M, Brglez V, Perez S, et al. Th17-Immune Response in Patients With Membranous Nephropathy Is Associated With Thrombosis and Relapses. Front Immunol. 2020;11:574997.

11. Tang D, Guo J, Zhang J. Variation of Peripheral Th17/Treg Imbalance in Patients with Idiopathic Membranous Nephropathy After Cyclosporin a Treatment: A Prognostic Marker of Idiopathic Membranous Nephropathy. Biomed J Sci Tech Res. 2018;7.

12. Li H, Wu H, Guo Q, et al. Myeloid-Derived Suppressor Cells Promote the Progression of Primary Membranous Nephropathy by Enhancing Th17 Response. Front Immunol. 2020;11:1777.

13. Linsley PS, Ledbetter JA. The role of the CD28 receptor during T cell responses to antigen. Annu Rev Immunol. 1993;11:191-212.

14. Cross AH, Girard TJ, Giacoletto KS, et al. Long-term inhibition of murine experimental autoimmune encephalomyelitis using CTLA-4-Fc supports a key role for CD28 costimulation. J Clin Invest. 1995;95(6):2783-9.

15. Finck BK, Linsley PS, Wofsy D. Treatment of murine lupus with CTLA4Ig. Science. 1994;265(5176):1225-7.

16. Borriello F, Sethna MP, Boyd SD, et al. B7-1 and B7-2 have overlapping, critical roles in immunoglobulin class switching and germinal center formation. Immunity. 1997;6(3):303-13.

17. Geara AS, Bhoj V, Hogan JJ. Bortezomib Treatment for Refractory PLA2R-Positive Membranous Nephropathy. Glomerular Dis. 2021;1(1):40-3.

18. Kwun J, Burghuber C, Manook M, et al. Successful desensitization with proteasome inhibition and costimulation blockade in sensitized nonhuman primates. Blood Adv. 2017;1(24):2115-9.

19. Jain D, Rajab A, Young JS, et al. Reversing donor-specific antibody responses and antibody-mediated rejection with bortezomib and belatacept in mice and kidney transplant recipients. Am J Transplant. 2020;20(10):2675-85.

20. Nishikawa K, Linsley PS, Collins AB, Stamenkovic I, McCluskey RT, Andres G. Effect of CTLA-4 chimeric protein on rat autoimmune anti-glomerular basement membrane glomerulonephritis. Eur J Immunol. 1994;24(6):1249-54

21. Heymann W, Hackel DB, Harwood S, et al. Production of nephrotic syndrome in rats by Freund's adjuvants and rat kidney suspensions. Proc Soc Exp Biol Med. 1959;100(4):660-4.

22. Mizuno S, Kurosawa T, Matsumoto K, et al. Hepatocyte growth factor prevents renal fibrosis and dysfunction in a mouse model of chronic renal disease. J Clin Invest. 1998;101(9):1827-34.

23. Schindelin J, Arganda-Carreras I, Frise E, et al. Fiji: an open-source platform for biological-image analysis. Nat Methods. 2012;9(7):676-82.

24. Wang YM, Zhang GY, Hu M, et al. CD8+ regulatory T cells induced by T cell vaccination protect against autoimmune nephritis. J Am Soc Nephrol. 2012;23(6):1058-67.

25. Eberl G. RORγt, a multitask nuclear receptor at mucosal surfaces. Mucosal Immunol. 2017;10(1):27-34.

26. Dolff S, Witzke O, Wilde B. Th17 cells in renal inflammation and autoimmunity. Autoimmun Rev. 2019;18(2):129-36.

27. Dong C. TH17 cells in development: an updated view of their molecular identity and genetic programming. Nat Rev Immunol. 2008;8(5):337-48.

28. Korn T, Bettelli E, Gao W, et al. IL-21 initiates an alternative pathway to induce proinflammatory T(H)17 cells. Nature. 2007;448(7152):484-7.

29. Nurieva R, Yang XO, Martinez G, et al. Essential autocrine regulation by IL-21 in the generation of inflammatory T cells. Nature. 2007;448(7152):480-3.

30. Coquet JM, Chakravarti S, Smyth MJ, et al. Cutting edge: IL-21 is not essential for Th17 differentiation or experimental autoimmune encephalomyelitis. J Immunol. 2008;180(11):7097-101.

31. Van Kooten C, Boonstra JG, Paape ME, et al. Interleukin-17 activates human renal epithelial cells in vitro and is expressed during renal allograft rejection. J Am Soc Nephrol. 1998;9(8):1526-34.

32. Bettelli E, Korn T, Oukka M, et al. Induction and effector functions of T(H)17 cells. Nature. 2008;453(7198):1051-7.

33. Shuai L, Cheng Q, Shen T, et al. CTLA4-Ig Abatacept Ameliorates Proteinuria by Regulating Circulating Treg/IL-17 in Adriamycin-Induced Nephropathy Rats. Biomed Res Int. 2020;2020:2347827.

34. Revu S, Wu J, Henkel M, et al. IL-23 and IL-1β Drive Human Th17 Cell Differentiation and Metabolic Reprogramming in Absence of CD28 Costimulation. Cell Rep. 2018;22(10):2642-53.

35. Krummey SM, Cheeseman JA, Conger JA, et al. High CTLA-4 expression on Th17 cells results in increased sensitivity to CTLA-4 coinhibition and resistance to belatacept. Am J Transplant. 2014;14(3):607-14.

36. Turner JE, Paust HJ, Steinmetz OM, et al. CCR6 recruits regulatory T cells and Th17 cells to the kidney in glomerulonephritis. J Am Soc Nephrol. 2010;21(6):974-85.

37. Zhang R, Borges CM, Fan MY, et al. Requirement for CD28 in Effector Regulatory T Cell Differentiation, CCR6 Induction, and Skin Homing. J Immunol. 2015;195(9):4154-61.

38. Wang Y, Wang YM, Wang Y, et al. DNA vaccine encoding CD40 targeted to dendritic cells in situ prevents the development of Heymann nephritis in rats. Kidney Int. 2013;83(2):223-32.

39. Li Q, Cao Q, Wang C, et al. Dendritic cell-targeted CD40 DNA vaccine suppresses Th17 and ameliorates progression of experimental autoimmune glomerulonephritis. J Leukoc Biol. 2019;105(4):809-19.

40. Pieper J, Herrath J, Raghavan S, et al. CTLA4-Ig (abatacept) therapy modulates T cell effector functions in autoantibody-positive rheumatoid arthritis patients. BMC Immunol. 2013;14:34.

41. Vincenti F, Rostaing L, Grinyo J, et al. Belatacept and Long-Term Outcomes in Kidney Transplantation. N Engl J Med. 2016;374(4):333-43

42. Rosenzwajg M, Languille E, Debiec H, et al. B- and T-cell subpopulations in patients with severe idiopathic membranous nephropathy may predict an early response to rituximab. Kidney Int. 2017;92(1):227-37.

43. Xu X, Wang G, Chen N, et al. Long-Term Exposure to Air Pollution and Increased Risk of Membranous Nephropathy in China. J Am Soc Nephrol. 2016;27(12):3739-46.

44. Krebs CF, Paust HJ, Krohn S, et al. Autoimmune Renal Disease Is Exacerbated by S1P-Receptor-1-Dependent Intestinal Th17 Cell Migration to the Kidney. Immunity. 2016;45(5):1078-92.

45. Krebs CF, Reimers D, Zhao Y, et al. Pathogen-induced tissue-resident memory T(H)17 (T(RM)17) cells amplify autoimmune kidney disease. Sci Immunol. 2020;5(50).

4.8 Figures

Figure 1

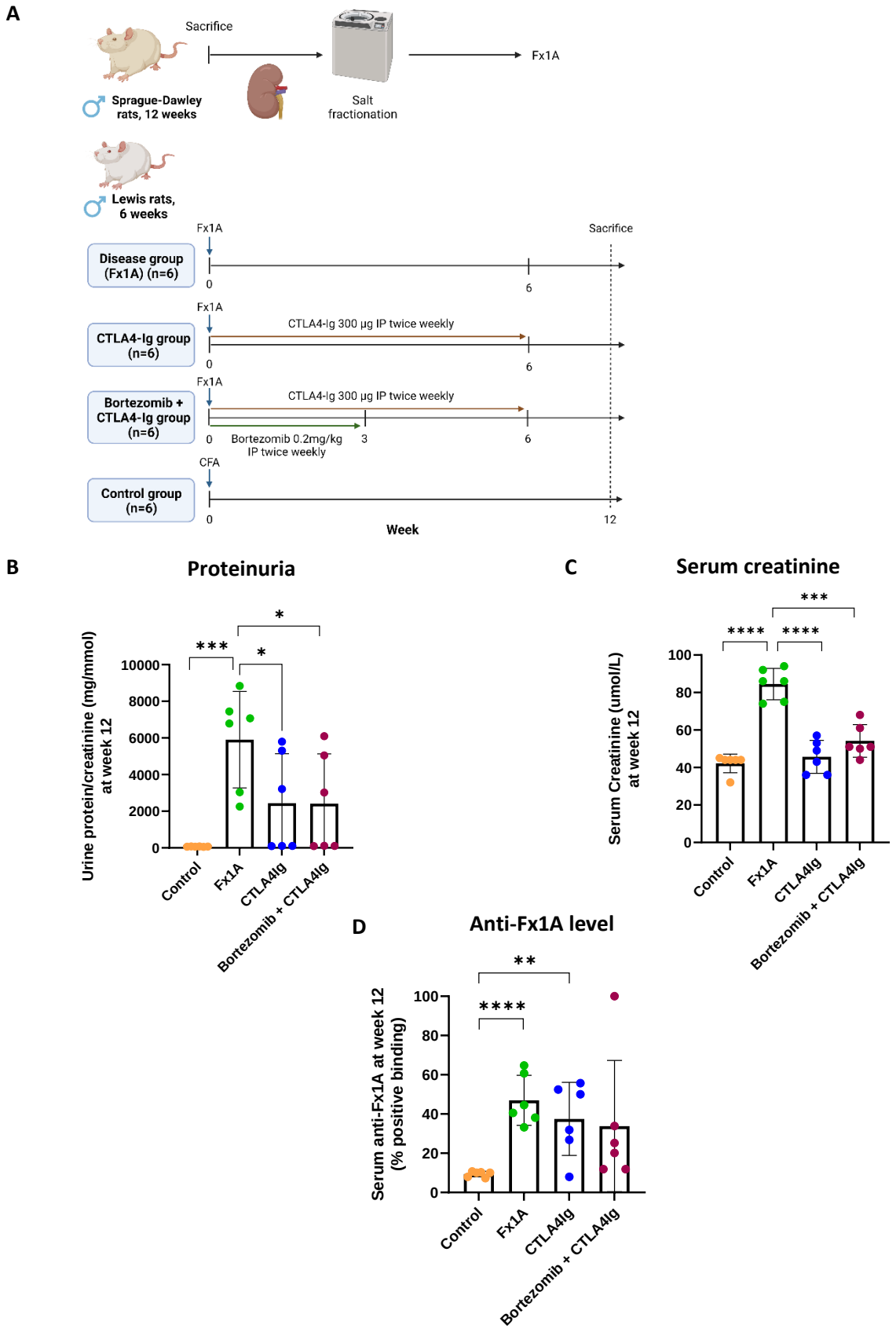

Figure 2

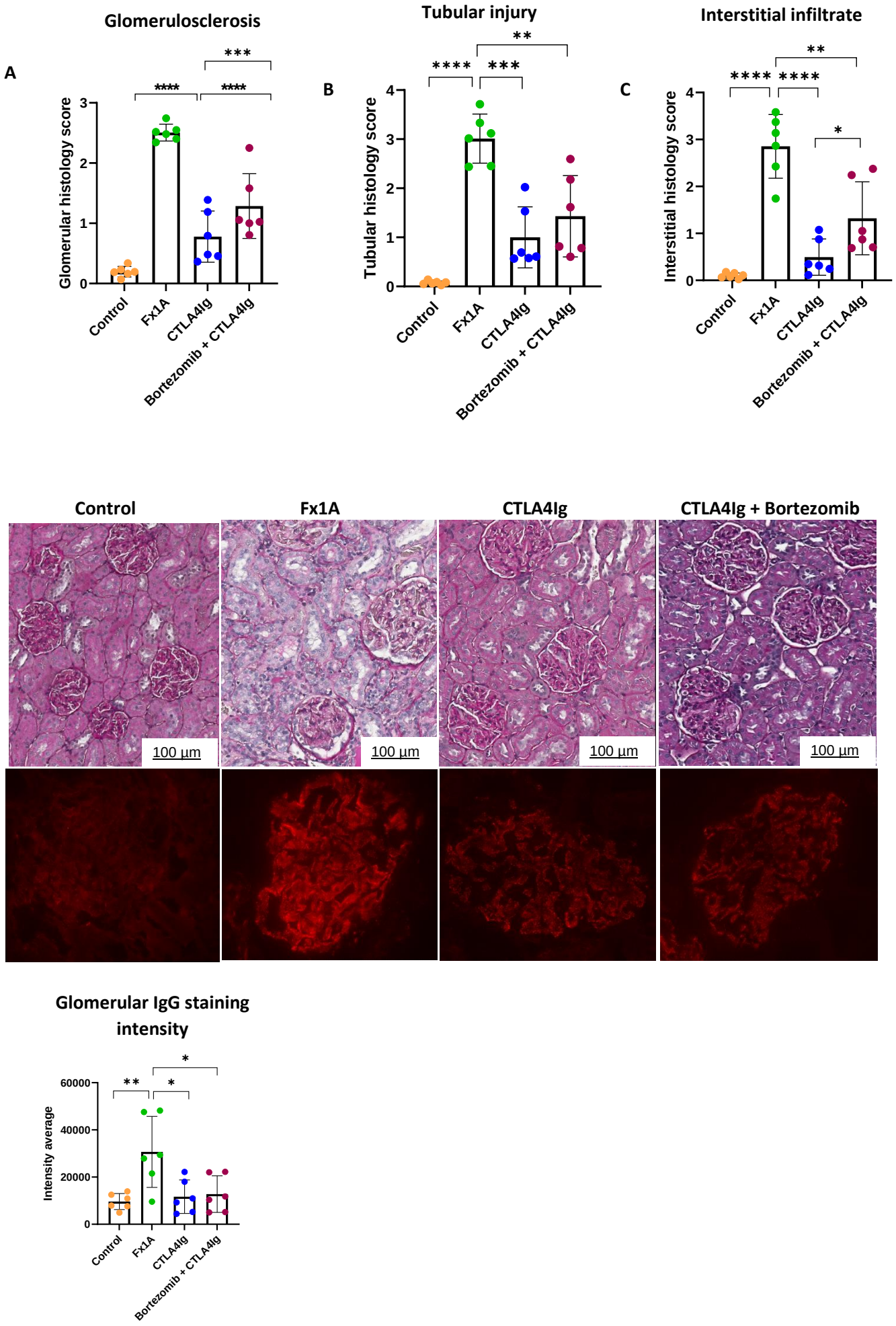
A
Glomerulosclerosis
Glomerular histology score
Control
Fx1A
CTLA4Ig
Bortezomib + CTLA4Ig
B
Tubular injury
Tubular histology score
C
Interstitial infiltrate
Interstitial histology score
D
Control
Fx1A
CTLA4Ig
CTLA4Ig + Bortezomib
100 µm
E
F
Glomerular IgG staining intensity
Intensity average

Figure 3

A

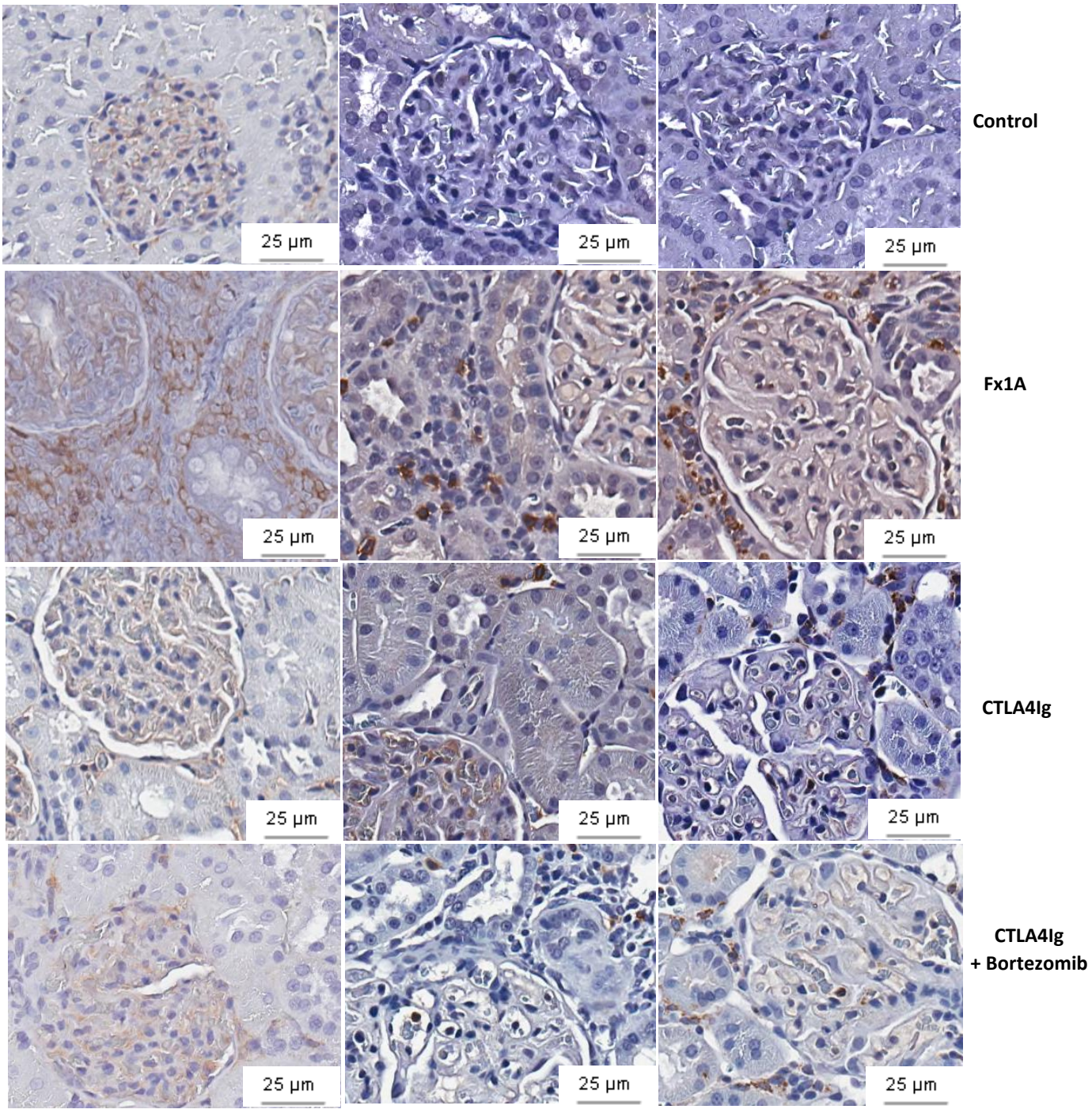
25 µm
Control
Fx1A
CTLA4Ig
CTLA4Ig
+ Bortezomib

B

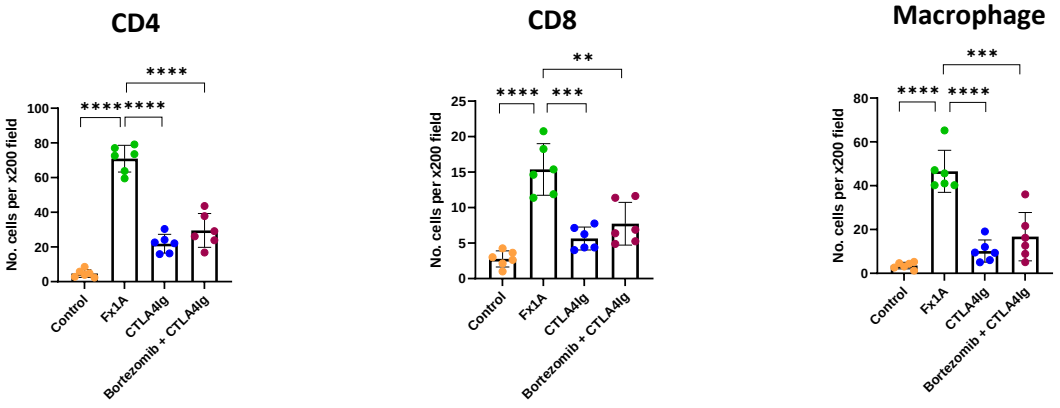
CD4
CD8
Macrophage
No. cells per x200 field
Control
Fx1A
CTLA4Ig
Bortezomib + CTLA4Ig

Figure 3

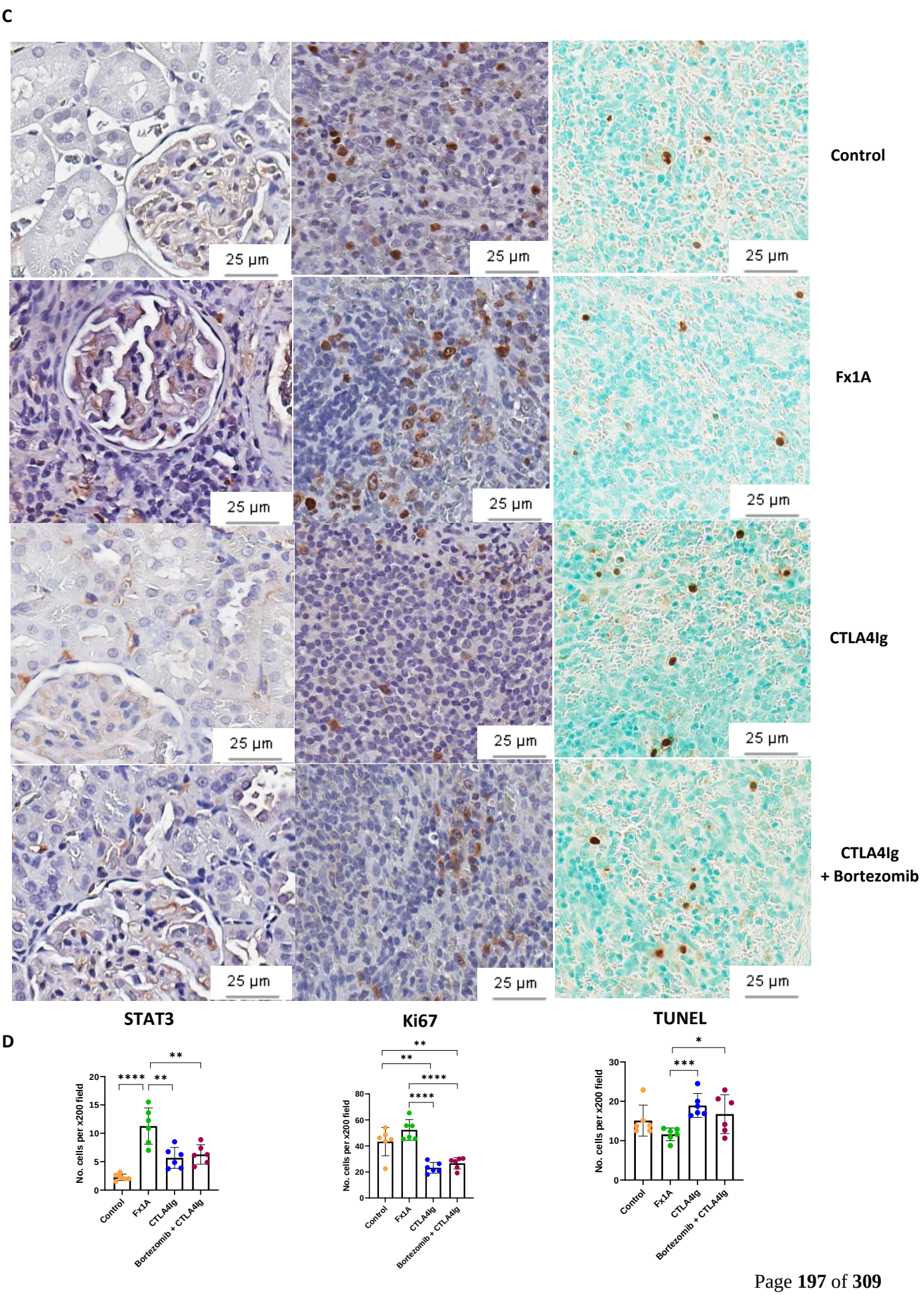
C
Control
Fx1A
CTLA4Ig
CTLA4Ig
+ Bortezomib
25 µm
D
STAT3
Ki67
TUNEL
No. cells per x200 field
Control
Fx1A
CTLA4Ig
Bortezomib + CTLA4Ig

Figure 4

A

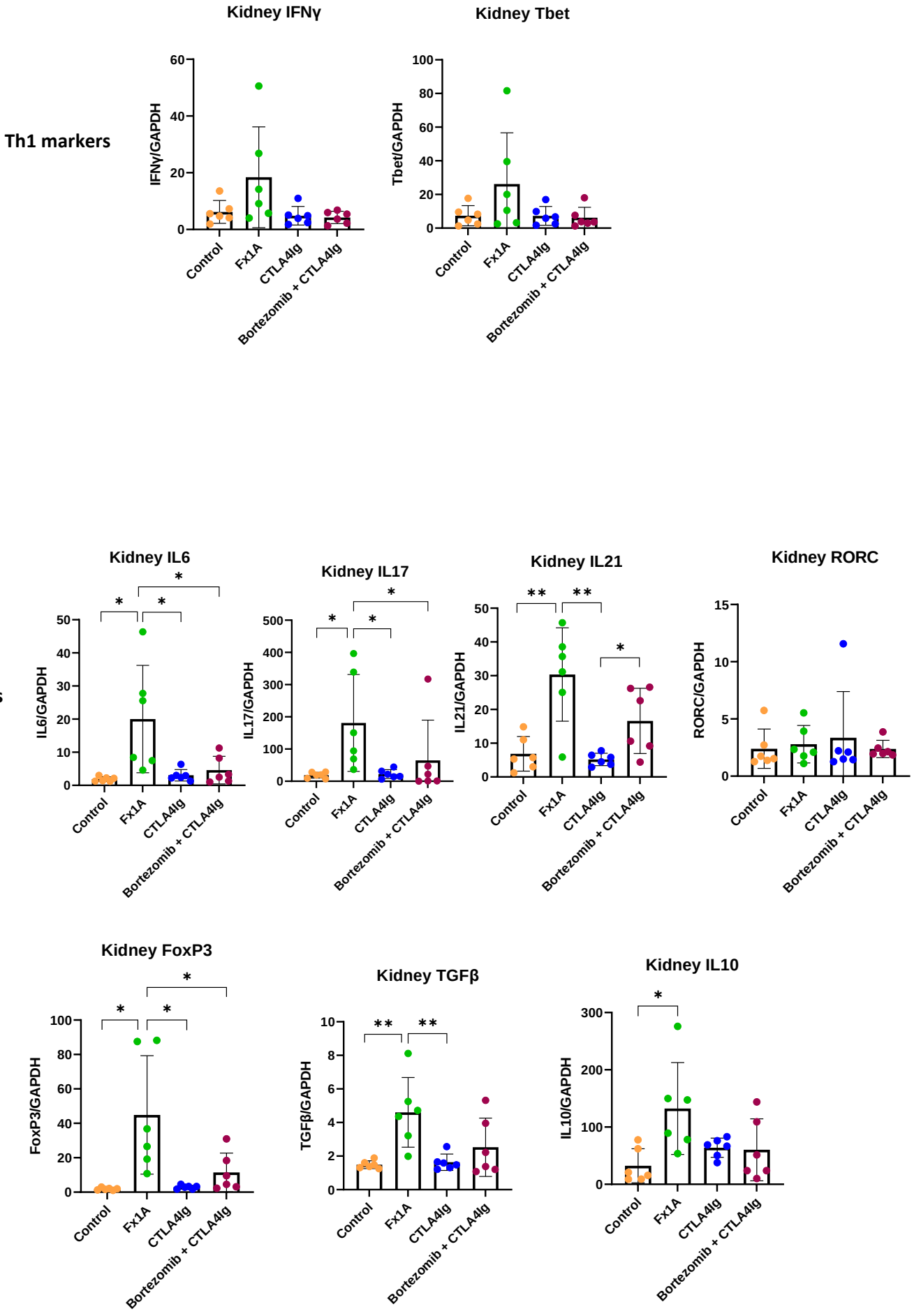
Th1 markers
Kidney IFNγ
IFNγ/GAPDH
Kidney Tbet
Tbet/GAPDH
Th17 markers
Kidney IL6
IL6/GAPDH
Kidney IL17
IL17/GAPDH
Kidney IL21
IL21/GAPDH
Kidney RORC
RORC/GAPDH
Treg markers
Kidney FoxP3
FoxP3/GAPDH
Kidney TGFβ
TGFβ/GAPDH
Kidney IL10
IL10/GAPDH
Control
Fx1A
CTLA4Ig
Bortezomib + CTLA4Ig

Figure 4

B

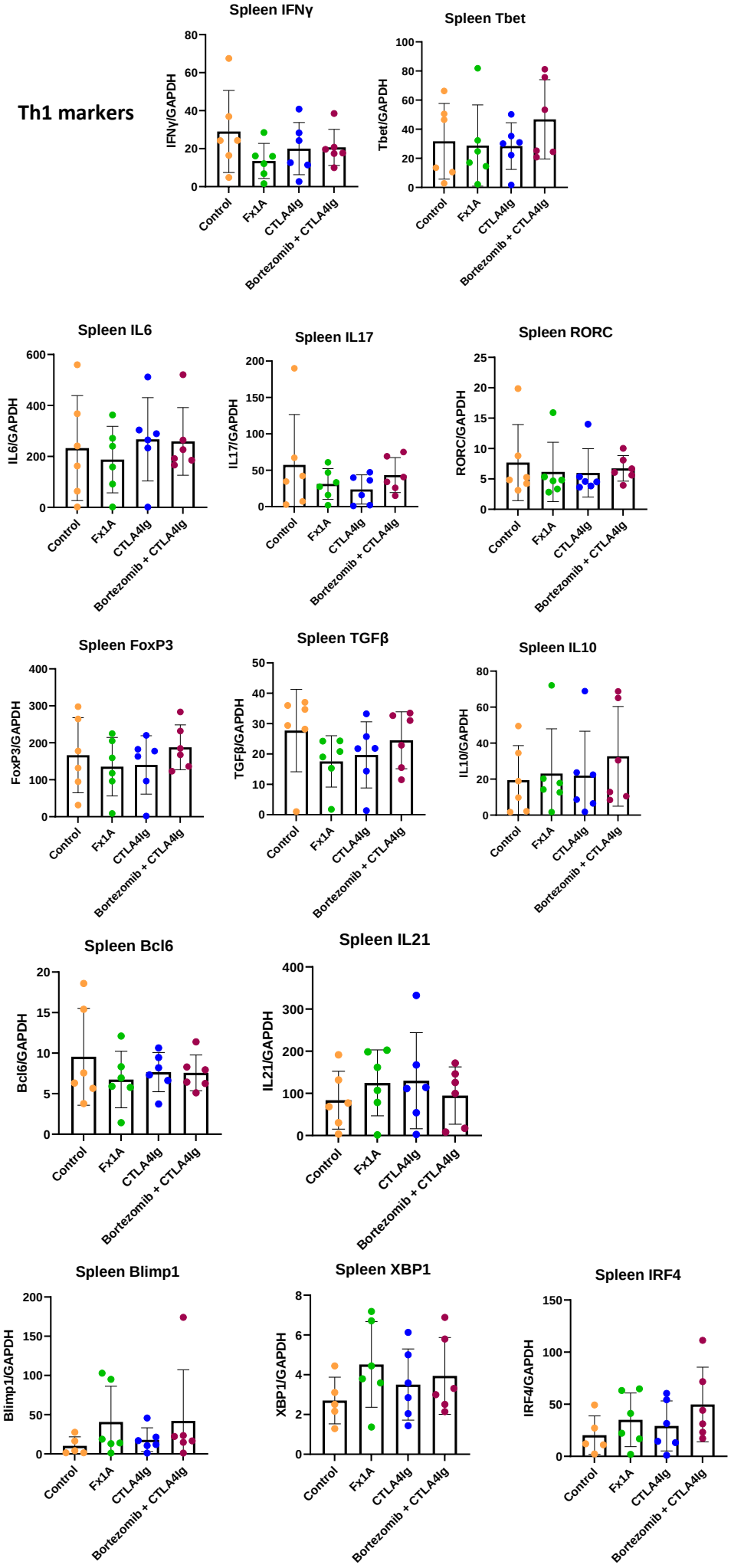
Th1 markers
Spleen IFNγ
IFNγ/GAPDH
Spleen Tbet
Tbet/GAPDH
Th17 markers
Spleen IL6
IL6/GAPDH
Spleen IL17
IL17/GAPDH
Spleen RORC
RORC/GAPDH
Treg markers
Spleen FoxP3
FoxP3/GAPDH
Spleen TGFβ
TGFβ/GAPDH
Spleen IL10
IL10/GAPDH
Tfh markers
Spleen Bcl6
Bcl6/GAPDH
Spleen IL21
IL21/GAPDH
Plasma cell markers
Spleen Blimp1
Blimp1/GAPDH
Spleen XBP1
XBP1/GAPDH
Spleen IRF4
IRF4/GAPDH
Control
Fx1A
CTLA4Ig
Bortezomib + CTLA4Ig

Figure 5

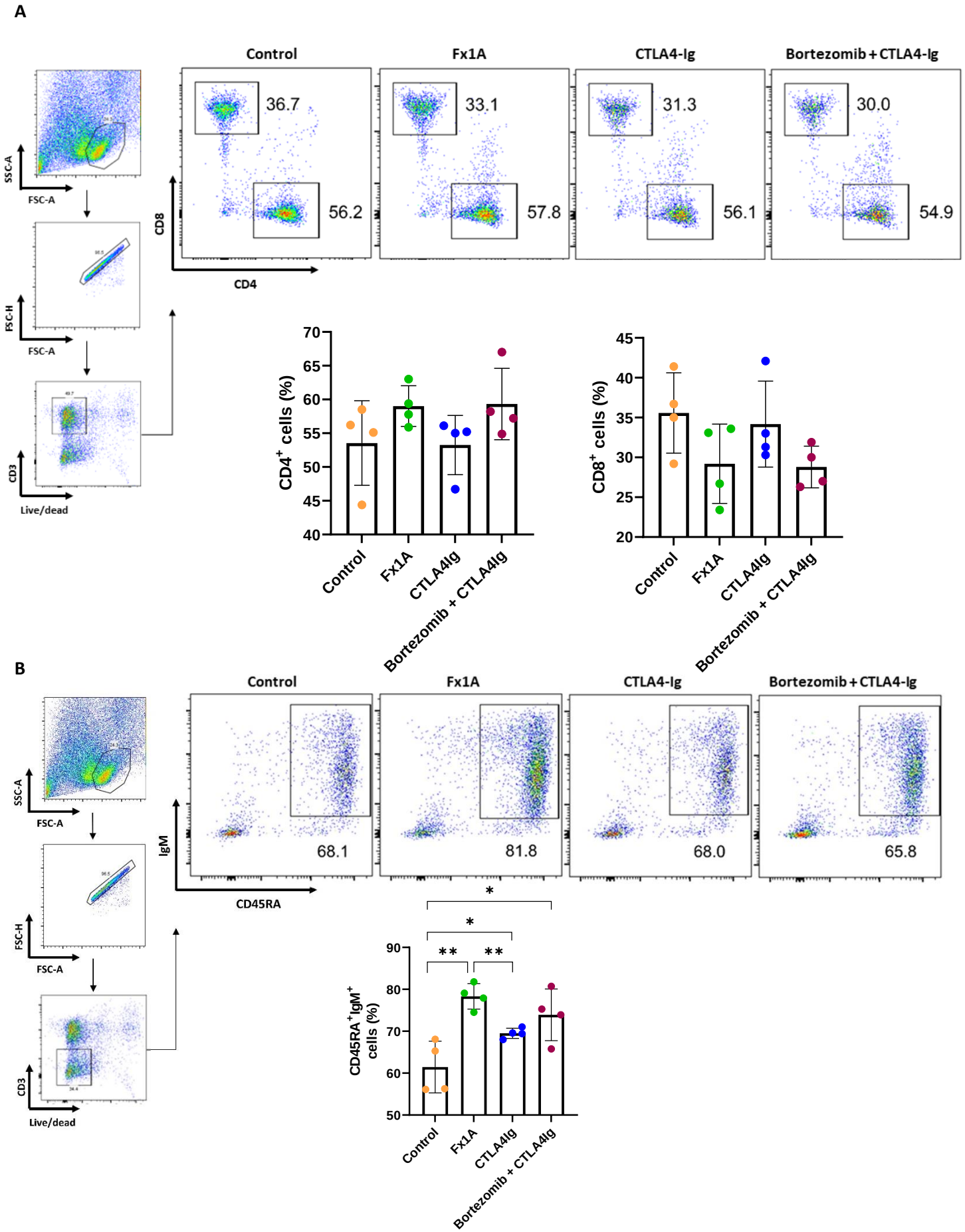
A
Control
Fx1A
CTLA4-Ig
Bortezomib + CTLA4-Ig
36.7
56.2
33.1
57.8
31.3
56.1
30.0
54.9
SSC-A
FSC-A
FSC-H
CD3
Live/dead
CD8
CD4
CD4+ cells (%)
CD8+ cells (%)
Control
Fx1A
CTLA4Ig
Bortezomib + CTLA4Ig
B
IgM
CD45RA
68.1
81.8
68.0
65.8
CD45RA+IgM+ cells (%)
*
**

Figure 5

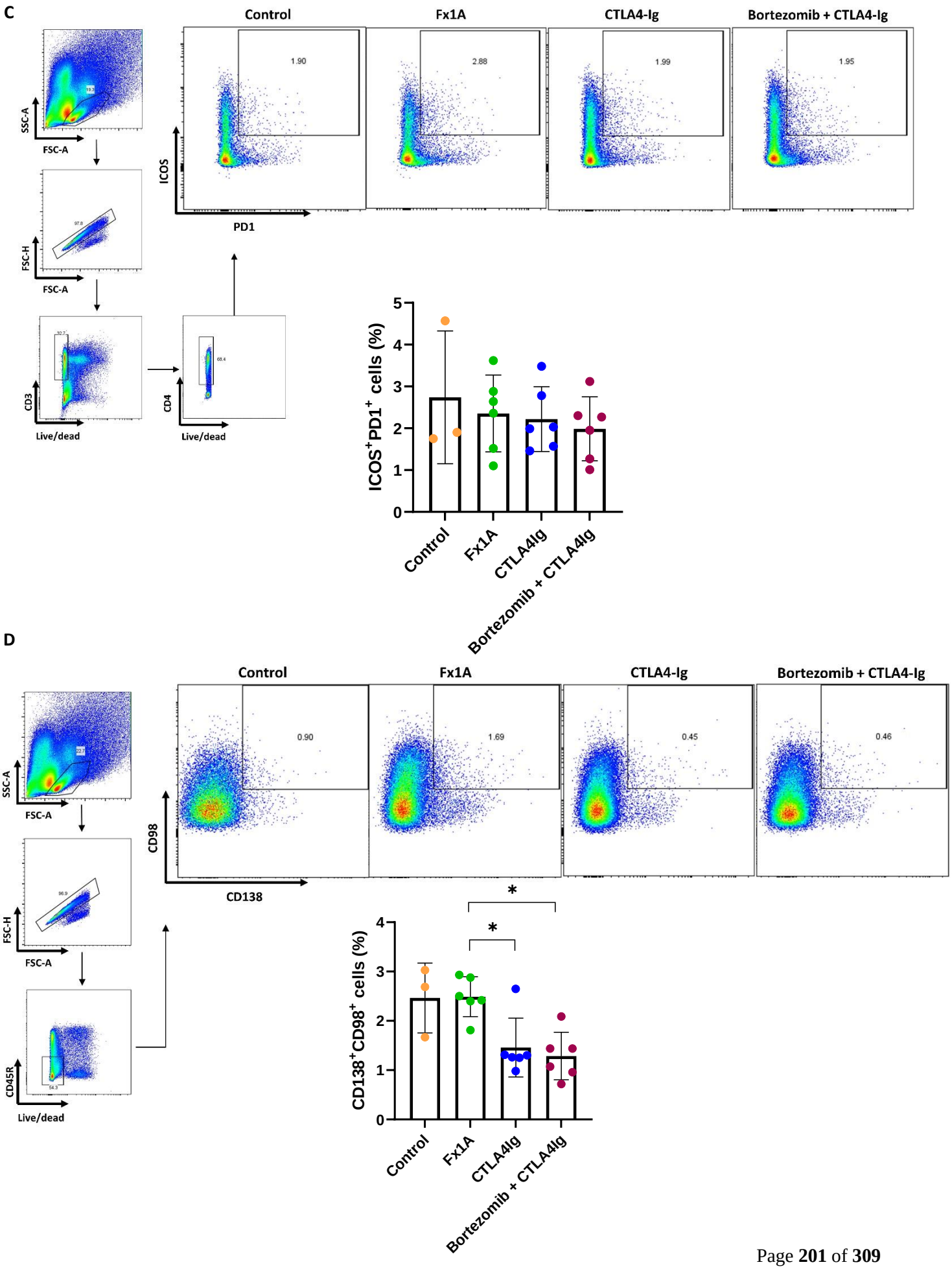
C
Control
Fx1A
CTLA4-Ig
Bortezomib + CTLA4-Ig
1.90
2.88
1.99
1.95
SSC-A
FSC-A
FSC-H
CD3
CD4
Live/dead
ICOS
PD1
ICOS+PD1+ cells (%)
Control
Fx1A
CTLA4Ig
Bortezomib + CTLA4Ig
D
0.90
1.69
0.45
0.46
CD98
CD138
CD45R
CD138+CD98+ cells (%)
*
*

E

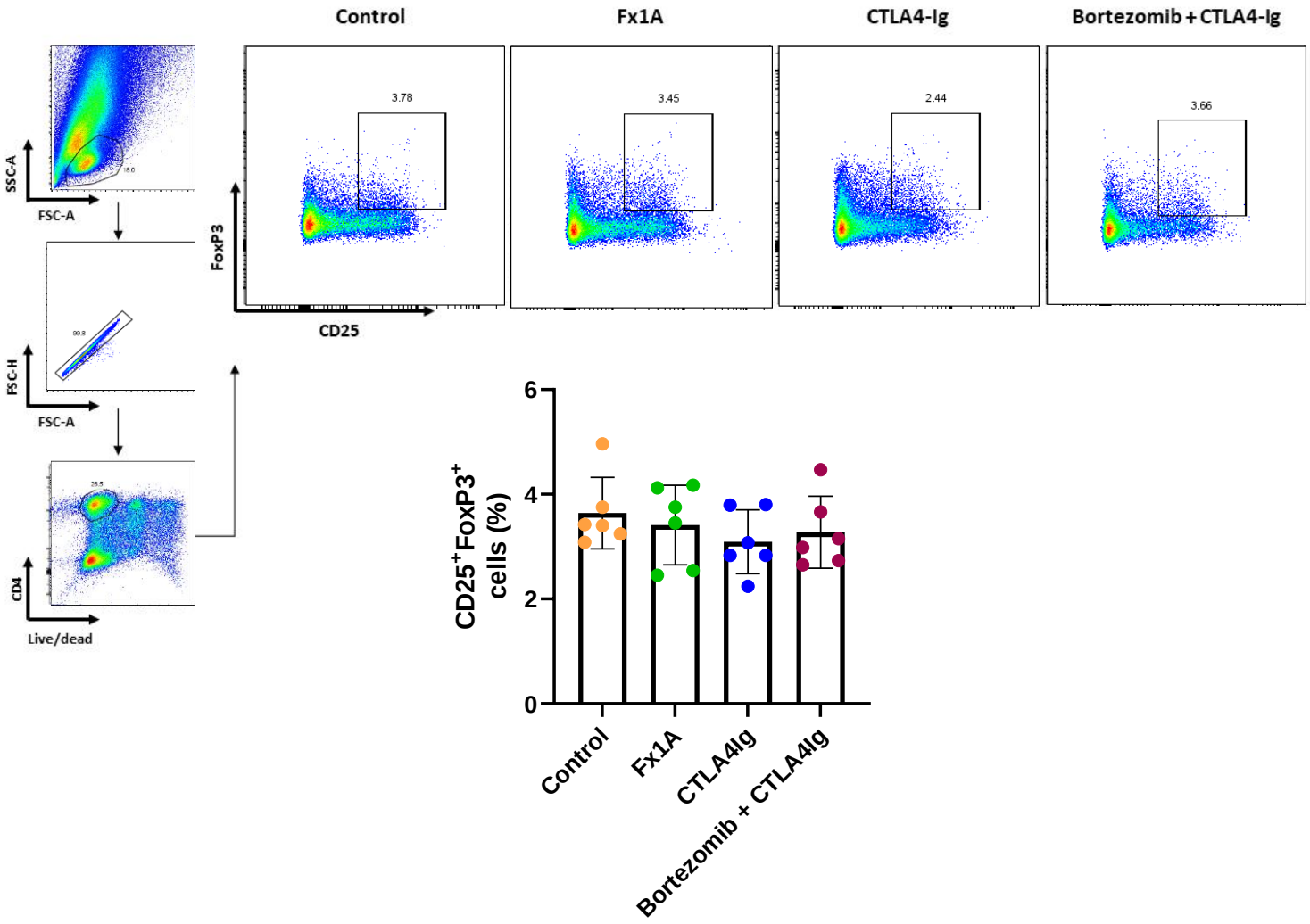
Control
Fx1A
CTLA4-Ig
Bortezomib + CTLA4-Ig
SSC-A
FSC-A
FSC-H
FSC-A
CD4
Live/dead
FoxP3
CD25
3.78
3.45
2.44
3.66
CD25+FoxP3+ cells (%)
0
2
4
6
Control
Fx1A
CTLA4Ig
Bortezomib + CTLA4Ig

Figure 6

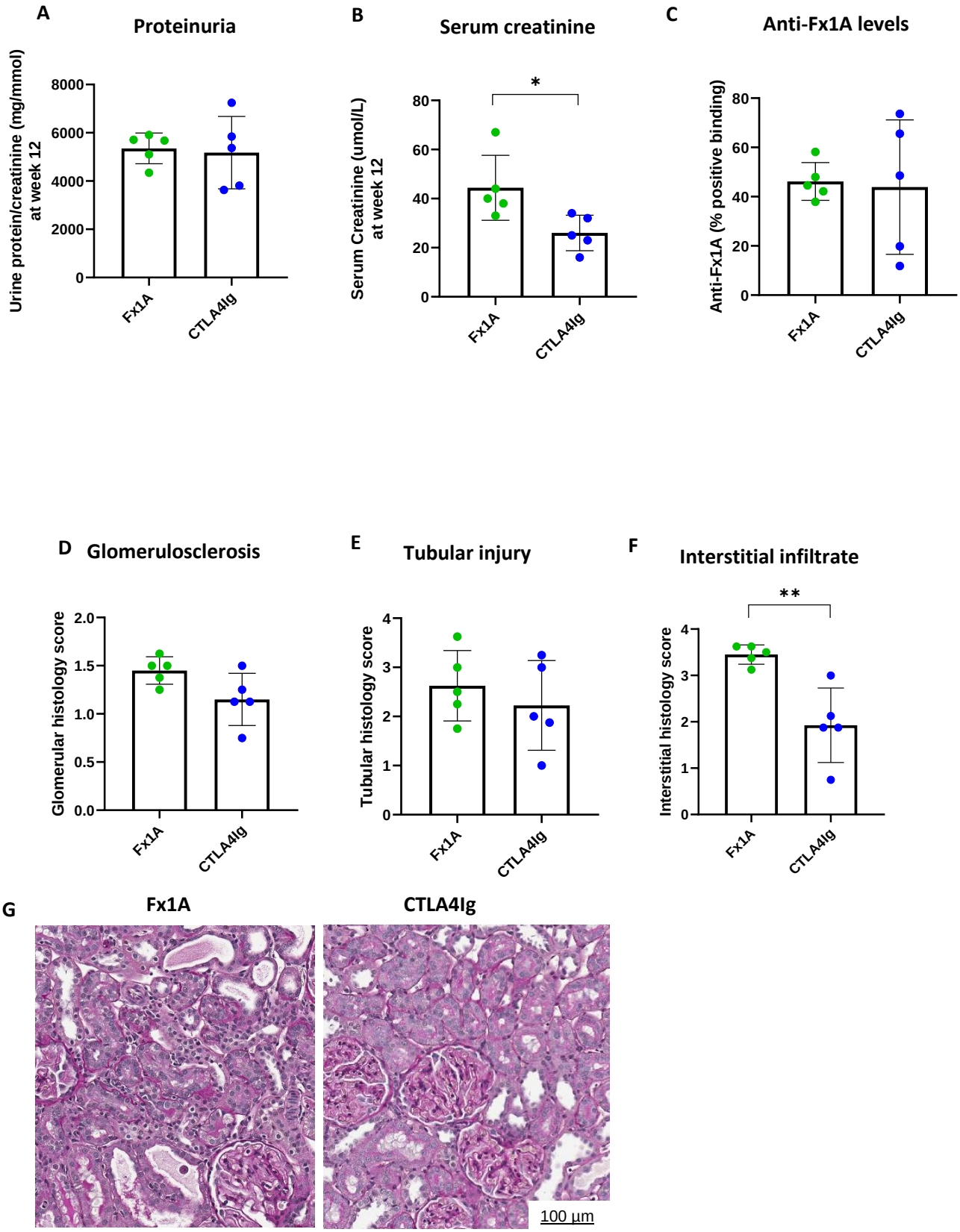
A
Proteinuria
Urine protein/creatinine (mg/mmol) at week 12
8000
6000
4000
2000
0
Fx1A
CTLA4Ig
B
Serum creatinine
Serum Creatinine (umol/L) at week 12
*
80
60
40
20
0
Fx1A
CTLA4Ig
C
Anti-Fx1A levels
Anti-Fx1A (% positive binding)
80
60
40
20
0
Fx1A
CTLA4Ig
D
Glomerulosclerosis
Glomerular histology score
2.0
1.5
1.0
0.5
0.0
Fx1A
CTLA4Ig
E
Tubular injury
Tubular histology score
4
3
2
1
0
Fx1A
CTLA4Ig
F
Interstitial infiltrate
**
Interstitial histology score
4
3
2
1
0
Fx1A
CTLA4Ig
G
Fx1A
CTLA4Ig
100 µm

Figure legends

Figure 1. CTLA4-Ig with or without bortezomib reduced proteinuria and serum creatinine in Heymann nephritis (HN) rats but did not significantly reduce anti-Fx1A autoantibody levels. (**A**) Lewis rats at 6 weeks of age were treated with CTLA4-Ig (300 μg intraperitoneal twice weekly for 6 weeks from Fx1A induction) or CTLA4-Ig plus bortezomib (0.2 mg/kg intraperitoneal twice weekly for 3 weeks from Fx1A induction) and sacrificed at 12 weeks after Fx1A induction. Fx1A was extracted from Sprague-Dawley rats at 12 weeks of age via salt fractionation. Figure was created using BioRender. (**B**) Urinary protein/creatinine ratio from a 16-hour urine collection and (**C**) serum creatinine were significantly lower in HN rats treated with CTLA4-Ig or CTLA4-Ig plus bortezomib compared to untreated HN rats (****$p<0.0001$, ***$p<0.001$, *$p<0.05$, n=6 per group). (**D**) Serum anti-Fx1A autoantibody levels (expressed as a percentage of positive binding, calculated by dividing the sample optical density by the optical density of a positive control sample of known strongly positive serum containing anti-Fx1A) were not significantly different between HN rats treated with CTLA4-Ig or CTLA4-Ig plus bortezomib and untreated HN rats, though significantly higher in untreated HN rats and HN rats treated with CTLA4-Ig compared to control rats (****$p<0.0001$, **$p<0.01$, n=6 in each group).

Figure 2. CTLA4-Ig with or without bortezomib reduced glomerulosclerosis, tubular injury, and interstitial mononuclear cell infiltrates in HN rats and reduced glomerular IgG deposition. (**A**) Semi-quantitative scores of morphological changes at week 12 showed significantly reduced (**A**) glomerulosclerosis, (**B**) tubular injury, and (**C**) interstitial infiltrates in the HN rats treated with CTLA4-Ig with or without bortezomib compared to untreated HN rats (****$p<0.0001$, ***$p<0.001$, **$p<0.01$, *$p<0.05$, n=6 per group). (**D**) Histology of kidney representative sections under PAS staining showed reduced kidney damage and cellular infiltration in the HN rats treated with CTLA4-Ig with or without bortezomib compared to untreated HN rats (n=6 per group, magnification X200).

(**E**) Representative sections of glomeruli showed CTLA4-Ig with or without bortezomib reduced but did not prevent glomerular capillary loop IgG deposition in HN rats compared to untreated HN rats (magnification X400). (**F**) Quantification of glomerular IgG staining using Fiji software (total fluorescence density quantified by the ratio of the integrated density over area of a representative glomerulus) showed reduced glomerular IgG staining in rats treated with CTLA4-Ig with or without bortezomib compared to untreated rats (*p<0.05, n=6 per group).

Figure 3. CTLA4-Ig with or without bortezomib reduced infiltration of $CD4^+$ T cells, $CD8^+$ T cells, macrophages ($CD68^+$), and Th17 cells ($STAT3^+$) into the kidney of HN rats. Photomicrographs of immunohistochemical kidney sections from control rats (CFA), untreated HN rats (HN), HN rats treated with CTLA4-Ig (CTLA4Ig), and HN rats treated with CTLA4-Ig plus bortezomib (CTLA4Ig+bortezomib) showed reduction in kidney infiltration of (**A**) $CD4^+$ T cells, (**B**) $CD8^+$ T cells, (**C**) macrophages and (**D**) $STAT3^+$ cells in the HN rats treated with CTLA4-Ig with or without bortezomib compared to untreated HN rats (****p<0.0001, ***p<0.001, **p<0.01, n=6 per group) (magnification, X400). Photomicrographs of immunohistochemical spleen sections from control rats (CFA), untreated HN rats (HN), HN rats treated with CTLA4-Ig (CTLA4Ig), and HN rats treated with CTLA4-Ig plus bortezomib (CTLA4Ig+bortezomib) showed reduction Ki67 staining and an increase in TUNEL staining in the HN rats treated with CTLA4-Ig with or without bortezomib compared to untreated HN rats (****p<0.0001, ***p<0.001, **p<0.01, *p<0.05, n=6 per group) (magnification, X400).

Figure 4. CTLA4-Ig with or without bortezomib reduced expression of Th17 cytokines (IL-6, IL-17, IL-21) and Treg markers (Foxp3, TGF-β) in the kidney but not spleen in HN rats. (**A**-**D**) Real-time quantitative PCR demonstrated reduced mRNA levels of IL-6, IL-17, IL-21, Foxp3 and TGF- β in the kidney (**A**-**C**) but not spleen (**D**) (**p<0.01, *p<0.05, n=6 per group, mRNA expression

normalized for GAPDH expression. Data shown are the mean ± standard error of the mean (SEM); each sample was run in triplicate). There was no significant difference in expression of RORC and IL-10 in the kidney or spleen between HN rats ($p>0.05$) though there was increased expression of IL-10 in the kidney of untreated HN rats compared to control rats (*$p<0.05$, n=6 per group. Data shown are the mean ± SD; each sample was run in triplicate). (**E-F**) There was no significant difference in Th1 (IFN-γ, Tbet) expression in the kidney (**E**) or spleen (**F**) between groups There were also no significant differences in expression of Tfh (Bcl-6, IL-21) or plasma cell (Blimp-1, IRF4, XBP1) markers in the spleen between groups (**F**). ($p>0.05$, n=6 per group, mRNA expression normalized for GAPDH expression. Data shown are the mean ± SD; each sample was run in triplicate).

Figure 5. In the spleen, CTLA4-Ig reduced total B cells and plasma cells but did not significantly alter total $CD4^+$ T cells, $CD8^+$ T cells, Tfh or Tregs. Representative flow cytometry showed total $CD4^+$ T cells and $CD8^+$ T cells gating on live $CD3^+$ cells (**A**). CTLA4-Ig significantly reduced total B cells ($CD45RA^+IgM^+$ gating on live $CD3^-$ cells) compared to untreated rats and there was increased B cells in all HN rats compared to control rats (**B**) (**$p<0.01$, *$p<0.05$, n=4 per group due to inadequate sample). Representative flow cytometry showed no between-group differences in Tfh cells ($ICOS^+PD1^+$gating on live $CD4^+$ cells) (n=3-6 per group due to inadequate sample) (**C**), reduced plasma cells ($CD138^+$ $CD98^+$ gating on live $CD45R^-$ cells) (*$p<0.05$, n=3-6 per group due to inadequate sample) (**D**) and no differences in Tregs ($CD25^+$ $Foxp3^+$ gating on live $CD4^+$ cells) (**E**) (n=6 per group).

Figure 6. CTLA4-Ig treatment after the onset of significant proteinuria at 8 weeks after Fx1A immunization reduced serum creatinine and interstitial infiltrate in HN rats but did not significantly reduce proteinuria or anti-Fx1A autoantibody levels. (**A**) Urinary protein/creatinine ratio from a 16-hour urine collection was not different between untreated HN rats and CTLA4-Ig-treated HN rats

though (**B**) serum creatinine was significantly lower in HN rats treated with CTLA4-Ig compared to untreated HN rats (*p<0.05, n=5 per group). (**C**) Serum anti-Fx1A autoantibody levels (expressed as a percentage of positive binding, calculated by dividing the sample optical density by the optical density of a positive control sample of known strongly positive serum containing anti-Fx1A) were not significantly different between HN rats treated with CTLA4-Ig and untreated HN rats (n=5 in each group). Semi-quantitative scores of morphological changes at week 12 showed no significant difference in (**D**) glomerulosclerosis or (**E**) tubular injury but reduced (**F**) interstitial infiltrates in the HN rats treated with CTLA4-Ig compared to untreated HN rats (*p<0.05, n=5 per group). (**G**) Histology of kidney representative sections under PAS staining showed similar kidney damage though reduced cellular infiltration in the HN rats treated with CTLA4-Ig compared to untreated HN rats (n=5 per group, magnification X200).

5.Peptide vaccination to induce $CD8^+$ regulatory T cells in Heymann Nephritis

5.1 Overview

Aim: $CD8^+$ regulatory T cells (Tregs) are cross-protective across multiple animal models of autoimmunity. Recently, specific peptides from a yeast-peptide-major histocompatibility complex library that expanded $CD8^+$ Tregs in murine experimental multiple sclerosis were reported. Whether these peptides also expand $CD8^+$ Tregs and protect against Heymann nephritis (HN), an experimental model of membranous nephropathy is unknown. We aimed to assess the efficacy of peptide vaccination to induce $CD8^+$ Tregs in HN.

Methods: Lewis rats were immunised with Fx1A/complete Freund's adjuvant to induce HN and received peptide vaccination 1 week before (prevention vaccination) or 1 week after disease induction (treatment vaccination). To understand whether the effect of peptide vaccination was mediated by $CD8^+$ Tregs, we adoptively transferred $CD8^+$ T cells from Lewis rats 1 week after vaccination with peptides and Fx1A into Lewis rats 1 week before induction of HN.

Results: Prevention vaccination, but not treatment vaccination, significantly reduced anti-Fx1A autoantibody levels and serum creatinine. Both prevention and treatment vaccination reduced histological kidney injury. mRNA expression of Helios, the major $CD8^+$ Treg transcription factor, was upregulated in both the spleen and kidney with prevention vaccination and in the kidney with treatment vaccination. Adoptive transfer of $CD8^+$ T cells after peptide vaccination significantly reduced serum creatinine, proteinuria, histological kidney injury, anti-Fx1A autoantibody levels, germinal centre formation, and mRNA expression of markers of T

follicular helper cells (Bcl6, interleukin-21), T helper 1 cells (interferon-γ, Tbet) and T helper 17 cells (interleukin-6, interleukin-17).

Conclusions: Peptide vaccination induces $CD8^+$ Tregs that ameliorate induction of experimental membranous nephropathy which may represent a further peripheral regulation of autoimmunity.

5.2 Introduction

Primary membranous nephropathy (MN) is a leading cause of adult-onset primary nephrotic syndrome caused by autoantibodies targeting podocyte antigens (phospholipase A2 receptor in 70%) and left untreated, around 30% of patients progress to kidney failure.[1] Despite growing understanding of the antigens and associated autoantibodies that drive MN, current treatments still rely on broadly suppressing the immune system, which are incompletely effective and often associated with significant toxicity. A desirable goal in treating autoimmune diseases is restoring immune tolerance, which is mediated by regulatory T cells (Tregs). While $CD4^+$ Tregs expressing forkhead box P3 (FoxP3) are the best-characterised Tregs their numbers were unchanged in Heymann nephritis (HN),[2] an experimental model of MN characterised by anti-Fx1A autoantibodies. However, adoptive transfer of $CD8^+$ T cells was previously found to suppress autoantibody production and proteinuria in HN.[3]

Earlier studies reported the mechanisms of $CD8^+$ T cell-mediated suppression to be dependent on Qa-1, the murine homolog of the non-classical major histocompatibility complex (MHC) class I molecule human leukocyte antigen-E (HLA-E), which is expressed on activated lymphocytes and dendritic cells.[4] Indeed, Qa-1 deficient mice are prone to experimental multiple sclerosis (experimental autoimmune encephalomyelitis (EAE)),[5] and Qa-1 mutations limited $CD8^+$ Tregs, with increased susceptibility to lupus in mice.[6] Our group has previously demonstrated that immunising HN rats with autoreactive $CD4^+$ T cells (T cell vaccination) expanded $CD8^+$ Tregs and eliminated T follicular helper (Tfh) cells, a subset of $CD4^+$ T-helper (Th) cells crucial for germinal B cell help and high affinity antibody production, in a Qa-1-dependent manner.[2] This is consistent with studies previously done in EAE showing T cell vaccination ameliorated autoimmunity via $CD8^+$ T cell-mediated immune suppression.[7-9]

Subsequent studies have further characterised Qa-1-restricted $CD8^+$ Tregs that express CD44, CD122, the MHC class I inhibitory receptor Ly49, and the transcription factor Helios, which is crucial for their stability.[6, 10] Using these markers, $CD8^+$ Tregs have been shown to be upregulated in human autoimmune disease (lupus, multiple sclerosis, and celiac disease) and infection (COVID-19 and influenza).[11] Similar to their murine counterparts, $CD8^+$ Tregs in human celiac disease eliminated gliadin-specific autoreactive $CD4^+$ T cells, which could be partially inhibited by antibodies blocking HLA-A/B/C and HLA-E, showing human $CD8^+$ Tregs engage with autoreactive T cells through both classical and non-classical MHC class I.[11] Adoptive transfer of $CD8^+$ T cells was equally cross-protective in experimental type 1 diabetes and EAE,[12] suggesting the T cell receptor (TCR) of $CD8^+$ Tregs is not restricted to the disease-specific antigen or antigens expressed on autoreactive $CD4^+$ T cells.[12]

Recently, the TCR of $CD8^+$ T cells in EAE was cloned and presented to a yeast-peptide-MHC library using mouse MHC class I ($H\text{-}2K^d$), identifying four peptides (ASRSNRYFWL, HDRVNWEYI, SMRPNHFFFL, YQPGNWEYI) demonstrating strong binding, which when immunised into mice expanded $CD8^+$ Tregs and protected against EAE.[13] In contrast to previous studies of $CD8^+$ Tregs, suppression was not Qa-1-restricted, likely since the yeast-peptide-MHC library was restricted to classical MHC class I, suggesting $CD8^+$ Treg induction can involve presentation by either classical and non-classical MHC class I.[13] The mouse and rat MHC class I are similar,[14-16] although *in silico* prediction tools for rat MHC class I binding to nonamers (HDRVNWEYI and YQPGNWEYI) and decamers (ASRSNRYFWLand SMRPNHFFFL) are lacking. Nevertheless, we hypothesised these peptides (ASRSNRYFWL,

HDRVNWEYI, SMRPNHFFFL, YQPGNWEYI) might also induce a $CD8^+$ Treg population and protect rats against HN.

5.3 Material and Methods

5.3.1 Induction of active Heymann nephritis with peptide vaccination

Male Lewis rats (4-6 weeks old weighing 120-280 g) were obtained from the Animal Resources Centre in Perth, Australia. Outbred male Sprague-Dawley (SD) rats were used for producing Fx1A as previously described.[17-19] Each group of six rats was immunised subcutaneously into one hind footpad and tail base each with 100 µl Fx1A emulsified in Complete Freund's Adjuvant (CFA) (Sigma-Aldrich #F5881), containing a total of 15 mg of Fx1A, 1 mg mycobacterium tuberculosis HRa37 (BD Biosciences #231141), 100 µl of Incomplete Freund's Adjuvant (IFA) (Sigma-Aldrich #F5506), and 100 µl of PBS. The control rats were immunised with an equivalent CFA emulsion prepared without Fx1A. A total of 24 rats was used for each experiment and randomisation was not performed. We repeated experiment twice and power calculations were not performed. All rat procedures carried out were approved by the Western Sydney Local Health District Animal Ethics Committee (protocol 4346.12.20).

We immunised HN rats in the tail base with 100 µg of all peptides (ASRSNRYFWL, HDRVNWEYI, SMRPNHFFFL, YQPGNWEYI), altogether diluted in 200 µl of PBS emulsified in 200 µl of CFA and 200 µg mycobacterium tuberculosis HRa37 either 1 week before Fx1A immunisation (prevention vaccination) or 1 week after Fx1A immunisation (treatment vaccination). Peptide dosage and vaccination adjuvant were based on the original study by Saligrama et al that identified the peptides and demonstrated they expanded $CD8^+$ Tregs in mice.[13] Peptides were synthesised by Thermo Scientific Custom Peptide synthesis service at >80% purity.

5.3.2 Adoptive transfer of $CD8^+$ T cells isolated after Heymann nephritis induction with or without peptide vaccination

Lewis rats were induced with HN (as described above) using Fx1A emulsion with or without 100 µg of each peptide (ASRSNRYFWL, HDRVNWEYI, SMRPNHFFFL, YQPGNWEYI). On day 7, spleen and draining lymph nodes were collected and $CD8^+$ cells were obtained using fluorescence-activated cell sorting (FACS). FACS-purified $CD8^+$ cells from rats that received Fx1A and peptide immunisation (peptide $CD8^+$ transfer) or Fx1A immunisation alone (control $CD8^+$ transfer) were adoptively transferred via tail vein (1 million cells per rat) 1 week before induction of HN.

5.3.3 Production of Fx1A

Adult male SD rats of at least 12 weeks age were used to prepare Fx1A, a crude tubular antigen, which is also expressed in the podocytes of rats. SD rats were anaesthetised using isoflurane and abdominal aorta puncture performed to perfuse PBS (Thermofisher #14190250) *in vivo* until kidneys became white. The kidney cortices were dissected and pushed through a 150-mesh steel sieve (bore size 104-106) in PBS. Filtrates were centrifuged twice with PBS (400g, 10 min, 4ºC) and supernatant collected each time. The supernatant (compromising of the tubular fraction containing the Fx1A antigen) was ultracentrifuged three times (Sorvall rotor SW-28 at 50,000g for 45 min at 4ºC), each time discarding the supernatant and resuspending the pellet in cold ultrapure Milli-Q water. The pellet was lyophilized and then stored at -80ºC. Experiments were performed using Fx1A from the same batch.

5.3.4 Purification of Fx1A by fractional salt precipitation

Fx1A 200 mg was solubilized in 10 ml of 1% deoxycholic acid (DOC) in 0.1M sodium chloride, 0.01M ethylenediaminetetraacetic acid and 0.01M Tris buffer at a pH of 8.0 and the suspension was stirred for 2 hours at 4ºC. The sample was ultracentrifuged (Sorvall rotor SW-55 Ti at 50,000g for 45 min at 4ºC) and supernatant (containing Fx1A) collected, to which 4.75 ml of saturated ammonium sulphate was slowly added with constant stirring at 4ºC. The sample was ultracentrifuged (Sorvall rotor SW-55 Ti at 50,000g for 45 min at 4ºC) again then supernatant collected and dialyzed in 0.9% NaCl overnight at 4ºC, then stored at -80ºC.

5.3.5 Anti-Fx1A autoantibody detection by enzyme-linked immunosorbent assay (ELISA)

Anti-Fx1A autoantibody titres were determined by ELISA at 12 weeks after Fx1A or CFA immunisation. Fx1A for ELISA was solubilised and purified by fractional salt precipitation.[18] Immulon 1B ELISA plates (John Morris Scientific #8045155) were coated with 100 µl of purified Fx1A (40 µg/mL, diluted in PBS) overnight at 4°C. The ELISA plate was washed with PBS + 0.05% Tween 20 twice and blocked with 300 µl of 2% bovine serum albumin (BSA, Sigma-Aldrich #A3983) for 1 hour at room temperature. The plate was washed with PBS + 0.05% Tween 20 three times and incubated with 100 µl of rat sera (diluted 1:20 in BSA 2%) for 1 hour at 37°C. The plate was subsequently washed with PBS + 0.05% Tween 20 three times and incubated with 100 µl of alkaline phosphatase-conjugated pre-absorbed goat antibody to rat IgG (Abcam #ab7098, diluted 1:1000 in BSA 2%) for 1 hour at 37°C. After washing the plate with PBS + 0.05% Tween 20 four times, 100 µl of p-nitrophenyl phosphate (PNPP) substrate (Thermofisher #37621) was added for 30 minutes. The yellow color reaction was read on a SpectraMax iD3 machine at 405 nm in triplicated samples. Anti-Fx1A

autoantibody titres were quantified as a percentage of positive binding, calculated by dividing the sample optical density by the optical density of a positive control sample of known strongly positive serum containing anti-Fx1A. Background based on blank wells incubated with BSA 2% was subtracted from optical density values.

5.3.6 Flow cytometry analysis

For surface staining, splenocytes were incubated with fluorochrome-conjugated anti-rat antibodies (CD3-FITC, Biolegend #201403; CD4-APC/Cy7, Biolegend #201518; CD8-PE/Cy7, Biolegend #201716; CD45RA-PE, Biolegend #202307; IgM-AF647, Biolegend #408909; ICOS-Pacific Blue, Biolegend #313522; PD1-CoraLite647, Proteintech #CL647-66220; CD45R-FITC, BD Bioscience #561876; CD138-PE, Abcam #ab209584; CD98-APC, Biolegend #206403; CD25-APC, Biolegend #202114; Live/Dead Fixable Aqua Dead Cell Stain Kit, Thermofisher #L34965) for 25 min on ice in the dark. Intracellular labelling was performed using fixed and permeabilised cells using PE Anti-mouse/rat forkhead box P3 (Foxp3) Staining Set (eBioscience #72-5775-40) and according to manufacturer's instructions. All samples were analysed by flow cytometry using a Fortessa Color Flow Cytometer (BD Biosciences, San Jose, USA). Data analyses were performed using the FlowJo™ software (Tree Star, Ashland, USA).

5.3.7 Measurement of protein and creatinine

Urine protein and creatinine levels, along with serum albumin and creatinine levels were measured at week 12. Blood samples for serum albumin and creatinine were obtained by inferior vena cava puncture at week 12. Urine protein/creatinine ratio was measured from a 16-hour urine collection using metabolic cages in which rats had access to water but not food.

Serum and urine creatinine was measured using the CREA method on the Ortho Vitros Fusion 5600 (Ortho Clinical Diagnostics, Egypt), serum albumin measured using the ALB method on the Ortho Vitros Fusion 5600, and total urine protein was measured using the Biuretic method (Randox Total Protein) on the Ortho Vitros Fusion 5600.

5.3.8 Histology and morphometric evaluation

The kidneys were removed on week 12. Sagittal slices of kidney tissue were fixed in neutral buffered formalin at room temperature for 24 hours and embedded in paraffin to evaluate their pathology. 4 μm slices were stained with Periodic Acid-Schiff (PAS) reagent and assessed by light microscopy. The remaining cortex of the same kidney was snap frozen in liquid nitrogen and used for RNA and immunohistochemistry. In each biopsy, a semi-quantitative score from two blinded trained observers was used to evaluate the degree of kidney injury as previously described.[20] The degree of glomerulosclerosis, tubular injury and interstitial infiltrate was evaluated on kidney sections embedded in paraffin, sections cut into 4 μm slices and stained with PAS stain. A minimum of 10 consecutive fields at 400x magnification were assessed and scored in one section per rat. Glomerulosclerosis was defined as glomeruli demonstrating any degree of sclerosis. Tubular injury was defined as tubular dilatation, epithelial cellular atrophy, and luminal cast formation. Interstitial infiltrate was defined as PAS-positive mononuclear cellular infiltration in the tubulointerstitial compartment. Each score was graded according to the extent of cortical involvement on a scale of 0 to 4: 0, normal; 1, involvement of 10-24% of the cortex; 2, involvement of 25-49% of the cortex; 3, involvement of up to 50–75% of the cortex; and 4, extensive damage involving >75% of the cortex. The degree of kidney injury was estimated by averaging each score across the 10 consecutive fields between two blinded trained observers.

5.3.9 Immunofluorescence

Immunofluorescence staining was performed for glomerular IgG deposition using the primary antibody goat anti-rat IgG H&L Alexa Fluor®-594 (Abcam #ab150160, diluted 1:100, incubated for 1 hour at room temperature) and for splenic germinal centre B cells using the primary antibody fluorescein labelled Peanut agglutinin (PNA) (Vector Labs #FL-1071-5, diluted 1:50, incubated for 1 hour at room temperature). Frozen kidney specimens were embedded in Tissue-Tek OCT (ProSciTech #IA018), 5 μm sections were cut on a Cryostat, dried overnight at room temperature, fixed in cold acetone at -20°C for 8 minutes, and dried for 30 minutes. Sections were incubated in blocking horse serum 2.5% (Vector Labs #S-2012) for 10 minutes. Images (magnification X400) were taken using a DeltaVision core microscope (Applied Precision, Washington). Glomerular IgG deposition fluorescence intensity was quantified by the ratio of the integrated density over area of a representative glomerulus using the Fiji software.[21]

5.3.10 Immunohistochemistry

Immunohistochemical staining was performed for $CD4^+$ T cells, $CD8^+$ T cells and macrophages. Primary antibodies used in immunohistochemistry were: rabbit anti-mouse/rat CAL4 for CD4 (Abcam #ab237722, diluted 1:2000, incubated at 4ºC overnight), mouse anti-rat MRC OX8 for CD8 (Biorad #MCA48GA, diluted 1:75, incubated for 1 hour at room temperature), and mouse anti-rat ED1 for CD68 (Biorad #MCA341GA, diluted 1:100, incubated for 1 hour at room temperature) for macrophages. The secondary antibody was obtained from the ImmPRESS Universal PLUS Polymer Kit, Peroxidase (horse anti-mouse/rabbit IgG) (Vector Labs #MP-7800).

Kidney and spleen specimens were embedded in paraffin, 5 μm sections of kidney and spleen were cut, deparaffinized in Xylene (three times for 5 minutes), rehydrated in alcohol 100% (three times for 5 minutes) and alcohol 70% (once for 5 minutes), then washed in tap water. Antigen retrieval was performed by placing slides in citrate buffer pH 6.0 (Sigma-Aldrich #C9999) and using a Decloaking Chamber NxGen at 95°C for 20 minutes. Endogenous peroxidase activity was blocked by incubating sections for 15 minutes in 0.3% (vol/vol) H_2O_2 solution. Blocking and slide development with peroxidase substrate were performed using the ImmPRESS Universal PLUS Polymer Kit according to manufacturer's instructions except for $CD4^+$ staining in which the secondary ImmPRESS Universal Polymer was diluted 1:3. Slides were counterstained with hematoxylin (Sigma-Aldrich). To assess levels of interstitial infiltration, positively stained cells were counted from five random cortical fields (magnification X400).

5.3.11 Real-time polymerase chain reaction (PCR)

RNA was isolated from the rat spleen, $CD8^+$ splenocytes (isolated using FACS), and kidney samples using TRIzol reagent (Thermofisher #15596018) to analyse messenger RNA (mRNA) expression. The total RNA was reverse transcribed to get cDNA as described previously.[2] To extract RNA, rat spleen and kidney samples were homogenized in an Eppendorf tube containing 1ml TRIzol reagent (Thermofisher #15596018). After 5 minutes to permit complete dissociation of the nucleoproteins complex, 0.2ml of chloroform (Sigma-Aldrich #C2432-500ml) was added, vortexed thoroughly and incubated for 3 minutes. Samples were subsequently centrifuged (12,000g for 15 min at 4ºC) and aqueous phase supernatant (containing the RNA) transferred into a new Eppendorf tube. Isopropanol 0.5ml (Sigma-

Aldrich #I9516-500ml) was added, incubated for 10 minutes then centrifuged (12,000g for 10 min at 4ºC), supernatant discarded, and pellet resuspended in 1ml of 75% ethanol. The sample was centrifuged (7500g for 5 min at 4ºC), supernatant discarded and RNA pellet air dried then resuspended in RNase-free water.

To synthesise complementary DNA (cDNA), 20 µl reaction mixture was made of 1 µg of RNA was combined with 1 µl of random primers (Thermofisher #48190011) and 1 µl of deoxynucleotide triphosphate (dNTP) mix (Thermofisher #10297018) (comprised of 10 µl each of adenine (dATP), cytosine (dCTP), guanine (dGTP), and thymine (dTTP) in 60 µl of DNase/RNase-free water (Thermofisher #10977015)) and up to 12 µl of sterile distilled water. This reaction mixture was heated at 65°C for 5 minutes then chilled on ice to which 4 µl of 5x First-Strand Buffer, 2 µl of 0.1M dithiothreitol (DTT), and 1 µl of RNaseOUT (40 units/µl) (Thermofisher #10777019) was added, then incubated at 25°C for 2 minutes. Subsequently, 1 µl (200 units) of SuperScript II Reverse Transcriptase (Thermofisher #18064-014) was added then incubated at 25°C for 10 minutes followed by 42°C for 50 minutes, then reaction inactivated by heating at 70°C for 15 minutes.

Real-time PCR was performed for 40 cycles (initial denaturation at 95°C for 5 minutes, denaturation at 95°C for 20 seconds, and primer annealing and elongation at 60°C for 50 seconds) with l µl of cDNA sample in the presence of 20 µl of PCR reaction mixture (consisting of 2 µl 10x PCR buffer, 1.6 µl dNTP mixture, 0.1 µl Taq polymerase, 0.3 µl TaqMan Gene Expression Assay, and 16 µl RNase free water) (Sigma-Aldrich #11596594001, Thermofisher #10297018). TaqMan Gene Expression Assays consisted of a pair of unlabelled PCR primers and a Taqman probe with a dye label (FAM) on the 5' end and a minor groove binder (MGB)

and non-fluorescent quencher (NFQ) on the 3' end. Primers were obtained specific for rat IKAROS family zinc finger 2 (Ikzf2) (Thermofisher #Rn01401535_m1), CD44 (Thermofisher #Rn00681157_m1), CD122 (Thermofisher #Rn00682353_m1), Perforin (Pf1) (Thermofisher #Rn00569095_m1), Granzyme B (Gzmb) (Thermofisher #Rn00821752_g1), interleukin (IL)-6 (Thermofisher #Rn0140330_m1), IL-17 (Thermofisher #Rn01757168_m1), IL-10 (Thermofisher #Rn99999012_m1), transforming growth factor (TGF)-β (Thermofisher #Rn00572010_m1), B cell lymphoma (Bcl)-6 (Thermofisher #Rn01404339_m1), IL-21 (Thermofisher #Rn01755623_m1), interferon (IFN)-γ (Thermofisher #Rn00594078_m1), T-box transcription factor 21 (Tbet) (Thermofisher #Rn01461633_m1), and glyceraldehyde 3-phosphate dehydrogenase (GAPDH) (Thermofisher #Rn01775763_g1). All samples were run in triplicate, normalised to glyceraldehyde 3-phosphate dehydrogenase (GAPDH) to account for complementary DNA variability, and analysed using the Rotogene Q PCR machine.

5.3.12 Statistical analysis

Results are expressed as group mean ± standard deviation (SD). Statistical analysis for multiple comparisons was performed using the one-way analysis of variance (ANOVA) test for normally distributed data and Kruskal-Wallis one-way ANOVA test for non-parametric data. Two group differences were analysed using the student's *t*-test for normally distributed data and the Mann-Whitney U test for non-parametric data. A two-tailed p value <0.05 was considered statistically significant. Statistical calculations were performed using GraphPad Prism 9.2.0.

5.4 Results

5.4.1 Peptide vaccination ameliorated induction of experimental MN but only prevention vaccination reduced anti-Fx1A antibody levels

Lewis rats were immunised with peptides (ASRSNRYFWL, HDRVNWEYI, SMRPNHFFFL, YQPGNWEYI) 1 week before (prevention vaccination) or 1 week after (treatment vaccination) induction of HN with Fx1A immunisation (**Figure 1A**). At 12 weeks after Fx1A immunisation, prevention vaccination (but not treatment vaccination) significantly reduced serum creatinine while treatment vaccination (but not prevention vaccination) significantly reduced proteinuria compared to untreated HN rats (**Figure 1B-C**, $p<0.05$ or $p<0.01$). Prevention vaccination (but not treatment vaccination) reduced serum anti-Fx1A antibody levels (**Figure 1D**, $p<0.01$).

5.4.2 Peptide vaccination limited kidney injury and reduced glomerular IgG deposition

Kidney histology revealed significantly less glomerulosclerosis, tubular injury, and interstitial cell infiltrates with prevention vaccination but only less glomerulosclerosis and tubular injury with treatment vaccination compared to untreated HN rats (**Figure 2A-D,** $p<0.05$ or $p<0.01$). Glomerular IgG deposition was significantly reduced with both prevention and treatment vaccination compared to untreated HN rats (**Figure 2E-F**, $p<0.01$ or $p<0.001$). Regarding the cellular infiltration, there was a marked reduction of infiltrating $CD4^+$ T cells with prevention and treatment vaccination compared to untreated HN rats (**Figure 3A-B,** $p<0.01$ or $p<0.001$), and reduced $CD8^+$ T cells with prevention vaccination (but not treatment vaccination) compared to untreated HN rats (**Figure 3A-B,** $p<0.05$). There was also a significant reduction of infiltrating macrophages with prevention vaccination compared to untreated HN rats (**Figure**

3A-B, $p<0.05$) and while there was a similar but non-significant reduction of infiltrating macrophages with treatment vaccination.

5.4.3 Peptide vaccination increased Helios expression and was associated with stimulation of the immune system

Twelve weeks post-Fx1A immunisation, Helios (encoded by *Ikzf2*) mRNA expression quantified by real-time quantitative PCR was significantly increased in the kidney with both prevention and treatment vaccination and increased in the spleen with prevention vaccination (but not treatment vaccination) compared to untreated HN rats (**Figure 4A-B**, $p<0.05$ or $p<0.01$). We isolated RNA from $CD8^+$ splenocytes using FACS and confirmed increased Helios expression in the spleen with prevention vaccination was specifically in $CD8^+$ cells but not reduced for non-CD8 cells (**Figure 4C**, $p<0.05$). There were no between-group differences in expression of perforin, granzyme B, CD44 and CD122 in $CD8^+$ splenocytes (**Figure 4D**).

Since Helios is also expressed by $CD4^+$ Tregs,[10] we assessed other markers of $CD4^+$ Tregs (FoxP3, TGF-β and IL-10). There was higher IL-10 expression in the kidney with treatment vaccination compared to untreated HN rats (**Figure 4E**, $p<0.05$). $CD8^+$ Tregs have been reported to produce IL-10,[22] though it is not essential to their regulatory function.[23] Other markers of $CD4^+$ Tregs were not significantly different in the kidney or spleen between peptide vaccination groups and untreated HN rats (**Figure 4E-F**), though increased expression of FoxP3 and TGF-β in the kidney in HN rats (with or without peptide vaccination) compared to control rats suggested inflammatory injury in the kidney caused by HN induced a $CD4^+$ Treg response (**Figure 4E**, $p<0.01$ or $p<0.05$).

We also examined markers of other $CD4^+$ Th subsets such as Tfh (Bcl6, IL-21), Th1 (IFN-γ, Tbet) and Th17 (IL-6, IL-17). There was higher IL-21 expression in the spleen with treatment vaccination compared to untreated HN rats (**Figure 4G**, $p<0.01$) but there were no differences between any groups in Bcl6 expression. As expected, HN rats expressed higher levels of markers of the Th1 and Th17 pathway in the kidney (**Figure 4H**, $p<0.05$, $p<0.01$ or $p<0.001$) but not the spleen (**Figure 4I**). However, peptide vaccination appeared to further stimulate these pro-inflammatory markers in kidney though this was not significant between the disease groups (**Figure 4H-I**). Given the existing literature on Helios downregulating inflammatory cytokines such as IFN-γ and IL-17,[10, 24] we hypothesised these data were indicative of peptide vaccination stimulating the immune system in addition to specifically $CD8^+$ Tregs.

5.4.4 Prevention peptide vaccination reduced plasma cell expansion but did not alter Tfh cells

Flow cytometry analyses of splenocytes showed an expansion of $CD4^+$ T cells in untreated HN rats compared to controls, which was reduced with treatment vaccination but not prevention vaccination (**Figure 5A**, $p<0.05$). While rat antibodies to $CD8^+$ Treg markers (CD44, CD122 and Ly49) were not available, peptide vaccination did not increase the total $CD8^+$ T cell population, which is consistent with $CD8^+$ Tregs normally constituting only 3-5% of total $CD8^+$ T cells.[6] Prevention vaccination (but not treatment vaccination) significantly reduced the expansion of plasma cells ($CD45R^-CD138^+CD98^+$) compared to untreated HN rats (**Figure 5B**, $p<0.01$), without alteration in total Tfh cell numbers ($CD4^+PD1^+ICOS^+$) (**Figure 5C**). There were also no between-group differences in B cells ($CD3^-CD45RA^+IgM^+$) or $CD4^+$ Tregs ($CD4^+CD25^+Foxp3^+$) (**Figure 5A-B**).

5.4.5 Adoptive transfer of $CD8^+$ T cells after peptide vaccination ameliorated experimental MN, reduced anti-Fx1A antibody levels, reduced germinal centre formation and reduced expression of markers of Tfh, Th1 and Th17 cells

To better understand whether the protective effect of peptide vaccination was mediated by $CD8^+$ Tregs, we collected $CD8^+$ T cells from Lewis rats immunised with Fx1A plus peptides (peptide $CD8^+$ transfer) or Fx1A alone (control $CD8^+$ transfer), which we adoptively transferred 1 week before induction of HN (**Figure 6A**). Both peptide and control $CD8^+$ transfer reduced serum creatinine compared to untreated HN rats, though only peptide $CD8^+$ transfer reduced proteinuria (**Figure 6B-C**, $p<0.01$, $p<0.001$, or $p<0.0001$). Peptide $CD8^+$ transfer reduced glomerulosclerosis, tubular injury, and interstitial infiltrate, whereas control $CD8^+$ transfer only reduced glomerulosclerosis compared to untreated HN rats (**Figure 6D-G**, $p<0.05$, $p<0.01$, or $p<0.001$).

Both peptide and control $CD8^+$ transfer significantly reduced anti-Fx1A autoantibody levels though only peptide $CD8^+$ transfer significantly reduced glomerular IgG deposition (**Figure 6H-J**, $p<0.05$ or $p<0.01$). Peptide $CD8^+$ transfer (but not control $CD8^+$ transfer) significantly reduced germinal centres in the spleen (**Figure 7A-B**, $p<0.05$). Peptide $CD8^+$ transfer also reduced expression of Tfh markers (Bcl6 and IL-21) in the spleen as well as markers of the Th1 (IFN-γ, Tbet) and Th17 (IL-6, IL-17) pathways in the kidney (**Figure 7C-E**, $p<0.05$ or $p<0.01$). In contrast, control $CD8^+$ transfer suppressed Tfh and Th1 markers to a lesser degree and did not suppress the Th17 pathway (**Figure 7C-E**, $p<0.05$ or $p<0.01$).

5.5 Discussion

Here we demonstrate that vaccination using peptides that induced $CD8^+$ Tregs in experimental multiple sclerosis in mouse models was able to also protect against autoimmunity in experimental rat MN. These effects were most pronounced with prevention vaccination, which reduced serum creatinine, histological kidney injury, glomerular IgG deposition, autoantibody production and plasma cell expansion, though treatment vaccination was able to ameliorate proteinuria and some measures of histological kidney injury. Peptide vaccination increased expression of Helios, the main transcription factor of $CD8^+$ Tregs, and adoptive transfer of $CD8^+$ T cells after immunisation with Fx1A plus peptides reduced serum creatinine, proteinuria, histological kidney injury, glomerular IgG deposition, and autoantibody production, demonstrating the protective effects of peptide vaccination were mediated through $CD8^+$ Tregs. Adoptive transfer of $CD8^+$ T cells after immunisation with Fx1A alone was partially protective, which was expected since immunisation with the disease antigen alone expanded $CD8^+$ Tregs and ameliorated experimental type 1 diabetes and EAE in mice, though the effects in our study were less pronounced likely due to a much lower dose of transferred cells (1 million $CD8^+$ T cells per rat compared to 2-5 million $CD8^+$ T cells per mouse).[12] Adoptive transfer of $CD8^+$ T cells after immunisation with Fx1A plus peptides demonstrated superior protection, likely through enhanced expansion of $CD8^+$ Tregs through peptides presented by rat MHC class I or potentially Qa-1 engaging their TCR. Adoptive transfer of $CD8^+$ T cells also suppressed Tfh, Th1 and Th17 pathways, unlike peptide vaccination, which may have additional effects on the immune system in addition to inducing $CD8^+$ Tregs.

In our study, adoptive transfer of $CD8^+$ Tregs suppressed Tfh-dependent autoantibody production and germinal centre formation which is consistent with existing studies in murine models of MN, lupus and heart allograft antibody-mediated rejection.[2, 6, 25, 26] We found $CD8^+$ Tregs did not alter the total B cell population, which is consistent with data showing B cells are not targeted by $CD8^+$ Tregs.[23] Our study also showed suppression of the Th1 and Th17 pathway in the kidney with adoptive transfer of $CD8^+$ Tregs, which is consistent with previous studies in murine models of multiple sclerosis, primary biliary sclerosis, systemic sclerosis, and immune tolerance.[27-29] We demonstrated prevention peptide vaccination reduced plasma cell expansion, likely due to $CD8^+$ Treg-mediated suppression of Tfh cells, which normally promote B cell differentiation into long-lived plasma cells. However, prevention peptide vaccination did not alter Tfh cells on flow cytometry, which may be due to our analysis being underpowered.

Our results suggest shared peptides induced $CD8^+$ Tregs across different models of autoimmune disease in different species (EAE and HN). Single-cell RNA sequencing of peripheral blood $CD8^+$ T cells in patients with lupus or multiple sclerosis found similarities across $CD8^+$ Tregs, namely Helios expression, but also differences such as higher expression of type I IFN responding genes in multiple sclerosis patients and higher expression of genes involved in glycolysis in lupus patients.[11] Furthermore, while the TCR repertoire of $CD8^+$ Tregs is less diverse than other $CD8^+$ T cells, it is still considerably diverse, potentially binding to a range of peptides presented on both classical and non-classical MHC class I.[11] While $CD8^+$ Tregs induced by peptide vaccination in EAE were not Qa-1-restricted, they still displayed a similar phenotype to Qa-1-restricted $CD8^+$ Tregs by eliminating autoreactive $CD4^+$ T cells in a perforin-dependent manner and were characterised on flow cytometry by co-expression of CD44, CD122 and Ly49, known markers of Qa-1-restricted $CD8^+$ Tregs.[13] In our study, $CD8^+$

Tregs reduced autoantibody production, likely via suppression of Tfh cells and associated inhibition of germinal centres and plasma cell expansion, similar to Qa-1-restricted $CD8^+$ Tregs.[2, 6, 25, 26]

Harnessing the therapeutic potential of $CD8^+$ Tregs is attractive due to its ability to protect against multiple autoimmune diseases without abrogating the immune response to foreign antigens,[12] thereby preserving anti-infection immunity. However, the optimal method of utilising $CD8^+$ Tregs therapeutically remains to be determined. A phase I trial (Eight-Treg supported by the ReSHAPE consortium) is being planned to test the safety and optimal dose of $CD8^+$ Tregs in kidney transplant recipients.[30] In our study, we demonstrated a greater efficacy of prevention vaccination compared with treatment vaccination. This may have therapeutic potential in preventing recurrence of MN after kidney transplantation. However, we also found the vaccine adjuvant had a stimulatory effect on the immune system and further study of the effects of peptide vaccination on preclinical models of kidney transplantation are needed to ensure peptide vaccination does not increase the risk of allograft rejection.

In conclusion, we demonstrated peptide vaccination induces $CD8^+$ Tregs that ameliorate the induction of experimental MN by reducing autoantibody production, germinal centre formation and plasma cell expansion. Suppression of Tfh, Th1, and Th17 cells was demonstrated with adoptive transfer of $CD8^+$ Tregs but not peptide vaccination, potentially due to secondary effects of vaccination on stimulating the immune system. Secondly, we demonstrated shared peptides that induce $CD8^+$ Tregs and protect against different autoimmune diseases, showing another mechanism of peripheral control against autoimmunity. These studies suggest that

further evaluation of $CD8^+$ Tregs in autoimmune kidney disease is warranted and may have therapeutic application.

5.6 References

1. Couser WG. Primary Membranous Nephropathy. Clin J Am Soc Nephrol. 2017;12(6):983-97.

2. Wang YM, Zhang GY, Hu M, et al. CD8+ regulatory T cells induced by T cell vaccination protect against autoimmune nephritis. J Am Soc Nephrol. 2012;23(6):1058-67.

3. de Heer E, Daha MR, Burgers J, et al. Reestablishment of self tolerance by suppressor T-cells after active Heymann's nephritis. Cell Immunol. 1986;98(1):28-33.

4. Eardley DD, Hugenberger J, McVay-Boudreau L, et al. Immunoregulatory circuits among T-cell sets. I. T-helper cells induce other T-cell sets to exert feedback inhibition. J Exp Med. 1978;147(4):1106-15.

5. Hu D, Ikizawa K, Lu L, et al. Analysis of regulatory CD8 T cells in Qa-1-deficient mice. Nat Immunol. 2004;5(5):516-23.

6. Kim HJ, Wang X, Radfar S, et al. CD8+ T regulatory cells express the Ly49 Class I MHC receptor and are defective in autoimmune prone B6-Yaa mice. Proc Natl Acad Sci U S A. 2011;108(5):2010-5.

7. Gaur A, Ruberti G, Haspel R, et al. Requirement for CD8+ cells in T cell receptor peptide-induced clonal unresponsiveness. Science. 1993;259(5091):91-4.

8. Jiang H, Zhang SI, Pernis B. Role of CD8+ T cells in murine experimental allergic encephalomyelitis. Science. 1992;256(5060):1213-5.

9. Koh DR, Fung-Leung WP, Ho A, et al. Less mortality but more relapses in experimental allergic encephalomyelitis in CD8-/- mice. Science. 1992;256(5060):1210-3.

10. Kim HJ, Barnitz RA, Kreslavsky T, et al. Stable inhibitory activity of regulatory T cells requires the transcription factor Helios. Science. 2015;350(6258):334-9.

11. Li J, Zaslavsky M, Su Y, et al. KIR(+)CD8(+) T cells suppress pathogenic T cells and are active in autoimmune diseases and COVID-19. Science. 2022;376(6590):eabi9591.

12. Wu Y, Zheng Z, Jiang Y, et al. The specificity of T cell regulation that enables self-nonself discrimination in the periphery. Proc Natl Acad Sci U S A. 2009;106(2):534-9.

13. Saligrama N, Zhao F, Sikora MJ, et al. Opposing T cell responses in experimental autoimmune encephalomyelitis. Nature. 2019;572(7770):481-7.

14. Kulski JK, Shiina T, Anzai T, et al. Comparative genomic analysis of the MHC: the evolution of class I duplication blocks, diversity and complexity from shark to man. Immunol Rev. 2002;190:95-122.

15. Hurt P, Walter L, Sudbrak R, et al. The genomic sequence and comparative analysis of the rat major histocompatibility complex. Genome Res. 2004;14(4):631-9.

16. Stevens J, Wiesmüller KH, Walden P, et al. Peptide length preferences for rat and mouse MHC class I molecules using random peptide libraries. Eur J Immunol. 1998;28(4):1272-9.

17. de Heer E, Daha MR, van Es LA. Lymph node cells from rats with Heymann's nephritis produce in vitro autoantibodies directed against purified renal tubular antigen. Immunology. 1984;52(4):743-52.

18. Edgington TS, Glassock RJ, Dixon FJ. Autologous immune complex nephritis induced with renal tubular antigen. I. Identification and isolation of the pathogenetic antigen. J Exp Med. 1968;127(3):555-72.

19. Wu H, Walters G, Knight JF, et al. DNA vaccination against specific pathogenic TCRs reduces proteinuria in active Heymann nephritis by inducing specific autoantibodies. J Immunol. 2003;171(9):4824-9.

20. Mizuno S, Kurosawa T, Matsumoto K, et al. Hepatocyte growth factor prevents renal fibrosis and dysfunction in a mouse model of chronic renal disease. J Clin Invest. 1998;101(9):1827-34.

21. Schindelin J, Arganda-Carreras I, Frise E, et al. Fiji: an open-source platform for biological-image analysis. Nat Methods. 2012;9(7):676-82.

22. Endharti AT, Rifa IM, Shi Z, et al. Cutting edge: CD8+CD122+ regulatory T cells produce IL-10 to suppress IFN-gamma production and proliferation of CD8+ T cells. J Immunol. 2005;175(11):7093-7.

23. Kim HJ, Verbinnen B, Tang X, et al. Inhibition of follicular T-helper cells by CD8(+) regulatory T cells is essential for self tolerance. Nature. 2010;467(7313):328-32.

24. Sebastian M, Lopez-Ocasio M, Metidji A, et al. Helios Controls a Limited Subset of Regulatory T Cell Functions. J Immunol. 2016;196(1):144-55.

25. Mishra S, Liao W, Liu Y, et al. TGF-β and Eomes control the homeostasis of CD8+ regulatory T cells. J Exp Med. 2021;218(1).

26. Choi JY, Eskandari SK, Cai S, et al. Regulatory CD8 T cells that recognize Qa-1 expressed by CD4 T-helper cells inhibit rejection of heart allografts. Proc Natl Acad Sci U S A. 2020;117(11):6042-6.

27. Jiang H, Braunstein NS, Yu B, et al. CD8+ T cells control the TH phenotype of MBP-reactive CD4+ T cells in EAE mice. Proc Natl Acad Sci U S A. 2001;98(11):6301-6.

28. Fenoglio D, Bernuzzi F, Battaglia F, et al. Th17 and regulatory T lymphocytes in primary biliary cirrhosis and systemic sclerosis as models of autoimmune fibrotic diseases. Autoimmun Rev. 2012;12(2):300-4.

29. Arnaboldi PM, Roth-Walter F, Mayer L. Suppression of Th1 and Th17, but not Th2, responses in a CD8(+) T cell-mediated model of oral tolerance. Mucosal Immunol. 2009;2(5):427-38.

30. Flippe L, Bézie S, Anegon I, et al. Future prospects for CD8(+) regulatory T cells in immune tolerance. Immunol Rev. 2019;292(1):209-24.

5.7 Figures

Figure 1

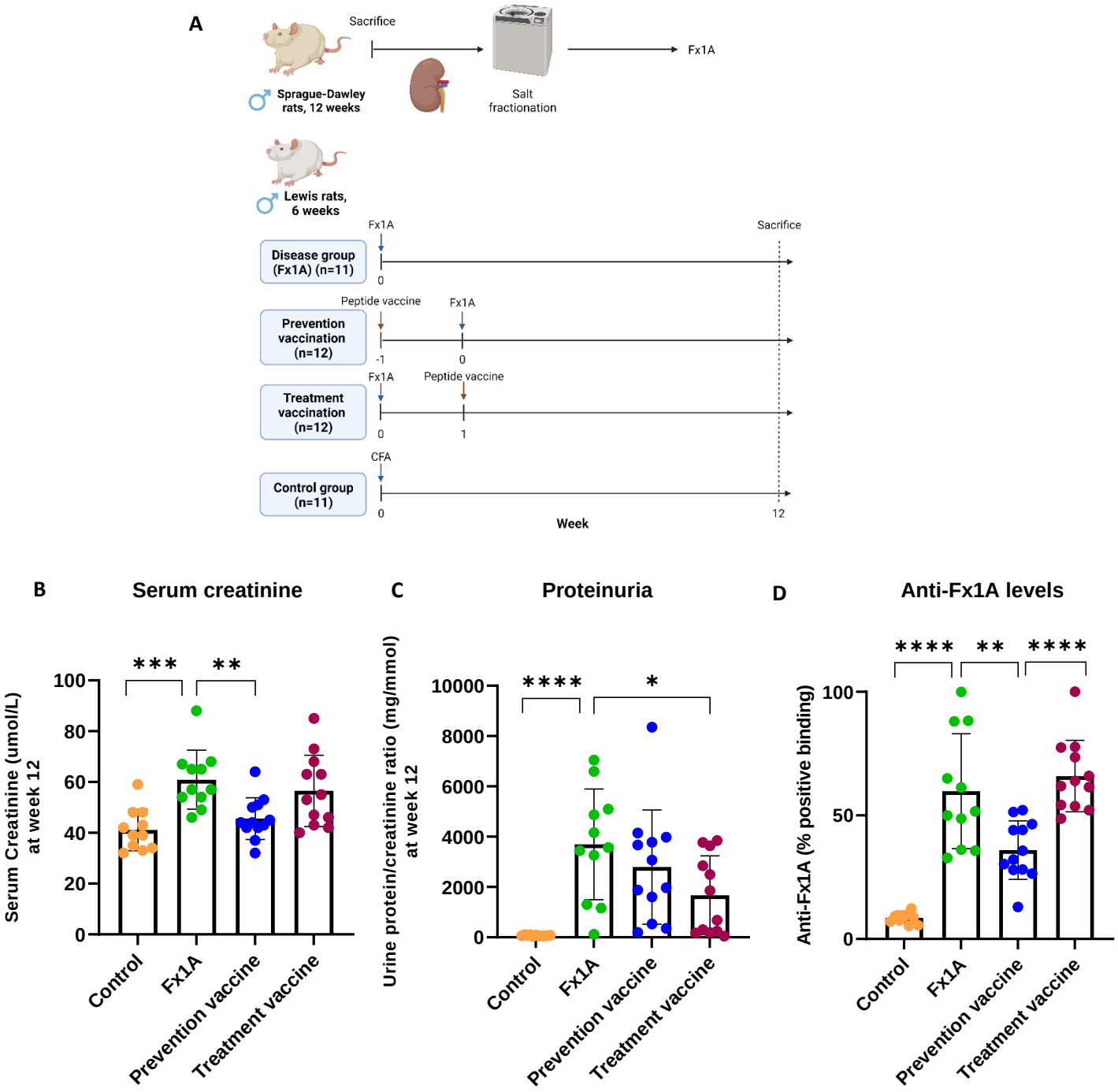

Figure 2

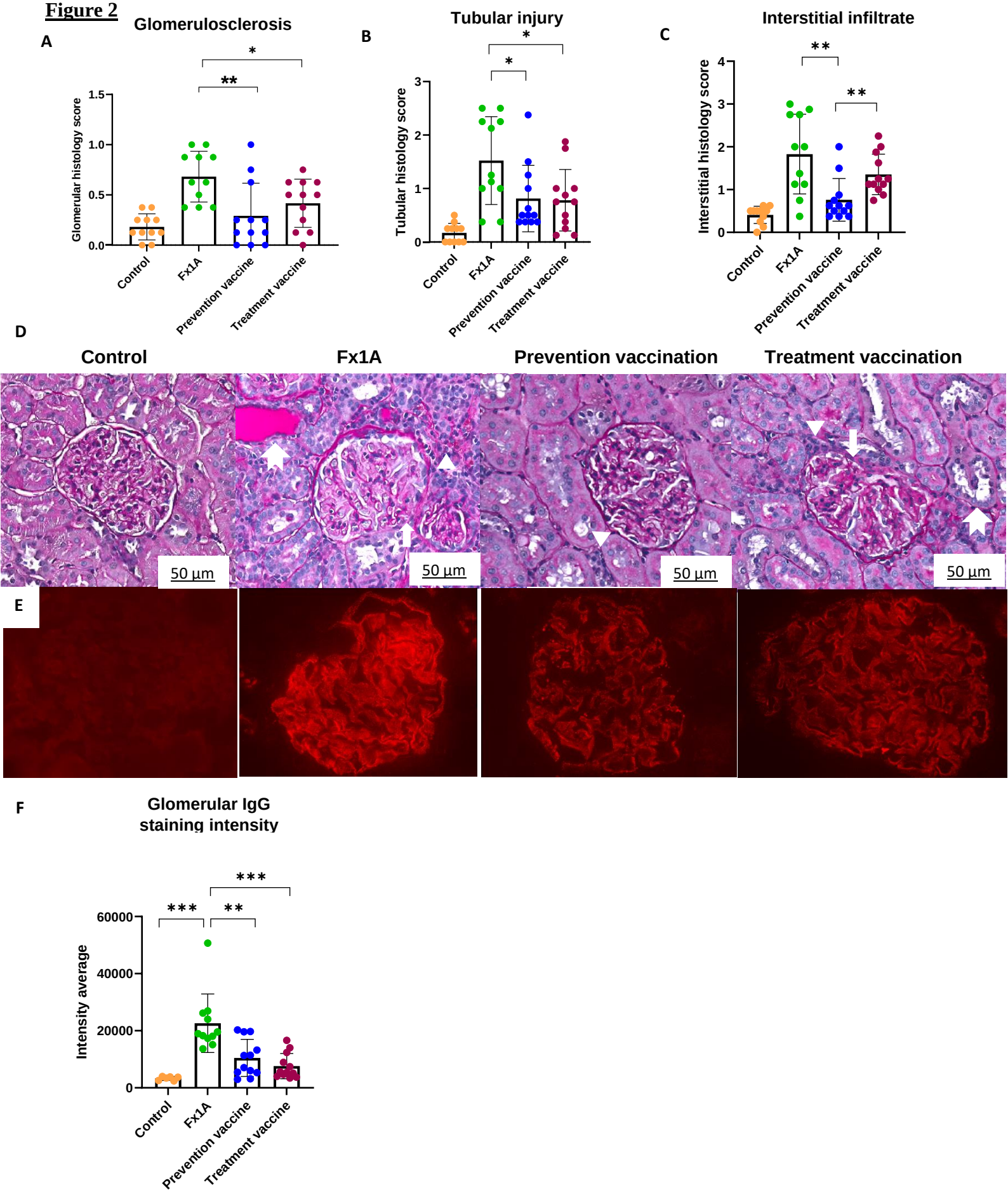
A
Glomerulosclerosis
Glomerular histology score
1.5
1.0
0.5
0.0
*
**
Control
Fx1A
Prevention vaccine
Treatment vaccine
B
Tubular injury
Tubular histology score
3
2
1
0
*
*
Control
Fx1A
Prevention vaccine
Treatment vaccine
C
Interstitial infiltrate
Interstitial histology score
4
3
2
1
0
**
**
Control
Fx1A
Prevention vaccine
Treatment vaccine
D
Control
Fx1A
Prevention vaccination
Treatment vaccination
50 µm
50 µm
50 µm
50 µm
E
F
Glomerular IgG staining intensity
Intensity average
60000
40000
20000
0
***
***
**
Control
Fx1A
Prevention vaccine
Treatment vaccine

Figure 3

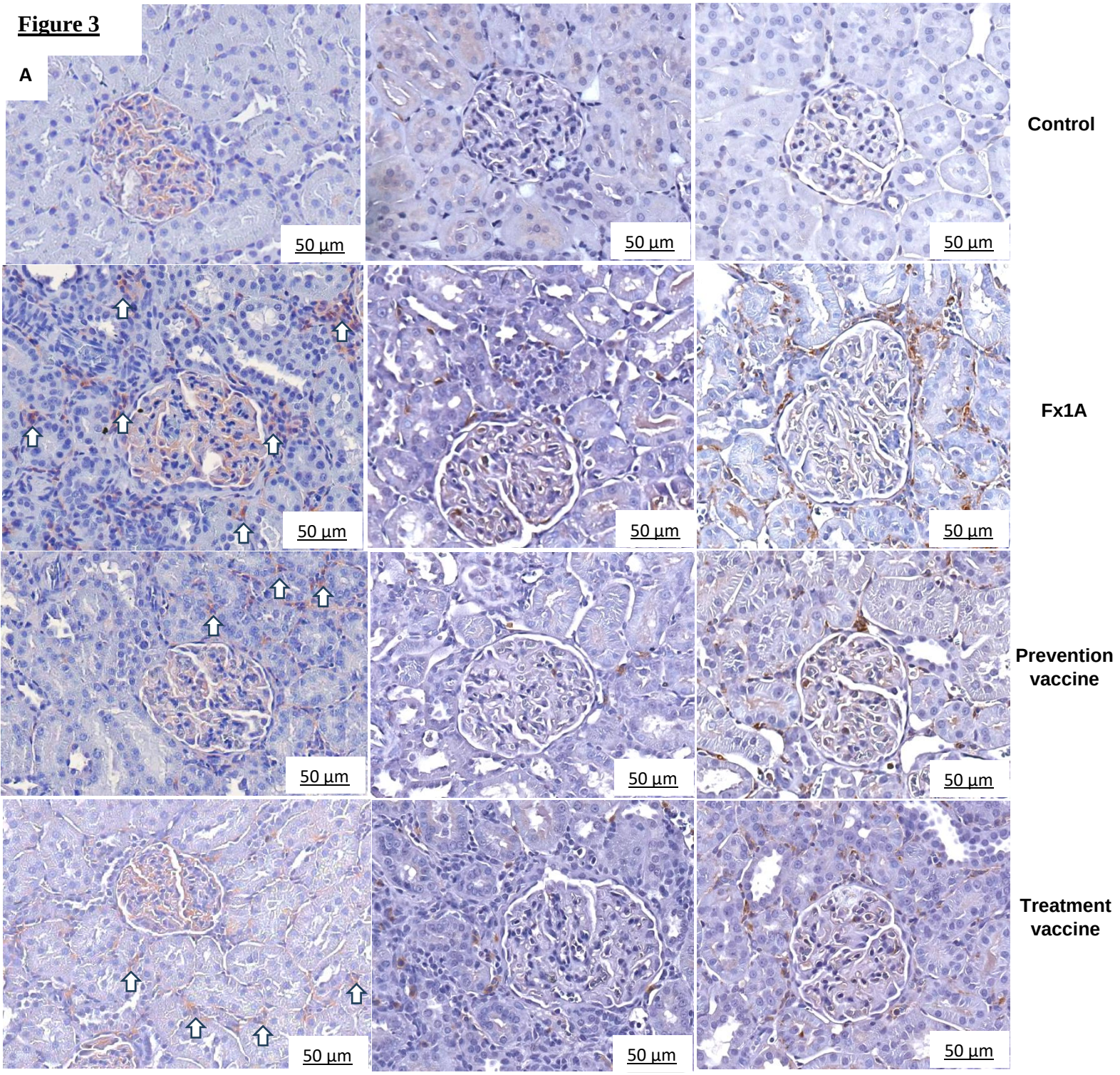
A
Control
Fx1A
Prevention vaccine
Treatment vaccine
50 µm

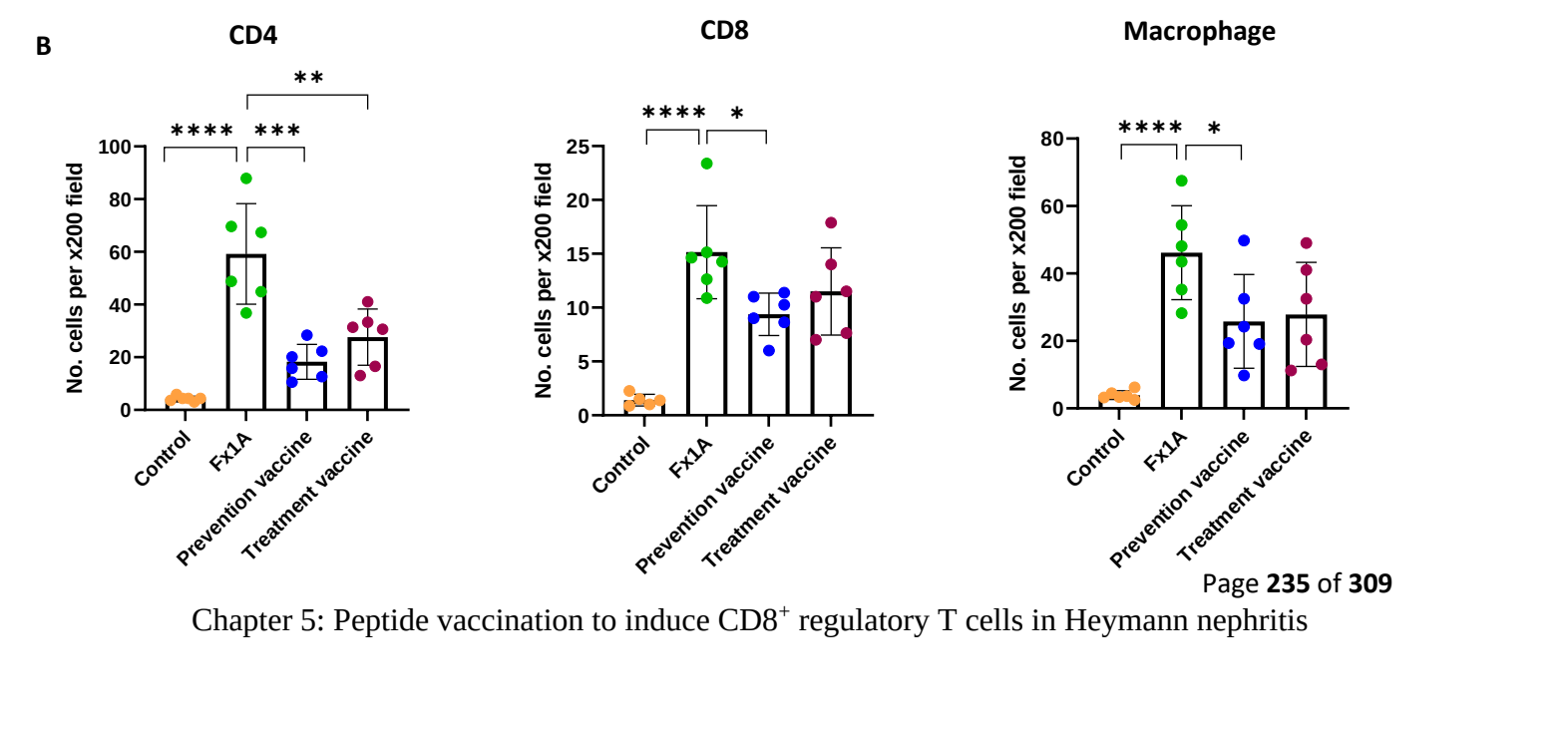
B
CD4
CD8
Macrophage
No. cells per x200 field
Control
Fx1A
Prevention vaccine
Treatment vaccine

Figure 4

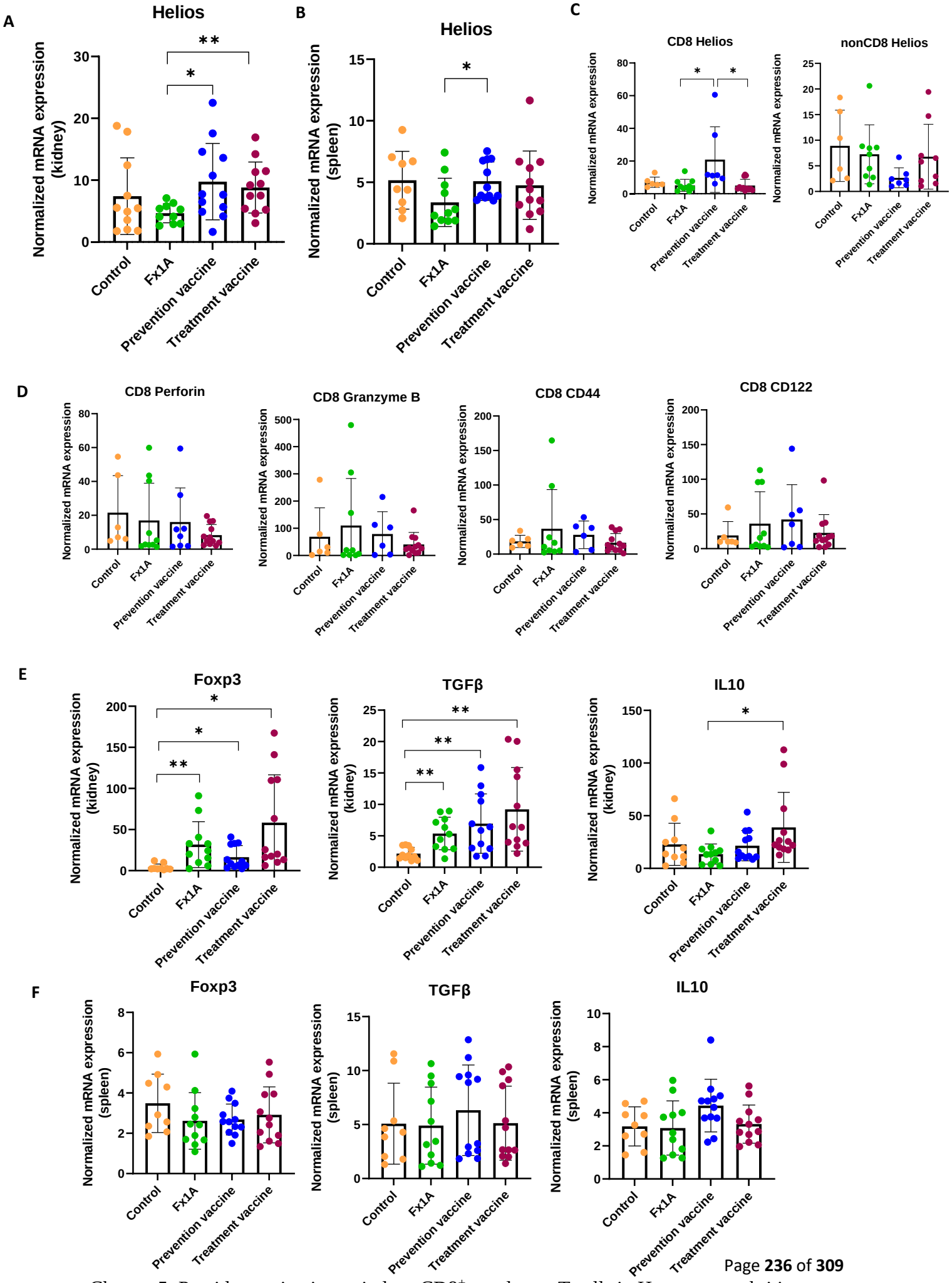
A
Helios
Normalized mRNA expression (kidney)
Control
Fx1A
Prevention vaccine
Treatment vaccine
B
Helios
Normalized mRNA expression (spleen)
C
CD8 Helios
nonCD8 Helios
Normalized mRNA expression
D
CD8 Perforin
CD8 Granzyme B
CD8 CD44
CD8 CD122
E
Foxp3
TGFβ
IL10
F
Foxp3
TGFβ
IL10

Figure 4

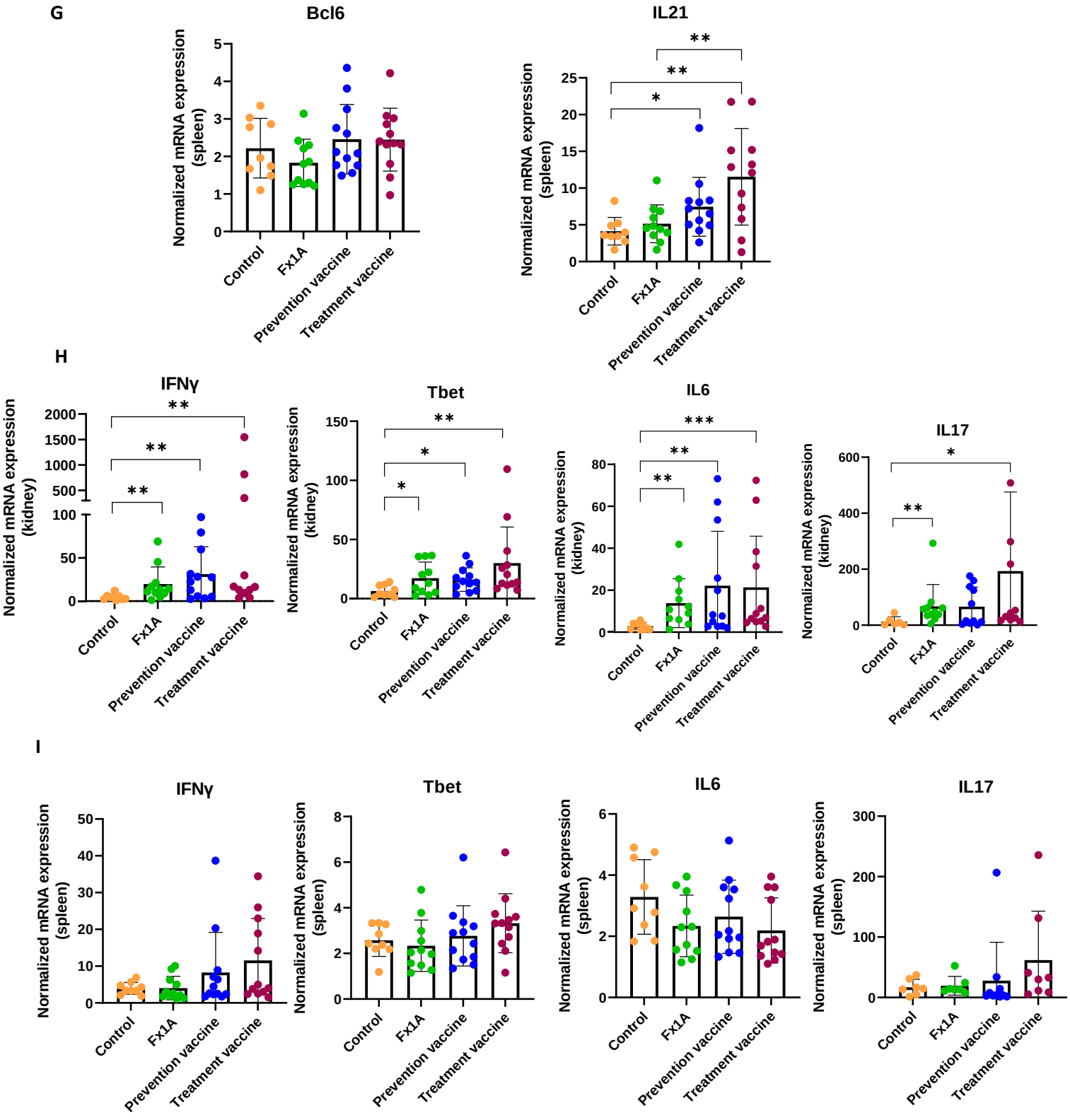
G
Bcl6
Normalized mRNA expression (spleen)
IL21
Normalized mRNA expression (spleen)
Control
Fx1A
Prevention vaccine
Treatment vaccine
H
IFNγ
Normalized mRNA expression (kidney)
Tbet
Normalized mRNA expression (kidney)
IL6
Normalized mRNA expression (kidney)
IL17
Normalized mRNA expression (kidney)
I
IFNγ
Normalized mRNA expression (spleen)
Tbet
Normalized mRNA expression (spleen)
IL6
Normalized mRNA expression (spleen)
IL17
Normalized mRNA expression (spleen)

Figure 5

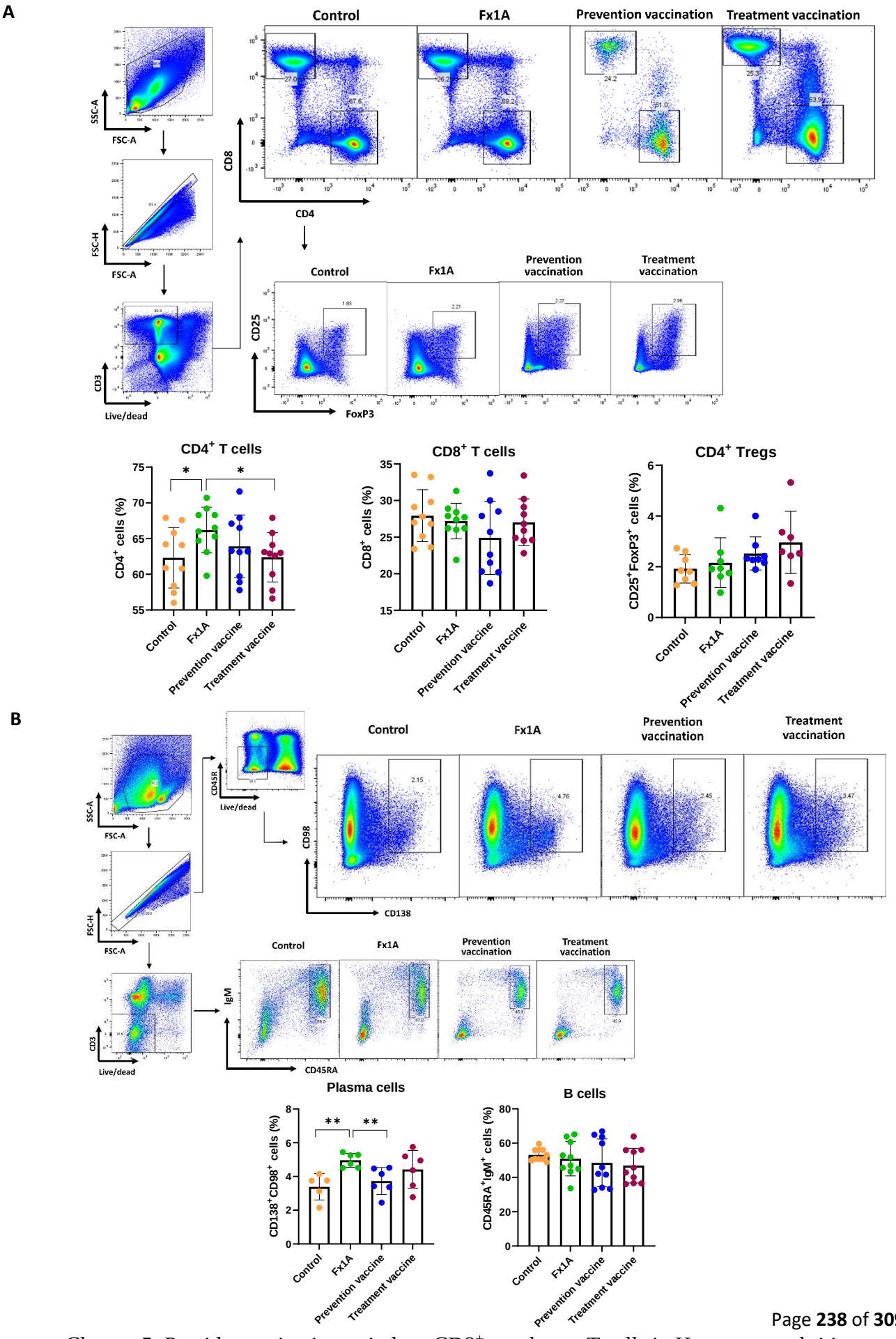
A
Control
Fx1A
Prevention vaccination
Treatment vaccination
SSC-A
FSC-A
FSC-H
CD3
Live/dead
CD8
CD4
CD25
FoxP3
CD4+ T cells
CD4+ cells (%)
CD8+ T cells
CD8+ cells (%)
CD4+ Tregs
CD25+FoxP3+ cells (%)
B
CD45R
CD98
CD138
IgM
CD45RA
Plasma cells
CD138+CD98+ cells (%)
B cells
CD45RA+IgM+ cells (%)

Figure 5

C

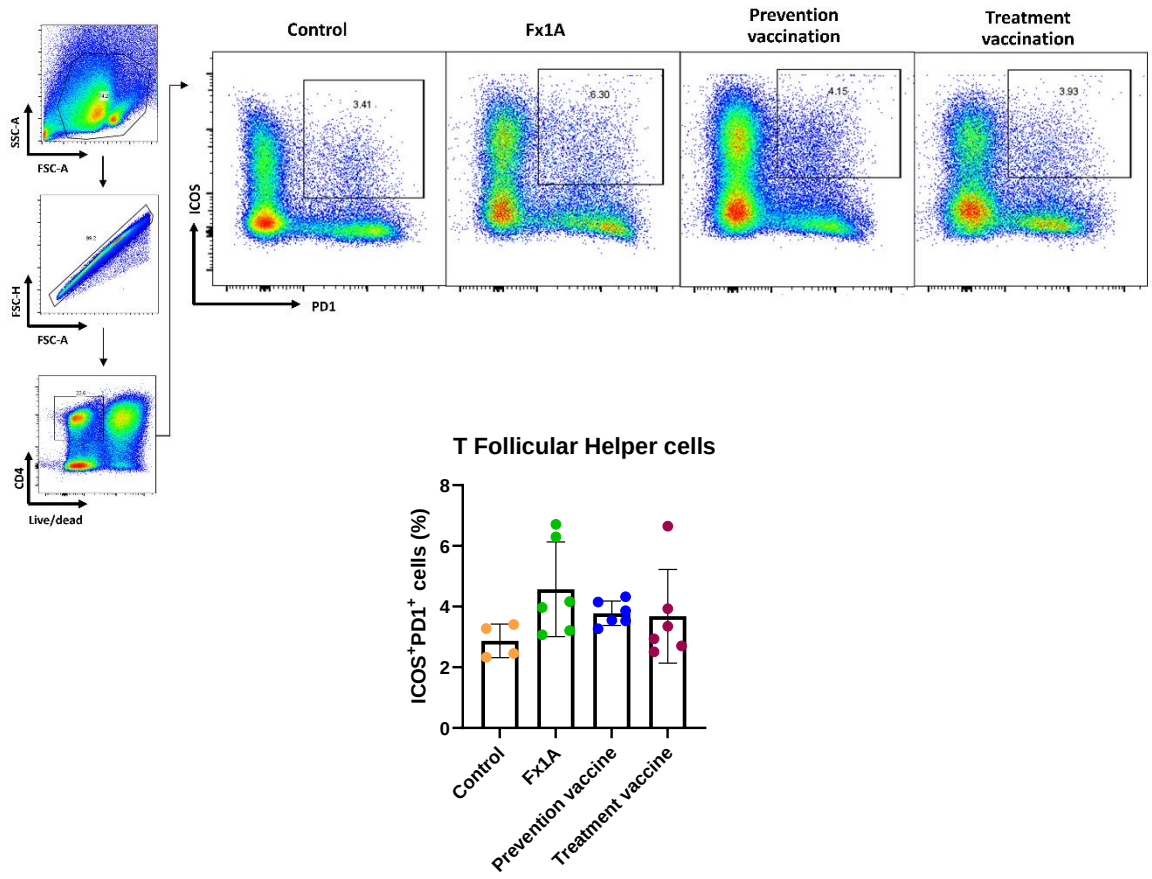
Control
Fx1A
Prevention vaccination
Treatment vaccination
SSC-A
FSC-A
FSC-H
FSC-A
CD4
Live/dead
ICOS
PD1
3.41
6.30
4.15
3.93
T Follicular Helper cells
ICOS+PD1+ cells (%)
0
2
4
6
8
Control
Fx1A
Prevention vaccine
Treatment vaccine

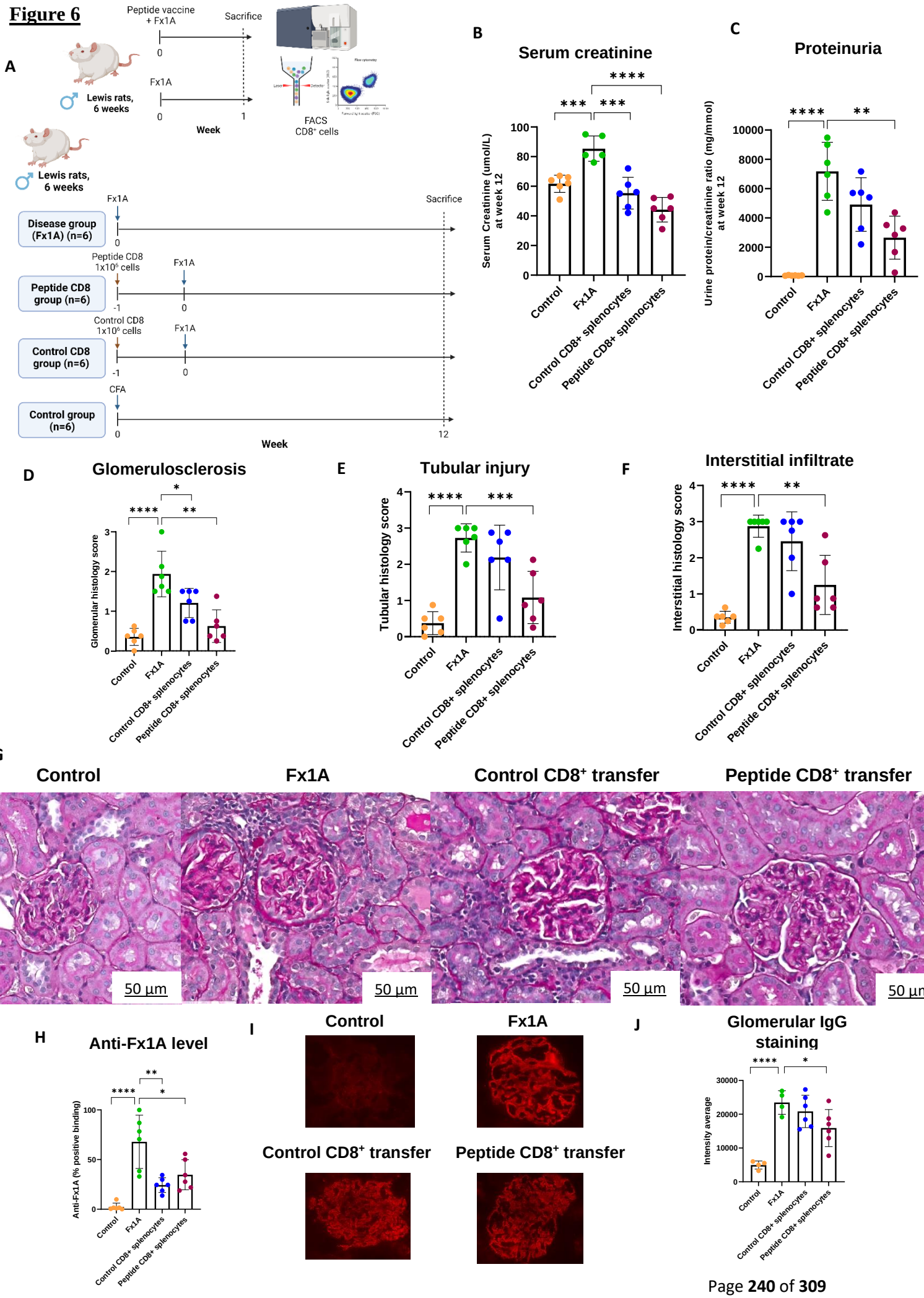
Figure 6
A
Peptide vaccine + Fx1A
Sacrifice
0
Fx1A
0
1
Week
Lewis rats, 6 weeks
FACS CD8+ cells
Lewis rats, 6 weeks
Fx1A
Sacrifice
Disease group (Fx1A) (n=6)
0
Peptide CD8 1x10⁶ cells
Fx1A
Peptide CD8 group (n=6)
-1
0
Control CD8 1x10⁶ cells
Fx1A
Control CD8 group (n=6)
-1
0
CFA
Control group (n=6)
0
12
Week
B
Serum creatinine
Serum Creatinine (umol/L) at week 12
Control
Fx1A
Control CD8+ splenocytes
Peptide CD8+ splenocytes
C
Proteinuria
Urine protein/creatinine ratio (mg/mmol) at week 12
D
Glomerulosclerosis
Glomerular histology score
E
Tubular injury
Tubular histology score
F
Interstitial infiltrate
Interstitial histology score
G
Control
Fx1A
Control CD8+ transfer
Peptide CD8+ transfer
50 µm
H
Anti-Fx1A level
Anti-Fx1A (% positive binding)
I
Control
Fx1A
Control CD8+ transfer
Peptide CD8+ transfer
J
Glomerular IgG staining
Intensity average

Figure 7

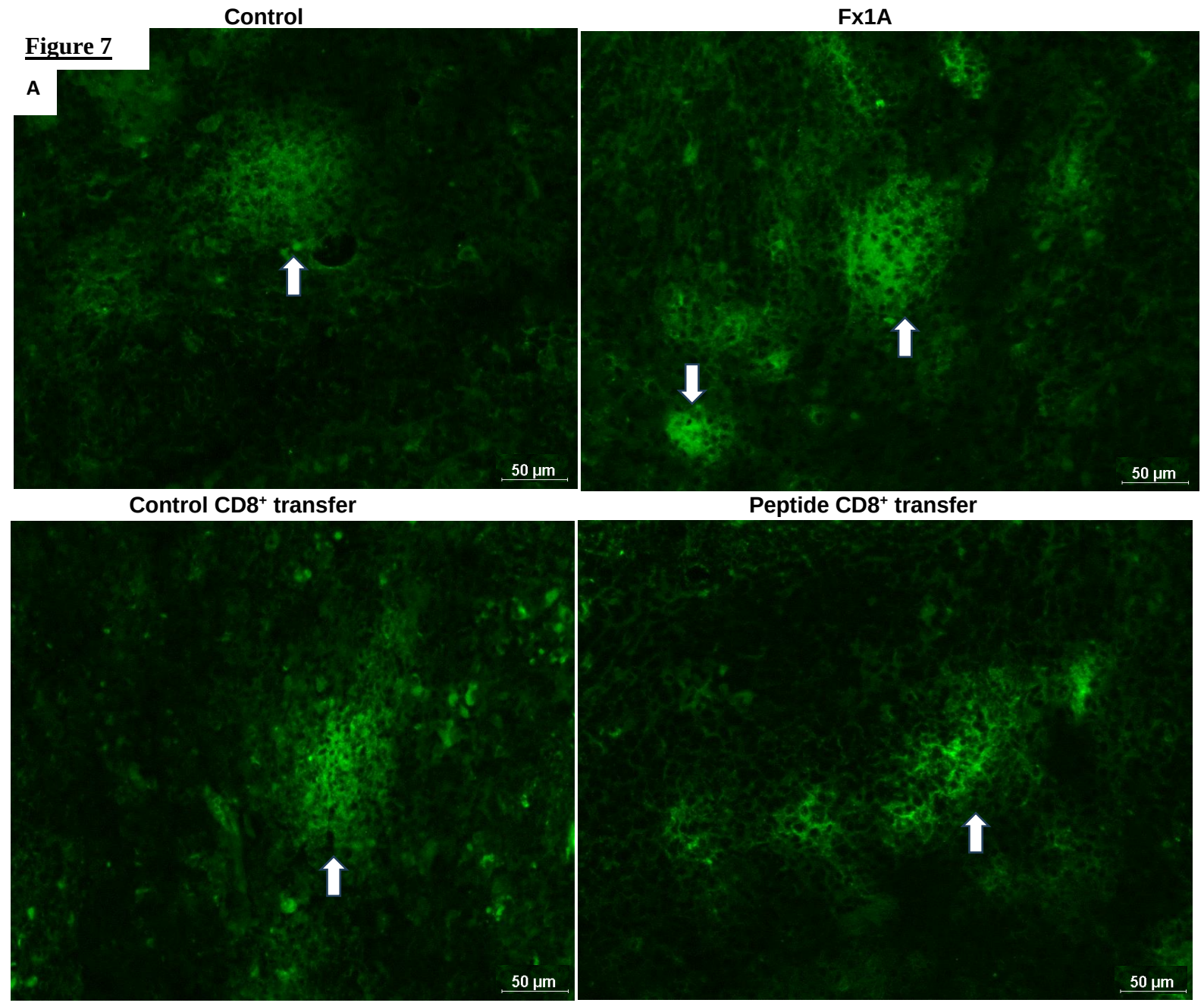
A
Control
Fx1A
50 µm
50 µm
Control CD8⁺ transfer
Peptide CD8⁺ transfer
50 µm
50 µm

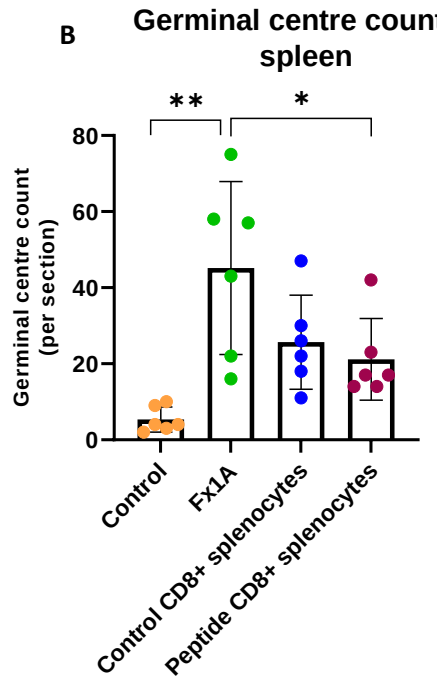
B
Germinal centre count in spleen
Germinal centre count (per section)
80
60
40
20
0
**
*
Control
Fx1A
Control CD8+ splenocytes
Peptide CD8+ splenocytes

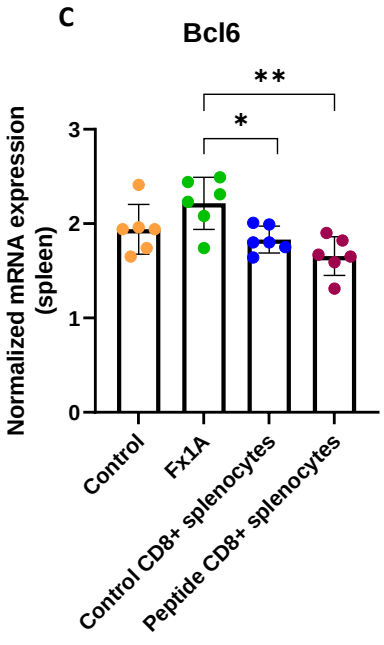
C
Bcl6
Normalized mRNA expression (spleen)
3
2
1
0
**
*
Control
Fx1A
Control CD8+ splenocytes
Peptide CD8+ splenocytes

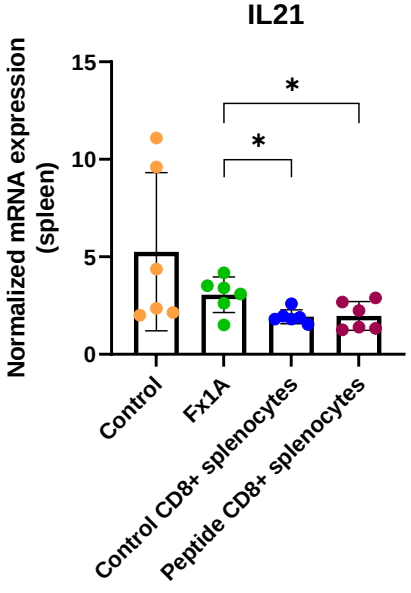
IL21
Normalized mRNA expression (spleen)
15
10
5
0
*
*
Control
Fx1A
Control CD8+ splenocytes
Peptide CD8+ splenocytes

Figure 7

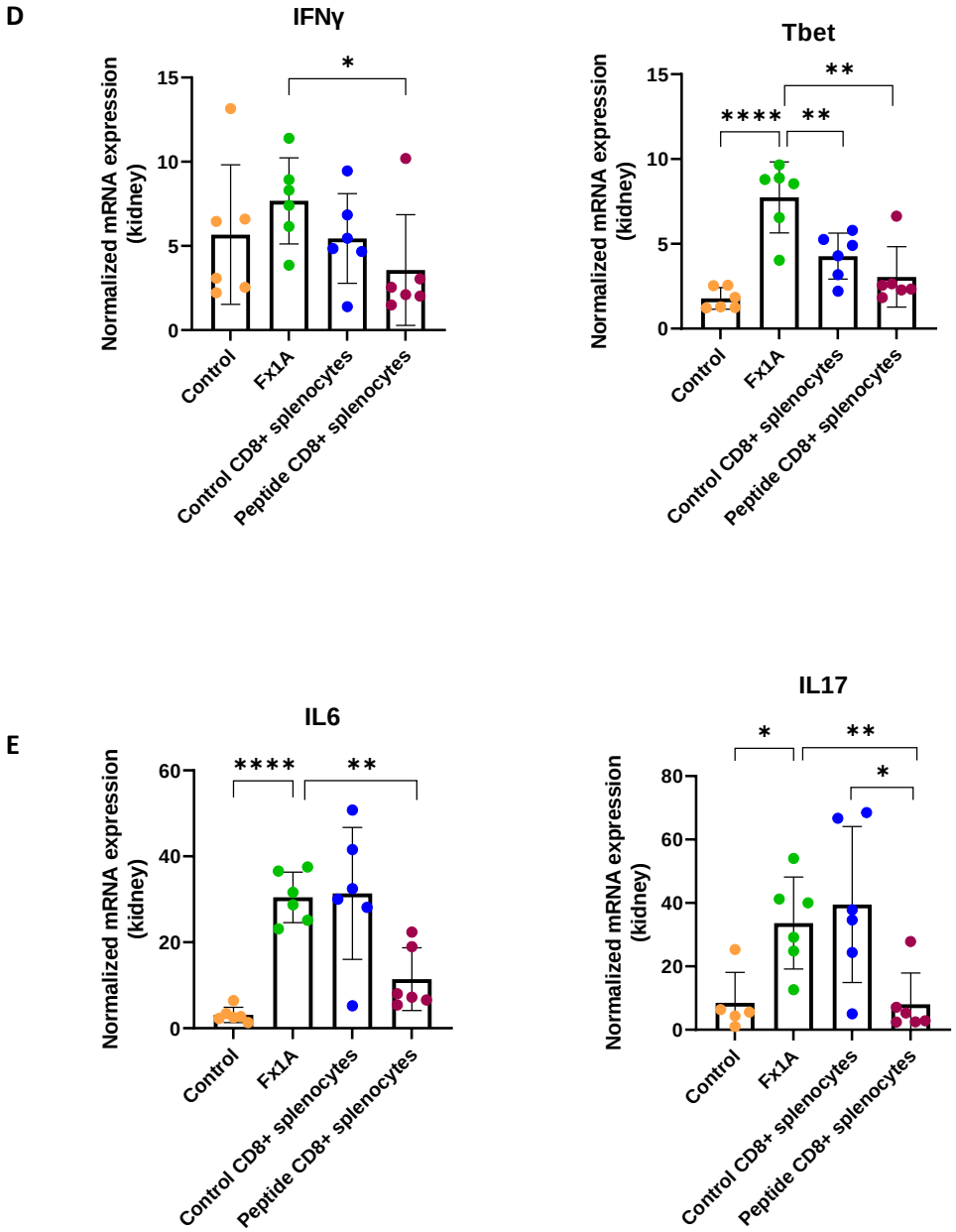
D
IFNγ
Normalized mRNA expression (kidney)
15
10
5
0
*
Control
Fx1A
Control CD8+ splenocytes
Peptide CD8+ splenocytes
Tbet
Normalized mRNA expression (kidney)
15
10
5
0
****
**
**
Control
Fx1A
Control CD8+ splenocytes
Peptide CD8+ splenocytes
E
IL6
Normalized mRNA expression (kidney)
60
40
20
0
****
**
Control
Fx1A
Control CD8+ splenocytes
Peptide CD8+ splenocytes
IL17
Normalized mRNA expression (kidney)
80
60
40
20
0
*
**
*
Control
Fx1A
Control CD8+ splenocytes
Peptide CD8+ splenocytes

Figure legends

Figure 1. Peptide vaccination ameliorated Heymann nephritis (HN) but only prevention vaccination reduced anti-Fx1A autoantibody levels. (**A**) Lewis rats at 4-6 weeks of age were immunised in the tail base with peptides (ASRSNRYFWL, HDRVNWEYI, SMRPNHFFFL, YQPGNWEYI) either 1 week before Fx1A immunisation (prevention vaccination) or 1 week after Fx1A immunisation (treatment vaccination) and sacrificed at 12 weeks after Fx1A immunisation. Fx1A was extracted from Sprague-Dawley rats at 12 weeks of age via salt fractionation. Figure was created using BioRender. (**B**) Serum creatinine was significantly lower in HN rats receiving prevention vaccination and (**C**) urinary protein/creatinine ratio from a 16-hour urine collection was significantly lower in HN rats receiving treatment vaccination compared to untreated HN rats (****$p<0.0001$, ***$p<0.001$, **$p<0.01$, *$p<0.05$, n=11-12 per group). (**D**) Serum anti-Fx1A autoantibody levels (expressed as a percentage of positive binding, calculated by dividing the sample optical density by the optical density of a positive control sample of known strongly positive serum containing anti-Fx1A) were lower in HN rats receiving prevention vaccination, but not treatment vaccination, compared to untreated HN rats (****$p<0.0001$, **$p<0.01$) (n=11-12 in each group).

Figure 2. Peptide vaccination reduced glomerulosclerosis (arrow) and tubular injury (notched arrow) but only prevention vaccination reduced interstitial cell infiltrates (arrowhead) and overall, peptide vaccination reduced glomerular IgG deposition. Semi-quantitative scores of morphological changes at week 12 showed significantly reduced (**A**) glomerulosclerosis and (**B**) tubular injury with prevention and treatment vaccination but only reduced (**C**) interstitial infiltrates with prevention vaccination compared to untreated HN rats (****$p<0.0001$, ***$p<0.001$, **$p<0.01$, *$p<0.05$, n=11-12 per group). (**D**) Histology of kidney representative sections under PAS staining showed reduced kidney damage and cellular infiltration in the HN rats treated with prevention and treatment vaccination compared to untreated HN rats (n=11-12 per group, magnification X200). (**E-F**) Representative sections of glomeruli showed prevention and treatment vaccination reduced but did

not prevent glomerular capillary loop IgG deposition in HN rats compared to untreated HN rats (magnification X400) (***p<0.001, **p<0.01, n=11-12 per group).

Figure 3. Peptide vaccination reduced infiltration of $CD4^+$ T cells, $CD8^+$ T cells and macrophages into the kidney of HN rats. (**A**) Photomicrographs of immunohistochemical kidney sections showed reduction in kidney infiltration of $CD4^+$ T cells (arrows), $CD8^+$ T cells and macrophages in the HN rats treated with peptide vaccination compared to untreated HN rats (magnification, X200), (**B**) which was statistically significant for both prevention and treatment vaccination for $CD4^+$ T cells (***p<0.001, **p<0.01, n=6 per group), and for prevention vaccination but not treatment vaccination for $CD8^+$ T cells and macrophages (****p<0.0001, *p<0.05, n=6 per group).

Figure 4. Peptide vaccination increased expression of Helios specifically in $CD8^+$ T cells in HN rats. (**A-I**) Real-time quantitative PCR demonstrated increased mRNA levels of Helios (*Ikzf2*) in the kidney with prevention and treatment vaccination (**A**) and in the spleen with prevention vaccination (**B**) (**p<0.01, *p<0.05, n=11-12 per group, mRNA expression normalised for GAPDH expression. Data shown are the mean ± standard deviation; each sample was run in triplicate). In the spleen, increased Helios mRNA expression was specific to $CD8^+$ splenocytes (isolated by FACS) but not $CD8^-$ splenocytes (**C**) (*p<0.05, n=6-12 per group). There was no significant difference in expression of Perforin, Granzyme B, CD44 and CD122 in $CD8^+$ splenocytes with peptide vaccination (**D**) (p>0.05, n=6-12 per group). (**E-F**) There was increased IL-10 mRNA expression in the kidney of HN rats with treatment vaccination compared to untreated HN rats (*p<0.05, n=11-12 per group) but no significant difference in expression of other markers of $CD4^+$ Tregs (FoxP3, TGF-β) in the spleen and kidney between HN rats (p>0.05, n=6-12 per group), though expression of FoxP3 and TGF-β was higher in the kidney of HN rats compared to controls (**p<0.01, *p<0.05, n=11-12 per group) (**G**). There was increased IL-21 mRNA expression in the spleen of HN rats with treatment vaccination

compared to untreated HN rats (**p<0.01, n=11-12 per group) but no between-group differences in expression of Bcl6. (**H-I**) There were also no differences in Th1 (IFN-γ, Tbet) or Th17 (IL-6, IL-17) mRNA expression in the kidney or spleen between HN rats, but higher expression in the kidney of HN rats compared to controls (***p<0.001, **p<0.01, *p<0.05, n=11-12 per group).

Figure 5. In the spleen, peptide vaccination reduced $CD4^+$ T cell expansion and prevention vaccination reduced plasma cell expansion but did not significantly alter total B cells or Tfh cells. (**A**) Peptide vaccination reduced total $CD4^+$ T cells (gating on live $CD3^+$ cells) compared untreated HN rats, which was statistically significant for treatment vaccination but not prevention vaccination (*p<0.05, n=7-10 per group). Peptide vaccination did not significantly alter total $CD8^+$ T cells (gating on live $CD3^+$ cells) or $CD4^+$ Tregs ($CD4^+CD25^+Foxp3^+$ gating on live $CD3^+$ cells). (**B**) Prevention vaccination significantly reduced plasma cells ($CD138^+CD98^+$ gating on live $CD45R^-$ cells) but did not alter total (**C**) Tfh cells ($ICOS^+PD1^+$ gating on live $CD4^+$ cells) compared to untreated HN rats (**p<0.01, n=4-6 per group). (**B**) Peptide vaccination also did not alter total B cells ($CD45RA^+IgM^+$ gating on live $CD3^-$ cells) (n=10 per group).

Figure 6. Adoptive transfer of $CD8^+$ T cells after peptide vaccination ameliorated HN and reduced anti-Fx1A autoantibody levels. (**A**) Lewis rats were induced with HN using Fx1A emulsion with or without 100 µg of each peptide (ASRSNRYFWL, HDRVNWEYI, SMRPNHFFFL, YQPGNWEYI). On day 7, spleen and draining lymph nodes were collected and FACS-purified $CD8^+$ cells from rats that received Fx1A and peptide vaccination (peptide $CD8^+$ transfer) or Fx1A immunisation alone (control $CD8^+$ transfer) were adoptively transferred (1 million cells per rat) 1 week before induction of HN. Figure was created using BioRender. (**B**) Serum creatinine and (**C**) urinary protein/creatinine ratio from a 16-hour urine collection were significantly lower with peptide $CD8^+$ transfer but only serum creatinine was lower with control $CD8^+$ transfer compared to untreated HN rats

(****p<0.0001, ***p<0.001, **p<0.01, n=6 per group). (**D-G**) There was less glomerulosclerosis, tubular injury, and interstitial infiltrates with peptide $CD8^+$ transfer, and less glomerulosclerosis with control $CD8^+$ transfer compared to untreated HN rats (***p<0.001, **p<0.01, *p<0.05, n=6 per group, magnification X200). (**H**) Serum anti-Fx1A autoantibody levels were significantly lower with peptide and control $CD8^+$ transfer compared to untreated HN rats (**p<0.01, *p<0.05, n=6 per group). (**I-J**) Representative sections of glomeruli showed peptide but not control $CD8^+$ transfer reduced glomerular capillary loop IgG deposition compared to untreated HN rats (*p<0.05, n=6 per group, magnification X200).

Figure 7. Adoptive transfer of $CD8^+$ T cells after peptide vaccination reduced germinal centre formation and reduced expression of markers of Tfh, Th1 and Th17 cells. (**A-B**) Peptide and control $CD8^+$ transfer reduced germinal centre formation (peanut agglutinin (PNA)-$FITC^+$ germinal centre B cells) (arrows) compared to untreated HN rats on immunofluorescent staining of spleen sections, though this only reached statistical significance with peptide $CD8^+$ transfer (*p<0.05, n=6 per group, magnification X100). (**C**) Real-time quantitative PCR demonstrated reduced mRNA levels of Tfh markers (Bcl6, IL-21) in the spleen with peptide and control $CD8^+$ transfer compared to untreated HN rats (**p<0.01, *p<0.05, n=6 per group, mRNA expression normalised for GAPDH expression. Data shown are the mean ± standard deviation; each sample was run in triplicate). (**D**) There was reduced mRNA expression of markers of Th1 cells (IFN-γ, Tbet) in the kidney with peptide and control $CD8^+$ transfer compared to untreated HN rats (**p<0.01, *p<0.05, n=6 per group), though this didn't reach statistical significance for control $CD8^+$ transfer on IFN-γ mRNA expression. (**E**) There was reduced mRNA expression of markers of Th17 cells (IL-6, IL-17) in the kidney with peptide $CD8^+$ transfer compared to untreated HN rats but not control $CD8^+$ transfer (**p<0.01, n=6 per group).

6.BAFF-expressing CAR T cell specifically eliminates B cells *in vitro*

6.1 Overview

B cell activating factor (BAFF) is a B cell growth factor that is involved in the development of autoreactive B cells by protecting against cell death. Serum concentrations of BAFF are associated with disease activity in autoimmune glomerulonephritis including primary membranous nephropathy. BAFF-expressing chimeric antigen receptor (CAR) T cells may redirect T cell killing towards autoreactive B cells that require high BAFF levels for survival. We have generated three BAFF-expressing CAR T cells (full-length BAFF monomer, truncated BAFF monomer, and truncated BAFF trimer) consisting of the extracellular domain of human BAFF using a PiggyBac transposon, a non-viral gene delivery method. All three BAFF-expressing CAR T cells demonstrated increased cytotoxicity against Raji B cells compared to unmodified T cells without significant cytotoxicity against a negative cell line human embryonic kidney (HEK)-293T cells. Co-culture of BAFF-expressing CAR T cells with Raji B cells resulted in induction of the degranulation marker CD107a and proinflammatory cytokines (tumour necrosis factor (TNF)-α, interferon (IFN)-γ and interleukin (IL)-2), compared to unmodified T cells co-cultured with Raji B cells. There was an effector memory T cell phenotype in BAFF-expressing CAR T cells, which overall did not exhibit a significantly increased expression of markers of T cell exhaustion (programmed death (PD)-1, T cell immunoglobulin and mucin domain-containing protein (Tim)-3, lymphocyte activation gene (LAG)-3). In conclusion, BAFF-expressing T cells eliminate B cells *in vitro* and may represent a novel treatment for B cell mediated autoimmunity, which underpins primary membranous nephropathy.

6.2 Introduction

Primary membranous nephropathy is an autoimmune kidney disease characterised by autoantibodies targeting podocyte antigens in the kidney, which in 70% of cases is the phospholipase A2 receptor (PLA2R).[1] Autoantibody formation represents a loss of tolerance to self-antigens, which normally causes apoptosis of autoreactive B cells via BCL2-interacting mediator of cell death (BIM) upon chronic self-antigen-induced signalling through the B cell receptor (BCR).[2] B cell activating factor (BAFF) is a cytokine that is critical for B cell survival and maturation into long-lived plasma cells, and excess BAFF is implicated in the development of autoreactive B cells since it overrides BIM-associated apoptosis, thus rescuing autoreactive B cells from clonal deletion and anergy.[3-5] The essential role of BAFF in autoimmunity is also demonstrated in BAFF-transgenic mice that develop lupus nephritis (another autoimmune kidney disease),[6, 7] genetic variants in BAFF conferring risk for lupus,[8] and serum BAFF levels correlating with disease activity in lupus and PLA2R-associated membranous nephropathy.[9, 10]

A monoclonal antibody against BAFF (belimumab) has been developed, which preferentially reduces autoantibody levels compared to total IgG levels in patients with lupus,[11] providing further evidence that excess BAFF favours the development of autoreactive B cells. However, belimumab has only shown marginal benefit in lupus nephritis where the absolute increase in disease remission over placebo was 10%.[12] This may be due to BAFF binding to three separate receptors on mature B cells and plasma cells (BAFF-receptor (BAFF-R), transmembrane activator and cyclophilin ligand interactor (TACI) and B cell maturation antigen (BCMA)), two of which are shared with another ligand, a proliferation-inducing ligand (APRIL). BAFF also induces B cell maturation into plasmablasts, which exhibit reduced expression of BAFF-R, increased expression of BCMA, and a resultant greater dependence on APRIL for survival in the bone marrow.[13, 14] In primary membranous nephropathy, a clinical trial (REBOOT,

NCT03949855) is underway combining belimumab with the anti-CD20 monoclonal antibody rituximab.

In this chapter, we propose utilising chimeric antigen receptor (CAR) T cells that genetically express BAFF to redirect T cell killing towards autoreactive B cells and plasma cells, which is likely superior to monoclonal antibodies targeting individual factors and receptors involved in their survival. CD19-targeted CAR T cells have revolutionised the treatment of B cell malignancies and recent preliminary data in refractory autoimmune disease has been remarkable, where a single infusion of CD19-targeted CAR T cell could induce drug-free remission for up to 2 years.[15] However, CD19 is expressed on all B cells (not just autoreactive B-cells) and is not expressed on plasma cells, which are increased and correlate with autoantibody levels in PLA2R-associated membranous nephropathy.[16] Therefore, BAFF-expressing CAR T cells may be more targeted against autoreactive B cell and plasma cell clones that require a high level of BAFF for survival and represent a promising precision treatment in primary membranous nephropathy and other forms of autoimmune kidney disease.

6.3 Material and Methods

Our research complies with all relevant ethical regulations, as determined by the Sydney Children's Hospitals Network Human Research Ethics Committee (2023/ETH01873).

6.3.1 Cell lines

The Raji Burkitt lymphoma cell line was supplied by the European Collection of Cell Cultures (ECACC; Salisbury, United Kingdom) as catalogue number 85011429, and was purchased from CellBank Australia (Westmead, NSW, Australia). This cell line was cultured in RPMI-

1640 media (Thermofisher #21870076) with 10% fetal bovine serum (FBS) (Thermofisher #26140079), 2mM glutamine (Thermofisher #25030081), and 1% penicillin-streptomycin (P/S) (Thermofisher #15140122). The Human Embryonic Kidney 293T (HEK293T) cell line was supplied by the European Collection of Cell Cultures (ECACC; Salisbury, United Kingdom) as catalogue number 85120602, and was purchased from CellBank Australia (Westmead, NSW, Australia). This cell line was cultured in Dulbecco's Modified Eagle Medium (DMEM) media (Thermofisher #11965092) with 10% FBS, 2mM glutamine, and 1% penicillin-streptomycin. All cell lines used throughout were subjected to Short Tandem Repeat profiling by CellBank Australia (Westmead, NSW, Australia) to confirm identity.

6.3.2 Flow cytometry

Flow cytometry antibodies were used to stain cell samples in phosphate-buffered saline (PBS) (Table 1). Live/Dead Fixable Aqua Dead Cell Stain Kit (Thermofisher #L34965) was used according to manufacturer instructions to distinguish live cells. For surface staining, splenocytes were incubated with fluorochrome-conjugated anti-human antibodies for 25 min on ice in the dark. Intracellular labelling of cytokines was performed using fixed and permeabilized cells using BD Cytofix/Cytoperm Fixation/Permeabilization Set (BD #554714) and according to manufacturer's instructions. All samples were analysed by flow cytometry using a Fortessa Color Flow Cytometer (BD Biosciences, San Jose, USA). Data analyses were performed using the FlowJo™ software (Tree Star, Ashland, USA).

6.3.3 BAFF CAR construct design

For the BAFF monomeric constructs, the BAFF CAR DNA sequence consists of: CD8α leader sequence; full-length or truncated BAFF ligand monomer; a glycine-serine (GGGGS)3 linker sequence; IgG1 hinge; CD28 transmembrane; CD28 and OX40 costimulatory; and CD3ζ domains. To prevent cleavage of membrane-bound BAFF, truncated BAFF consists of its extracellular domain distal to the cleavage site and we mutated the cleavage site in the full-length BAFF construct (K132A/R133A).[17] In both constructs, we also introduced mutations (H218A/E223K) to prevent BAFF aggregation into multimers,[18] which we hypothesise would cause CAR T cells to aggregate and impair their function. The BAFF CAR DNA sequence was synthesised (Genscript Biotech) and subcloned into a modified HIV-1-based lentiviral expression vector using the PmlI and SalI restriction enzyme sites for the full-length BAFF-CAR construct and using the BstEII and XbaI restriction enzyme sites for the truncated BAFF-CAR construct. The lentiviral vector backbone was modified to co-express the full-length extracellular domain of human CD20 downstream of the BAFF CAR construct, separated by a P2A self-cleaving peptide sequence. Transcription of both BAFF CAR and CD20 were controlled by a full-length elongation factor 1-alpha 1 (EF1α) promoter. An ampicillin resistance gene was inserted to facilitate cloning in Escherichia coli (E.coli) competent cells.

The BAFF trimer construct on a Piggybac backbone was provided by Dr Kavitha Gowrishankar (Children's Cancer Research Unit, The Children's Hospital at Westmead). This BAFF CAR DNA sequence consists of: CD8α leader sequence; truncated BAFF ligand trimer each separated by a glycine-serine (GGGGS)4 linker sequence; CD28 transmembrane; 4-1BB (CD137) costimulatory; and CD3ζ domains. The truncated BAFF sequence consisted of the extracellular domain of BAFF distal to the cleavage site with E223K mutation to prevent BAFF multimerisation.[18] Enhanced green fluorescent protein (EGFP) was expressed downstream of the BAFF CAR construct, separated by a T2A self-cleaving peptide sequence. Transcription of

both BAFF CAR and EGFP were controlled by a EF1α core promoter. A kanamycin resistance gene was inserted to facilitate cloning in E.coli competent cells.

6.3.4 T cell isolation

Anonymised healthy donor buffy coats were provided by the Australian Red Cross (agreement no. 23-09NSW-14). Peripheral blood mononuclear cells (PBMCs) were isolated from blood via density gradient centrifugation using Ficoll-Paque Plus (Sigma-Aldrich # GE17-1440-02), according to manufacturer instructions. T cells were purified from PBMCs using the EasySep human CD3 Negative selection kit (StemCell Technologies #17951), according to manufacturer instructions.

6.3.5 CAR T cell generation using lentiviral gene delivery

To clone the lentiviral BAFF CAR DNA plasmid, we added 1 µl of plasmid DNA synthesised by Genscript Biotech (diluted 10 ng/µl in sterile water) to 50 µl JM109 competent E.coli cells at 4ºC for 10 minutes, then heat shocked the cells in a 42ºC water bath for 45 seconds before immediately chilling it at 4ºC for 2 minutes. We added 450 µl of super optimal medium with catabolic repressor (SOC) medium at room temperature, incubated it in a shaker for 60 minutes at 37ºC and 225 rpm, then cultured it on Agar plates (1:10 and 1:100 dilutions in Luria-Bertani (LB) broth) at 37ºC overnight. Agar plates were created by mixing 2.25g of Agar with 150 ml LB broth (mix 10 g of Bacto Trypton, 5 g of Bacto Yeast Extract, 5 g of sodium chloride, and 1 g of D-glucose in 1 L of Milli-Q water then autoclave) which was autoclaved then antibiotic of choice added (ampicillin 100 µg/ml). Colonies, from the Agar plate, were further cultured in a shaker at 37ºC and 225 rpm in 8 ml of LB broth with ampicillin (100 µg/ml) for 6 hours then in 300 ml of LB broth with ampicillin (100 µg/ml) overnight. Plasmid DNA was isolated

and purified using an EndoFree® Plasmid Maxi Kit (Qiagen #12362), using the high-copy number vector protocol, according to manufacturer instructions.

Lentivirus was produced by colleagues at the Vectorology Facility at the Children's Medical Research Institute (Westmead, NSW, Australia). In brief, they transfected HEK293T cells using polyethylenimine max. The media was changed the next day, then viral supernatant collected at 24 and 48 hours afterwards. The viral supernatant was subsequently ultracentrifuged with a sucrose cushion. The pellet from both the 24 hour and 48 hour harvests were resuspended in PBS and ultracentrifuged again to concentrate.

Isolated T cells were activated with T Cell TransAct CD3/CD28 microbeads (Miltenyi Biotec #130-111-160) for 48 hours in complete RPMI-1640 media (10% FBS, 2 mM L-glutamine, 1% penicillin–streptomycin; ThermoFisher) supplemented with IL-7 (Miltenyi Biotec #130-093-937; 200 IU/mL) and IL-15 (Miltenyi Biotec #130-095-760; 150 IU/mL), followed by lentiviral transduction. T cells (0.5×10^6 cells per well in a 24-well tissue culture plate (In Vitro Technologies #FAL353504)) were incubated with lentivirus in 500 µl of complete RPMI-1640 media supplemented with IL-7 (200 IU/mL), and IL-15 (150 IU/mL) for 6 hours at 37ºC before adding an additional 500 µl of complete RPMI-1640 media supplemented with IL-7 (200 IU/mL), and IL-15 (150 IU/mL). CAR T cells were expanded in complete RPMI-1640 media supplemented with IL-7 (200 IU/mL), and IL-15 (150 IU/mL) every two days.

For some experiments, a 24-well tissue culture plate was coated with 300 µl of retronectin (40 µg/ml in PBS) and incubated overnight at 4ºC. The lentivirus is subsequently added to the coated wells and centrifuged at 2000g for 2 hours and 30 minutes at 4ºC. Following centrifugation, the supernatant was removed, and 0.5×10^6 T cells added to virus-coated wells

in 500 µl of complete RPMI-1640 media supplemented with IL-7 (200 IU/mL), and IL-15 (150 IU/mL) every two days.

6.3.6 Subcloning BAFF CAR construct into a PiggyBac backbone

To isolate the CAR constructs from both the lentiviral plasmids and PiggyBac transposon plasmid from their respective vector backbones, we performed a double digest combining 10 µg of lentiviral BAFF CAR DNA plasmid (full-length BAFF monomer or truncated BAFF monomer) or 5 µg of PiggyBac vector plasmid encoding a EPH receptor A2 (EphA2) CAR (supplied by Dr Kavitha Gowrishankar (Children's Cancer Research Unit, The Children's Hospital at Westmead)) with 1 µl of each unique restriction enzyme (FseI (New England Biolabs #R0588) and SalI-HF (New England Biolabs #R3138)), 1x rCutSmart Buffer (New England Biolabs) and made up to 100 µl (for lentiviral BAFF CAR plasmid) or 50 µl (for PiggyBac vector plasmid) with nuclease-free water, which was incubated at 37ºC in a heat block for 3 hours then heat inactivated at 65ºC in a heat block for 15 minutes.

We subsequently loaded a 1.5% Agarose gel (0.75g of Agarose low electroendosmosis (LE) mixed in 50 ml of 1x Tris-acetate-ethylenediaminetetraacetic acid (EDTA) (TAE) buffer (Thermofisher #B49) with 10 µl of each digest mixture, which we ran in an electrophoresis bath containing 1x TAE buffer at 180V for 3 hours until good separation of bands. The gel was stained with ethidium bromide (20 µl ethidium bromide (Sigma-Aldrich #E1510-10ml) in 200 ml distilled water) for 15 minutes then visualised under ultraviolet (UV) light using the Molecular Imager Gel Doc XR system (Biorad). Bands containing the full-length BAFF monomer CAR construct, truncated BAFF monomer CAR construct, and the PiggyBac transposon plasmid were cut and isolated from their respective vector backbones on the UV

visualiser UView™ Mini Transilluminator (Biorad), then purified the DNA using a gel extraction kit (Qiagen #28704), according to manufacturer instructions.

To ligate the full-length BAFF monomer and truncated BAFF monomer CAR constructs onto a PiggyBac vector backbone, we combined 300 ng of BAFF CAR construct DNA, 100 ng of PiggyBac vector backbone DNA, and made up to 20 µl with nuclease-free water, which was incubated at 65ºC for 3 minutes and cooled at room temperature for 5 minutes. We subsequently added 1 µl of T4 DNA ligase (New England Biolabs #M0202S) and 2 µl of 10x ligation buffer (New England Biolabs) then incubated at room temperature overnight.

To clone the BAFF CAR PiggyBac vector plasmid, we added 10 µl of ligation mixture to 50 µl JM109 competent E.coli cells at 4ºC for 10 minutes, then heat shocked the cells in a 42ºC water bath for 45 seconds before immediately chilling it at 4ºC for 2 minutes. We added 450 µl of SOC medium at room temperature, incubated it in a shaker for 60 minutes at 37ºC and 225 rpm, then cultured it on Agar plates (with kanamycin 50 µg/ml) at 37ºC overnight. Six colonies from the Agar plate were further cultured separately in a shaker at 37ºC and 225 rpm in 8 ml of LB broth with kanamycin (50 µg/ml) for 6 hours then the plasmid DNA for each clone was isolated and purified using a QIAprep Spin Miniprep Kit (Qiagen #27104). Clones of full-length BAFF monomer CAR PiggyBac plasmid and truncated BAFF monomer CAR PiggyBac plasmid were confirmed with both diagnostic digest and Sanger sequencing. The diagnostic digest protocol was identical to the gel electrophoresis protocol outlined above but only 1 µg of plasmid DNA was digested with a total reaction volume 20 µl and two different restriction enzymes in separate reactions were used: AseI (New England Biolabs #R0526S) and SacI-HF (New England Biolabs #R3156S). We designed two primers: 1. F: 5'AGTCTTGTAAATGCGGGCCA3', R: 5'CGCTTTTTGACGGCTACGAA3'; and 2. F:

5’CGATGACCACCCCAAGGAAT3’; R: 5’AGCAGCGTATCCACATAGCG3’ to confirm the DNA sequence of the ligation sites of both BAFF CAR PiggyBac plasmids. Primer 1 was designed for the ligation site after FseI enzyme digest and primer 2 was designed for the ligation site after SalI-HF enzyme digest. Sanger sequencing was performed by the Australian Genome Research Facility.

Clones with confirmed successful ligation by Sanger sequencing were cultured in separate Agar plates with kanamycin (50 μg/ml). Colonies from these Agar plate was further cultured in a shaker at 37ºC and 225 rpm in 8 ml of LB broth with kanamycin (50 μg/ml) for 6 hours then in 300 ml of LB broth with kanamycin (50 μg/ml) overnight. Plasmid DNA was isolated and purified using an EndoFree® Plasmid Maxi Kit (Qiagen #12362), using the low-copy number vector protocol, according to manufacturer instructions.

6.3.7 CAR T cell generation using PiggyBac transposon gene delivery

T cells (5 x 10^6 cells for each electroporation reaction) isolated from PBMCs were mixed with 82 μl of nucleofector solution and 18 μl of supplement (Lonza #VPA-1002) then added to 5 μg of BAFF CAR PiggyBac plasmid (full-length BAFF monomer, truncated BAFF monomer or truncated BAFF trimer) and 5 μg of PiggyBac Transposase plasmid. The cell suspension is pipetted into the cuvette, placed in the electroporation Nucleofector 2b machine (Lonza) and run on program T023 for human T cells. Electroporated T cells were incubated in complete RPMI-1640 media overnight at 37ºC then stimulated with twice the number of irradiated PBMCs (30 Gray delivered in a CellRad+ Benchtop X-ray Irradiator (Precision X-ray)) from the same donor and supplemented with IL-15 (Miltenyi Biotec #130-095-765; 200 IU/mL) every two days. Irradiated PBMCs were added to culture every 7 days to stimulate and activate

BAFF-expressing CAR T cells, which should bind to B cells expressing BAFF receptor within the irradiated PBMCs.

6.3.8 *In vitro* cytotoxicity assay

Raji cells (positive target cells) or HEK293T cells (negative target cells) were labelled with 0.025 mM of Calcein for 30 minutes in a 37ºC water bath. Cells were then washed twice and cocultured with CAR T cells or unmodified T cells at various effector:target (E:T) ratios in a 96-well round-bottom tissue culture plate (In Vitro Technologies #FAL353077) in 200 µL complete RPMI-1640 media without phenol red for 4 hours in a 37ºC incubator. Wells containing Calcein-labelled Raji or HEK293T cells alone were used as a negative control. Wells containing Calcein-labelled Raji cells or HEK293T cells with 2% Triton X (MP-Biomedicals #02194854-CF) to achieve complete cell lysis, were used a positive control. After co-culture, the 96-well round-bottom tissue culture plate was centrifuged (1200 rpm, 3 minutes), 100 µL of supernatant from each well were collected and fluorescence read on a SpectraMax iD3 machine (excitation 485nm and emission 538nm) in triplicated samples. Target cell death was measured using the following formula:

$$Specific\ lysis\ (\%) = 100\ \times \frac{\text{test well}\ -\ \text{negative control}}{\text{positive control}\ -\ \text{negative control}}$$

6.3.9 CD107a degranulation assay

T cells were co-cultured with Raji cells (5:1 E:T ratio) in complete RPMI-1640 media containing GolgiStop (BD Biosciences #554724) and Golgiplug protein transport inhibitor (BD Biosciences #555029) and CD107a FITC (Biolegend #328606) or CD107a BV785 flow antibody (Biolegend #328643) for 4 hours in a 37ºC incubator. Cells were then labelled with CD3 BV510 antibody (Biolegend #317331) and analysed using flow cytometry. To measure

the percentage of $CD107a^+$ cells, BAFF-expressing CAR T cell samples were gated on live $CD3^+BAFF^+$ cells, while unmodified T cell samples were gated on live $CD3^+$ cells.

6.3.10 Statistical analysis

Results are expressed as group mean ± standard deviation (SD). Statistical analysis for multiple comparisons was performed using the one-way analysis of variance (ANOVA) test for normally distributed data and Kruskal-Wallis one-way ANOVA test for non-parametric data. Two group differences were analysed using the student's *t*-test for normally distributed data and the Mann-Whitney U test for non-parametric data. A two-tailed p value <0.05 was considered statistically significant. Statistical calculations were performed using GraphPad Prism 9.2.0.

6.4 Results

6.4.1 Lentiviral gene delivery did not generate stable BAFF CAR expression

We evaluated BAFF CAR expression (full-length BAFF monomer and truncated BAFF monomer) at day 4, 7, 11, 15, 19, 23, and 27 after lentiviral transduction at a multiplicity of infection (MOI) of 1, 10, 20, 50 and 100. Across all tested MOI, lentiviral gene delivery did not generate stable BAFF CAR expression based on either $CD3^+BAFF^+$ expression (Figure 1A) and $CD3^+CD20^+$ expression (Figure 1B) in either construct. There were different kinetics between BAFF expression and CD20 expression across the different time points with CD20 expression occurring earlier and BAFF expression occurring later. As a result, we did not see a significant population of $CD3^+BAFF^+CD20^+$ cells. Overall, CAR expression was low with both full-length BAFF monomer and truncated BAFF monomer constructs with the highest

transduction efficiency based on $CD3^+BAFF^+$ expression of 7.3% (mean 1.3 ± SD 1.7% at MOI 100) and 2.8% (0.9 ± 0.7% at MOI 100) respectively, and highest transduction efficiency based on $CD3^+CD20^+$ expression of 5.1% (0.7 ± 1.3% at MOI 100) and 4.0% (0.5 ± 1.0% at MOI 100) respectively. Furthermore, both constructs exhibited near complete loss of CAR expression after day 23 based on $CD3^+BAFF^+$ expression and after day 15 based on $CD3^+CD20^+$ expression. We tested high MOIs of 500 and 700, which produced higher CAR expression initially but similarly resulted in near complete loss of CAR expression by day 15 (Figure 1C). We also used retronectin with spinoculation to improve lentiviral transduction and while it initially exhibited higher CAR expression based on $CD3^+CD20^+$ expression, it also failed to produce stable BAFF CAR expression (Figure 1D).

To test whether loss of CAR expression was due to non-transduced T cells having a proliferative and/or survival advantage compared to BAFF-expressing CAR T cells, we sorted for $CD3^+CD20^+$ cells using fluorescence-activated cell sorting (FACS) at day 7 after lentiviral transduction at MOI 500 ($CD3^+CD20^+$ expression of 34% and 19% at time of FACS for full-length BAFF monomer and truncated BAFF monomer constructs respectively). However, after 2 weeks in culture, there was complete loss of CD20 expression (Figure 1E) with both full-length BAFF monomer and truncated BAFF monomer constructs.

6.4.2 Subcloning lentiviral BAFF CAR constructs onto a PiggyBac backbone

Since we could not generate stable BAFF CAR expression using a lentiviral vector, we subcloned both full-length BAFF monomer and truncated BAFF monomer constructs onto a PiggyBac backbone to utilise the PiggyBac transposon system, a non-viral gene delivery approach. We used unique restriction enzymes (FseI and SalI-HF) to isolate the CAR

constructs from both the lentiviral plasmids and PiggyBac transposon plasmid from their respective vector backbones, then ligated the full-length BAFF monomer and truncated BAFF monomer constructs separately onto a PiggyBac vector backbone. We confirmed successful ligation with diagnostic digest and Sanger sequencing using two primers for each construct (one primer for each ligation site). We performed diagnostic digest using two different restriction enzymes: 1. AseI, which cuts full-length BAFF monomer/PiggyBac and truncated BAFF monomer/PiggyBac plasmids at 3 sites, and PiggyBac backbone plasmid at 2 sites (Figure 2A) and 2. SacI-HF, which cuts full-length BAFF monomer/PiggyBac and truncated BAFF monomer/PiggyBac plasmids at 4 sites, and PiggyBac backbone plasmid at 3 sites (Figure 2B).

6.4.3 PiggyBac-based, non-viral gene delivery generated stable BAFF CAR expression

In addition to the full-length BAFF monomer/PiggyBac and truncated BAFF monomer/PiggyBac plasmids, we were provided with a truncated BAFF trimer PiggyBac transposon plasmid by Dr Kavitha Gowrishankar (Children's Cancer Research Unit, The Children's Hospital at Westmead). We evaluated BAFF CAR expression (full-length BAFF monomer, truncated BAFF monomer and truncated BAFF trimer) at day 8, 15, 22, and 29 after co-electroporation of BAFF CAR-encoding transposon plasmid and Piggybac transposase-encoding vector. Overall, PiggyBac-based gene delivery generated improved and more stable BAFF CAR expression in full-length BAFF monomer and truncated BAFF monomer constructs compared to lentiviral gene delivery based on $CD3^+BAFF^+$ expression (Figure 3A). However, there was lower $CD3^+CD20^+$ expression in both full-length BAFF monomer and truncated BAFF monomer constructs using PiggyBac-based gene delivery (Figure 3B). BAFF CAR expression in the truncated BAFF trimer construct was not significantly different to full-

length BAFF monomer and truncated BAFF monomer constructs. The highest $CD3^+BAFF^+$ expression in the full-length BAFF monomer, truncated BAFF monomer and truncated BAFF trimer constructs were 9.8% (mean 6.1 ± standard deviation (SD) 2.4%), 13.0% (mean 6.4 ± SD 3.1%) and 37.0% (mean 11.3 ± SD 8.2%) respectively. In comparison, the highest $CD3^+CD20^+$ expression in both full-length BAFF monomer and truncated BAFF monomer constructs using PiggyBac-based gene delivery were 4.0% (mean 1.4 ± SD 0.9%) and 5.9% (mean 2.3 ± SD 1.7%) respectively while the highest $CD3^+GFP^+$ expression for the truncated BAFF trimer construct was 82.0% (mean 49.6 ± SD 23.0%). Therefore, we successfully generated CAR T cells with stable BAFF expression, which we utilised for downstream assays detailed below.

6.4.4 BAFF-expressing CAR T cells specifically eliminated B cells *in vitro*

We evaluated the *in vitro* cytotoxicity of BAFF-expressing CAR T cells against Raji cells, a B cell lymphoma cell line known to express all three receptors for BAFF (BAFF-receptor, TACI and BCMA),[19, 20] and HEK293T cells, which do not express any of the three BAFF receptors.[21] Raji and HEK293T cells were fluorescently labelled with Calcein then co-cultured with CAR T cells or unmodified T cells at different concentrations. After 4 hours, BAFF-expressing CAR T cells exhibited significant cytotoxicity against Raji cells compared to unmodified T cells and in a dose-dependent manner (Figure 4A). Cytotoxicity was not significantly different between the constructs but cytotoxicity in all constructs reduced at an E:T cell concentration of 20:1 or lower. In comparison, full-length BAFF monomer displayed some cytotoxicity against HEK293T cells (Figure 4B) but truncated BAFF monomer and truncated BAFF trimer CAR T cells did not display significant cytotoxicity against HEK293T cells. Therefore, we demonstrated BAFF-expressing CAR T cells generated using the non-viral PiggyBac gene

delivery system was cytotoxic against B cells without significant cytotoxicity to a negative target cell line.

6.4.5 BAFF-expressing CAR T cells degranulate and release proinflammatory cytokines after co-culture with B cells

We co-cultured BAFF-expressing CAR T cells (full-length BAFF monomer, truncated BAFF monomer and truncated BAFF trimer) or unmodified T cells with Raji cells for 4 hours before characterising BAFF-expressing CAR T cells by flow cytometry. There was significantly higher expression of the degranulation marker CD107a with BAFF-expressing CAR T cells compared with unmodified T cells and BAFF-expressing CAR T cells alone (Figure 5A). We also found BAFF-expressing CAR T cells released more TNFα, IFNγ and IL2 compared to unmodified T cells (Figure 5B-D). There were no differences between the constructs regarding degranulation or cytokine release. When comparing BAFF-expressing CAR T cells co-cultured with Raji cells to BAFF-expressing CAR T cells alone, there was significantly increased release of TNFα, only truncated BAFF monomer CAR T cells released significantly more IL2 but there was no significantly increased release of IFNγ.

6.4.6 BAFF-expressing CAR T cells exhibited an effector phenotype and did not exhibit increased markers of T cell exhaustion

There was significant donor variability in the CD8/CD4 ratio and BAFF-expressing CAR T cells exhibited an effector memory T (Tem) phenotype ($CD62L^{-}CD45RA^{-}$) with a shift away from stem-like central memory T (Tscm) cells ($CD62L^{+}CD45RA^{+}CD95^{+}$) but no differences in central memory T (Tcm) cells ($CD62L^{+}CD45RA^{-}$), and terminally differentiated effector memory re-expressing CD45RA T (Temra) cells ($CD62L^{-}CD45RA^{+}$) compared to unmodified

T cells (Figure 6A). There was increased expression of programmed death 1 (PD1) in full-length BAFF monomer CAR T cells compared to unmodified cells but otherwise no significant difference in expression of other T cell exhaustion markers (Tim3 and Lag3) between BAFF T cells (full-length BAFF monomer, truncated BAFF monomer and truncated BAFF trimer) and unmodified T cells (Figure 6B-D).

6.5 Discussion

High levels of BAFF are crucial for the survival and maturation of autoreactive B cells that drive autoantibody-mediated diseases such as primary membranous nephropathy. Here, we demonstrated that BAFF-expressing CAR T cells can specifically eliminate a B cell line (Raji cells) with degranulation and release of pro-inflammatory cytokines such as TNFα, IFNγ and IL2 when exposed to B cells and without significant cytotoxicity against HEK293T cells which do not express the receptors for BAFF. BAFF-expressing CAR T cells overall do not display a significant increase in markers of exhaustion, which improves its likelihood of retaining effector function. We compared three BAFF CAR constructs (BAFF full-length monomer, BAFF truncated monomer, and BAFF truncated trimer), which demonstrated similar effector functions and cytokine release though there was a trend towards increased degranulation and pro-inflammatory cytokine release with the BAFF truncated trimer CAR construct compared to the two monomeric constructs. BAFF, like other TNF receptor-associated factors (TRAFs), is a trimeric ligand that binds linear TRAF-binding sequences on BAFF-R, TACI, and BCMA.[22] In contrast, the affinity of TRAFs for a monomeric receptor is low. Therefore, BAFF truncated trimer CAR T cells may bind better to its receptors and facilitate effector functions such as degranulation and cytokine release, compared to BAFF monomeric CAR T cells. There was significant variability in cytotoxicity against Raji cells for all three BAFF CAR constructs,

which is likely due to relatively low and variable transduction efficiency, thus influencing the amount of CAR T cells for each co-culture experiment.

While CAR T cell technology was developed for the treatment of B cell malignancies, the design principles are also applicable to non-malignant diseases such as autoimmune diseases, which are often driven by autoantibodies and autoreactive B cells. Clinical trials of CD19-targeting CAR T cells for relapsed or refractory B cell malignancies have demonstrated the potential for this technology to cure otherwise incurable disease,[23-25] in some cases achieving cancer remission for over a decade.[26] CD19-targeting CAR T cells was effective in the treatment of a murine model of lupus and early clinical studies in patients with refractory lupus and other autoimmune diseases have shown impressive efficacy.[15, 27-29] Many of these patients had already received B cell depleting monoclonal antibodies such as rituximab and the superiority of CAR T cells may be due to their ability to penetrate tissues to eliminate tissue-resident B cells, which can escape antibody-mediated targeting.[30] In primary membranous nephropathy, up to a 30% of patients will not respond to current immunosuppression, which carries a poor prognosis with 50% progressing to kidney failure within 8-10 years.[31] Therefore, CAR T cells targeting autoantibody-producing cells is an attractive treatment option for refractory or relapsed membranous nephropathy. We demonstrate BAFF-expressing CAR T cells have similar cytotoxicity against Raji B cells *in-vitro* compared to CD19-targeting CAR T cells.[32] BAFF-expressing CAR T cells also have theoretical advantages over CD19-targeting CAR T cells: 1. Immature B cells will not be targeted as they do not express any receptors for BAFF but do express CD19, which will limit the severity of B cell aplasia, and 2. Plasma cells, which correlate with disease activity in primary membranous nephropathy,[16] will be targeted as they express BCMA but not CD19. However, early clinical studies of CD19-targeting CAR T cells in autoimmune disease suggests B cell aplasia only lasts 2-6 months and plasma cells

not being targeted by CD19-targeting CAR T cells may be advantageous as antibody titres against vaccinations was maintained with only a mild decrease in total IgG levels.[15, 28] Further research will be required to evaluate the efficacy and safety of BAFF-expressing CAR T cells compared to CD19-targeting CAR T cells in different models of autoimmune disease such as primary membranous nephropathy.

In our study, we generated BAFF-expressing CAR T cells using the PiggyBac transposon non-viral gene delivery system. The PiggyBac system is derived from the cabbage looper moth *Trichoplusia ni* and is comprised of a PiggyBac element (transposon vector) that can be divided by a PiggyBac transposase enzyme to cut out a transgene (in our case the BAFF CAR construct) between the inverted terminal repeat sequences located on both ends of the transposon vector and efficiently integrate it into TTAA chromosomal sites of the target cell.[33, 34] An advantage of the PiggyBac system is its ability to deliver large transgenes (over 200 kb) compared to lentiviral gene delivery (limit of 10 kb),[35, 36] and the lentiviral plasmids of our BAFF full-length monomer and BAFF truncated monomer constructs were 9.7 kb and 9.5 kb respectively, which explains the improved BAFF CAR expression using PiggyBac gene delivery compared to lentiviral gene delivery. Both PiggyBac and lentiviral gene transfer insert the transgene randomly into the genome of the target cell, which carries the risk of insertional mutagenesis. Indeed, a phase I study of CD19-targeting CAR T cells produced using the PiggyBac system resulted in 2 of 10 participants developing CAR T cell lymphoma, which may be related to a high transgene copy number per cell of 24 in one participant.[37, 38] In comparison, secondary malignancies were reported in 536 of 12,394 (4.3%) adverse event reports following commercial CAR T cell therapy, which is predominantly delivered using lentiviral vectors, of which 22 were T cell malignancies.[39] In one case of T cell lymphoma following a BCMA-targeting CAR T cell infusion, CAR transgene integration was detected in

the Pre-B-cell leukemia transcription factor 2 *(PBX2)* gene but other potential driving mutations (Tet methylcytosine dioxygenase *(TET)-2*, nuclear factor-kappa-B *(NFKB)-2*, Protein Tyrosine Phosphatase Receptor Type B *(PTPRB)* and Janus Kinase *(JAK)-3*) were also found, some of which were present prior to CAR T cell treatment.[40] Overall, lentiviral gene delivery appears safer than the PiggyBac system, which is still a feasible system to evaluate the delivery and function of BAFF constructs *in vitro* and *in vivo*. While we demonstrated stable expression and function of BAFF-expressing CAR T cells using the PiggyBac system, safety concerns will likely limit its translation into the treatment of autoimmune diseases such as primary membranous nephropathy.

In contrast, we found that lentiviral transduction of either BAFF monomer full-length or BAFF monomer truncated CAR constructs did not yield stable or persistent expression. Lentiviral vectors are derived from human immunodeficiency virus (HIV)-1, which can stably integrate into the genome of T cells for up to 5 years and a failure of lentiviral vectors to cause stable integration has not been previously reported.[41] Rather, loss of gene expression after lentiviral, retroviral and murine leukaemia virus (MLV)-based gene delivery has been linked to epigenetic changes, specifically DNA hypermethylation at cytosine phosphate guanine (CpG) sites.[42-46] Differences in culture technique (type of media, and manual or automated production) did not alter DNA methylation.[42] Gene silencing due to DNA methylation was only partially reversed by using DNA methylation antagonists such as 5-azacytidine or histone deacetylase inhibitor trichostatin A,[43-45] though combining both medications was more effective.[46] Of more relevance is evidence that decitabine, an inhibitor of DNA methyltransferases (DNMT), or deletion of DNMT3A in T cells improved anti-tumour activity of CAR T cells in mice, which was associated with improved proliferation and pro-inflammatory cytokine release, decreased exhaustion, and maintained memory phenotype.[47-49] Culture-associated DNA methylation is

highly reproducible but does not display evidence of a targeted mechanism as methylation does not develop in an additive manner at neighbouring CpGs or at interacting chromatin domains, therefore suggesting stochastic epigenetic drift that mimics aging.[50-52] Reducing *in vitro* culture time during CAR T cell production may reduce CAR T cell dysfunction due to gene silencing from DNA methylation though at the cost of reduced CAR T cell expansion. How this impacts the efficacy of CAR T cells would be an important area for future research.

An alternative explanation for the low BAFF CAR expression using lentiviral gene delivery is due to toxicity of the BAFF CAR leading to a proliferative disadvantage compared to untransduced T cells,[53] or the mutations we introduced the BAFF molecule resulted in protein misfolding and subsequent degradation in the proteasome.[54] The near complete loss of BAFF CAR expression after 2 weeks of culture post-FACS sorting, which should eliminate the presence of untransduced T cells, suggests our BAFF CAR constructs do not simply confer a proliferative disadvantage. The mutations we introduced into our BAFF CARs (H218A/E223K with or without K132A/R133A) were previously reported in studies evaluating mutated BAFF molecules in HEK293T cells and downstream assays were performed using cell culture supernatant containing soluble BAFF cleaved off the cell membrane.[17, 18] While a previous study by Wong et al has also generated BAFF-expressing CAR T cells with good expression of around 40% with both lentiviral and non-viral gene delivery, details of the BAFF construct were not reported apart from it being a truncated BAFF sequence that encompassed the majority of the extracellular domain of the human BAFF molecule with no mention of additional mutations.[21] Therefore, it is possible the mutations we introduced into our BAFF CAR constructs caused protein misfolding and toxicity specifically in T cells. This explanation would also affect BAFF CAR expression using the PiggyBac transposon system, which resulted in relatively stable BAFF CAR expression over 4 weeks though in the BAFF truncated

trimer, BAFF CAR expression was markedly lower than GFP expression despite expression of both being controlled by the same promoter. The CD20 safety switch in our BAFF full-length monomer and BAFF truncated monomer constructs should not confer T cell toxicity as CD20 has been expressed in T cells using a retroviral vector previously with no signs of toxicity over 3 weeks of culture.[55] Overall, our results suggest the mutated BAFF CAR constructs may confer some toxicity to T cells limiting their expression, but additional factors present in our lentiviral experiments and not in our PiggyBac transposon experiments, resulted in near complete loss of BAFF CAR expression over time, which may be related to either the lentiviral plasmid or lentivirus itself. In our PiggyBac transposon experiments, CD20 expression was significantly lower than monomeric BAFF CAR expression, which may be due to a lack of codon optimisation of the CD20 sequence, which has been shown to improve expression in T cells.[56]

Our findings are consistent with existing literature where BAFF-expressing CAR T cells have been generated by Wong et al. who demonstrated its cytotoxicity against multiple B cell cancer lines but not against negative cell lines including HEK293T cells.[21] Memory and exhaustion phenotypes were not reported but Wong et al. showed the efficacy of BAFF-expressing CAR T cells in multiple *in vivo* models of B cell malignancy.[21] Limitations of our study include a lack of cytotoxicity data in other target cell lines with differing expression of BAFF's three cognate receptors (eg. THP-1 cells express BAFF-R with no TACI or BCMA and MM1.R cells express BCMA but low levels of BAFF-R and TACI)[19, 20] as well as other negative cell lines, lack of integration site analysis to assess the risk of insertional mutagenesis, and lack of evaluation of its efficacy and safety *in vivo* in models of autoimmune kidney disease such as Heymann nephritis. While our BAFF CAR construct is fully humanised, we still expect

efficacy in murine models of autoimmunity since the receptor binding domains in human and mouse BAFF have 93% homology.[57]

In conclusion, we generated three different BAFF-expressing CAR T cells using the non-viral PiggyBac gene delivery system, which demonstrated efficacy in specifically killing B cells *in vitro* while not showing significant T cell exhaustion. Further evaluation of BAFF-expressing CAR T cells in models of autoantibody-mediated autoimmune kidney diseases such as Heymann nephritis will be of great interest, which if effective and safe, may facilitate their use in refractory or relapsed primary membranous nephropathy.

6.6 References

1. Beck LH, Jr., Bonegio RG, Lambeau G, et al. M-type phospholipase A2 receptor as target antigen in idiopathic membranous nephropathy. N Engl J Med. 2009;361(1):11-21.

2. Nemazee D. Mechanisms of central tolerance for B cells. Nat Rev Immunol. 2017;17(5):281-94.

3. Lesley R, Xu Y, Kalled SL, et al. Reduced competitiveness of autoantigen-engaged B cells due to increased dependence on BAFF. Immunity. 2004;20(4):441-53.

4. Thien M, Phan TG, Gardam S, et al. Excess BAFF rescues self-reactive B cells from peripheral deletion and allows them to enter forbidden follicular and marginal zone niches. Immunity. 2004;20(6):785-98.

5. Cambier JC, Gauld SB, Merrell KT, et al. B-cell anergy: from transgenic models to naturally occurring anergic B cells? Nat Rev Immunol. 2007;7(8):633-43.

6. Stohl W, Xu D, Kim KS, et al. BAFF overexpression and accelerated glomerular disease in mice with an incomplete genetic predisposition to systemic lupus erythematosus. Arthritis Rheum. 2005;52(7):2080-91.

7. Mackay F, Woodcock SA, Lawton P, et al. Mice transgenic for BAFF develop lymphocytic disorders along with autoimmune manifestations. J Exp Med. 1999;190(11):1697-710.

8. Steri M, Orrù V, Idda ML, et al. Overexpression of the Cytokine BAFF and Autoimmunity Risk. N Engl J Med. 2017;376(17):1615-26.

9. Netti GS, Infante B, Spadaccino F, et al. Serum Levels of BAFF and APRIL Predict Clinical Response in Anti-PLA2R-Positive Primary Membranous Nephropathy. J Immunol Res. 2019;2019:8483650.

10. Petri M, Stohl W, Chatham W, et al. Association of plasma B lymphocyte stimulator levels and disease activity in systemic lupus erythematosus. Arthritis Rheum. 2008;58(8):2453-9.

11. Wallace DJ, Stohl W, Furie RA, et al. A phase II, randomized, double-blind, placebo-controlled, dose-ranging study of belimumab in patients with active systemic lupus erythematosus. Arthritis Rheum. 2009;61(9):1168-78.

12. Furie R, Rovin BH, Houssiau F, et al. Two-Year, Randomized, Controlled Trial of Belimumab in Lupus Nephritis. N Engl J Med. 2020;383(12):1117-28.

13. Avery DT, Kalled SL, Ellyard JI, et al. BAFF selectively enhances the survival of plasmablasts generated from human memory B cells. J Clin Invest. 2003;112(2):286-97.

14. Belnoue E, Pihlgren M, McGaha TL, et al. APRIL is critical for plasmablast survival in the bone marrow and poorly expressed by early-life bone marrow stromal cells. Blood. 2008;111(5):2755-64.

15. Müller F, Taubmann J, Bucci L, et al. CD19 CAR T-Cell Therapy in Autoimmune Disease - A Case Series with Follow-up. N Engl J Med. 2024;390(8):687-700.

16. Cantarelli C, Jarque M, Angeletti A, et al. A Comprehensive Phenotypic and Functional Immune Analysis Unravels Circulating Anti-Phospholipase A2 Receptor Antibody Secreting Cells in Membranous Nephropathy Patients. Kidney Int Rep. 2020;5(10):1764-76.

17. Nardelli B, Belvedere O, Roschke V, et al. Synthesis and release of B-lymphocyte stimulator from myeloid cells. Blood. 2001;97(1):198-204.

18. Vigolo M, Chambers MG, Willen L, et al. A loop region of BAFF controls B cell survival and regulates recognition by different inhibitors. Nat Commun. 2018;9(1):1199.

19. Lyu MA, Cheung LH, Hittelman WN, et al. The rGel/BLyS fusion toxin specifically targets malignant B cells expressing the BLyS receptors BAFF-R, TACI, and BCMA. Mol Cancer Ther. 2007;6(2):460-70.

20. Zhang L, Jiang Y, Zheng Y, et al. Selective killing of Burkitt's lymphoma cells by mBAFF-targeted delivery of PinX1. Leukemia. 2011;25(2):331-40.

21. Wong DP, Roy NK, Zhang K, et al. A BAFF ligand-based CAR-T cell targeting three receptors and multiple B cell cancers. Nat Commun. 2022;13(1):217.

22. Mackay F, Schneider P. Cracking the BAFF code. Nat Rev Immunol. 2009;9(7):491-502.

23. Grupp SA, Kalos M, Barrett D, et al. Chimeric antigen receptor-modified T cells for acute lymphoid leukemia. N Engl J Med. 2013;368(16):1509-18.

24. Kalos M, Levine BL, Porter DL, et al. T cells with chimeric antigen receptors have potent antitumor effects and can establish memory in patients with advanced leukemia. Sci Transl Med. 2011;3(95):95ra73.

25. Porter DL, Levine BL, Kalos M, et al. Chimeric antigen receptor-modified T cells in chronic lymphoid leukemia. N Engl J Med. 2011;365(8):725-33.

26. Melenhorst JJ, Chen GM, Wang M, et al. Decade-long leukaemia remissions with persistence of CD4(+) CAR T cells. Nature. 2022;602(7897):503-9.

27. Kansal R, Richardson N, Neeli I, et al. Sustained B cell depletion by CD19-targeted CAR T cells is a highly effective treatment for murine lupus. Sci Transl Med. 2019;11(482).

28. Mackensen A, Müller F, Mougiakakos D, et al. Anti-CD19 CAR T cell therapy for refractory systemic lupus erythematosus. Nat Med. 2022;28(10):2124-32.

29. Mougiakakos D, Krönke G, Völkl S, et al. CD19-Targeted CAR T Cells in Refractory Systemic Lupus Erythematosus. N Engl J Med. 2021;385(6):567-9.

30. Anolik JH, Barnard J, Owen T, et al. Delayed memory B cell recovery in peripheral blood and lymphoid tissue in systemic lupus erythematosus after B cell depletion therapy. Arthritis Rheum. 2007;56(9):3044-56.

31. Troyanov S, Wall CA, Miller JA, et al. Idiopathic membranous nephropathy: definition and relevance of a partial remission. Kidney Int. 2004;66(3):1199-205.

32. Maschan M, Caimi PF, Reese-Koc J, et al. Multiple site place-of-care manufactured anti-CD19 CAR-T cells induce high remission rates in B-cell malignancy patients. Nat Comm. 2021;12(1):7200

33. Fraser MJ, Ciszczon T, Elick T, et al. Precise excision of TTAA-specific lepidopteran transposons piggyBac (IFP2) and tagalong (TFP3) from the baculovirus genome in cell lines from two species of Lepidoptera. Insect Mol Biol. 1996;5(2):141-51.

34. Wilson MH, Coates CJ, George AL, Jr. PiggyBac transposon-mediated gene transfer in human cells. Mol Ther. 2007;15(1):139-45.

35. Woodard LE, Wilson MH. piggyBac-ing models and new therapeutic strategies. Trends Biotechnol. 2015;33(9):525-33.

36. Larson RC, Maus MV. Recent advances and discoveries in the mechanisms and functions of CAR T cells. Nat Rev Cancer. 2021;21(3):145-61.

37. Bishop DC, Clancy LE, Simms R, et al. Development of CAR T-cell lymphoma in 2 of 10 patients effectively treated with piggyBac-modified CD19 CAR T cells. Blood. 2021;138(16):1504-9.

38. Micklethwaite KP, Gowrishankar K, Gloss BS, et al. Investigation of product-derived lymphoma following infusion of piggyBac-modified CD19 chimeric antigen receptor T cells. Blood. 2021;138(16):1391-405.

39. Elsallab M, Ellithi M, Lunning MA, et al. Second primary malignancies after commercial CAR T-cell therapy: analysis of the FDA Adverse Events Reporting System. Blood. 2024;143(20):2099-105.

40. Harrison SJ, Nguyen T, Rahman M, et al. CAR+ T-Cell Lymphoma Post Ciltacabtagene Autoleucel Therapy for Relapsed Refractory Multiple Myeloma. Blood. 2023;142:6939.

41. Mok HP, Javed S, Lever A. Stable gene expression occurs from a minority of integrated HIV-1-based vectors: transcriptional silencing is present in the majority. Gene Ther. 2007;14(9):741-51.

42. Salz L, Seitz A, Schäfer D, et al. Culture expansion of CAR T cells results in aberrant DNA methylation that is associated with adverse clinical outcome. Leukemia. 2023;37(9):1868-78.

43. Kuriyama S, Sakamoto T, Kikukawa M, et al. Expression of a retrovirally transduced gene under control of an internal housekeeping gene promoter does not persist due to methylation and is restored partially by 5-azacytidine treatment. Gene Ther. 1998;5(10):1299-305.

44. McInerney JM, Nawrocki JR, Lowrey CH. Long-term silencing of retroviral vectors is resistant to reversal by trichostatin A and 5-azacytidine. Gene Ther. 2000;7(8):653-63.

45. Zentilin L, Qin G, Tafuro S, et al. Variegation of retroviral vector gene expression in myeloid cells. Gene Ther. 2000;7(2):153-66.

46. Lorincz MC, Schübeler D, Goeke SC, et al. Dynamic analysis of proviral induction and De Novo methylation: implications for a histone deacetylase-independent, methylation density-dependent mechanism of transcriptional repression. Mol Cell Biol. 2000;20(3):842-50.

47. Wang Y, Tong C, Dai H, et al. Low-dose decitabine priming endows CAR T cells with enhanced and persistent antitumour potential via epigenetic reprogramming. Nat Commun. 2021;12(1):409.

48. You L, Han Q, Zhu L, et al. Decitabine-Mediated Epigenetic Reprograming Enhances Anti-leukemia Efficacy of CD123-Targeted Chimeric Antigen Receptor T-Cells. Front Immunol. 2020;11:1787.

49. Prinzing B, Zebley CC, Petersen CT, et al. Deleting DNMT3A in CAR T cells prevents exhaustion and enhances antitumor activity. Sci Transl Med. 2021;13(620):eabh0272.

50. Franzen J, Georgomanolis T, Selich A, et al. DNA methylation changes during long-term in vitro cell culture are caused by epigenetic drift. Commun Biol. 2021;4(1):598.

51. Teschendorff AE, West J, Beck S. Age-associated epigenetic drift: implications, and a case of epigenetic thrift? Hum Mol Genet. 2013;22(R1):R7-r15.

52. Hernando-Herraez I, Evano B, Stubbs T, et al. Ageing affects DNA methylation drift and transcriptional cell-to-cell variability in mouse muscle stem cells. Nat Commun. 2019;10(1):4361.

53. Rosano GL, Ceccarelli EA. Recombinant protein expression in Escherichia coli: advances and challenges. Front Microbiol. 2014;5:172.

54. Goldberg AL. Protein degradation and protection against misfolded or damaged proteins. Nature. 2003;426(6968):895-9.

55. Introna M, Barbui AM, Bambacioni F, et al. Genetic modification of human T cells with CD20: a strategy to purify and lyse transduced cells with anti-CD20 antibodies. Hum Gene Ther. 2000;11(4):611-20.

56. Vogler I, Newrzela S, Hartmann S, et al. An improved bicistronic CD20/tCD34 vector for efficient purification and in vivo depletion of gene-modified T cells for adoptive immunotherapy. Mol Ther. 2010;18(7):1330-8.

57. Schneider P, MacKay F, Steiner V, et al. BAFF, a novel ligand of the tumor necrosis factor family, stimulates B cell growth. J Exp Med. 1999;189(11):1747-56.

6.7 Table and Figures

Table 1. Flow cytometry antibodies

Marker	Fluorochrome	Detector	Clone	Product code	Dilution
CD3	BV510	V525_50E	OKT3	Biolegend 317331	1:100
CD4	AF700	R730_45B	SK3	Biolegend 344621	1:50
CD8	APC-Cy7	R780_60A	SK1	Biolegend 344713	1:50
BAFF	PE	Y586_15D	T7-241	Biolegend 318606	1:50
CD107a	FITC	B530_30B	H4A3	Biolegend 328606	1:20
CD107a	BV785	V780_60A	H4A3	Biolegend 328643	1:20
IFNγ	PE-Cy7	Y780_60A	4S.B3	Biolegend 502527	1:20
TNFα	APC	R670_14C	Mab11	Biolegend 502913	1:100
IL2	BV421	V440_40F	MQ1-17H12	Biolegend 500327	1:20
CD45RA	APC	R670_14C	HI100	Biolegend 304111	1:50
CD62L	PE-Cy7	Y780_60A	DREG-56	Biolegend 304821	1:50
CD95	PE-Dazzle	Y610_20C	DX2	Biolegend 305633	1:50
PD1	BV421	V440_40F	EH12.2H7	Biolegend 329919	1:50
Tim3	BV785	V780_60A	F38-2E2	Biolegend 345031	1:50
Lag3	PerCP-Cy5.5	B710_50A	11C3C65	Biolegend 369311	1:50
Live/Dead Fixable Aqua Dead Cell Stain Kit	LIVE/DEAD™ Fixable Aqua	U515_30B	N/A	Thermofisher L34965	1:400

Figure 1

A

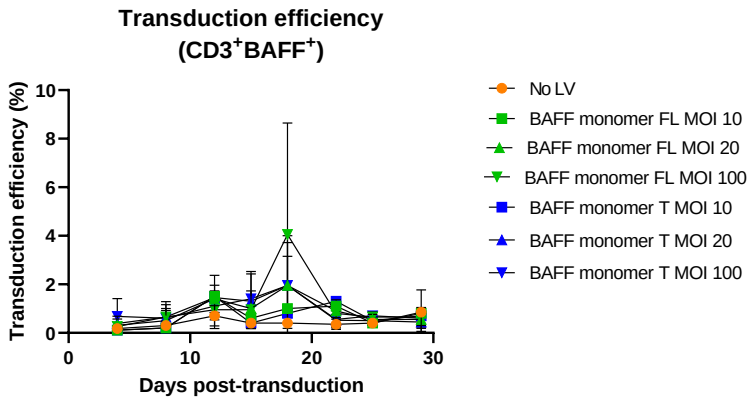

B

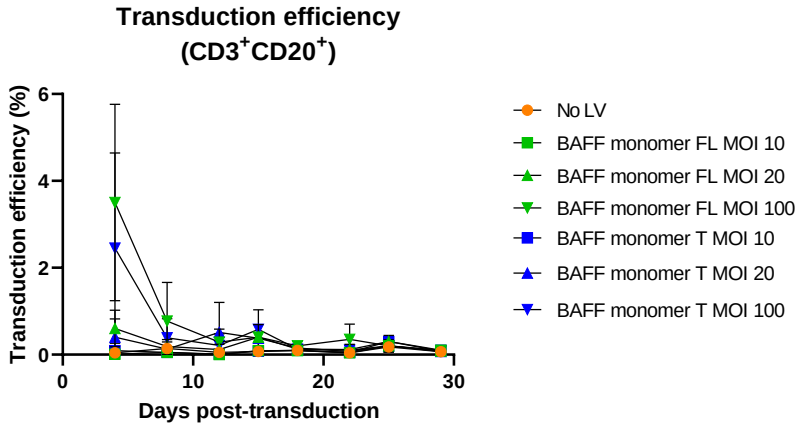

C

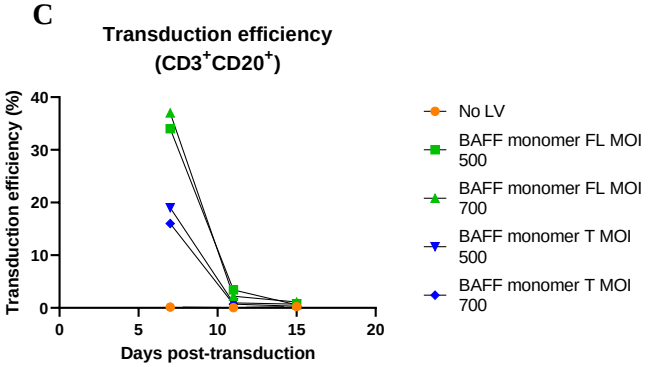

D

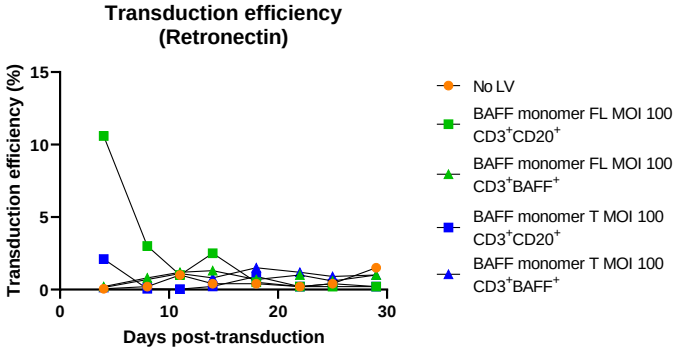

E

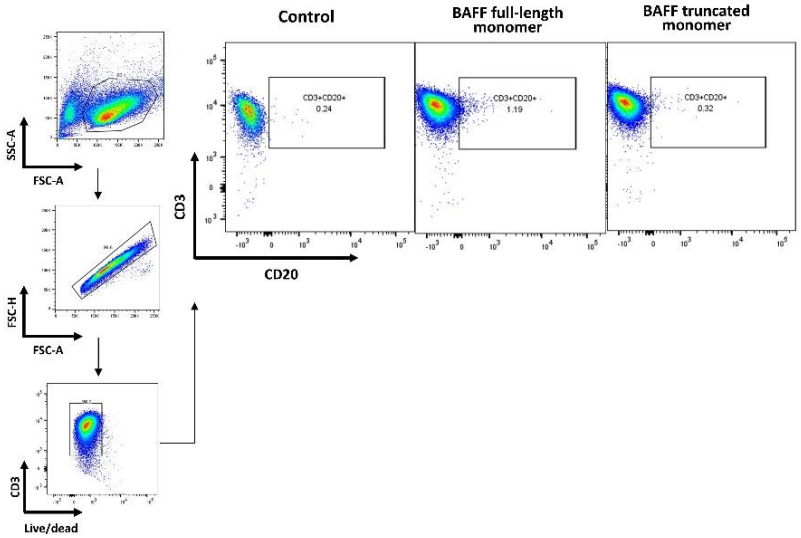

Figure 2

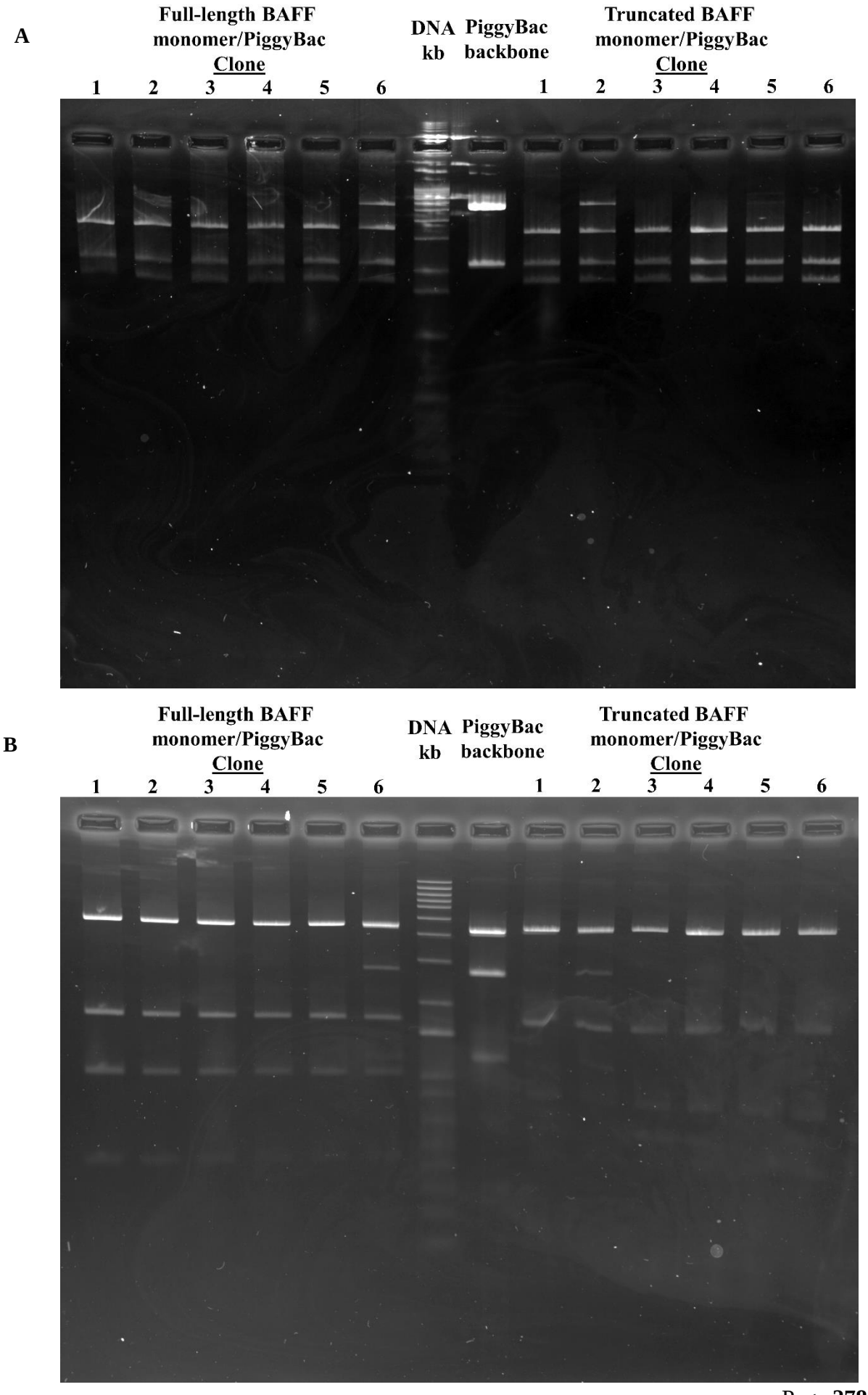
A
Full-length BAFF monomer/PiggyBac
Clone
1 2 3 4 5 6
DNA kb
PiggyBac backbone
1
Truncated BAFF monomer/PiggyBac
Clone
2 3 4 5 6
B
Full-length BAFF monomer/PiggyBac
Clone
1 2 3 4 5 6
DNA kb
PiggyBac backbone
1
Truncated BAFF monomer/PiggyBac
Clone
2 3 4 5 6

Figure 3

A

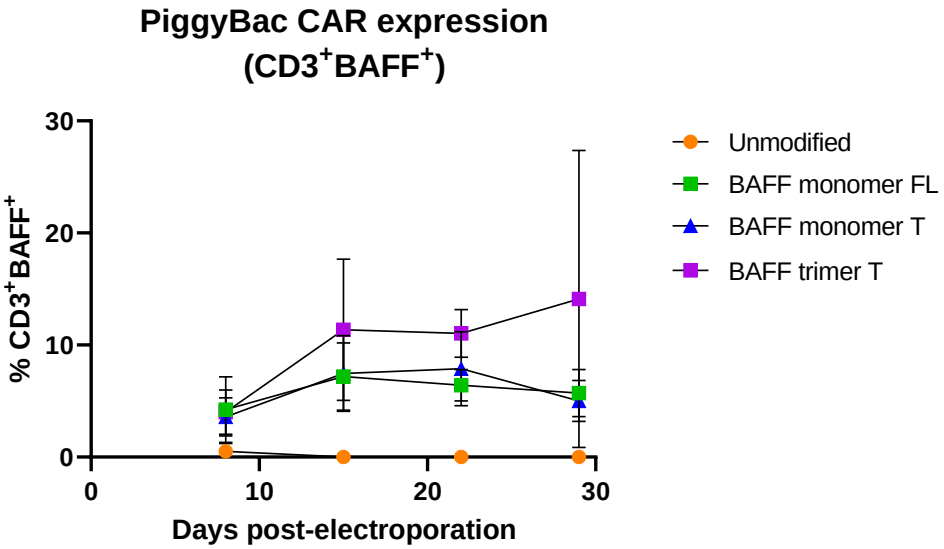
PiggyBac CAR expression
(CD3+BAFF+)
% CD3+BAFF+
30
20
10
0
0
10
20
30
Days post-electroporation
Unmodified
BAFF monomer FL
BAFF monomer T
BAFF trimer T

B

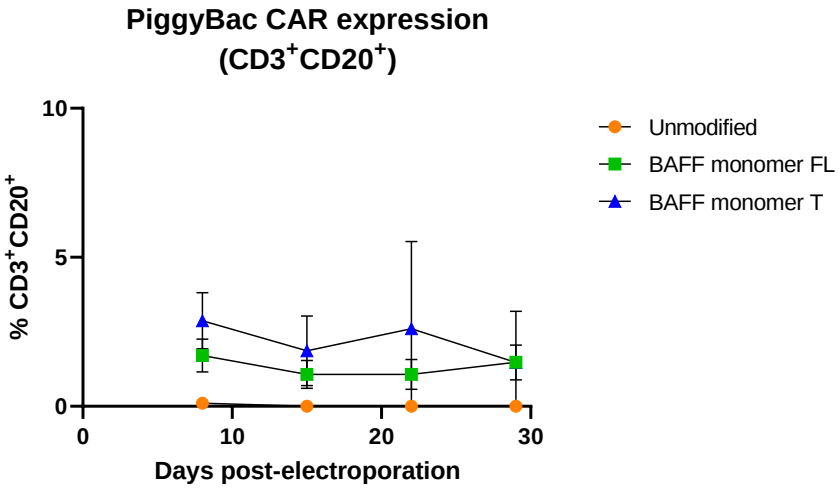
PiggyBac CAR expression
(CD3+CD20+)
% CD3+CD20+
10
5
0
0
10
20
30
Days post-electroporation
Unmodified
BAFF monomer FL
BAFF monomer T

Figure 4

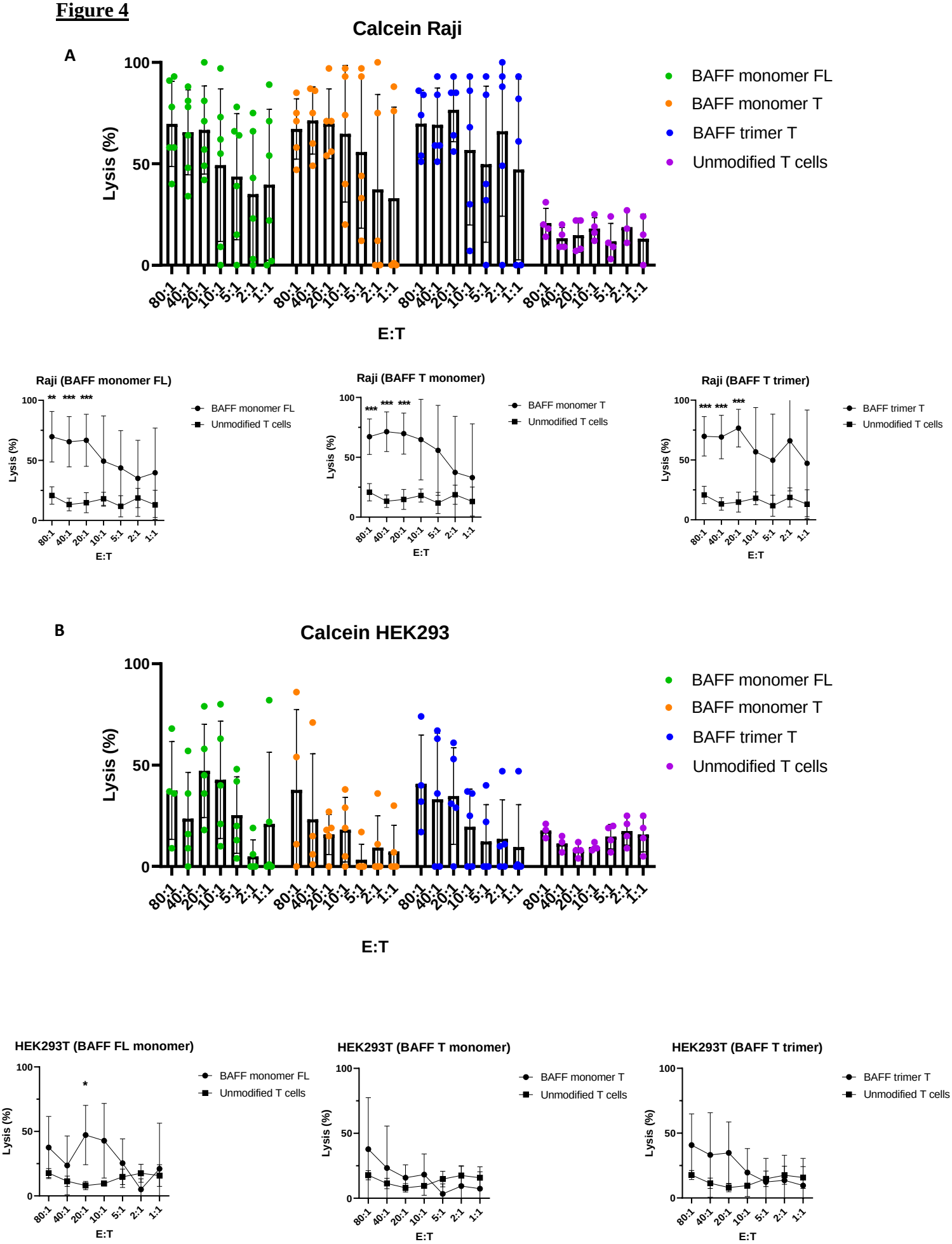
A
Calcein Raji
Lysis (%)
E:T
BAFF monomer FL
BAFF monomer T
BAFF trimer T
Unmodified T cells
Raji (BAFF monomer FL)
Raji (BAFF T monomer)
Raji (BAFF T trimer)
B
Calcein HEK293
HEK293T (BAFF FL monomer)
HEK293T (BAFF T monomer)
HEK293T (BAFF T trimer)

Figure 5

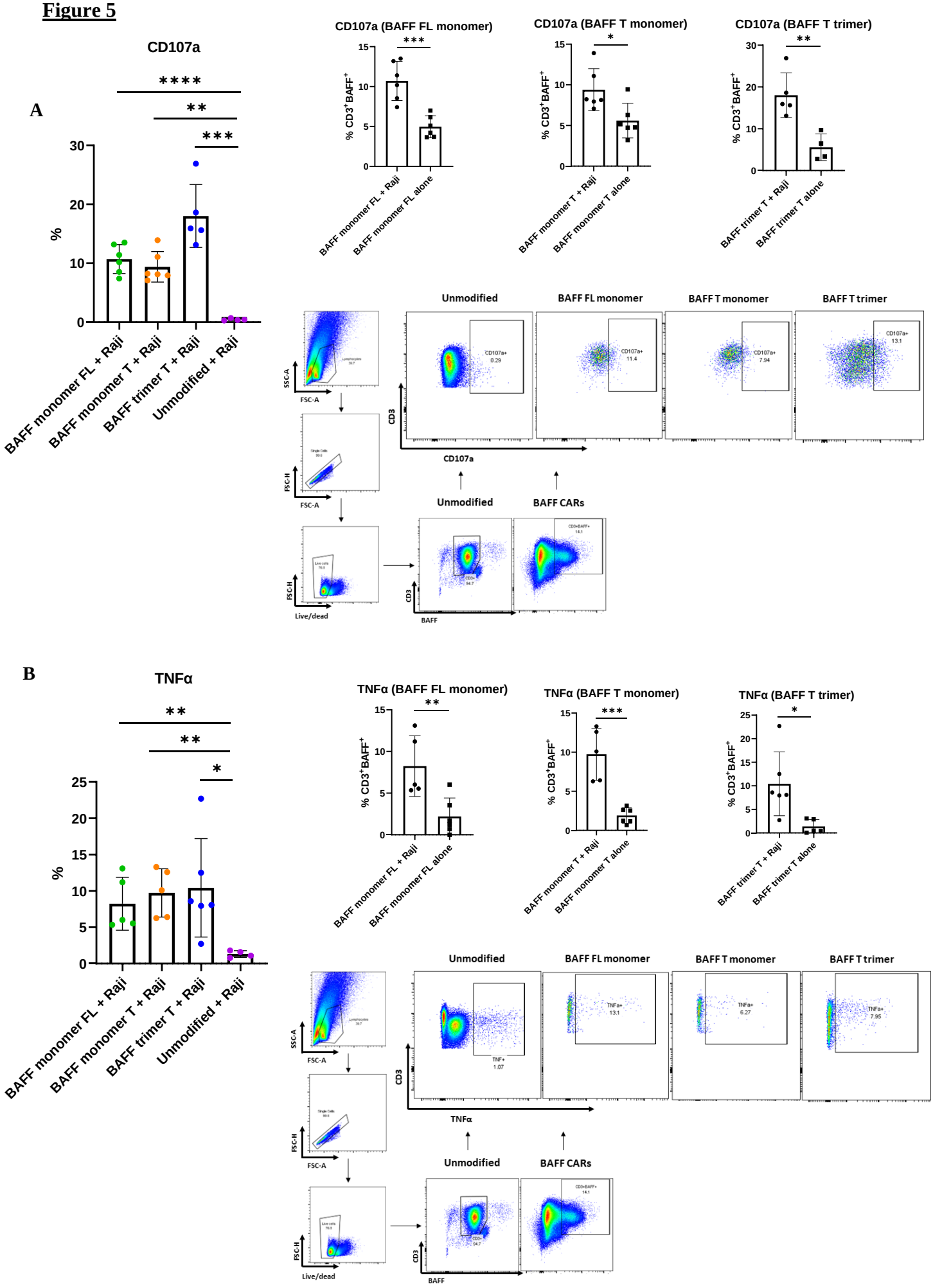
A
CD107a
%
BAFF monomer FL + Raji
BAFF monomer T + Raji
BAFF trimer T + Raji
Unmodified + Raji
CD107a (BAFF FL monomer)
CD107a (BAFF T monomer)
CD107a (BAFF T trimer)
% CD3+BAFF+
BAFF monomer FL alone
BAFF monomer T alone
BAFF trimer T alone
Unmodified
BAFF FL monomer
BAFF T monomer
BAFF T trimer
SSC-A
FSC-A
FSC-H
Live/dead
CD3
CD107a
BAFF CARs
BAFF
B
TNFα
TNFα (BAFF FL monomer)
TNFα (BAFF T monomer)
TNFα (BAFF T trimer)

Figure 5

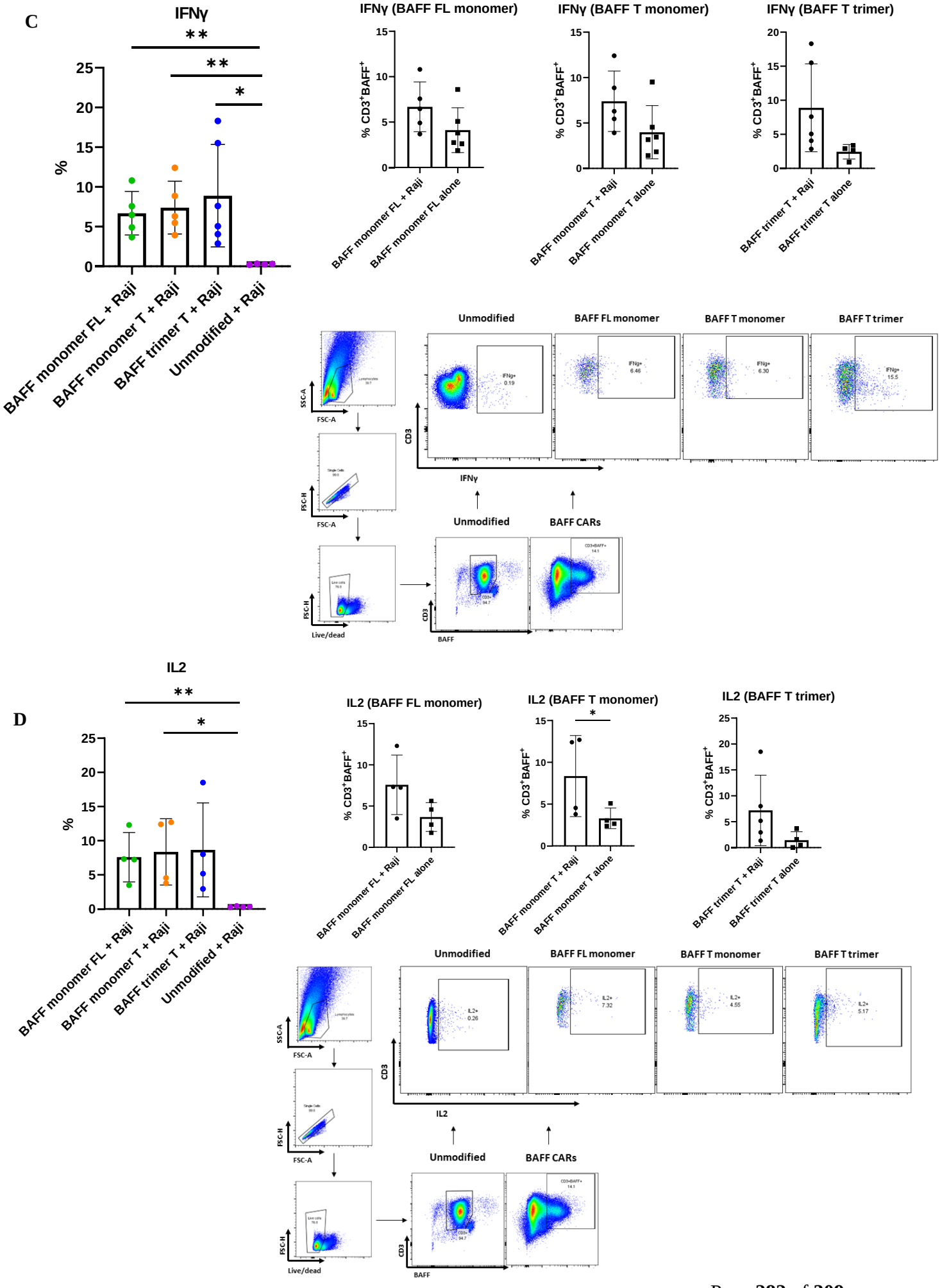
C
IFNγ
%
BAFF monomer FL + Raji
BAFF monomer T + Raji
BAFF trimer T + Raji
Unmodified + Raji
IFNγ (BAFF FL monomer)
IFNγ (BAFF T monomer)
IFNγ (BAFF T trimer)
% CD3+BAFF+
BAFF monomer FL + Raji
BAFF monomer FL alone
BAFF monomer T + Raji
BAFF monomer T alone
BAFF trimer T + Raji
BAFF trimer T alone
Unmodified
BAFF FL monomer
BAFF T monomer
BAFF T trimer
SSC-A
FSC-A
FSC-H
Live/dead
CD3
IFNγ
BAFF
BAFF CARs
D
IL2
IL2 (BAFF FL monomer)
IL2 (BAFF T monomer)
IL2 (BAFF T trimer)

Figure 6

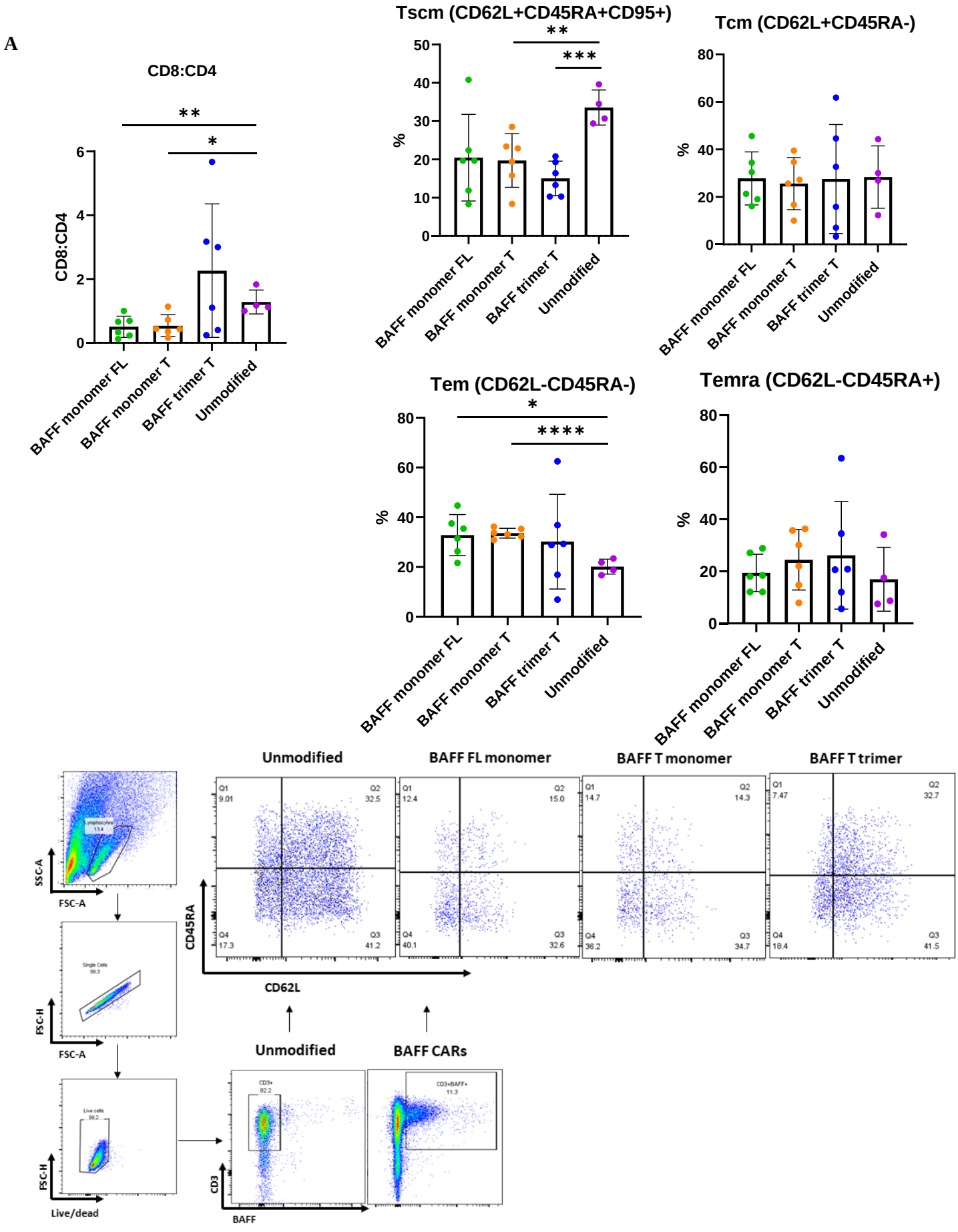
A
CD8:CD4
CD8:CD4
BAFF monomer FL
BAFF monomer T
BAFF trimer T
Unmodified
Tscm (CD62L+CD45RA+CD95+)
Tcm (CD62L+CD45RA-)
Tem (CD62L-CD45RA-)
Temra (CD62L-CD45RA+)
%
Unmodified
BAFF FL monomer
BAFF T monomer
BAFF T trimer
SSC-A
FSC-A
FSC-H
Live/dead
CD45RA
CD62L
BAFF CARs
CD3
BAFF

Figure 6

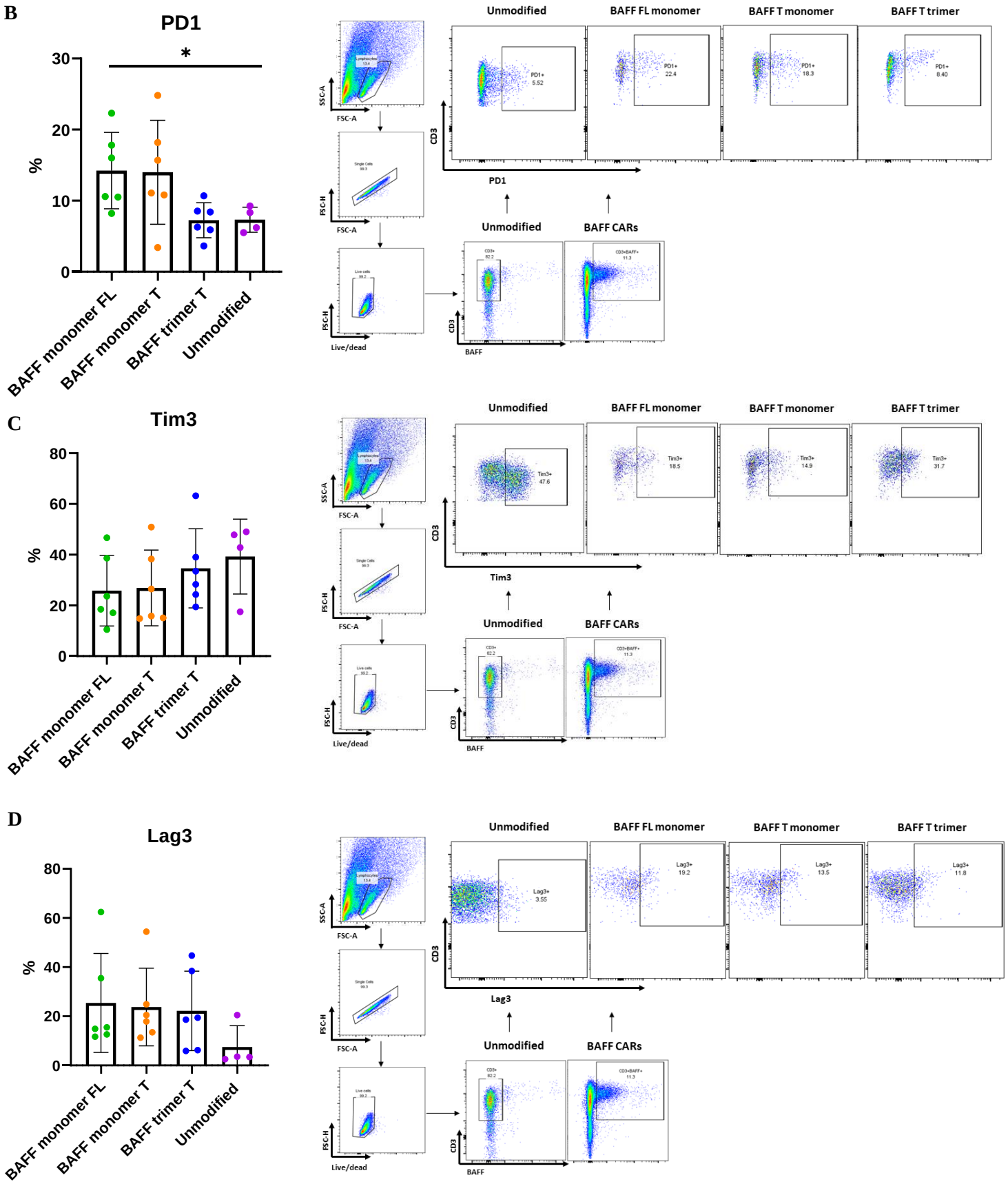
B
PD1
*
30
20
10
0
%
BAFF monomer FL
BAFF monomer T
BAFF trimer T
Unmodified
Unmodified
BAFF FL monomer
BAFF T monomer
BAFF T trimer
SSC-A
FSC-A
FSC-H
Live/dead
CD3
PD1
PD1+ 5.52
PD1+ 22.4
PD1+ 18.3
PD1+ 8.40
Unmodified
BAFF CARs
BAFF
C
Tim3
80
60
40
20
0
%
Tim3
Tim3+ 47.6
Tim3+ 18.5
Tim3+ 14.9
Tim3+ 31.7
D
Lag3
Lag3
Lag3+ 3.55
Lag3+ 19.2
Lag3+ 13.5
Lag3+ 11.8

Figure legends

Figure 1. Lentiviral gene delivery failed to generate stable expression of BAFF CAR constructs. Transduction efficiency by $CD3^+BAFF^+$ expression (**A**) and $CD3^+CD20^+$ expression (**B**) was transient across both BAFF full-length (FL) monomer and truncated (T) monomer constructs at different lentivirus (LV) multiplicity of infection (MOI) (n=3), including very high MOIs of 500 and 700 (**C**) (n=1). Retronectin and spinoculation to improve lentiviral transduction efficiency was also unable to generate stable BAFF CAR expression (**D**) (n=1). We sorted for $CD3^+CD20^+$ cells using fluorescence-activated cell sorting (FACS) at day 7 after lentiviral transduction at MOI 500 ($CD3^+CD20^+$ expression of 34% and 19% at time of FACS for BAFF monomer FL and BAFF monomer T constructs respectively) but after 2 weeks of culture, $CD3^+CD20^+$ expression dropped to 1.2% and 0.3% respectively (**E**) (n=1).

Figure 2. Diagnostic digest confirming successful subcloning of full-length BAFF monomer and truncated BAFF monomer CAR constructs into a PiggyBac vector backbone. Diagnostic digest was performed after subcloning procedure using two different restriction enzymes: 1. AseI, which cuts full-length BAFF monomer/PiggyBac and truncated BAFF monomer/PiggyBac plasmids at 3 sites, and PiggyBac backbone plasmid at 2 sites (**A**) and 2. SacI-HF, which cuts full-length BAFF monomer/PiggyBac and truncated BAFF monomer/PiggyBac plasmids at 4 sites, and PiggyBac backbone plasmid at 3 sites (**B**). Subcloning was unsuccessful in clone 6 for full-length BAFF monomer/PiggyBac and clone 2 for truncated BAFF monomer/PiggyBac. The remaining clones were confirmed to be correct by Sanger sequencing.

Figure 3. PiggyBac transposon gene delivery generated stable expression of BAFF CAR constructs. Compared to lentiviral gene delivery, the PiggyBac transposon system generated relatively stable BAFF CAR T cells based on $CD3^+BAFF^+$ expression (**A**) (n=5) and

$CD3^+CD20^+$ expression (**B**) (n=5), though expression of CD20 was low compared to expression of BAFF.

Figure 4. BAFF-expressing CAR T cells exhibited cytotoxicity against B cells with less cytotoxicity against HEK293 T cells. Using the Calcein assay, all three BAFF CAR constructs (BAFF monomer full-length (FL), BAFF monomer truncated (T) and BAFF trimer truncated) displayed cytotoxicity against Raji B cells after 4 hours of incubation (**A**), particularly at effector:target (E:T) concentrations of 80:1, 40:1 and 20:1 (n=4-5, *** $p<0.001$, ** $p<0.01$). BAFF-expressing CAR T cells did not display significant cytotoxicity against HEK293T cells (a negative cell line) after 4 hours of incubation apart from BAFF monomer full-length CAR T cells at an E:T concentration of 20:1 (**B**) (n=5, * $p<0.05$).

Figure 5. BAFF-expressing CAR T cells degranulate and release pro-inflammatory cytokines were exposed to B cells. BAFF-expressing CAR T cells (BAFF full-length (FL) monomer, BAFF truncated (T) monomer and BAFF truncated trimer) were co-cultured with Raji B cells at an E:T concentration of 5:1 for 4 hours then analysed by flow cytometry. Representative flow cytometry for each panel was gated on live $CD3^+$ cells for unmodified T cells and live $CD3^+BAFF^+$ cells for BAFF-expressing CAR T cells. There was a significantly higher expression of the degranulation marker CD107a (**A**) and pro-inflammatory cytokines tumour necrosis factor (TNF)-α (**B**), interferon (IFN)-γ (**C**), and interleukin (IL)-2 (**D**) in BAFF-expressing CAR T cells compared to unmodified T cells and higher expression of CD107a and TNF-α between BAFF-expressing CAR T cells cultured with Raji B cells compared to BAFF-expressing CAR T cells alone (n=4-6, **** $p<0.0001$, *** $p<0.001$, ** $p<0.01$, * $p<0.05$). While there was a trend towards increased IFN-γ and IL-2 expression in BAFF-expressing CAR T cells co-cultured with Raji B cells compared to BAFF-expressing CAR T cells alone, this was only significant for IL-2 expression in BAFF truncated monomer CAR T cells (n=4, * $p<0.05$).

Figure 6. There was lower CD8:CD4 ratio and an effector phenotype in BAFF full-length and truncated monomer CAR T cells, which overall did not exhibit increased markers of T cell exhaustion. Representative flow cytometry for each panel was gated on live $CD3^+$ cells for unmodified T cells and live $CD3^+BAFF^+$ cells for BAFF-expressing CAR T cells. The ratio of CD8 to CD4 T cells and stem-like central memory T (Tscm) cells ($CD62L^+CD45RA^+CD95^+$) were significantly lower in BAFF full-length and truncated monomer CAR T cells with an associated increase in effector memory T (Tem) cells ($CD62L^-CD45RA^-$) compared to unmodified T cells with no significant difference in other memory T cell subsets such as central memory T (Tcm) cells ($CD62L^+CD45RA^-$) and terminally differentiated effector memory re-expressing CD45RA T (Temra) cells ($CD62L^-CD45RA^+$) (**A**) (n=4-6, **** $p<0.0001$, ** $p<0.01$, * $p<0.05$). In contrast, there was significant donor variability in CD8:CD4 ratio and memory phenotype in BAFF truncated trimer CAR T cells though Tscm cells were also significantly reduced compared to unmodified T cells (n=4-6, *** $p<0.001$). There was significantly increased expression of the T cell exhaustion marker programmed death (PD)-1 in BAFF full-length monomer CAR T cells compared to unmodified T cells (n=4-6, * $p<0.05$) (**B**), but otherwise there was no significant difference in PD-1 or other markers of T-cell exhaustion (T cell immunoglobulin and mucin domain-containing protein (Tim)-3 (**C**), lymphocyte activation gene (LAG)-3 (**D**)) between BAFF-expressing T cells and unmodified T cells (n=4-6).

7.Discussion

7.1 Overview

Precision medicine is the concept of individualising treatments for each patient, which can be achieved through both understanding the pathophysiology underpinning the disease and computational tools for analysing large datasets to characterise the disease.[1] This thesis adopts a multimodal approach to developing and implementing novel therapeutic strategies in primary membranous nephropathy, the treatment of which still relies on non-specific broad immunosuppression that are incompletely effective and often toxic. Over the past two decades, our understanding of the immune mechanisms that drive primary membranous nephropathy has deepened, revealing a heterogeneous disease associated with different disease antigens in the kidney but unified by the immune phenotype of loss of immune tolerance to singular antigens expressed on the podocyte of the kidney with subsequent autoantibody formation. Therefore, limiting autoantibody production and expanding regulatory T cells (Tregs) to restore immune tolerance have emerged as attractive therapeutic strategies. In contrast, our understanding of recurrent membranous nephropathy after kidney transplantation remains poor, though large transplant registries allow a computational approach to analysing these large datasets to better understand predictors of recurrent membranous nephropathy, which may inform monitoring post-transplantation and identify high risk patients for potential early treatment. This chapter summarises the main findings of this thesis, discusses their significance, the limitations of our studies, and outlines future research directions.

7.2 Summary of main findings

Through combining machining learning algorithms to a large national transplant registry dataset, targeting specific components of the immune system in an established model of membranous nephropathy, and developing a novel chimeric antigen receptor (CAR) T cell product to target B cells *in vitro*, this thesis has generated new knowledge that can be utilised to develop and implement novel therapeutic strategies in primary membranous nephropathy. Specifically, this thesis has: 1. Developed prediction models for recurrent membranous nephropathy after kidney transplantation, 2. Demonstrated that T cell costimulatory blockade using cytotoxic-T-lymphocyte-associated antigen 4 (CTLA4)-Ig protects against experimental membranous nephropathy by limiting T helper (Th)-17 cells, 3. Demonstrated that $CD8^+$ Tregs induced by peptide vaccination protects against experimental membranous nephropathy and suppressed autoantibody production, and 4. Demonstrated that B cell activating factor (BAFF)-expressing CAR T cells specifically eliminate B cells *in vitro*, which may be used to target B cell-mediated autoantibody production that underpins primary membranous nephropathy.

7.2.1 A penalised Cox regression model could predict recurrent membranous nephropathy with reasonable performance, and identified donor-recipient HLA characteristics as important predictors

In chapter 3, we used data from the Australian and New Zealand Dialysis and Transplant Registry (ANZDATA) (n=554 with primary membranous nephropathy) to develop prediction models for recurrent membranous nephropathy using three machine learning algorithms: 1. Group Least Absolute Shrinkage and Selection Operator (LASSO), 2. Penalised Cox regression, and 3. Random Forest. Models were derived in a subset of the dataset with complete human leukocyte antigen (HLA) serotyping for both donor and recipient HLA-A/B/DR/DQ (n=199) due to existing literature linking recurrent membranous nephropathy with HLA characteristics in both donors and recipients.[2, 3] Group LASSO and penalised Cox regression

(AUC-ROC 0.85, 95% confidence interval 0.76-0.94 and 0.91, 0.85-0.96 respectively) outperformed random forest (0.62, 0.57-0.69) in the derivation cohort for predicting recurrent membranous nephropathy. In the validation cohort, consisting of the ANZDATA dataset with incomplete HLA serotyping for both donor and recipient HLA-A/B/DR/DQ but containing HLA included in the prediction models (n=275), the penalised Cox regression model performed reasonably (area under the receiver operating characteristic curve (AUC-ROC) 0.73, 0.59-0.86 and model accuracy 59%, 49-68%) and better than the Group LASSO model (AUC-ROC 0.60, 0.49-0.70). The random forest model utilised variables from all recipient and donor HLA serotypes and therefore a validation cohort could not be generated. Variables chosen by all models included recipient HLA-A2, donor HLA-DR12, donor-recipient HLA-B65 and HLA-DR12 match, highlighting the importance of both donor and recipient HLA characteristics to recurrent membranous nephropathy.

7.2.2 CTLA4-Ig ameliorated induction of experimental membranous nephropathy potentially by limiting Th17 cells in the kidney without a significant effect on autoantibody production

In chapter 4, we used Heymann nephritis, a rat model of membranous nephropathy, to evaluate the effects of T cell costimulatory blockade (CTLA4-Ig) with or without proteasome inhibition (bortezomib) on disease induction and autoantibody production. While both CTLA4-Ig and CTLA4-Ig plus bortezomib reduced glomerular IgG deposition, there was no significant difference in serum anti-Fx1A autoantibody levels. Rather, CTLA4-Ig and CTLA4-Ig plus bortezomib significantly reduced Th17 cell infiltration in the kidney (reduced $CD4^+$ T cell and $STAT3^+$ cell infiltration) and Th17-associated cytokines (interleukin (IL)-6, IL17 and IL21). There were no significant between group differences in the CTLA4-Ig alone and CTLA4-Ig plus bortezomib groups, suggesting the effects were mediated by CTLA4-Ig alone. These

results were unexpected and neither CTLA4-Ig or bortezomib demonstrated significant effects on T follicular helper (Tfh) cells or plasma cells respectively as we had hypothesised. Furthermore, CTLA4-Ig suppressed markers of $CD4^+$ Tregs in the kidney, suggesting that while CTLA4-Ig may prevent pathogenic Th17 cells in experimental membranous nephropathy, it also has effects on $CD4^+$ Tregs that are involved in maintaining immune tolerance. Therefore, CTLA4-Ig may be useful as an adjunctive treatment in primary membranous nephropathy in cases where Th17 cell activation is contributing to disease activity.

7.2.3 $CD8^+$ Tregs induced by peptide vaccination ameliorated induction of experimental membranous nephropathy and suppressed autoantibody production

In chapter 5, we used the Heymann nephritis model to evaluate the effects of vaccinating four peptides, which had previously been shown to induce $CD8^+$ Tregs in another rodent model of autoimmune disease - experimental multiple sclerosis. Peptide vaccination ameliorated Heymann nephritis, predominantly when given as prevention rather than as a treatment. Both prevention and treatment vaccination induced Helios expression, the main transcription factor of $CD8^+$ Tregs, which reduced histological kidney injury and when given as a prevention vaccination, reduced glomerular IgG deposition, autoantibody production and plasma cell expansion. Adoptive transfer of $CD8^+$ T cells after peptide vaccination also ameliorated Heymann nephritis by reducing glomerular IgG deposition, reducing autoantibody production and suppressing markers of the Tfh, Th1 and Th17 pathways, demonstrating the protective effects of peptide vaccination were mediated through $CD8^+$ Tregs. Overall, these findings demonstrate $CD8^+$ Tregs can suppress autoreactive $CD4^+$ T cells that contribute to disease through multiple pathways (Tfh cells and associated autoantibody production, and possibly kidney infiltrating Th1 and Th17 cells). These results also suggest $CD8^+$ Tregs can be induced

by shared peptides, which are independent of disease-specific antigens and potentially MHC, and therefore mechanisms to harness $CD8^+$ Tregs may have broad application across different autoimmune diseases in addition to primary membranous nephropathy.

7.2.4 BAFF-expressing CAR T cells specifically eliminated B cells *in vitro*

In chapter 6, we generated BAFF-expressing CAR T cells using the PiggyBac transposon system, a non-viral gene delivery method to target B cells that drive autoantibody-mediated diseases such as primary membranous nephropathy. Three BAFF CAR constructs were evaluated (BAFF full-length monomer, BAFF truncated monomer, and BAFF truncated trimer), all of which demonstrated significant cytotoxicity against a B cell line (Raji cells) with no significant cytotoxicity against a negative cell line (human embryonic kidney (HEK)-293T cells). BAFF-expressing CAR T cells exposed to B cells also exhibited increased degranulation and release of pro-inflammatory cytokines such as tumour necrosis factor (TNF)-α, interferon (IFN)-γ and IL2, which were similar between all three constructs. BAFF-expressing CAR T cells did not display significant markers of T cell exhaustion, which are linked with poor CAR T cell performance and unfavourable clinical outcomes.[4, 5] Lentiviral gene delivery did not yield stable BAFF-expressing CAR T cells, which may reflect gene silencing due to epigenetic DNA methylation,[6] though the exact mechanism in this case remains unclear. Overall, BAFF-expressing CAR T cells specifically eliminated B cells *in vitro* and represents a novel treatment for B cell-mediated autoimmune diseases such as primary membranous nephropathy.

7.3 Significance of findings

This section discusses the clinical and research implications of the findings from this thesis on the development and implementation of novel therapeutic strategies in primary membranous

nephropathy. Rituximab emerged as a novel treatment to deplete B cells in primary membranous nephropathy in 2019 but failed to induce disease remission in 40% of patients.[7] Prior to this, the treatment landscape for 20 to 30 years was limited to either cyclophosphamide and corticosteroids, and calcineurin inhibitors, which carried significant toxicities and risk of relapse respectively.[8-10] In contrast, our understanding of the immune mechanisms driving primary membranous nephropathy have dramatically improved with discoveries of over 20 antigens targeted by autoantibodies,[11] key immune cells that contribute to disease aside from B cells (eg. increased Tfh cells, Th17 cells, and plasma cells, and reduced $CD4^+$ Tregs),[12-16] and molecules (eg. BAFF) that support immune cells in primary membranous nephropathy.[17] Translating this knowledge into developing and implementing novel treatment strategies is crucial to improving patient care in this chronic relapsing disease, which carries a high risk of kidney failure in up to 30% of patients who do not respond to existing treatments.[18]

In contrast, our understanding of recurrent membranous nephropathy after kidney transplantation remains poor. Existing studies have identified risk factors including detectable pre-transplant anti-phospholipase A2 receptor (PLA2R) autoantibody, steroid-free immunosuppression, recipient HLA-A3 and donor risk HLA-D and PLA2R1 alleles.[2, 3, 19-21] A genetic risk score based on donor risk HLA-D and PLA2R1 alleles was able to identify patients at high risk of disease recurrence.[2] However, next-generation sequencing of HLA-D and PLA2R1 loci are not routinely available to assist in the prediction of recurrent membranous nephropathy after kidney transplantation and since genetic testing of the donor is required, this is currently not possible in settings of deceased donor kidney transplantation. Furthermore, existing studies were limited to small cohort studies with limited clinical variables which were modelled using stepwise logistic regression. Therefore, in chapter 3, we developed prediction models for recurrent membranous nephropathy in a national registry of kidney transplant

recipients using routinely collected clinical data. For this high dimensional dataset with 222 variables including donor-recipient HLA serotypes and HLA mismatch characteristics, stepwise logistic regression to build models would be inappropriate due to the risk of overfitting and multiple testing with stepwise feature selection across the 222 variables. Therefore, we utilised machine learning algorithms such as Group LASSO, penalised Cox regression and random forest models to both build prediction models and select predictive features of recurrent membranous nephropathy, which has not been previously performed. The penalised Cox regression model performed reasonably though requires further validation in larger datasets in other population groups. Features predictive of recurrent membranous nephropathy across all three prediction models were donor-recipient HLA characteristics, which may influence decisions regarding the choice of kidney donor in patients with membranous nephropathy though this needs to be weighed against the poor quality of life and significant risk of cardiovascular disease and death for patients on dialysis.[22, 23] Overall, these prediction models allow identification of patients at high risk of recurrent membranous nephropathy at time of transplantation using routinely collected data, which facilitates a tailored management approach to counsel high risk patients pre-transplantation and monitor them closely post-transplantation for signs of recurrent membranous nephropathy (eg. monitoring of proteinuria or early signs of membranous nephropathy on protocol transplant biopsies) to allow early diagnosis and treatment.

The need for kidney transplantation in people with membranous nephropathy reflects the ineffectiveness of current treatments. With over 20 antigens linked with membranous nephropathy,[11] it is apparent that primary membranous nephropathy is not a single disease but rather a group of conditions unified by a common immunological phenotype – the development of autoantibodies against mostly singular proteins on the podocyte of the kidney glomerulus

due to a loss of immune tolerance. While the disease antigen in Heymann nephritis, megalin, is not implicated in human membranous nephropathy, this experimental rat model of membranous nephropathy remains relevant since it recapitulates the common immunological phenotype of membranous nephropathy and therefore is suitable for testing treatments working at reducing autoantibody production and promoting immune tolerance. In chapters 4 and 5, we used the Heymann nephritis model to test T cell costimulatory blockade (CTLA4-Ig) with or without proteasome inhibition (bortezomib) and peptide vaccination to induce $CD8^+$ Tregs, to reduce autoantibody production and promote immune tolerance respectively. Unexpectedly, we did not see a significant reduction in serum autoantibody levels with CTLA4-Ig with or without bortezomib though treatment did attenuate the degree of autoantibody deposition in the kidney. Rather, CTLA4-Ig appeared to suppress Th17 cells in the kidney, which is being increasingly recognised in primary membranous nephropathy,[15, 16, 24] though it remains unclear whether Th17 cell infiltration in the kidney is a key upstream immune mechanism driving disease or a downstream consequence of proteinuria, which is known to drive production of pro-inflammatory cytokines and chemokines (eg. endothelin-1, monocyte chemoattractant protein-1 (MCP-1), regulated upon activation normal T-cell expressed and secreted (RANTES) and nuclear factor κβ (NF-κβ) activation) with resultant immune cell infiltration into the kidney and fibrosis.[25, 26] A study demonstrating an association between the incidence of primary membranous nephropathy and levels of pollution, which also correlated with IL17 levels in patients with primary membranous nephropathy suggests it may act upstream as a driving immune mechanism since fine particular matter theoretically activates antigen-presenting cells to release IL6, subsequent Th17 activation and IL17 release.[15] Indeed, IL17 is known to promote B cell proliferation and isotype switching by downregulating the chemokine CXCL12, which retains B cells in the germinal centre.[27, 28] However, serum autoantibody levels were not significantly reduced despite significant reductions in Th17 cells and associated cytokines with

CTLA4-Ig in Heymann nephritis, making a link between Th17 and autoantibody production less likely in primary membranous nephropathy. Instead, Th17 cell activation may represent an independent immune mechanism in primary membranous nephropathy which is present in a subset of patients for whom CTLA4-Ig may represent an effective adjuvant treatment in addition to treatments for depleting autoantibody production. The ALPHAGEM trial (NCT05941845) which is evaluating interferon-alpha for Th17-associated membranous nephropathy reflects this current hypothesis that Th17 cells are important in a subset of patients with membranous nephropathy.

The ultimate goal in the treatment of autoimmune diseases is to re-establish immune tolerance through inducing Tregs since the most upstream immune mechanism is a loss of tolerance towards disease antigens. In chapter 5, we found that peptides that induce $CD8^+$ Tregs in mice with experimental multiple sclerosis could also induce $CD8^+$ Tregs in rats and protect them from Heymann nephritis. This is consistent with our understanding that $CD8^+$ Tregs are equally cross-protective between autoimmune diseases suggesting their T cell receptor binds to peptides not related to the disease antigen.[29] Therefore methods to harness $CD8^+$ Tregs may be helpful in treating multiple autoimmune diseases, not just primary membranous nephropathy. However, in our work, the benefits of peptide vaccination to induce $CD8^+$ Tregs was most pronounced when given prior to disease induction and while peptide vaccination given after disease induction reduced proteinuria and histological kidney injury, it did not reduce autoantibody production. Furthermore, peptide vaccination also increased expression of multiple cytokines associated with the Th1 and Th17 pathway in the kidney, which reflects the non-specific effects of vaccine adjuvants on stimulating the immune system, which is well-described and uncommonly linked with the development and exacerbation of autoimmune diseases, hypothesised to be due to molecular mimicry, epitope spreading, bystander activation

and/or polyclonal activation.[30-32] Indeed, we confirmed the vaccine adjuvant caused stimulation of the immune system in Heymann nephritis, not $CD8^+$ Tregs, since adoptive transfer of $CD8^+$ Tregs after peptide vaccination significantly reduced disease activity, autoantibody production and reduced expression of markers of the Tfh, Th1 and Th17 pathway. Therefore, due to the potential risk of vaccination in exacerbating autoimmune disease, it may be preferable to harness $CD8^+$ Tregs through adoptive cell therapy, which may be enhanced *ex vivo* using peptide vaccination. The Eight-Treg phase I trial testing the safety and optimal dose of $CD8^+$ Tregs in kidney transplant recipients will be of great interest. However, while utilising $CD8^+$ Tregs may hold great promise across autoimmune diseases not limited to primary membranous nephropathy, currently the optimal method of developing and implementing $CD8^+$ Tregs-related therapies remain challenging.[33]

Cellular therapies, in particular CD19-targeting CAR T cells, in refractory B cell-mediated autoimmune diseases such as lupus has recently shown impressive results.[34] Primary membranous nephropathy also involves a B cell-mediated autoimmune component of disease whereby autoantibody-producing B cells and/or plasma cells are driven in part by the B cell growth factor BAFF.[17] In chapter 6, we developed an orthogonal approach to targeting autoreactive B cells using CAR T cells where instead of genetically engineering a receptor to target surface proteins on B cells (such as CD19), we genetically altered CAR T cells to express a BAFF molecule, which specifically eliminated B cells *in vitro* and released pro-inflammatory cytokines without showing significant signs of exhaustion. This may be advantageous to CD19-targeting CAR T cells since they may also target pathogenic plasma cells that do not express CD19 while not eliminating naïve B cells that do not express any of the receptors for BAFF, thus limiting B cell aplasia. Furthermore, a major cause of CAR T cell resistance in the treatment of malignancy is antigen loss or downregulation,[35, 36] which BAFF-expressing CAR

T cells may be less prone to than CD19-targeting CAR T cells since BAFF binds to three different receptors (BAFF-receptor (BAFF-R), transmembrane activator and cyclophilin ligand interactor (TACI) and B cell maturation antigen (BCMA)). However, whether antigen loss occurs and results in CAR T cell resistance in autoimmune disease is unclear as the use of CAR T cells in autoimmunity is still in its infancy.

7.4 Limitations

In this thesis, we utilised a range of research methods from machine learning algorithms in large datasets to animal models to *in vitro* studies in primary human T cells, which all play an important role in translational research but also have limitations. In chapter 3, while we built prediction models in a large national registry (ANZDATA), membranous nephropathy is a rare disease and therefore rates of recurrent membranous nephropathy were low to leverage the computational power of machine learning algorithms. Furthermore, anti-PLA2R antibody levels are a known risk factor for recurrent membranous nephropathy,[19-21, 37] but is not collected in ANZDATA, and the rates of recurrent membranous nephropathy were lower than expected in existing literature, which limits the prediction models developed from this database and represents a disadvantage of using a broad registry that covers all dialysis and transplant recipients across Australia and New Zealand but is unlikely to collect tests specific for or have standardised protocols to detect the recurrence of rare diseases such as membranous nephropathy.

In chapter 4 and 5, the Heymann nephritis model was used, which has distinct effector mechanisms downstream of glomerular autoantibody deposition compared to primary membranous nephropathy but is similar in terms of upstream immunopathogenesis. While we

found CTLA4-Ig ameliorated Heymann nephritis, likely through suppression of Th17 cells in the kidney, it remains unclear whether Th17 cells act independently or are involved in glomerular autoantibody deposition. Therefore, it remains unclear whether the effectiveness of CTLA4-Ig will translate effectively to treating primary membranous nephropathy. Furthermore, a lack of commercially available rat reagents to detect Th17 cells limited our ability to confirm Th17 cell infiltration in the kidney, which was detected by one method ($STAT3^+$ immunohistochemical staining in the kidney) along with indirect evidence from mRNA expression of Th17 cytokines (IL6, IL17 and IL21). In chapter 5, we demonstrated prevention peptide vaccination ameliorated Heymann nephritis through upstream mechanisms by reducing autoantibody production, likely through inducing immune tolerance through $CD8^+$ Tregs. However, the effects of peptide vaccination were less pronounced when given as a treatment after disease induction and the lack of a control peptide means we cannot be confident that the specific peptides (ASRSNRYFWL, HDRVNWEYI, SMRPNHFFFL, YQPGNWEYI) used were responsible for inducing $CD8^+$ Tregs. *In silico* prediction tools to assess binding of these peptides to rat major histocompatibility complex (MHC) classical and non-classical class I are also lacking to evaluate the likelihood of these peptides, which induce $CD8^+$ Tregs in mice, also engaging with $CD8^+$ Tregs in rats. While there is emerging evidence for the importance to $CD8^+$ Tregs in human autoimmune diseases such as lupus, multiple sclerosis, and celiac disease, their importance in primary membranous nephropathy is yet to be established.[38] Therefore, the translational potential of therapeutics to induce $CD8^+$ Tregs such as peptide vaccination (either given directly or to expand $CD8^+$ Tregs *ex vivo*) remains unclear for primary membranous nephropathy.

In chapter 6, we developed BAFF-expressing CAR T cells in primary healthy human T cells, which effectively eliminated a B cell line (Raji cells) without significant cytotoxicity towards

a negative cell line. While Raji cells express all three receptors for BAFF, we cannot confidently determine the cytotoxicity of BAFF-expressing CAR T cells is mediated through BAFF binding to its cognate receptors. Such work has previously been shown by Wong et al, who demonstrated cytotoxicity of BAFF-expressing CAR T cells to a cell line engineered to expressed only BAFF-R, TACI or BCMA.[39] As stated in the previous chapter, we have not shown BAFF-expressing CAR T cells are effective in treating autoimmune kidney diseases such as Heymann nephritis nor safety in terms of insertional mutagenesis and lack of cytotoxicity towards other negative cell lines such as brain, heart, lung, and liver. Due to the cost of CAR T cell therapies, it will likely be used in patients with refractory or relapsed autoimmune diseases who have been exposed to multiple lines of immunosuppression previously. Therefore, generating BAFF-expressing CAR T cells in human T cells from patients who have had previous immunosuppression will also be crucial since insufficient CAR T cell expansion is an important cause of CAR T cell failure.[36] Lastly, we were not able to generate stable and persistent BAFF-expressing CAR T cells using lentiviral gene delivery. Although we could use the PiggyBac transposon system, this has been linked to increased risk of insertional mutagenesis with evidence of malignant T cell transformation,[40] which limits its translation into the clinic.

7.5 Future research directions

The aims of this thesis were to develop and implement novel therapeutic strategies in primary membranous nephropathy. While our work makes important steps towards this goal, further research is required to translate our findings into improved patient care. Validation of our prediction models developed in chapter 3 in larger datasets such as other national transplant registries would be important to improve the generalisability of the model. Furthermore, data

linkage between transplant registries and existing biorepositories may facilitate access to other important variables known to predict recurrent membranous nephropathy, such as anti-PLA2R antibody levels and molecular HLA typing, which will likely improve prediction model performance and better guide decision-making regarding post-transplant monitoring and treatment of recurrent disease.

In chapter 4 and 5, we identified treatments that suppress the Th17 pathway (CTLA4-Ig) and induce $CD8^+$ Tregs (peptide vaccination) in Heymann nephritis respectively. However, the exact role of the Th17 pathway and $CD8^+$ Tregs in primary membranous nephropathy remain unclear and warrants further characterisation to improve the likelihood of translational success. To determine whether the Th17 pathway acts upstream or downstream of autoantibody production, the effect of IL17 administration or IL17 receptor knock-out on autoantibody levels and germinal centre B cells could be evaluated in Heymann nephritis rats or recently developed models of PLA2R-associated membranous nephropathy in mice, which better represent primary membranous nephropathy.[41, 42] Characterising $CD8^+$ Tregs in the peripheral blood and kidney biopsies of patients with primary membranous nephropathy, and assessing their correlation with disease activity is important to establish their relevance as a therapeutic target. To translate the concept of peptide vaccination into the clinic would require further research evaluating whether the four peptides described by Saligrama et al also expand human $CD8^+$ Tregs *in vitro*,[43] which is possible since the mechanism of cutting proteins into peptides for loading onto MHC class I is conserved between different species.[44] However, there are also distinct differences between human and mouse MHC class I, and peptide generation machinery (eg. proteasome, transporter associated with antigen processing (*TAP*) and tapasin) that may impact peptides recognised by human $CD8^+$ Tregs,[45] though the methodology described by Saligrama et al can be applied to identify peptides that induce human $CD8^+$ Tregs.[43]

Preliminary studies demonstrating the efficacy of CD19-targeting CAR T cells in B cell-mediated autoimmune diseases have laid the foundation for the translational potential of BAFF-expressing CAR T cells.[34, 46] In chapter 6, while we demonstrated efficacy of BAFF-expressing CAR T cells against B cells *in vitro*, further research into their efficacy *in vivo* in models of autoimmune kidney disease such as Heymann nephritis is needed. Furthermore, due to concern from the Food and Drug Administering (FDA) regarding insertional mutagenesis and subsequent T cell malignancy with existing gene delivery methods to generate CAR T cells,[47] it is also essential to perform integration site analysis by assessing vector copy number (VCN) via droplet digital polymerase chain reaction (PCR), aiming for a VCN less than 5 per cell as recommended by the FDA.[48] While we were able to generate stable BAFF-expressing CAR T cells using the PiggyBac transposon system, it has been associated with cases of high VCN that resulted in T cell malignancy.[40] In contrast, we were unable to generate stable BAFF-expressing CAR T cells using lentiviral gene delivery, which has much more real world data, suggesting an overall low risk of secondary T cell malignancy (1 of 449 patients and 1 of 724 patients in recent reports).[49, 50] Therefore, future research should include evaluating alternative gene delivery methods, such as the non-viral TcBuster transposon system, which inserted less frequently into transcript-coding DNA regions than lentiviral gene delivery while still retaining good CAR expression.[39] Alternatively, future research into reasons why lentiviral gene delivery failed to yield stable BAFF-expressing CAR T cells may reveal mechanisms that inform the translational potential of this method. Analysis of DNA methylation or rescue of BAFF CAR expression using DNA methylation antagonists such as decitabine may confirm gene silencing, which limits the translation of these BAFF CAR constructs. Evaluation of additional constructs such as truncated BAFF monomer or trimer CAR constructs without additional mutations may elucidate whether the mutations we introduced into the BAFF molecule inhibited protein

expression, potentially through misfolding and subsequent degradation in the proteasome. To evaluate whether our lentiviral plasmid requires optimisation, we could replace our BAFF CAR constructs with a simple construct (eg. green fluorescent protein (GFP)) expected to be highly expressed without conferring toxicity to T cells. Lastly, lentivirus quality may influence gene delivery and repeating our experiments with a new batch of lentivirus may reveal whether batch-to-batch variability in lentivirus quality impacted on the degree and durability of BAFF CAR expression.

7.6 Conclusions

Research in primary membranous nephropathy has dramatically improved our understanding of the immune mechanisms driving this autoimmune kidney disease, which is characterised by a loss of immune tolerance to antigens expressed on podocytes and subsequent autoantibody production. However, treatments for primary membranous nephropathy have lagged behind with only one new medication (rituximab) successfully implemented for this condition over the past 20 years. This thesis addresses the limited translational research in primary membranous nephropathy, required to develop and implement new treatments, which ideally target the upstream immune mechanisms by depleting autoantibody production and/or expanding Tregs to restore immune tolerance. The findings of this thesis identify promising therapeutic strategies, which have translational potential in primary membranous nephropathy. Additionally, treatments inducing $CD8^+$ Tregs and generating BAFF-expressing CAR T cells have the potential to benefit other autoimmune diseases as well. Therefore, our work will also stimulate further research into how novel treatments to deplete autoantibody production and/or expand Tregs can improve the care of patients with primary membranous nephropathy or other autoimmune diseases.

7.7 References

1. Collins FS, Varmus H. A new initiative on precision medicine. N Engl J Med. 2015;372(9):793-5.

2. Berchtold L, Letouzé E, Alexander MP, et al. HLA-D and PLA2R1 risk alleles associate with recurrent primary membranous nephropathy in kidney transplant recipients. Kidney Int. 2021;99(3):671-85.

3. Batal I, Vasilescu ER, Dadhania DM, et al. Association of HLA Typing and Alloimmunity With Posttransplantation Membranous Nephropathy: A Multicenter Case Series. Am J Kidney Dis. 2020;76(3):374-83.

4. Fraietta JA, Lacey SF, Orlando EJ, et al. Determinants of response and resistance to CD19 chimeric antigen receptor (CAR) T cell therapy of chronic lymphocytic leukemia. Nat Med. 2018;24(5):563-71.

5. Deng Q, Han G, Puebla-Osorio N, et al. Characteristics of anti-CD19 CAR T cell infusion products associated with efficacy and toxicity in patients with large B cell lymphomas. Nat Med. 2020;26(12):1878-87.

6. Salz L, Seitz A, Schäfer D, et al. Culture expansion of CAR T cells results in aberrant DNA methylation that is associated with adverse clinical outcome. Leukemia. 2023;37(9):1868-78.

7. Fervenza FC, Appel GB, Barbour SJ, et al. Rituximab or Cyclosporine in the Treatment of Membranous Nephropathy. N Engl J Med. 2019;381(1):36-46.

8. Ponticelli C, Altieri P, Scolari F, et al. A randomized study comparing methylprednisolone plus chlorambucil versus methylprednisolone plus cyclophosphamide in idiopathic membranous nephropathy. J Am Soc Nephrol. 1998;9(3):444-50.

9. Jha V, Ganguli A, Saha TK, et al. A randomized, controlled trial of steroids and cyclophosphamide in adults with nephrotic syndrome caused by idiopathic membranous nephropathy. J Am Soc Nephrol. 2007;18(6):1899-904.

10. Cattran DC, Appel GB, Hebert LA, et al. Cyclosporine in patients with steroid-resistant membranous nephropathy: a randomized trial. Kidney Int. 2001;59(4):1484-90.

11. Avasare R, Andeen N, Beck L. Novel Antigens and Clinical Updates in Membranous Nephropathy. Annu Rev Med. 2024;75:219-332.

12. Cantarelli C, Jarque M, Angeletti A, et al. A Comprehensive Phenotypic and Functional Immune Analysis Unravels Circulating Anti-Phospholipase A2 Receptor Antibody Secreting Cells in Membranous Nephropathy Patients. Kidney Int Rep. 2020;5(10):1764-76.

13. Shi X, Qu Z, Zhang L, et al. Increased ratio of ICOS(+) /PD-1(+) follicular helper T cells positively correlates with the development of human idiopathic membranous nephropathy. Clin Exp Pharmacol Physiol. 2016;43(4):410-6.

14. Zhang Z, Shi Y, Yang K, et al. Higher frequencies of circulating ICOS(+), IL-21(+) T follicular helper cells and plasma cells in patients with new-onset membranous nephropathy. Autoimmunity. 2017;50(8):458-67.

15. Cremoni M, Brglez V, Perez S, et al. Th17-Immune Response in Patients With Membranous Nephropathy Is Associated With Thrombosis and Relapses. Front Immunol. 2020;11:574997.

16. Li H, Wu H, Guo Q, et al. Myeloid-Derived Suppressor Cells Promote the Progression of Primary Membranous Nephropathy by Enhancing Th17 Response. Front Immunol. 2020;11:1777.

17. Netti GS, Infante B, Spadaccino F, et al. Serum Levels of BAFF and APRIL Predict Clinical Response in Anti-PLA2R-Positive Primary Membranous Nephropathy. J Immunol Res. 2019;2019:8483650.

18. Troyanov S, Wall CA, Miller JA, et al. Idiopathic membranous nephropathy: definition and relevance of a partial remission. Kidney Int. 2004;66(3):1199-205.

19. Grupper A, Cornell LD, Fervenza FC, et al. Recurrent Membranous Nephropathy After Kidney Transplantation: Treatment and Long-Term Implications. Transplantation. 2016;100(12):2710-6.

20. Kattah A, Ayalon R, Beck LH, Jr., et al. Anti-phospholipase A_2 receptor antibodies in recurrent membranous nephropathy. Am J Transplant. 2015;15(5):1349-59.

21. Quintana LF, Blasco M, Seras M, et al. Antiphospholipase A2 Receptor Antibody Levels Predict the Risk of Posttransplantation Recurrence of Membranous Nephropathy. Transplantation. 2015;99(8):1709-14.

22. Chaudhry D, Chaudhry A, Peracha J, et al. Survival for waitlisted kidney failure patients receiving transplantation versus remaining on waiting list: systematic review and meta-analysis. Bmj. 2022;376:e068769.

23. Reese PP, Shults J, Bloom RD, et al. Functional status, time to transplantation, and survival benefit of kidney transplantation among wait-listed candidates. Am J Kidney Dis. 2015;66(5):837-45.

24. Xu J, Shen C, Lin W, et al. Single-Cell Profiling Reveals Transcriptional Signatures and Cell-Cell Crosstalk in Anti-PLA2R Positive Idiopathic Membranous Nephropathy Patients. Front Immunol. 2021;12:683330.

25. Remuzzi G, Bertani T. Pathophysiology of progressive nephropathies. N Engl J Med. 1998;339(20):1448-56.

26. Perico N, Codreanu I, Schieppati A, et al. Pathophysiology of disease progression in proteinuric nephropathies. Kidney Int Suppl. 2005(94):S79-82.

27. Mitsdoerffer M, Lee Y, Jäger A, et al. Proinflammatory T helper type 17 cells are effective B-cell helpers. Proc Natl Acad Sci U S A. 2010;107(32):14292-7.

28. Hsu HC, Yang P, Wang J, et al. Interleukin 17-producing T helper cells and interleukin 17 orchestrate autoreactive germinal center development in autoimmune BXD2 mice. Nat Immunol. 2008;9(2):166-75.

29. Wu Y, Zheng Z, Jiang Y, et al. The specificity of T cell regulation that enables self-nonself discrimination in the periphery. Proc Natl Acad Sci U S A. 2009;106(2):534-9.

30. Agmon-Levin N, Paz Z, Israeli E, et al. Vaccines and autoimmunity. Nat Rev Rheumatol. 2009;5(11):648-52.

31. Pellegrino P, Clementi E, Radice S. On vaccine's adjuvants and autoimmunity: Current evidence and future perspectives. Autoimmun Rev. 2015;14(10):880-8.

32. Petrovsky N. Comparative Safety of Vaccine Adjuvants: A Summary of Current Evidence and Future Needs. Drug Saf. 2015;38(11):1059-74.

33. Flippe L, Bézie S, Anegon I, et al. Future prospects for CD8(+) regulatory T cells in immune tolerance. Immunol Rev. 2019;292(1):209-24.

34. Müller F, Taubmann J, Bucci L, et al. CD19 CAR T-Cell Therapy in Autoimmune Disease - A Case Series with Follow-up. N Engl J Med. 2024;390(8):687-700.

35. Labanieh L, Mackall CL. CAR immune cells: design principles, resistance and the next generation. Nature. 2023;614(7949):635-48.

36. Shah NN, Fry TJ. Mechanisms of resistance to CAR T cell therapy. Nat Rev Clin Oncol. 2019;16(6):372-85.

37. Hullekes F, Uffing A, Verhoeff R, et al. Recurrence of membranous nephropathy after kidney transplantation: A multicenter retrospective cohort study. Am J Transplant. 2024;24(6):1016-26.

38. Li J, Zaslavsky M, Su Y, et al. KIR(+)CD8(+) T cells suppress pathogenic T cells and are active in autoimmune diseases and COVID-19. Science. 2022;376(6590):eabi9591.

39. Wong DP, Roy NK, Zhang K, et al. A BAFF ligand-based CAR-T cell targeting three receptors and multiple B cell cancers. Nat Commun. 2022;13(1):217.

40. Micklethwaite KP, Gowrishankar K, Gloss BS, et al. Investigation of product-derived lymphoma following infusion of piggyBac-modified CD19 chimeric antigen receptor T cells. Blood. 2021;138(16):1391-405.

41. Tomas NM, Dehde S, Meyer-Schwesinger C, et al. Podocyte expression of human phospholipase A2 receptor 1 causes immune-mediated membranous nephropathy in mice. Kidney Int. 2023;103(2):297-303.

42. Tomas NM, Schnarre A, Dehde S, et al. Introduction of a novel chimeric active immunization mouse model of PLA2R1-associated membranous nephropathy. Kidney Int. 2023;104(5):916-28.

43. Saligrama N, Zhao F, Sikora MJ, et al. Opposing T cell responses in experimental autoimmune encephalomyelitis. Nature. 2019;572(7770):481-7.

44. Rammensee HG, Falk K, Rötzschke O. Peptides naturally presented by MHC class I molecules. Annu Rev Immunol. 1993;11:213-44.

45. Pascolo S. HLA class I transgenic mice: development, utilisation and improvement. Expert Opin Biol Ther. 2005;5(7):919-38.

46. Mackensen A, Müller F, Mougiakakos D, et al. Anti-CD19 CAR T cell therapy for refractory systemic lupus erythematosus. Nat Med. 2022;28(10):2124-32.

47. Levine BL, Pasquini MC, Connolly JE, et al. Unanswered questions following reports of secondary malignancies after CAR-T cell therapy. Nat Med. 2024;30(2):338-41.

48. Ayala Ceja M, Khericha M, Harris CM, et al. CAR-T cell manufacturing: Major process parameters and next-generation strategies. J Exp Med. 2024;221(2).

49. Ghilardi G, Fraietta JA, Gerson JN, et al. T cell lymphoma and secondary primary malignancy risk after commercial CAR T cell therapy. Nat Med. 2024;30(4):984-9.

50. Hamilton MP, Sugio T, Noordenbos T, et al. Risk of Second Tumors and T-Cell Lymphoma after CAR T-Cell Therapy. N Engl J Med. 2024;390(22):2047-60.